# LABILE ZINC AND ITS ROLE IN REGULATION OF PRO-CASPASE-3 AND NF-κB ACTIVATION IN MAST CELLS

**A thesis submitted to the University of Adelaide as the requirement of the Degree of Doctor of Philosophy**

**by**

**Lien Ha Ho B. Health. Sc. (Hons).**

Department of Medicine
The University of Adelaide
The Queen Elizabeth Hospital

June 2003

Errata

General changes:
All Zn supplementation experiments were performed using Zn pyrithione as the ionophore.

In some graphs, data were pooled from several experiments and results were normalized by expressing them as % apoptosis of control. At least one figure was included to show the absolute values.

Specific changes:
Table of Contents: 1.6.4 refers to the heading 'Mediators'
Page 83; change 2.2.3 to 2.3.3 and 2.2.4 change to 2.3.4

Page 123; 'section 2.6.7' change to 'section 2.6.4' and 'section 2.6.13' change to 'section 2.6.6'
Page 107 (line 14); change 'section 2.7.4 to 'section 2.6.3, change 'section 2.9' to 'section 2.6.5' and change 'section 2.9' to 'section 2.6.6'

Page 8- section 1.2.5: Since the writing of this thesis a new member of the ZnT family has been described, ZnT7. Kirschke, CP, Huang, L. ZnT7, a novel mammalian zinc transporter, accumulates zinc in the Golgi apparatus. J. Biol Chem, Feb 2003 7;278(6):4096-12.

Figure 1.5: Bid: is a cytosolic, proapoptotic BH3 domain containing protein.

Page 66: ZEN: change abbreviation from zinc enriched neurons to zinc enriched

Page 67: at least one report of an increase of Zn in AD has been published. Danscher G, Jensen KB, Frederickson CJ, Kemp K, Andreasen A, Juhl S, Stoltenberg M, Ravid, R. Increased amount of zinc in the hippocampus and amygdala of Alzheimer's diseased brains: a proton-induced X-ray emission spectroscopic analysis of cryostat sections from autopsy material. J. Neurosci. Meth. 76: 53-59.

Chapter 3: Zinquin fluorescence was not quantified because there was no sensitive or reliable technique currently available at that time.

Chapter 4: Negative controls were included for the expression of pro-caspase-3 mRNA experiments, however due to space limitations they were not shown.

Figure 4.11E: scroll like structures are shown which may either be granules or mitochondria.

Page 137: mast cells were activated for 18h with compound 48/80 according to a commonly used technique

Table 6.4: significances were determined for all comparisons. For clarity, only the most relevant ones were shown in the table.

Grammatical corrections:

Page 12- line 16 change peak to peaks
Page 13- line 6 change tool to tools
Page 29- line 14 deletion of bracket
Figure 1.7- line 4 change turns to turn
line 7 change caspase to caspase-9
line 10 change molecule to molecules
Page 34- line 16 change mitochondrial intramembranous to intramembrane region of mitochondria
Page 35-line 13 change Down to Downs
Page 36- line 1 change requires to require
line 15 change play to plays
line 16 change response to responses
line 17 change protein to proteins
line 18 change compromised to comprises

Page 41-line 3 change TRAF to TRAF-associated
line 13 change debatable to debated
Page 49- line21 change rats to rat
Page 50- line change MCM to MMC
Page 52- line 18 change mechanism to mechanisms
Page 53- line 14 delete 'the' from 'the tyrosine'
Page 54- line 9 change result to results
Page 55- line 12 change activate to activates
Page 58- last line 'Kazimierczak and Maslinski, and Uvnas' delete first 'and' and omit comma.
Page 80- line 12; 'depleted' refer to action of TPEN and 'supplemented' refer to $ZnSO_4$.
Page 85- line 14 change degraunlation to degranulation
Page 90- line 12 change spin to spins
Page 117- line 7 change is to in
Page 139- line 16 change increases to increase
line 18 change caspases to caspase
Page 165- line 2 change regulate to regulates
line 3 change regulate to regulates

## TABLE OF CONTENTS

# SUMMARY

# SUMMARY

The main aim of this thesis was to further investigate the relationship between Zinquin-detectable intracellular pools of labile Zn and caspase activation since caspases have now been shown to be important effector enzymes in apoptosis. This was largely studied in mast cells and some findings confirmed in neuronal cells, a cell type with quite different function and cell physiology.

Mast cells were chosen because these cells are important inflammatory cells that have been shown to contain Zn rich granules. However, there have been no previous studies of labile Zn in these cells, the mechanisms by which it is accumulated and its function in relationship to apoptosis. Labile Zn was shown to be rich in mast cells by Zinquin fluorescence with a granular like staining pattern and the fluorescence decreased during degranulation. A major issue is how mast cells regulate their uptake of Zn from their environment. The experiments reported here are the first to describe the localization of a Zn transporter, $ZnT_4$ in mast cells. There was high expression of both the mRNA and its protein in mast cells, suggesting that it is likely to be involved in the transportation of Zn either across the plasma membrane or into the granules. The absence of overlap between Zn and $ZnT_4$ may imply that only a subset of granules require $ZnT_4$ as their major Zn transporter. Other transporters need to be investigated.

The distribution of pro-caspases, important components in apoptosis signaling has not been a focus of mast cell biologists. It was important to determine whether these were

present in mast cells and their relationship to mast activation. In mast cells, expression of pro-caspase-3 mRNA was shown and the detection of its protein by immunocytochemistry indicated that it was translated. One unexpected finding was that pro-caspase-3 (and -4) were localized within granules of the mast cells as shown by immunoelectron microscopy. This was confirmed by their loss during degranulation.

Explanations for why pro-caspases are localized in mast cell granules include: 1) pro-caspases may be released and activated during degranulation and cleave extracellular substrates, 2) caspases maybe released and induce apoptosis in other cells, 3) caspases may have a special function in cleaving proteins within the granules and 4) in order to prolong their survival during activation, mast cells may shed their caspases during degranulation and thereby become more resistant to noxious stimuli.

Depletion of Zn by one mechanism (TPEN chelation) but not by degranulation increased the activation of pro-caspase-3, either spontaneously or in cells treated with the apoptotic inducer butyrate. The experiments described in this thesis show that at least under *in vitro* conditions, degranulated mast cells can recover their granular content of Zn and do not undergo apoptosis spontaneously. Similar results were obtained for a range of degranulators and various mast cell types. These findings suggest that there are two labile pools of Zn; one regulates caspase activation and apoptosis while the other (the granular pool) has other functions.

To further understand the mechanism by which Zn may regulate apoptosis in mast cells, the effects of Zn supplementation and depletion on activation of NF-κB were

investigated. NF-κB is thought to be an anti-apoptotic factor prolonging the survival of inflammatory cells. Zn supplementation by the ionophore pyrithione blocked nuclear translocation of NF-κB, an important step in the activation of this transcription factor. Furthermore, Zn depletion by TPEN was found to be an effective inducer of nuclear NF-κB translocation. This has not previously been demonstrated. These findings suggest that Zn is a regulator of NF-κB translocation and raise questions as to whether abnormalities in NF-κB activation occur in Zn deficiency.

The studies with neuroblastoma cells confirmed some of these findings. BE(2)-C neuroblastoma cells had cytoplasmic/cytoskeletal pools of intracellular labile Zn which were further increased by Zn ionophore or decreased by Zn chelator TPEN. As for mast cells there was synergy between TPEN and butyrate in caspase activation and this was suppressed by Zn supplementation, suggesting that the effect of Zn on caspase regulation is a general phenomenon.

As a summation of the findings reported in this thesis, a general model is proposed describing possible interactions between Zn, pro-caspases and NF-κB. Some of these findings were reported in Ho et al 2000 and form part of a submitted manuscript Ho et al 2003.

## DECLARATION

This work contains no material which has been accepted for the award of any other degree or diploma in any university or other tertiary institution and, to the best of my knowledge and belief, contains no material previously published or written by another person, except where due reference has been made in the text.

I give consent to this copy of my thesis, when deposited in the University Library, being available for loan and photocopying.

*Signed.* *Date* 2/06/03

Lien Ha Ho

# ACKNOWLEDGMENTS

I would like to thank the Department of Medicine, the University of Adelaide for providing me with the resources for my PhD candidature. I would also like to thank the following people for their endless support, knowledge and friendship.

To two very brave persons namely **Dr Peter Zalewski** and **Professor Richard Ruffin** who took me under their wings and provided me with constant support, insightful advice and friendship in the past four years. Your belief and support has made it worthwile. It has been a privilege and an inspiration to be working beside two wonderful people.

**Peter (Zinc man)**: thank you so much for your support and never say no attitude to my cries for help and sitting through the harrowing months of writing up. Thank you for being a great teacher and showing me the passionate side of science and teaching me that perserverance and hard work builds an honourable chararacter. I wish you all the successes in the future years. May you always keep that passion for science alive.

To my family: thank you so much for your love and support over the years. Without all of you here this would not be possible. To my brother Long, thank you for cheering me up with all of your Simpsons antedotes. Groove on Bart!

Ms Sarah Appleton: it has been a privilege to share my time in the department with you. You have become a wonderful and supportive friend. Thank you for giving so much and asking for so little back. Thank you for making my time here such a wonderful experience. Your friendship has helped me through so many difficult times.

I shall miss our lunches and lively discussions on all things great and small. I wish you love and happiness for always.

Mrs Ermioni Mourtzios: thank you for being the most knowledgeable person about anything and everything and being a super organizer. Without your help I would be a very lost girl. Thank you for always being there in times of great need.

Mr Austil Milton: thank you for your help with all things computer as well as non-computer. Thank you for always being ready to lend a hand and give helpful advice. Best wishes to you and your family.

Dr Prue Cowled: thank you for your support and constant encouragment through the past years. Your words have truly motivated me and restore my sanity in the darkest of times. Thank you for letting me roam freely on your floor and trust that I did not destroyed more than I created. I wish you all the best.

Ms Lefta Leonardas: thank you for being my saviour for so many things. You have have been so generous to take time out to help me and put up with my constant questions. You are the best, and I wish you and your family a wonderful future ahead filled with love.

Dr Lorwai Tan: thank you for giving me making me laugh every time we talk and for your understanding of my strange working hours. I am very grateful for the opportunity that you have given me. I wish you all the successes in the world and keep powering on girl.

Ms Sue Millard: thank you for your help throught the years, your advice and encouragement. You are never without a smile and a laugh or two, a truly inspirational person.

Miss Joanne Carter: thank you for being a great friend and I miss our chats and silly laughter. I am so glad that you are spreading your wings and feeling so happy. Enjoy life to the fullest Joanne.

Ms Rachel Gibson: thank you for your close friendship and constant support. I have enjoyed our outings and I hope we remain friends for many years to come. Thank you for always finding a way to cheer me up.

Dr Fugui Chai: thanks for being such a great office mate and putting up with me, because it is a very hard task to do. Wishing you the very best.

I would also like to thank the following people who have laughed, cheered and shared their knowledge and life with me: Dr Ranjit Ratnaike, Mary Denys, Sue Dowset, Melanie Bagg, Andrea Varga, Gwenda Graves, Lan Lan, Marj, Dr Dion Grosser and Evelyn Douglas. *To Joshua*: thank you for being a great friend and I have enjoyed our yummy lunches. Thanks for fixing the impossible. I wish you the best of luck and hope to see you soon for more food.

To my dearest friend in the world: Kelly Chau, you are truly an inspirational person. For 17 years you have stood by me through thick and thin and never given up on me. There are not enough thank yous' to express what our friendship means to me. I am humble to be a part of your wonderful life.

To a dear friend that never fails to lift my spirit: Lien Vo (my better half), you are never far away from my side when I need that all important uplifting talk. You have carried me through so many dark moments and I feel stronger as a result. Thank you for being such a wonderful friend for so many years. I wish you happiness.

To the Cox/McClimont family: thank you so much for your love, support and endless encouragement. I am so grateful to know all of you and see it as a blessing to be a part of your daily lives. Thank you for welcoming me into your family with open arms and I look forward to many more happy times with you.

And finally I would like to thank my wonderful Daniel, my tower of strength. Without you, my struggles would have been so much harder to bear. Your support and love have made every moment worthwhile and made me a better person. I could not imagine any other person than you to share my life with. You make me realised that it is a wonderful life afterall. For always.

To Chloe: my ever-smiling golden retriever, thank you for making me understand the meaning of unconditional love.

***"This is the true joy in life, the being used for a purpose recognized by yourself as a mighty one; the being thoroughly worn out before you are thrown on the scrap heap; the being a force of Nature instead of a feverish selfish little clod of ailments and grievances complaining that the world will not devote itself to making you happy"***

**George Bernard Shaw**

## PUBLICATIONS ARISING FROM THESIS

---

**Chai F, Truong-Tran AQ, Ho LH and Zalewski PD.** Regulation of caspase activation and apoptosis by cellular zinc fluxes and zinc deprivation: A review. *Immunology and Cell Biology.* 77: 272-278 (1999).

**Ho LH, Ratnaike, RN and Zalewski, PD.** Involvement of intracellular labile zinc in suppression of DEVD-caspase activity in human neuroblastoma cells. *Biochemical and Biophysical Research Communications.* 268: 148-154 (2000).

**Truong-Tran AQ, Ho LH, Chai F and Zalewski PD.** Cellular zinc fluxes and the regulation of apoptosis/gene-directed cell death. *Journal of Nutrition.* 130 (5S Suppl): 1459S-1466S (2000).

**Ho LH, Richard RE, Murgia C, Li L, Krilis SA and Zalewski PD.** Labile Zinc And Zinc Transporter $ZnT_4$ In Mast Cell Granules: Role In Regulation Of Caspase Activation and NF-κB Translocation. (Submitted, 2003)

## CONFERENCE PRESENTATIONS

-Oral presentation at The 1998 Australian Association of Gerontology Scientific Conjoint Meeting: Mapping The Future: Expressions of the science and Art of Aged Care, held at Westlakes, South Australia on August 6th.

-Oral presentation at the Annual Scientific Meeting by The Australian Society for Medical Research (ASMR), South Australian division: visualisation of zinc (zn) in mast cells and its role in suppression of nf-κb in airway epithelial cells June 2000 .

-Oral presentation at the 2000 European Respiratory Society International conference: high basal caspase-2, 3, 4 and 6 activity in rat rbl-2h3 mast cells. August 30-September 4, Florence, Italy.

-Oral presentation at the 2001 Allergy, Asthma and Immunology Conference: Suppression of nf-kb transcription factor in airway epithelial cells by zinc released from inflammatory cells: anti-inflammatory role for zinc in respiratory diseases November 21-26, Orlando, Florida, USA.

-Oral presentation at the Allen & Hanbury's Young Investigator Award: Release of intracellular zinc and increased caspase-3 and -4 levels in mast cells. June 2001, Adelaide, South Australia, Australia.

-Oral presentation at the Australian-New Zealand Thoracic society conference:
Release of intracellular zinc and increased caspase-3 and -4 levels following mast cell degranulation. March 22-24, 2002, Cairns, Australia.

# LIST OF FIGURES

# LIST OF TABLES

# ABBREVIATIONS

| | |
|---|---|
| AD | Alzheimer's disease |
| Apaf-1 | Activating factor-1 protein |
| BMMC | Bone marrow mast cells |
| BSA | Bovine serum albumin |
| $Ca^{2+}$ | Calcium ions |
| CARD | Caspase Recruitment Domain |
| CBMC | Cord blood mast cells |
| CDF | Cation diffusion facilitator |
| $CO_2$ | Carbon Dioxide |
| CRIP | Cysteine-rich intestinal protein |
| °C | Degree celsius |
| DCT | Divalent Cation Transporter |
| DED | Death effector domain |
| DEVD-AFC | 7-amino-4(trifluoromethyl) coumarin |
| DNA | Deoxyribonucleic acid |
| ssDNA | single strand Deoxyribonucleic acid |
| DMSO | Dimethylsulphoxide |
| DNP-IgE | dinitrophenyl-IgE |
| DNP-BSA | dinitrophenyl – BSA |
| EM | electron microscope |
| FBS | Foetal bovine serum |
| FITC | Fluorescein isothiocyanate |
| GSU | Gray Scale Units |
| $H_2O_2$ | Hydrogen peroxide |
| HBSS | Hanks balanced buffered salt solution |
| g | g- force in gravity |

| | |
|---|---|
| h | hour |
| IAP | Inhibitor of apoptosis protein |
| IKK | IkappaB kinase |
| IKB | Ikappa B |
| IL- | Interleukin- |
| LHS | Left hand side |
| min | minute |
| MOPS | 3-[N-Morpholino]propanesulfonic acid |
| NF-κB | Nuclear factor-kappa B |
| PARP | Poly(ADP-ribose) polymerase |
| PBS | Phosphate buffered saline |
| PMA | phorbol 12-myristate 13-acetate |
| PKC | Protein kinase C |
| RIP | Receptor interacting protein |
| RPMC | Rat peritoneal mast cells |
| RNA | Ribonucleic acid |
| mRNA | Messenger RNA |
| RHS | Right hand side |
| RT | Room temperature |
| RT-PCR | Reverse transcriptase |
| SCF | Stem cell factor |
| SDS | Sodium dodecyl sulphate |
| SEM | Standard Error of Mean |
| SSC | Sodium citrate buffer |
| TAE | Tris-acetate-EDTA |
| TNF | Tumour necrosis factor |
| TNFR | Tumour necrosis factor recpetor |
| TPEN | N, N, N', N'-tetrakis(2-pyridylmethyl)ethylendiamine |
| TRAF | TNF receptor associated factor |
| UV | Ultraviolet |

| | |
|---|---|
| Zn | Zinc |
| Zinquin | ethyl(2-methyl-8-p-toluenesulphonamido-6-quinolyloxy |
| $ZnSO_4$ | Zinc sulphate |
| ZnT | Zinc transporter |
| µg | micro gram |
| µM | micro Molar |
| mM | milli Molar |
| nM | nano Molar |

# CHAPTER ONE

# INTRODUCTION

# AND

# LITERATURE REVIEW

## 1.1 Introduction

This thesis addresses a number of hypotheses relating to the role of intracellular pools of labile Zn in the regulation of activation of caspases and NF-κB transcription factor, as well as the role of a major Zn transporter, $ZnT_4$. Two major cell types, mast cells and neuroblastoma cells, were studied. Chapter one begins with a review of the cellular biology of Zn. This includes a historical overview of Zn, its chemical properties, its bioavailability and absorption in the body, its transport within tissues and in plasma focusing on Zn transporters, particularly the transporter $ZnT_4$. This is followed by evidence for two distinct pools of intracellular Zn: the tightly bound and the labile pools, their detection methods, and the mechanisms by which chemical agents can manipulate them in cells. The effects of Zn deficiency in the proper functioning of biological systems are also reviewed and this section ends with an outline of the various biological functions of Zn.

The biochemical signaling pathways leading to apoptosis are described along with the morphological characteristics of apoptosis. The techniques used to detect caspases-3 activation and the action of apoptotic inducers are outlined. This is followed by a section on the relationship between Zn and apoptosis and possible mechanisms for Zn to act as an anti-apoptotic agent. The role of the transcription factor NF-κB as a regulator of apoptosis is also outlined along with its general functions and link with Zn.

Finally a description of both neuronal and mast cells used in the experiments are described with relation to their biological characteristics, Zn and their apoptotic mechanisms.

## 1.2 Zinc (Zn)

### 1.2.1 Historical Background

The therapeutic uses of Zn dates back to 1500 BC where it was recorded in the Eber's papyrus that topical use of Zn in the form of calamine was used to heal eye lesions (Cassel, 1978). Zinc compounds such as Zn oxide and Zn sulfate were used to treat convulsions and urethral discharge in the late 1700s and early 1800s in Western Europe (Barceloux, 1999). Characteristics of Zn deficiency were first shown in various animal models in the early 1940s when tissues of rats fed with a low Zn diet were examined (Follis, 1941). The importance of Zn in growth and development of humans was highlighted when the first cases of Zn deficiency were described in populations with severe growth retardation, hypogonadism, hepatosplenomegaly, rough, dry skin and mental lethargy existing on diets of unleavened bread and beans, low animal protein but rich in phytic acid (Prasad, 1963). These individuals also practiced geophagia, clay eating and were also suffering from anemia (Prasad, 1963). The anemia in these individuals was corrected with iron, while the other abnormalities were reversed by Zn supplementation (Prasad, 1963). Subsequent studies in the past decades have established the biological importance of Zn in organ tissues systems, as a structural component for metalloenzymes and Zn fingers in health and disease states.

### 1.2.2 Chemistry

Zn is a group IIB transition metal reacting readily with organic as well as inorganic compounds (Barceloux, 1999). It performs its biochemical functions as a divalent cation and does so when bound to enzymes and other proteins (Vallee and Falchuk, 1993). Its ability to assume multiple co-ordination geometries makes it extremely versatile to meet the demands of its various ligands (Cotton and Wilkinson, 1988). Under physiological conditions, Zn does not undergo oxidation or reduction and it is this lack of redox activity that makes it a stable ion in a biological medium (Williams, 1987). Therefore Zn is an ideal metal cofactor for redox-stable reactions such as proteolysis and hydration of carbon dioxide (Butler, 1998).

### 1.2.3 Bioavailability And Absorption

Zn is contained from meat, seafood, dairy products, nuts, legumes and whole grains (Solomons, 1988). The recommended daily allowances (USA) for Zn are 5 mg/day for infants, 10 mg/day for children, 15 mg/day for teenagers, adults and pregnant women and 16-19 mg/day for lactating women (Sciences, 1989). The total Zn content in the human body is 2-3 g distributed throughout organs, secretion fluids and body tissues; the bulk of this is contained within cells (Vallee and Falchuk, 1993).

The bioavailability of Zn is dependent on a variety of factors. These include the presence of ligands (phosphates and oxalates), which decrease absorption, as well as other ligands (carboxylic acids, glucose and amino acids such as histidine and methionine), which increase uptake. Some of the latter have been utilized to facilitate

Zn absorption in Zn supplements. The amount of protein in a meal can have an effect on Zn absorption, although each protein affects Zn absorptivity differently. Factors including lactoferrin and whey factor in human milk have been shown to promote Zn absorption (Lonnerdal, 1997). One important dietary factor that negatively influences Zn absorption is phytate, commonly present in staple foods such as cereals, corn and rice (Lonnerdal, 1997). Lowering of phytate levels via the enzymic activity of phytase (commonly found in fermented soy bean meals) can increase Zn bioavailability as it results in the degradation of phytic acid (Hirabayashi, 1998).

There are no Zn stores, though bone and liver may act as reservoirs. In humans, Zn is absorbed mainly in the second portion of the distal duodenum or proximal jejunum, and the amount absorbed is dependent on the type of food and the body's requirement (Lee, 1989). In mice, the ileum is also a site of significant Zn absorption (Sorensen, 1998). Fractional absorption of Zn decreases as the gastrointestinal concentration of Zn is increased while low Zn concentrations in the gut have the opposite effect. Increased fractional absorption of Zn occurs in pregnancy, lactation and infancy, where Zn demands are high (Krebs, 1998).

### 1.2.4 Zn Transporters

It is assumed that transportation of Zn requires energy and is dependent on time, temperature, pH and involving saturable and nonsaturable components (Reyes, 1996). The mechanisms by which Zn is transported across intestinal membranes are not defined. Absorption of Zn appears to be by passive diffusion of either ionic Zn or Zn

complexed to various ligands including histidine, picolinic acid and citric acid (Vallee and Falchuk, 1993) and carrier-mediated processes (Davies, 1980; Hoadley, 1987).

A schema showing some of the known Zn transporters is described in Figure 1.1. A possible candidate for an enterocyte apical membrane transporter of Zn is the divalent cation transporter-1 (DCT-1), recognized as one of the major transporter of iron (Conrad, 1999). DCT-1 may also serve as a transporter of other metals such as copper, though this has yet to be established. Another candidate is hZTL1, a protein of 523 amino acids which when expressed in Xenopus laevis oocytes increased zinc uptake across the plasma membrane. The localization, regulatory properties, and function of hZTL1 indicate a role in regulating the absorption of dietary zinc across the apical enterocyte membrane (Cragg, 2002).

Once across the border Zn is thought to be coupled with either of the two intracellular transporters, metallothionein or cysteine-rich intestinal protein (CRIP). CRIP is a 77 amino acid protein located in the mucosal cytosol, which consists of two cysteine- and/or histidine-rich Zn-finger motifs which bind Zn and may be involved in protein protein interactions (Fernandes, 1997; Khoo, 1997). It is thought that CRIP shuttles Zn from apical to basolateral surfaces. CRIP has been shown to bind to a large proportion of the Zn entering the intestinal cells of rats that have been given a moderate amount of Zn. In instances where Zn intake was excessive, the bulk of intestinal cellular Zn was associated with the other cysteine-rich protein, metallothionein. A study by Davis and colleagues has shown that metallothionein retains Zn in the enterocyte either for local use or to prevent excess Zn absorption during periods of elevated intakes (Davis, 1998).

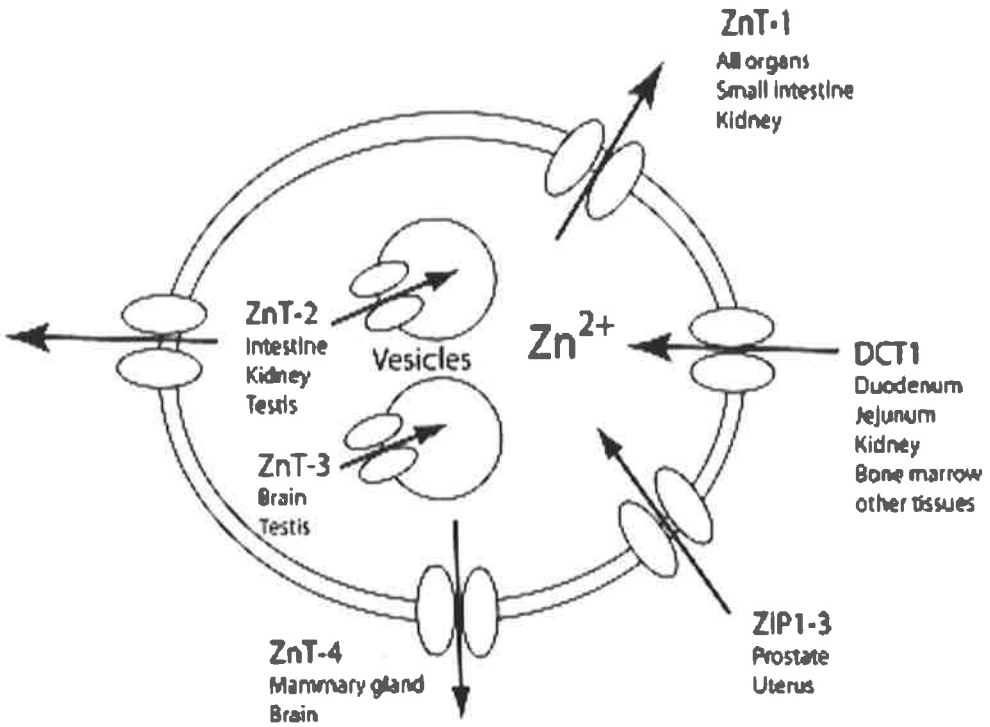


**Figure 1.1: Localization and Roles of Zn Transporters.**

Schema showing the localisation and roles of some of the known Zn transporters. The arrows indicate the direction of movement of Zn. Figure adapted from McMahon and Cousins, 1998.

Metallothioneins are a group of low molecular weight proteins (6-7 kDa), consisting of single-polypeptide chains of 61-62 amino acids residues, which contain 20 cysteine residues. These cysteine residues bind several bivalent cations including Zn, copper, cadmium and mercury (Dreosti, 2001). Metallothioneins are ubiquitous in most organs and are induced by both endogenous and exogenous stimuli including heavy metals and glucocorticoids (Kagi and Schaffer, 1988; Vallee and Auld, 1995).

At the basolateral surface, Zn export is likely to be mediated by the Zn efflux protein ZnT-1 (Figure 1.1), similar to the action of Cu-ATPase in the export of copper (McMahon and Cousins, 1998). ZnT-1 was the first Zn-specific transporter cloned (Palmiter and Findley, 1995). In rats, ZnT-1 is located on the basolateral membrane of villous enterocytes lining the duodenum and jejunum, but is absent in the ileum and colon (McMahon and Cousins, 1998). ZnT-1 is a member of a larger family of Zn transporters, which will be described below.

In plasma, the total Zn content is approximately 100 μg/100 ml, varying with age, gender pregnancy and time of the day (Pilch and Senti, 1984). It is thought that approximately 2/3 of Zn is bound to albumin, and the rest bound to $\alpha_2$globulins (Calesnick and Dinan, 1988). However, due to the high affinity for metals, including both free and bound Zn, the role of albumin in the transportation of Zn remains unclear (Vallee and Falchuk, 1993). The liver has a major role in Zn transfer and distribution to organs such as the pancreas and kidneys (Endre, 1990). Uptake of Zn from plasma by the liver may be an early sign of the body's response to physiological stimuli.

### 1.2.5 Other Zn Transporters

There are two families of Zn transporters, ZnT (Zn transporter) and ZIP (ZRT1, IRT1-like protein) (Gaither and Eide, 2000; Huang and Gitschier, 1997; Lioumi, 1999; Palmiter, 1996; Palmiter and Findley, 1995). The ZnT proteins are members of the cation diffusion facilitator (CDF) family and act to either transport Zn out of cells or to sequester Zn into intracellular compartments (Cole, 1999; Murgia, 1999; Palmiter and Findley, 1995). The ZIP proteins are involved in the uptake of Zn into the cytoplasm (Gaither and Eide, 2001; Lioumi, 1999). The ZnT proteins are thought to have similar protein structures with six transmembrane domains and a histidine-rich cytoplasmic loop between transmembrane domain IV and V (Palmiter and Findley, 1995). In addition to ZnT1, other ZnT transporters include the following: $ZnT_2$ was cloned from experiments in which cells were rescued from Zn toxicity (Palmiter, 1996). It is expressed in the membrane of intracellular vesicles and is involved in sequestration of Zn (Figure 1.1) (Cousins and McMahon, 2000). $ZnT_3$ incorporates Zn into vesicles at neuronal pre-synaptic terminals (Palmiter, 1996). $ZnT_4$, is discussed separately below. $ZnT_5$ is thought to transport Zn into insulin-containing secretory granules of pancreatic β-cells (Kambe, 2002). $ZnT_6$ is a new member of the ZnT family, which may function in transporting the cytoplasmic zinc into the Golgi apparatus as well as the vesicular compartment (Huang, 2002).

### 1.2.6 $ZnT_4$ Transporter

$ZnT_4$ is the fourth member of the ZnT family identified from a cDNA clone called *Dri* 27 obtained from rat intestine (Barila, 1994) and Huang and Gitschier isolated its sequence in 1997 (Huang and Gitschier, 1997) (Figure 1.2). $ZnT_4$ has 6 trans-membrane domains, with N and C termini located on the cytoplasmic side of the membrane. They also have a conserved histidine-rich domain between trans-membrane segments IV and V, which binds Zn (Murgia, 1999). $ZnT_4$ shares the most homology with $ZnT_2$ and $ZnT_3$. Expression of $ZnT_4$ provides Zn resistance to the yeast strain Δzrc1, which has a defect in a vacuolar Zn transporter, indicating a role for $ZnT_4$ in the removal of cytoplasmic Zn into vacuoles (Huang and Gitschier, 1997). Identification of a mutation of $ZnT_4$ gene in the lethal mouse (lm) strain indicated a role for $ZnT_4$ in the transportation of Zn into breast milk. Lethal mouse syndrome is due to a single point mutation resulting in premature death of pups nursed by lm/lm mothers (Piletz and Ganschow, 1978). Administration of Zn to the pups or lm/lm mothers can prevent early death of the pups (Ackland and Mercer, 1992). The level of Zn in the milk of homozygous lm/lm mice is approximately 50% of normal lactating mice (Piletz and Ganschow, 1978).

$ZnT_4$ appears to be expressed ubiquitously with high expression in mammary gland, brain and small intestine of mice suggesting a more general role in Zn metabolism (Huang and Gitschier, 1997). The rat homolog for murine $ZnT_4$ has been localized in the membrane of intracellular vesicles, with the majority found in the basal cytoplasmic region of polarized enterocytes (Murgia, 1999). In the same study, $ZnT_4$ was strongly expressed in brain and testes, followed by the small intestine, medulla,

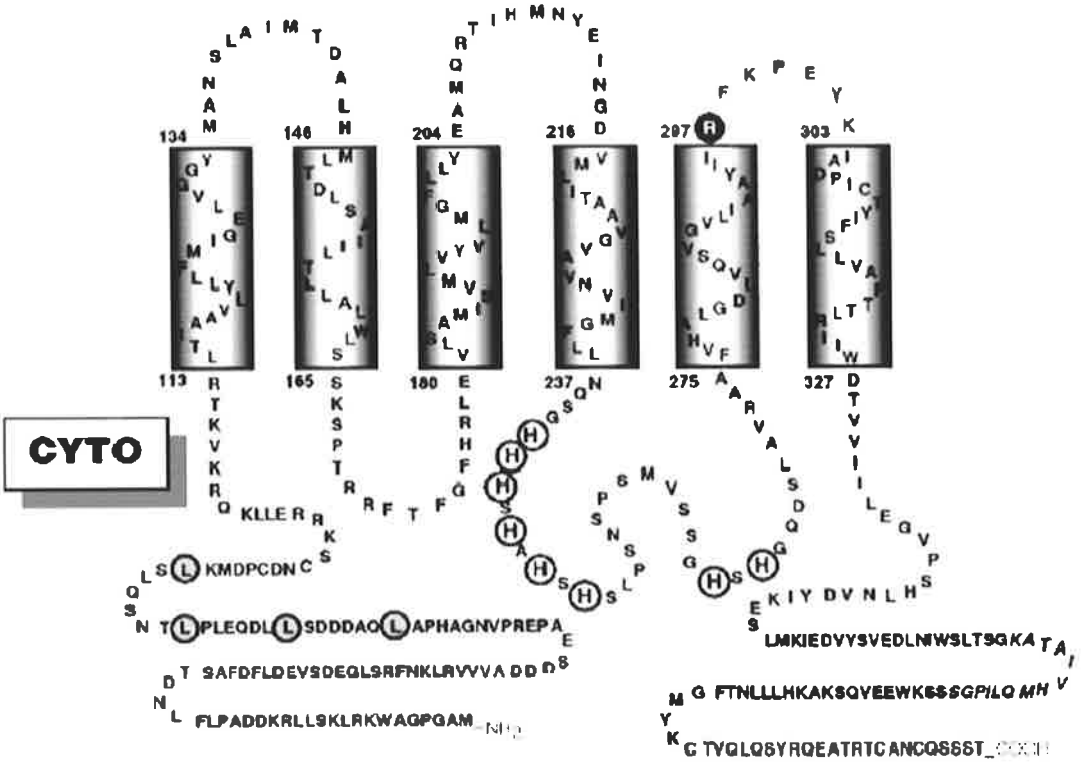


**Figure 1.2: Secondary Structure and Putative Functional Domains of $ZnT_4$.**

Primary sequence of protein is depicted according to insertion topology within membrane bilayer. Positions of consensus sequences for protein-protein interaction (Leu zipper) and metal binding (His region) are circled. Dark circle around the arginine residue at *position 297* marks point mutation that leads to synthesis of a truncated protein in the lethal milk mutant allele. Sequence of 14-amino-acid synthetic peptide used to raise polyclonal antibodies is indicated in italics. CYTO, cytoplasmic side. Figure adapted from Murgia et al 1999.

lung, kidney and the proximal and distal portions of the gastrointestinal tract (Murgia, 1999).

A study by Michalczyk and colleagues demonstrated for the first time that the human orthologue of $ZnT_4$, *h*$ZnT_4$ was constitutively expressed in the human breast and might be involved in the transport of Zn into milk. Using the Zn-specific fluorophore Zinquin, the study also found that h$ZnT_4$ was distributed in a granular pattern in the human breast epithelial cell line PMC42, consistent with a vesicular localization (Michalczyk, 2002). However, in a double-labelling experiment with Zinquin and *h*$ZnT_4$, it was observed that there was no clear overlap between Zinquin and *h*$ZnT_4$ protein, indicating that *h*$ZnT_4$ may not have direct involvement in the transport of Zn into vesicles (Michalczyk, 2002). This study is the first to show $ZnT_4$ localization in human cells. Similarly, another study by Ranaldi and colleagues in MDCK kidney cells have also shown that double fluorescence labelling of both Zinquin and anti-$ZnT_4$ antibody demonstrated distinct staining pattern for Zn and $ZnT_4$ (Ranaldi, 2002). Thus it would be of interest to determine whether $ZnT_4$ is expressed in other human cell types, in particular mast cells, where Zn is rich in the granules.

### 1.2.7 Two Distinct Pools Of Cellular Zn

Zn exists in two distinct intracellular pools. The bulk of cellular Zn exists tightly bound to metalloenzymes, where it serves both catalytic and structural functions. Zn can function catalytically by forming complexes with the substrate that promote the formation of active states; alternatively Zn act structurally by promoting the formation of protein domains within the enzyme structure (Coleman, 1992). The tightly bound

pool of Zn is largely non-exchangeable and is little affected by dietary intake of Zn. The remaining Zn (5-10 per cent in most cells) exists in a more dynamic pool, which is rapidly exchangeable and readily depleted in Zn deficiency (Bettger and O'Dell, 1981; Chesters, 1989). Therefore the rate of Zn turnover in the body is tissue-specific; labile Zn pools (e.g. in liver and bone) turn over rapidly and are very susceptible to alterations in dietary Zn while other non-readily exchangeable pools (e.g. in muscle and brain) turn over more slowly (Zalewski and Forbes, 1993). These exchangeable intracellular pools include vesicular Zn, free cytosolic Zn ions, loosely bound Zn in the membrane to metallothionein or cytosolic proteins and pools of Zn within the nucleus.

### 1.2.8 Detection of Zn

A range of techniques have been used to detect Zn in biological tissues including: atomic absorption and emission spectroscopy, atomic fluorescence, X-ray fluorescence, tracer with Zn stable isotopes and autometallography (Krebs and Hambidge, 2001; Stoltenberg and Danscher, 2000; Vallee and Falchuk, 1993). The Timm's Sulphide Silver method has been used to detect labile Zn at an ultrastructural level (Danscher, 1996)]. This method allows Zn to bind chemically to form Zn sulphide crystals and these nanometer size crystals can be silver amplified in vibratome and cryostat sections by exposure to an autometallographic developer (Danscher, 1996). Areas of interests from these tissue sections are cut and block stained with osmium tetroxide and embedded in Epon and view under high magnifications of an electron microscope.

Labile Zn has best been detected using compounds, which fluoresce in contact with it (fluorophores). The fluorophore TSQ, (6-methoxy-8-p-toluenesulphonamido-quinolone) was initially used as a histochemical stain for Zn in sections of brain, heart, and other tissues (Frederickson, 1987). TSQ forms UV-excitable fluorescent complexes with Zn.

Zalewski and colleagues developed a Zn-specific membrane-permeable fluorophore, Zinquin [ethyl (2-methyl-8-p-toluenesulphonamido-6-quinolyloxy) acetate (Figure 1.3) and used it to detect intracellular labile Zn in a variety of tissues and cell types (Ward, 2000; Zalewski, 1993; Zalewski, 1996; Zalewski, 1994). The incorporation of ester groups into Zinquin gave the fluorophore an anionic form following the cleavage of the esters by intracellular esterases (Zalewski, 1993). This allows the fluorophore to remain within the cells. Zinquin was the first practical Zn-specific fluorophore to study the role of Zn in regulation of cell growth. Using Zinquin, the importance of cellular Zn distribution in apoptosis was assayed in hepatocytes and pancreatic islet $\beta$-cells in which both were rich in Zn (Zalewski, 1994). Zinquin has excitation and emission fluorescence peak at 363 and 485 nm, respectively (Zalewski, 1994). Fluorescence is specific for Zn, except for a weak reaction with Cadmium (Cd II) and Zn-dependent fluorescence is not affected by the mM concentrations of important biological divalent cations of Calcium (Ca II) and Magnesium (Mg II) (Zalewski, 1994). Due to its low affinity for Zn, Zinquin is likely to detect only the less tightly bound Zn in cells, which include free Zn and those loosely bound to proteins and lipids (Zalewski, 1993).

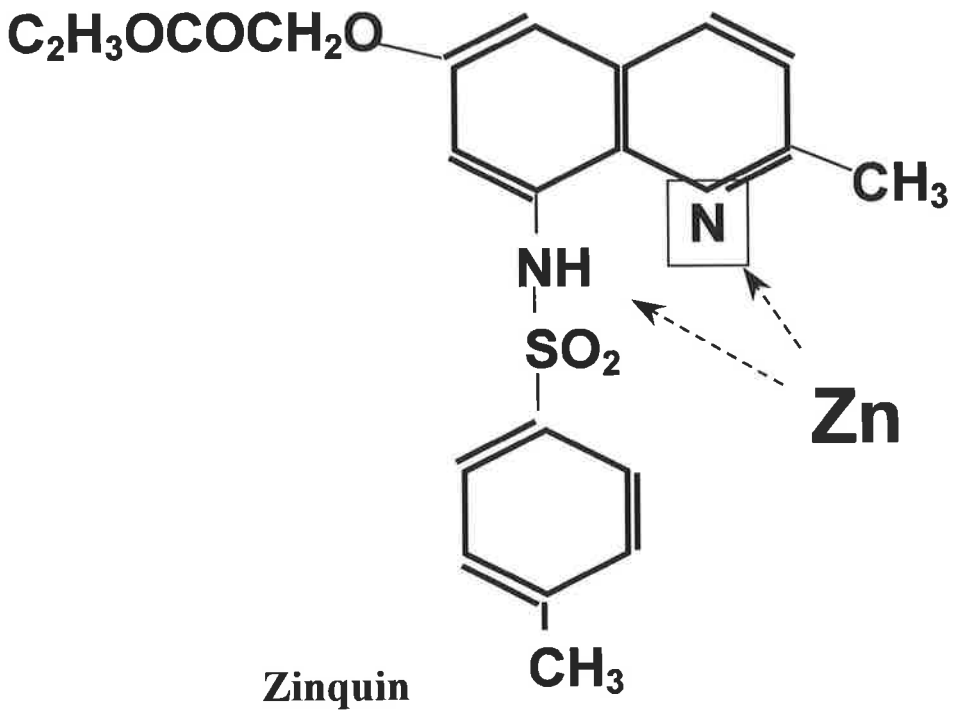


**Figure 1.3: Structure of Zinquin [ethyl (2-methyl-8-p-toluenesulphonamido-6-quinolyloxy) acetate].**

A Zn-specific membrane-permeant fluorophore used to detect intracellular labile Zn. Zn binds to the two nitrogens and the complex is fluorescent under UV light.

Other Zn fluorophores have been developed. These include dansyl-labeled macrocyclic amines (Kimura and Kioke, 1998), Znpyr-1 which has been shown to stain Zn in the golgi and acidic cellular compartments of cells (Walkup, 2000), Newport Green, FluoZin-2 and FuraZin-1 (Dineley, 2002; Thompson, 2002). These and other fluorophores, some more practical and/or specific than others have all provided researchers with the suitable tool to study the role of Zn in various compartments and tissues in biological mechanisms.

Advantages of using fluorophores over more traditional techniques such as atomic absorption spectrometry include the ability to visualize the pools in cells without disrupting them, to detect the more labile pools which is not possible with most of the other techniques and to detect Zn fluxes. The technique of autometallography (Stoltenberg and Danscher, 2000) does allow the detection of subcellular labile pools of Zn in electron microscopy, but this technique was not available in our laboratory. The major disadvantage of fluorophores is that it is still not possible to determine real concentrations of Zn from fluorescent values.

### 1.2.9 Techniques For Manipulating Intracellular Zn Levels

Zn has been depleted from cells *in vitro* by a range of techniques (Cui, 2002; Zalewski, 1993; Zalewski, 1991) including culture in Zn free medium and use of membrane permeable Zn chelators such as 1, 10 phenanthroline and TPEN (N, N, N', N'-tetrakis(2-pyridylmethyl)ethylendiamine) (Figure 1.4). Depletion of intracellular Zn in the experiments of this thesis was induced by TPEN, a selective chelator of transition metals due to the pyridines groups acting as soft electron donators. It is

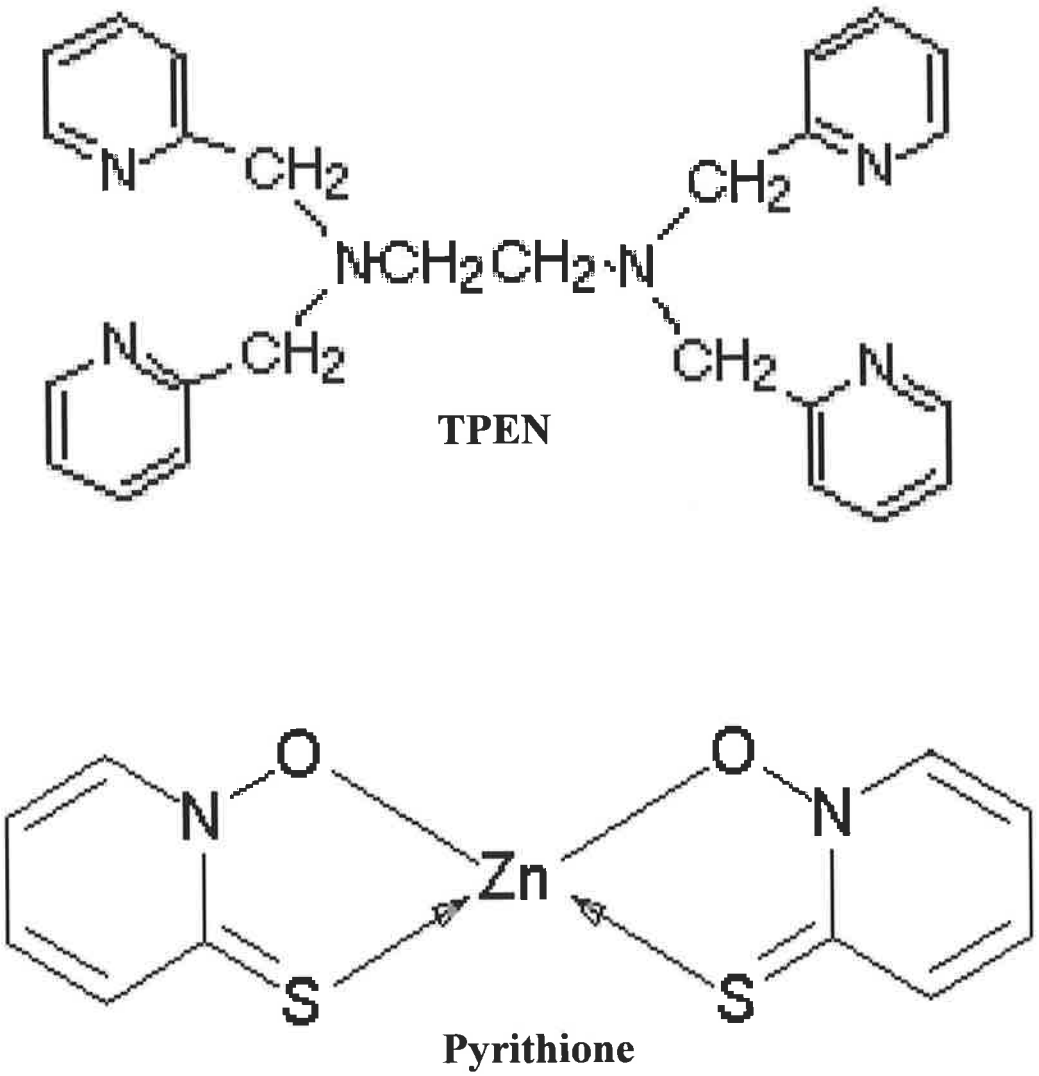


**Figure 1.4: Structure of TPEN [N, N,N',N'-tetrakis-2-pyridylmethyl-ethylenediamine] and Zn Pyrithione.**

TPEN is a Zn chelator used to deplete cellular Zn while pyrithione is a Zn ionophore, which binds Zn, as shown above and transports it across cell membranes.

water-soluble and cell membrane-permeable with a very high affinity for Zn (logKZn = 15.58). It also binds iron (logKFe = 14.61) but has negilible affinity for calcium and magnesium (logKCa = 4.4, logKMg = 1.7) (Arslan, 1985). TPEN was used because it acts more rapidly than culturing in Zn free medium and its action is more specific than that of phenanthroline.

Various methods have been used to increase intracellular Zn including addition of high concentrations of Zn salts to the medium or the use of lower concentrations of Zn salts in the presence of Zn ionophores such as di-iodoquinoline and sodium pyrithione (Takano, 1991; Zalewski, 1993; Zalewski, 1991). In these experiments, supplementation of exogenous Zn into cells used 25 μM $ZnSO_4$ (a typical plasma concentration) and sodium pyrithione (Figure 1.4). Sodium pyrithione forms lipophilic complex with Zn, nickel and cadmium (Jasim and Tjalve, 1986). Pyrithione acts more rapidly than exposing cells to $ZnSO_4$ alone and avoids the use of very high Zn concentrations, which may be toxic to cells.

### 1.2.10 Zn Deficiency

Zn deficiency in man is associated with hypogonadism and growth retardation, loss of taste and poor wound healing (Solomons, 1988). Even in severe Zn deficiency, the total cellular Zn (as measured by atomic absorption spectroscopy) is decreased only slightly or not at all. Therefore, the Zn, which is most susceptible to depletion, resides in the minor, readily exchangeable labile pools (Zalewski and Forbes, 1993).

There are two types of Zn deficiency, primary and secondary. Primary Zn deficiency occurs when there is insufficient intake of Zn due to one of several mechanisms including low Zn diet or malabsorption of Zn (Sandstead, 1991). Secondary Zn deficiency is acquired and can occur when there is excessive loss of Zn from the body such as in the urine in diabetes (Kinlaw, 1983). One of the major pathophysiological abnormalities contributing to secondary Zn deficiency is Zn malabsorption. An important factor is the functional integrity of the intestinal mucosa, which is compromised in a number of disorders including alcoholism and gastrointestinal disorders (Solomons, 1988). Acrodermatitis enteropathica is an inherited disease of abnormal Zn absorption transmitted as an autosomal recessive trait, characterized by ulcerated skin, chronic diarrhoea and muscle wasting (Hambidge, 1977). Oral therapy of Zn sulphate ($ZnSO_4$) produces complete remission, however the exact mechanism of this abnormality is not known (Campo and McDonald, 1976).

Mild Zn deficiency states have been associated with diets low in readily bioavailable Zn, and can occur as a result of conditions such as diarrhoea and pregnancy (Solomons, 1988). The frequency of mild Zn deficiency in developed countries is unclear. In Australia, according to the 1983 National Dietary Survey of Adults; 27% of males and 54% females had Zn intakes of less than 70% the recommended daily intake. Earlier studies in North America have shown that Zn deficiency was present in otherwise healthy infants, toddlers and preschoolers even after the fortification of Zn into infant formulas (Walravens and Hambidge, 1976). One important dietary factor that negatively influences Zn absorption is phytate, commonly present in staple foods such as cereals, corn and rice (Lonnerdal, 1997). Lowering of phytate levels via the enzymic activity of phytase (commonly found in fermented soy bean meals) can

increase Zn bioavailability as it results in the degradation of phytic acid (Hirabayashi, 1998). Thus, Zn status needs to be measured and monitored in subjects at risk of Zn deficiency.

Zn deficiency has profound effects on the immune system. A study by Fraker showed depressed responses to T cell-dependent and independent antigens in Zn-deficient mice (Fraker, 1983). A subsequent study by Fernandes and colleagues reported a progressive decline in the activity of cytotoxic lymphocytes and natural killer cells of Zn-deficient mice (Fernandes, 1979). Lack of Zn also impairs the function of the thymic hormone thymulin, where Zn is an important co-factor. Zn binds 1:1 to thymulin to induce a conformational change, which results in the active form of the hormone (Dardenne, 1982). Host resistance to parasitic infection is markedly impaired in Zn-deficient mice (Vallee and Falchuk, 1993), resulting in a diminished ability to phagocytose pathogens and kill them (Fraker, 1982).

### 1.2.11 Biological Functions

The function of Zn is characterized in three main areas: catalytic, structural and regulatory. Zn is involved at various stages of growth and development, DNA synthesis, behavioural response, reproduction, membrane stability, bone formation and regulation of hormone receptor structures (Barceloux, 1999). It is a constituent of over 300 metalloenzymes in all of the six recognizable classes of enzyme and in Zn-finger proteins (Cousins, 1998). The first Zn metalloenzyme was discovered in 1940 when Zn was found in carbonic anhydrase, establishing its role in catalysis (Keilin and Mann, 1940). Metalloenzymes participate in carbohydrate, protein and lipid

metabolism and nucleic acid synthesis, while Zn-finger proteins participate in signaling and transcription (Cousins, 1998). With respect to its role in regulation of protein function, Zn has the added advantage of being less toxic than other chemicals and it is chemically stable but stereochemically flexible (Vallee, 1995).

The properties of Zn include membrane stabilisation, suppression of inflammation agent, antioxidant and anti-apoptotic effects (Vallee and Falchuk, 1993). Zn has been shown to promote re-epithelialisation in partial-thickness skin wounds in pigs (Agren, 1991).

**Secretion**

Zinc has also been linked to the secretion of various products including insulin, neurotransmitters and nerve growth factor (Frederickson, 1989). In the presence of Zn in the islet cell, insulin monomers assemble to a dimeric form for and storage and secretion as the Zn crystal (Chausmer, 1998). The dimeric insulin further assembles into a hexamer consisting of three dimeric units in the presence of Zn and at neutral pH (Emdin, 1980; Foster, 1993). Decrease of Zn has been shown to affect the ability of islet cells to produce and secrete insulin, particularly in Type 2 diabetes (Chausmer, 1998). Removal of Zn has been suggested to make insulin less immunologically active than insulin complex to Zn, suggesting a possible relationship involving Zn in the degradation and binding of insulin (Arquilla, 1978).

**Anti-Oxidant**

Studies have suggested that Zn is also protective against oxidative stress and the production of free radicals. A decrease in the production of oxidative stress-related agents in various Zn-sufficient *in vitro* models have been observed compared to an increase in these products in Zn-deficient models (Powell, 2000). Thus this supports the hypothesis that Zn deficiency is associated with oxidative damage. In conditions where major tissue damage is caused by production of oxygen reactive species, a decrease in plasma Zn levels is a common observation (Grennan, 1980). Two mechanisms have been proposed to for the action of Zn as an antioxidant. The first involves replacement of redox active metals $Fe^{2+}$ and $Cu^{2+}$ by redox non-reactive $Zn^{2+}$ (Hanada, 1991). The second mechanism relies on the action of Zn metallothioneins as target substrates for oxidant attacks thus providing protection for cells and surrounding tissues (Hanada, 1992).

**Zn and Inflammation**

The inflammatory process involves complex interactions between inflammatory mediators and effector cells such as mast cells and eosinophils (Horwitz and Busse, 1995). Zn is delivered to sites of inflammation and tissue damage via the blood. Plasma Zn level decreases in inflammatory conditions such as rheumatoid arthritis, ulcerative colitis (Sturniolo, 1998), trauma and infections (Whitehouse, 1990). In these conditions, Zn is redistributed to the liver where it binds to newly synthesised metallothioneins (Fukushima, 1988). This redistribution of Zn reduces its levels to other tissues and sites of injury. Various studies have suggested that a reduction in the serum Zn level might promote platelet aggregation (Prasad, 1986) degranulation of

platelets (Huo, 1988), and decrease in phagocytic functions and motility of granulocytes (Briggs, 1982).

A prolonged state of low serum Zn could compromise acute inflammatory Zn-dependent functions such as antioxidant defenses (Wilson, 1987), wound healing and membrane stability (Prasad, 1986) and granulocyte activity (Yatsuyanagi, 1987). A subsequent study performed by the same author reported similar results when Zn levels were decreased in blood and inflamed paws, but increased in liver, kidneys and spleen of adjuvant-induced arthritic rats (Milanino, 1988). These results suggest that the redistribution rate of Zn to the liver is dependent on the severity and duration of the inflammatory reaction.

The importance of Zn was also demonstrated in chronic inflammatory rat models. Studies of arthritis induced-rats have shown that supplementation of Zn markedly reduced or suppressed the development of the condition in these animals (Yatsuyanagi, 1987). $ZnSO_4$ supplementation has been shown to be beneficial in patients with psoriatic arthritis (Frigo, 1989) as well as in cutaneous inflammatory conditions such as papulopustular acne (Norris, 1985). Zn supplementation in rheumatoid arthritis patients has been suggested to be of benefit, especially those who are Zn deficient (Simkin, 1997). Another important function that Zn has been shown to regulate is apoptosis, details of which are described below.

## 1.3 Apoptosis

Apoptosis is a programmed physiological process of cell death consisting of both morphological and biochemical changes. The idea of cell death being a part of development and homeostasis was recognized and described by the early work of Glucksmann in 1952 and Saunders and Fallon in 1966 (Glucksmann, 1951; Saunders and Fallon, 1966). Kerr and colleagues first described the morphological characteristics of this type of cell death in 1972 and coined the term "apoptosis" (Kerr, 1972). However, it was not until the discovery of the *ced*-gene in the nematode *Caenorhabditis elegans*, which was found to encode a protein, required for cell death that a specific and conserved pathway for programmed cell death was seriously studied (Hengartner and Horvitz, 1994; Horvitz, 1994; Schwartzman and Cidlowski, 1993). Many important findings about the apoptotic process have been discovered from this organism model. However, apoptosis in vertebrates is far more complex than that of nematodes and this is likely to be due to the differences in various cell types or developmental stages (Bortner and Cidlowski, 2002). The ability of cells to undergo apoptosis seems to be an innate, normal process essential for the development and homeostasis of multi-cellular organisms (Kerr, 1987; Wyllie, 1997).

### 1.3.1 Cellular Changes in Apoptosis

Characteristic morphological changes of apoptosis include the loss of cell volume, cytoplasmic and organelle shrinkage, plasma membrane blebbing, nuclear chromatin condensation and DNA fragmentation of the nucleus and cytoplasm. Eventually, apoptotic bodies are formed from cell contents and rapidly ingested by phagocytosis

from neighboring cells and resident tissue macrophages (Arends, 1990; Strasser, 2000). The biochemical changes involve input of signalling pathways from the nucleus, plasma membrane and cytoskeleton (Sun, 1999). This highly efficient process eliminates cells quickly and without inflammation or damage (Savill and Fadok, 2000). By contrast, in the other process of cell death termed necrosis, different cellular changes occur. During necrosis cells undergo nuclear and mitochondrial swelling, dissolution of organelles, collapsed plasma membrane and condensation of chromatin around the nucleus (Kanduc, 2002; Martin, 2001). Necrotic cell death is usually accompanied by rapid efflux of cell constituents into extracellular space, which can trigger infiltration of inflammatory cells thereby promoting inflammation (Manjo and Joris, 1995).

### 1.3.2 Apoptosis Signalling Pathways

Currently there are two major interacting pathways of apoptotic signaling (Figure 1.5). The first pathway is initiated by withdrawal of growth factors, by exposure to chemicals or toxins, or viruses. This pathway involves the mitochondria and the Bcl-2 family of proteins, which consist of 16 members in humans with roles in either promoting (pro-apoptotic) or preventing (anti-apoptotic) apoptosis (Chao and Korsmeyer, 1998). The levels of these pro- or anti-apoptotic proteins are suggested to modulate the apoptotic threshold of cells (Yang and Korsmeyer, 1996). Some of these agents induce the phosphorylation of p53 (Evan and Littlewood, 1998). Once activated, p53 either induces growth arrest or apoptosis depending on the cell type and the surrounding environment (Evan and Littlewood, 1998).

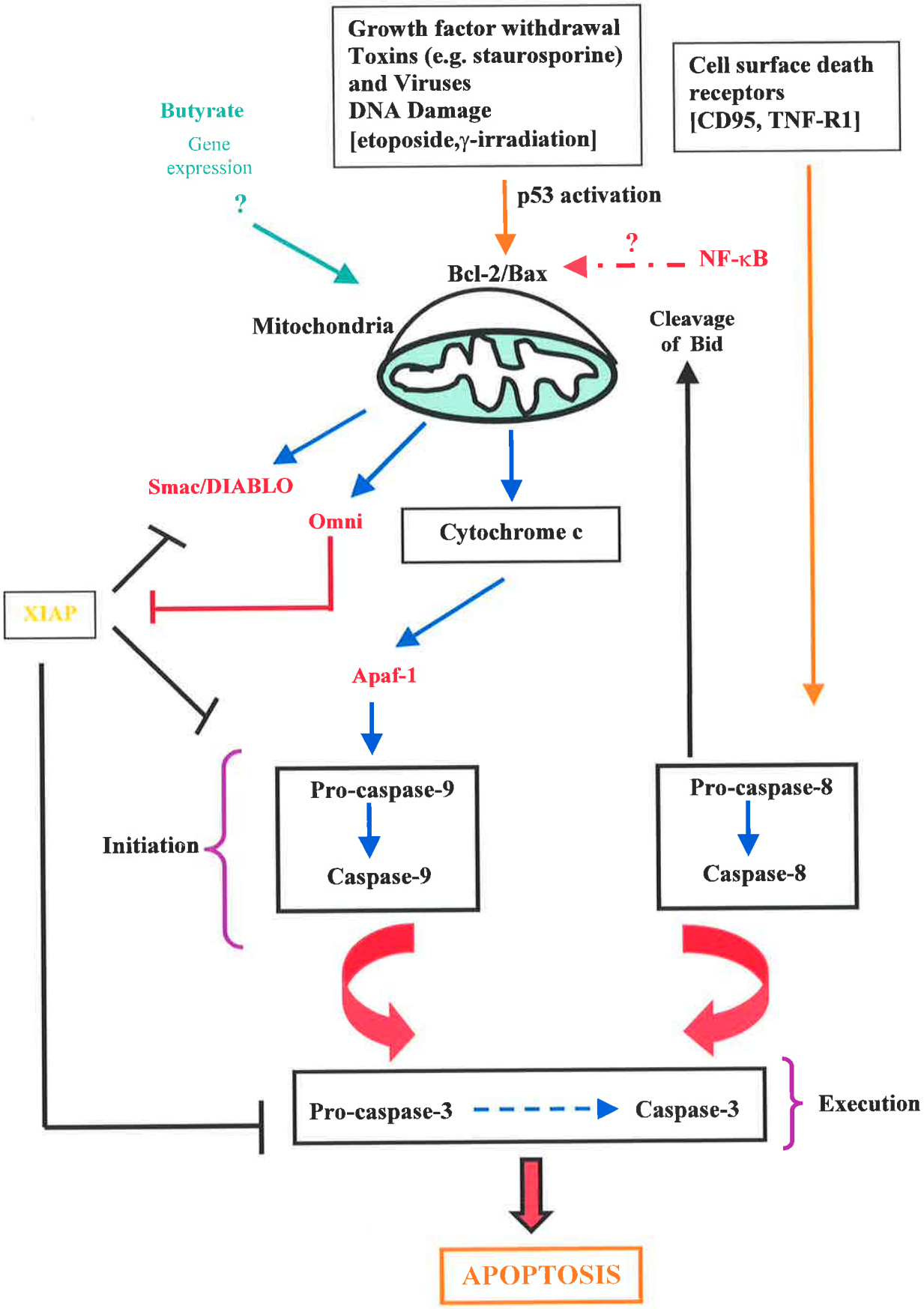


**Figure 1.5: Apoptotic Signaling Pathways**

**Figure 1.5: Apoptotic Signaling Pathways**

There are two major pathways of apoptotic signaling, one mediated by caspase-9 and the other by caspase-8. Pathway one is initiated by toxins, DNA damage and growth factor withdrawal and causes the activation of the initiator caspase-9 resulting in the downstream activation of executioner caspase-3. The other pathway results in the activation of initiator caspase-8 induced by death receptors such as CD95 or TNF-R1, leading to the activation of caspase-3. Both pathways lead to morphological and biochemical changes characteristics of apoptosis. Butyrate, one of the apoptotic inducers used in my experiments acts via a gene expression but it is not clear which of the two pathways it interacts with.

Cell death pathways regulated by mitochondria through the release, of cytochrome *c*, Smac/DIABLO and Omni. Both Smac/DIABLO and Omni induce caspase activation by binding and inhibiting IAPs. Omni is also a serine protease that can induce apoptosis through a caspase-independent pathway Whereas IAPs serve to block apoptosis via caspase inactivation. The two pathways can interact with each other at the level of the mitochondria since caspase-8 can cleave Bid, resulting in release of mitochondroial cytochrome *c*.

The second pathway is via cell surface death receptors in which members belong to the tumour necrosis factor (TNF) receptor gene family. The most extensively studied members are CD95 (Fas/Apo-1)] and TNF-R1 (p55/CD120a) (Smith, 1994). These receptors have similar cysteine-rich extracellular domains and a homologous cytoplasmic sequence called death domain (Baker and Premkumar Reddy, 1998), which interacts with other intracellular signal transduction molecules that contain death domains (Tartaglia, 1993), and interact with downstream molecules that initiate the cascade of caspase activation (Figure 1.5). There is evidence that apoptotic response to CD95 ligation occurs within an hour after reagent addition (Vaughan, 2002). This may explain the fewer steps in activating caspase-3 after death receptor binding compared to the longer caspase-9 activating process due to DNA damage. This pathway results in the activation of pro-caspase-8 leading to the activation of caspase-3.

**Other mechanisms: SMAC and Omni**

In the past three years, an indication that there are other caspase regulatory mechanisms have come from the identification of a mitochondrial-derived factor named SMAC (second mitochondrial-derived activator of caspase) or DIABLO (direct IAP binding protein with low pI) (Du, 2000). SMAC promotes caspase activation in the cytochrome c/Apaf-1/caspase-9 pathway by binding to inhibitor of apoptosis proteins (IAPs) (Du, 2000; Verhagen, 2000). SMAC is normally a mitochondrial protein and is released into the cytosol when cells undergo apoptosis. The IAP family of proteins has the ability to inhibit apoptotic execution (Deveraux and Reed, 1999).

XIAP is the most potent inhibitor in the family with its mechanism via domain specific inhibition of caspase-9 and the activated forms of caspase-3 (Datta, 2000). A second mitochondrial protein involved is Omni, which binds to and inhibits the activity of IAPs following its release into the cytosol from the mitochondria (Martins, 2001; Suzuki, 2001). Therefore these recently discovered proteins and their role in apoptosis might indicate that other caspase regulatory mechanisms are yet to be found.

### 1.3.3 Caspases

The identification of caspases stemmed from the discovery of the gene *ced* 3 which is required for all programmed deaths in *C. elegans*. It was found that several related genes were present in the mammalian genome, termed caspases (Whyte, 1996). The first member in the mammalian caspase family to be identified was the interleukin 1β converting enzyme (ICE), responsible for the cleavage and activation of inflammatory cytokine IL-1β (Yuan, 1993).

The caspase family comprises of at least 14 members expressed in almost all cell types as inactive pro-enzymes (zymogens, also termed as pro-caspase) and divided into three groups. The initiator caspases, the inflammatory caspases and the effector caspases, which cleave target proteins at specific aspartate residues (Alnemri, 1996). The initiator caspases, which include caspases-2, -8, -9, -10 and -12 all act upstream, while inflammatory caspases include caspases-1, -4, -5, -11, and -13, and the executioner caspases (pro-apoptotic), which include caspases-3, -6 and -7 acting downstream, resulting in cleavage of substrates leading to apoptosis (Earnshaw, 1999). Caspase-14 has not yet been placed in any of the above groups, though it has been

suggested to be involved in differentiation of keratinocytes in artificial skin models (Eckhart, 2000).

Caspases share two characteristics: 1) they all have a conserved QACXG pentapeptide, containing the active-site cysteine and 2) they have a preference for cleavage for the peptide bond C-terminal to aspartate residues (Cohen, 1997). Both initiator and inflammatory caspases contain long pro-domains of up to 100 amino acids, while pro-domains in effector caspases are shorter and usually less than 20 amino acids (Earnshaw, 1999). The long pro-domains consist of distinct motifs including death effector domains (DEDs) present in pro-caspase-8 and -10, and caspase recruitment domains (CARDs) in pro-caspase-1, -2, -4 -5 and -9, important for the activation of these enzymes (Hengartner, 2000) (Figure 1.6). In contrast, executioner caspases have short distinct N-terminal peptide spanning often less than 20 amino acids (Earnshaw, 1999).

**Role of Initiator Caspases**

The initiator caspases translate apoptotic signals to proteolytic activity (Denault and Salvesen, 2002). Recruitment and activation of these caspases are via adapter molecules that connect to the death receptors via DED's for caspase-8 and 10 or CARD for the interaction of caspase-9 and Apaf-1 (Fesik, 2000; Wang and Lenardo, 2000). Denault and Salvesen have proposed three possible roles for these caspases which include: sensing and integrating signals towards the execution phase; amplification of the apoptotic process through activation of executioner caspases; and a regulatory step before commitment to cell death (Denault and Salvesen, 2002).

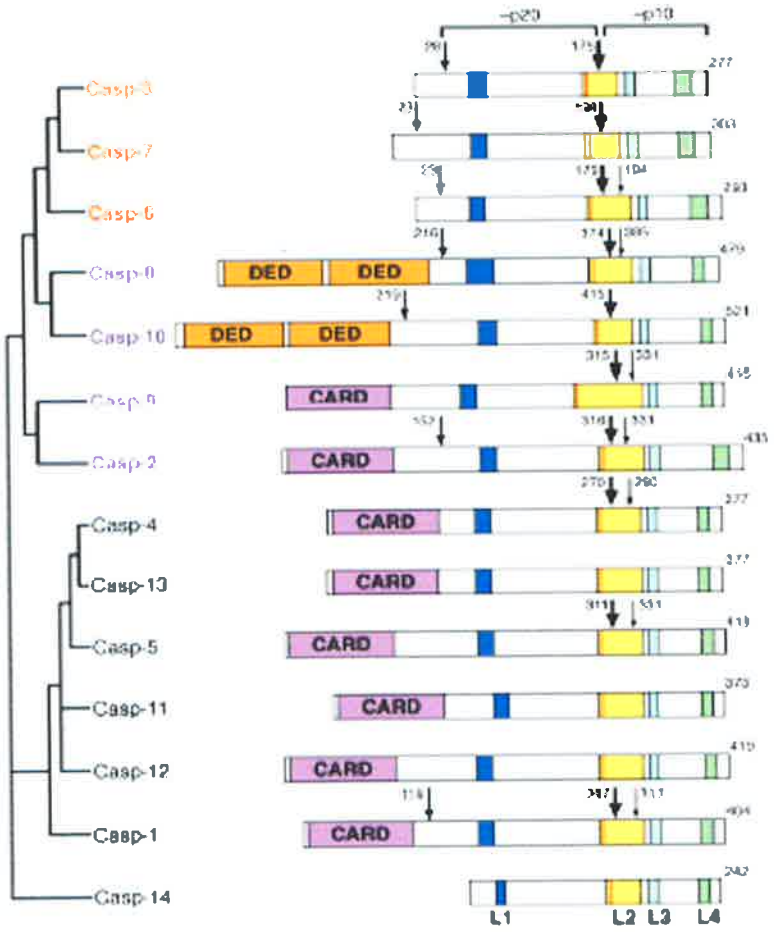


**Figure 1.6: Schematic Diagram of the Mammalian Caspases**

The initiator and effector caspases are labeled in purple and red, respectively. Their phylogenetic relationship (left) appears to correlate with their functionin apoptosis or inflammation. The position of the first activation cleavage (between the large and small subunits) is highlighted with a large arrow while additional sites of cleavage are represented by medium and small arrows. Removal of the prodomain of a caspase is unnecessary for its catalytic activity. The catalytic residue Cys is shown as a red line at the beginning of loop L2. This diagram is scaled according to the lengths of caspases and the location of functional segments. Figure adapted from Shi, 2002.

Caspase-2 was the first mammalian apoptotic caspase to be identified (Kumar, 1994; Wang, 1994). Early studies suggest roles for caspase-2 in removal of excess oocytes in female mice (Bergeron, 1998) and in cell death pathways (Bergeron, 1998; MacFarlane, 1997). Recent studies have suggested that it is closest to the caspase cascade during stress signaling and is needed for mitochondrial permeabilisation and release of cytochrome *c* and Diablo (Lassus, 2002; Robertson, 2002).

Caspase-8 is another initiator caspase. In caspase-8 deficient mice, these die at the embryonic stage and were also found to have abnormal heart muscle development (Varfolomeev, 1998). Hence caspase-8 is important for early embryonic development, production of heart muscle and hematopoietic progenitor cells (Varfolomeev, 1998). Capase-8 has also been shown to be important for death-receptor signaling in fibroblasts of mice (Varfolomeev, 1998). Studies have shown that the death receptor CD95 interacts with caspase-8 via the adaptor molecule FADD leading to the initiation of apoptotic cascade (Boldin, 1996). Its ability to activate all known caspases including caspase-1, -7, -9 and -10 re-affirms the hypothesis that its place is the top of the apoptotic cascade (Boldin, 1996; Muzio, 1996).

The third member of the initiator caspases is caspase-9, an important caspase in the apoptotic cascade where it is activated by Apaf-1 and cytochrome *c*. It has been shown to have a very similar phenotype to caspase-3 (Srinivasula, 1996). In studies using caspase-9 deficient mice, it was found that these animals displayed both a protruded and expanded brain and cranial tissues due to defective apoptosis of neuroepithelium (Hakem, 1998; Kuida, 1998). Apart from causing severe defects in

the nervous system, caspase-9 deficient thymocytes treated with either dexamethasone and γ-radiation were found to be resistant to apoptosis accompanied by retention of the mitochondrial membrane potential (Hakem, 1998).

The last member of this group is caspase-10. Caspase-10 has a similar structure to that of caspase-8 and can interact with death receptors through the same adaptor molecule. FADD/Mort 1 (Vincenz and Dixit, 1997). Caspase-10 is downstream of various death receptors hence mutations of this caspase affects various death receptor pathways, for example the TRAIL-receptor pathways in T-cells of patients suffering from autoimmune lymphoproliferative syndrome (Wang, 1999).

**Role of Pro-Inflammatory Caspases**

Caspase-1 is a cytokine activator and is important for the processing of pro-forms of IL-1β and IL-18 and their maturation. This role was suggested from studies that reported an absence of mature IL-1β (Fantuzzi, 1998) and IL-18 (Li, 1995) in caspases-$1^{-/-}$ mice. These mice have also been shown to not produce cytokines such as IL-1α, IL-16, TNF-α and IFN-γ properly (Kuida, 1995; Li, 1995).

Both caspase-4 and -5 have been poorly studied and their exact functions are not known. However, it has been proposed that both of these caspases are cytokine activators due to their similar amino acid sequences and substrate specificity to caspase-1 (Nicholson and Thornberry, 1997; Thornberry and Lazebnik, 1998). It has also been suggested that these two caspases process cytokines brought on by inflammatory stimuli either differently from caspase-1 or in concert with caspase-1 to

produce an inflammatory response (Denault and Salvesen, 2002). Caspase-4 has also been implicated in FAS-mediated apoptosis (Kamada, 1997). In addition, over expression of both caspase-4 and -5 results in apoptosis of fibroblasts when their pro-domains were truncated (Munday, 1995).

Similar to caspase-1, caspase-11 is required for the maturation of cytokines (Wang, 1998). It has been shown to be an important mediator of septic shock response and is up regulated by lipopolysaccharide (Wang, 1996).

**Role of Pro-Apoptotic/Executioner Caspases**

Caspase-3 is considered as one of the main executioner enzyme with a N-terminal pro-domain, central large domain and a small domain at the C-terminal. Activation of caspase-3 results in the removal of the pro-domain and the separation of the large and small domain. The large and small domains then reassemble to become the active form of caspase-3. In the execution phase of apoptosis, caspase-3 is involved in the cleavage of a large number of substrates including PARP, enzymes that function in mRNA processing and DNA fragmentation (Bossy, 1998) and cellular substrates such as actin and lamin (Enari, 1998). Studies on the central nervous system have shown a significant reduction in apoptosis of neuroepithelial cells in caspase-3 deficient mice (Kuida, 1996). Caspase-3 has been shown to be involved in the late stage of apoptosis from observations that morphological changes associated with apoptosis were absent or delayed when hepatocytes and thymocytes were exposed to Fas (Zheng, 1998).

The other members in this group are caspases-6 and -7. The precise role of caspase-6 in the downstream pathway of apoptosis is still debatable. Conflicting results have suggested that pro-caspase-6 activation results in caspase-3 activation and vice versa (Srinivasula, 1996). Caspase-7 has been shown to share similar functions and substrate specificities with caspase-3 and it has been suggested that cleavage of PARP occurs via the combined effort of these two caspases (Fernandes-Alnemri, 1995).

**Granzyme B**

Granzyme B belongs to a family of serine proteases. The Granzyme B perforin pathway is an important part of granule exocytosis and the main cell death pathway involving cytotoxic T-cells and natural killer cells (Greenberg, 1996). It is the only protease that has similar substrate specificity with caspases. Its action is similar to that of an initiator caspase to induce target cell apoptosis (Barry and Bleackley, 2002; Trapani, 2001). Granzyme B has the ability to directly activate almost all the mammalian caspases and other apoptosis-related proteins and substrates (Browne, 2000; Li, 1997; Thomas, 2000).

**Distribution Of Pro-Caspases**

Pro-caspases are found in various intracellular compartments, including mitochondria, endoplasmic reticulum, Golgi apparatus, cytosol and nucleus (Porter, 1999; Susin, 1999; Zhivotovsky, 1999). Porter further showed pro-caspase-3 was translocated from cytosol to mitochondria early in apoptosis, similar to pro-caspase-2 and -9 (Porter, 1999). They are normally present as zymogens (pro-caspases) in the cytoplasm of vertebrate and other organisms. Samali and colleagues have shown that pro-caspase-3

is localized to cytosol and mitochondria of various rat tissues (brain, heart, kidney, liver, spleen and thymus). The ratio of cytosolic to mitochondrial pools of pro-caspase-3 varied between different tissues with higher amount of mitochondrial pro-caspase-3 in thymus and spleen. It was suggested that mitochondrial pro-caspase-3 is involved in mitochondrial apoptosis (Samali, 1998). Pro-caspase-3 has also been shown to translocate from cytosol to nuclei in some cells undergoing apoptosis, for example apoptotic neuroblastoma (Nakagawara, 1997). Nuclei caspases may be involved in nuclear related events such as activation of the endonuclease responsible for DNA fragmentation (Enari, 1998).

### 1.3.4 Activation Of Caspases

The pro-caspases contain four domains; an N-terminal pro-domain, a large subunit (17-21 kDa), a small subunit (10-13 kDa) and a shorter region between the large and small subunits (Earnshaw, 1999). Several intracellular pathways can activate caspases; one pathway is dependent on ligation of the death receptor and another (is dependent on the release of apoptogenic factors from mitochondria and formation of the apoptosome (Hengartner, 2000) (Figure 1.7).

The extrinsic pathway starts with ligation of death receptors such as Fas/CD95 resulting the recruitment of pro-caspase-8 to the DISC and its activation via interaction with DEDs. Active caspase-8 cleaves and activates caspase-3 (Hengartner, 2000). This also results in activation of pro-caspases-10 and -2.

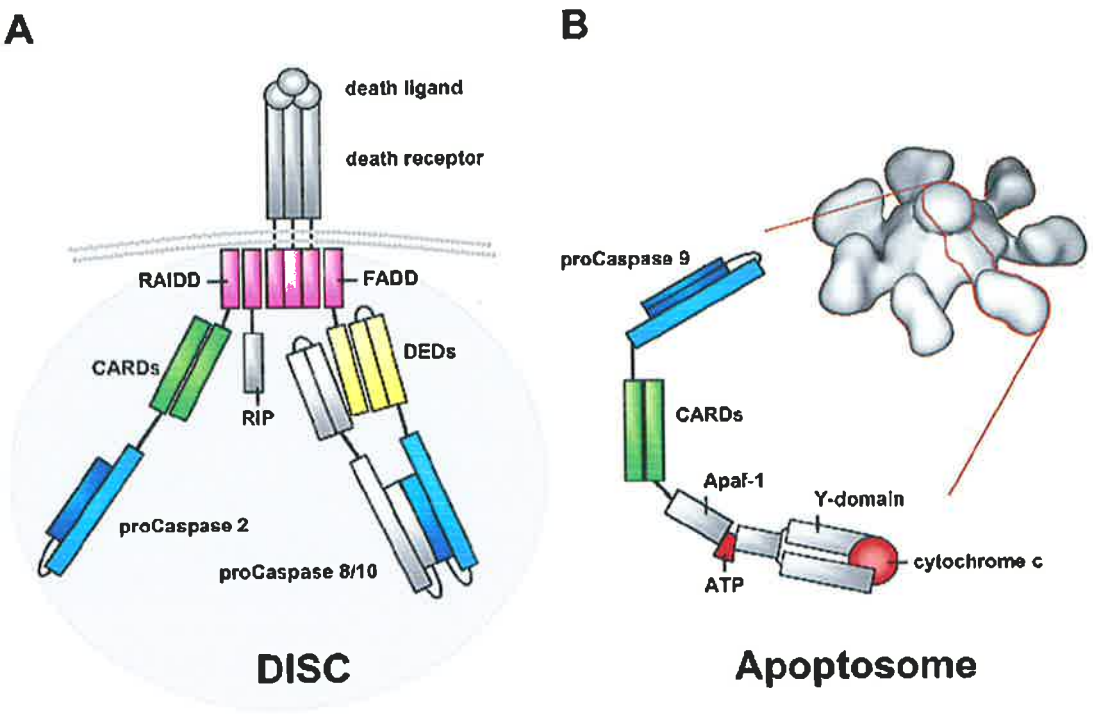


**Figure 1.7: Activation of Caspases.**

Two major pathways of caspase activation are shown.

**A**: The extrinsic pathway starts with ligation of death receptors such as Fas/CD95. This results in activation of pro-caspase-8, pro-caspases-10 and 2 which in turns activate executioner caspases.

**B**: The intrinsic pathway also results in caspase activation but dominantly of pro-caspase-. The mechanism involves the formation of the apoptosome. Release of cytochrome *c* by the mitochondria is the initial step of this pathway. Apaf 1 is activated in the presence of ATP and oligomerizes forming the apoptosome. This structure binds several molecule of pro-caspase 9 via CARD/CARD interactions, thereby significantly increasing the local pro-caspase -9 concentration. Active caspase-9 in turn activates pro-caspase-3. Figure adapted from [Denault, 2002].

The other pathway involve caspases acting downstream of mitochondrial release of cytochrome *c* and other inter-membrane proteins, including apoptosis inducing factor, heat shock proteins, adenylate kinase-2 and other pro-caspases (Kohler, 1999; Mancini, 1998; Samali, 1999; Susin, 1999). Entering the cytosol, cytochrome *c* binds to Apaf-1, which oligomerizes in the present of dATP/ATP and binds pro-caspase-9 to form the apoptosome complex (Li, 1997; Zou, 1999). This leads to activation of pro-caspase-9, which cleaves downstream effector caspases (Figure 1.5).

In addition the two pathways can interact with each other since caspase-8 also induces the release of cytochrome *c* and formation of apoptosome by cleavage of the cytosolic protein Bid (Gross, 1999).

### 1.3.5 Methods For Analysis Of Caspase Activation

There are several ways to detect caspase activation. Commonly used techniques include 1) immunoblotting to detect both proteolytic processing of the pro-caspaes, 2) immunoblotting to detect cleavage of caspase substrates, 3) affinity labelling of activated caspases and 4) cleavage of synthetic substrates. The experiments in this thesis largely employed synthetic fluorogenic substrates. The method is described in detail in chapter two. Briefly, cleavage of the fluorogenic substrate z-asp-glu-val-asp-7-amino-4-methyl-coumarin (z-DEVD-AFC) by caspase-3 results release of the AFC group, which is now fluorescent. This increase in fluorescence is measured in a fluorescence spectrophotometer. Different caspases have slightly different substrate specificities allowing different fluorogenic substrates to be used to measure the

different caspases. However, there is some overlap between caspase specificities. In particular, both caspases-3 and -7 can cleave DEVD-AFC (Fattman, 2001).

### 1.3.6 Inducers Of Apoptosis: Butyrate, Staurosporine

The two main inducers of apoptosis used in the experiments in this thesis were butyrate and staurosporine.

Butyrate is a 4-carbon fatty acid which is thought to act by inhibition of histone deacetylase and hyperacetylation of histones resulting in unpacking of the chromatin and new gene expression that may include pro-apoptotic genes (Hassig, 1997; Medina, 1997) (Figure 1.8). Butyrate inhibits histone deacetylase (Candido, 1978), the enzyme responsible for removing acetyl groups; once inhibited, hyperacetylation of the histones occurs, which loosens the local chromatin structure and increases the accessibility of transcriptional regulatory proteins to specific DNA sequences (Lee, 1993). In this way, butyrate influences a number of genes (Boffa, 1994) either turning a repressed gene on or inactivating a gene engaged in transcription. Therefore, it is possible that some death genes may be activated and apoptosis could be triggered in butyrate-treated cells. Butyrate synergises with staurosporine in inducing apoptosis of Jurkat and colon cancer cell lines (Medina, 1997).

Butyrate has been shown to induce several colon cancer cell lines to undergo apoptosis at concentrations of 1-5 mM, well within the physiological range (Hague, 1993). This effect was also confirmed in the human myeloid HL-60 cell line (Calabresse, 1993) and in the Burkitt's lymphoma BL-30 cell line (Filippovich,

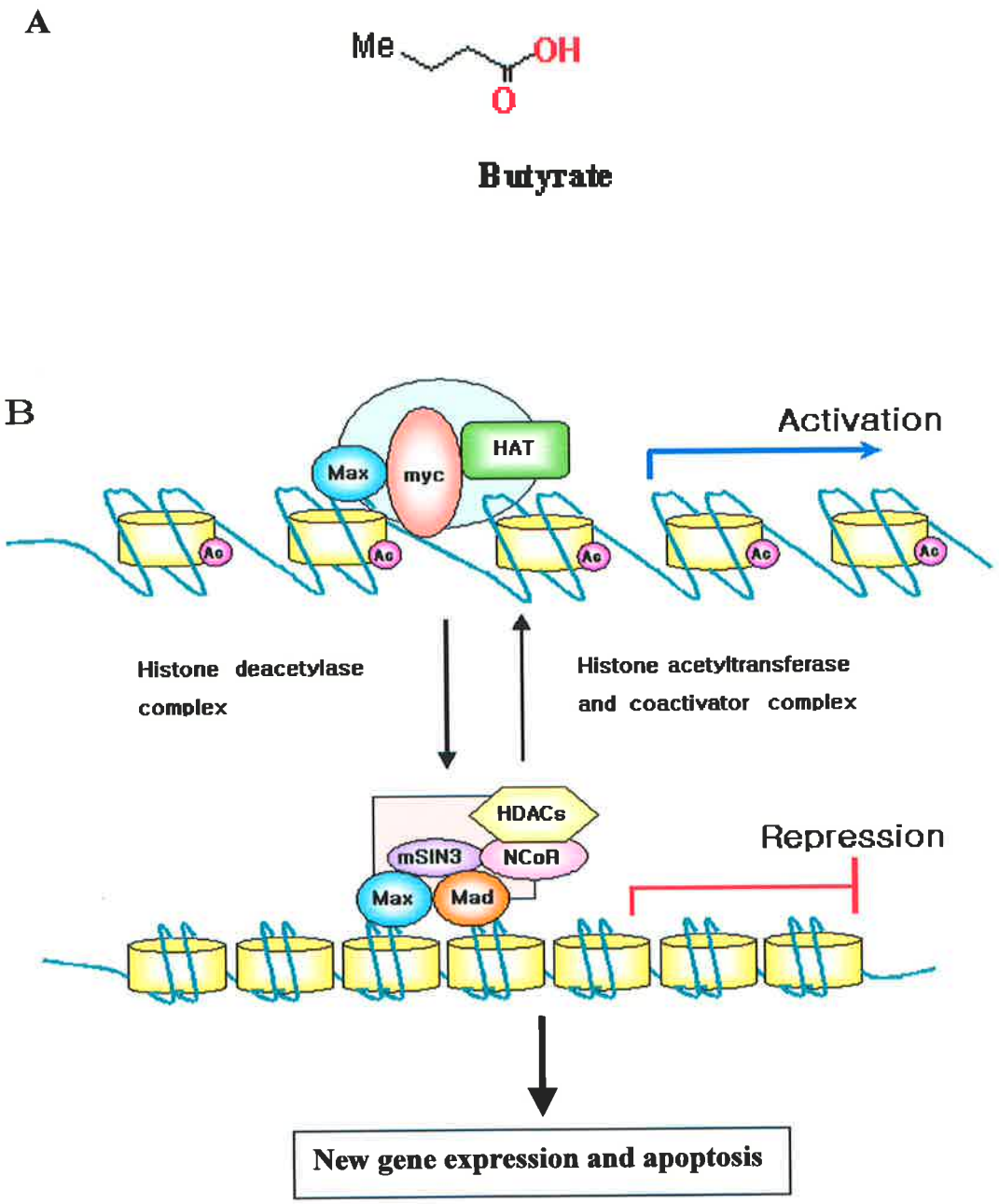


**Figure 1.8: Mechanisms of Action of Butyrate**

Butyrate inhibits histone deacetylase resulting in hyper-acetylation of histones, relaxation of chromatin packing around the nucleosome and enhanced access of RNA polymerase and other enzymes to the promoter regions of genes. This leads to an up-regulation of gene expression. Included amongst the new genes are pro-apoptotic genes. Figure adapted from:

http://dasan.sejong.ac.kr/~bioprobe/Histone%20deacetylase.htm.

1994). Little is known about the molecular mechanism of butyrate-induced apoptosis though butyrate-induced apoptosis involves activation of caspase-3 (and/or related caspases) (Medina, 1997). In MCF-7 cells, the butyrate-induced apoptosis was closely associated with the down-regulation of expression of Bcl-2 mRNA and Bcl-2 protein. In colorectal carcinoma, butyrate-induced apoptosis of DiFi cells was accompanied by inhibition of expression of Bcl-2 and this cellular effect of butyrate was inhibited by Bcl-2 over expression (Mandal, 1997).

Staurosporine, an indolo[2,3-alpha] carbazole (Figure 1.9) was discovered in the extracts of the bacterium *Streptomyces* sp. It was found to be a potent inhibitor of protein kinase C, with an IC50 of around $10^{-9}$ M. Although staurosporine does modulate gene expression via effects on PKC, it is capable of inducing apoptosis in cytoplasts (lacking in nuclei) indicating that its apoptotic effects are not mediated by alteration in gene expression (Raff, 1992). Staurosporine induces apoptosis by inhibiting protein kinases and causing mitochondrial changes such as cytochrome *c* release that lead to apoptosis (Kluck, 1997).

### 1.3.7 Zn and Apoptosis

#### Early Studies

The strongest evidence suggesting the suppression of apoptosis by Zn have come from Zn-depleted animal studies. The first study was that of Elmes who reported significantly increased frequencies of apoptotic cells in the small intestinal crypts of zinc-deficient rats (Elmes, 1977; Elmes and Jones, 1980). It was proposed that this

**A**

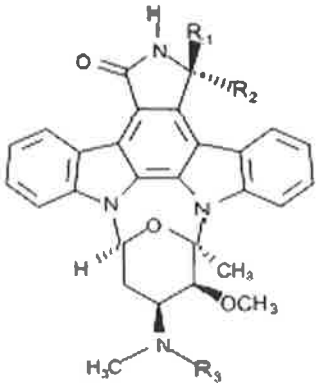

R1, R2, R3 = H: staurosporine;

**B**

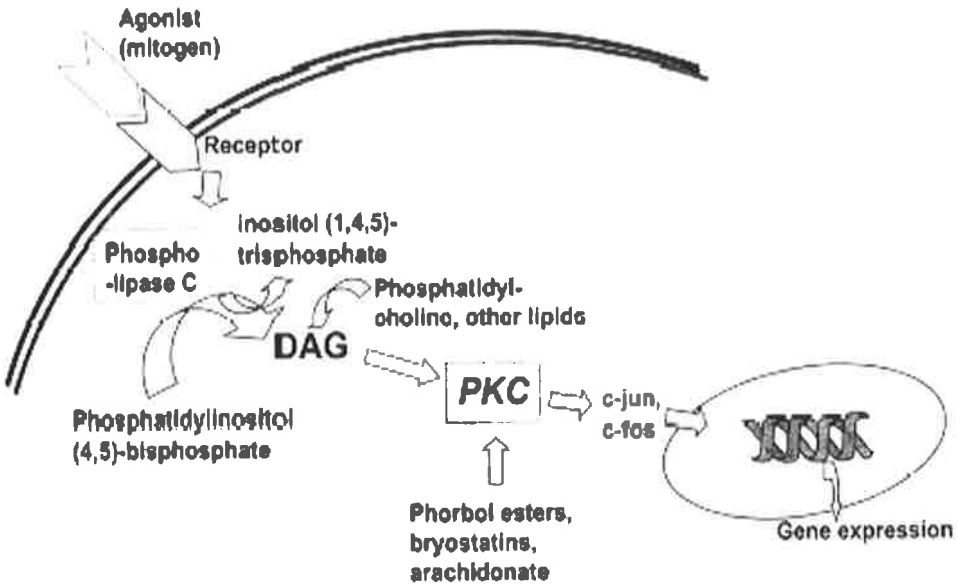


**Figure 1.9: Staurosporine and Mechanism of Action.**

A: Structure of staurosporine as indolo[2,3-alpha] carbazole.

B: Staurosporine interacts with PKC signaling pathway in cells affecting a number of cellular processes including gene expression. Figures adapted from [Gescher, 2000].

apoptosis was triggered by a failure of DNA synthesis in these cells (Elmes and Jones, 1980). Subsequent studies by the same author and by others showed that the frequency of apoptotic cells was also markedly increased in various tissues of adult animals as well as in the neuroepithelium of foetal rats borne by Zn-deficient dams (Record, 1985).

The following series of experiments investigated the effect of *in vitro* Zn depletion on apoptosis of cultured cells. Experiments in cells cultured in Zn-depleted medium or treatment with chelators such as TPEN showed that Zn depletion resulted in apoptosis (Martin, 1991; Zalewski, 1993). It appears that the more exchangeable or labile pools of Zn influence cell susceptibility to apoptosis and these pools are sensitive to depletion and supplementation (Zalewski, 1993).

Conversely, increasing intracellular Zn by supplementation protects various types of cells (eg anterior and stromal keratinocytes in rabbits (Kuo, 1997) and hippocampal neurons in gerbils (Matsushita, 1996) from apoptotic death *in vivo*, while supplementation *in vitro* prevents apoptotic DNA fragmentation. In some cases Zn supplementation prevents cell death in diverse types of cell treated with various apoptosis-inducers (Zalewski and Forbes, 1993).

**Molecular Targets of Zn in Apoptosis**

Earlier studies on Zn and apoptosis suggested that Zn prevents DNA fragmentation by inhibiting the $Ca^{2+}$-$Mg^{2+}$-dependent endonuclease in various cell lines (Cohen and Duke, 1984). However, recent studies have demonstrated that apoptosis can still occur

without DNA fragmentation and Zn was still inhibitory towards the process. This suggests that Zn may act at an earlier stage of apoptosis than DNA fragmentation. Lazebnik and colleagues described a cell-free model of apoptosis where cytosols from cells primed for apoptosis were added to nuclei resulting in nuclear condensation and DNA fragmentation (Lazebnik, 1993). Interestingly the amount of Zn required to inhibit apoptotic changes in the nuclei were lower than that needed to prevent DNA fragmentation.

A study by Perry and colleagues identified caspase-3 as a target of Zn inhibition of apoptosis. The study reported that pre-treatment of intact Molt4 leukemic cells with Zn at micro molar concentration (100 μM) resulted in the inhibition of the proteolysis of the death substrate poly (ADP-ribose) polymerase (PARP) (Perry, 1997). The same study also investigated the effects of Zn in a cell free model similar to that of Lazebnik's. Zn was found to inhibit PARP proteolysis from soluble extracts of etoposide-treated cells incubated with bovine PARP as a substrate (Perry, 1997). A study by Kolenko and colleagues has shown that TPEN induces the translocation of cytochrome c from mitochondrial intramembranous into the cytosol in lymphocytes (Kolenko, 2001). Another mechanism of action of Zn in regulating caspases has been proposed. According to this model, Zn bound to caspase-3 exerts an inhibitory effect on this enzyme and removal of Zn by chelators including thionein activates it (Maret, 1999).

Another recent study has implicated Zn in the regulation of the anti-apoptotic Bcl-2-like and pro-apoptotic Bax-like mitochondrial membrane proteins (Fukamachi, 1998). Fukamachi and colleagues reported a significant increase in the ratio of Bcl-2/Bax in

Zn-supplemented U937 cells, this ratio is thought to determine the susceptibility of damaged cells to apoptotic death, for instance high ratios increasing cellular resistance to apoptosis (Korsmeyer, 1993). Other potential targets for Zn are the microtubular cytoskeleton, which is stabilized by Zn and disrupted in apoptosis (Zalewski and Forbes, 1993) and the cytoplasmic glucocorticoid receptor in thymocytes (Fraker and Telford, 1997). At least in neurons, Zn may also influence events at the level of gene expression since Zn deprivation-induced apoptosis was suppressed by cycloheximide (Anh, 1998).

**Implications For Diseases**

The relationship between Zn deficiency induced apoptosis and the pathogenesis of diseases is not fully understood. One of the main interests is whether fluxes of tissue and organ Zn concentrations during physiopathological events influence the susceptibility of cells to undergo caspase activation and apoptosis. Down syndrome, a disease associated with Zn deficiency; peripheral leukocytes of these patients were reported to have increased incidence of features characteristic of early stage apoptosis and this was abolished following long-term oral Zn supplementation (Antonucci, 1997). Decreased uptake and utilization of Zn by aged cells (Prasad, 1993) could contribute to the increased susceptibility to apoptosis of senescent cells, as occurs in patients with Alzheimer's disease. Mori and colleagues (Mori, 1996) have proposed a role for increased apoptosis in the formation of vesicular skin lesions in patients with acquired zinc deficiency, although not in the formation of hyperkeratotic skin lesions.

There are still a number of issues that requires clarification. Firstly, the relationship between levels of intracellular Zn and regulation of apoptosis has not been defined both in disease states and in normal tissues. There is also little known about the roles of distinct cytoplasmic pools of Zn in regulation of apoptosis such as, Zn within secretory granules. In this thesis one of the issues addressed is the relationship between granular Zn and regulation of caspases.

### 1.4 Nuclear factor kappa-B (NF-κB)

Nuclear factor-kappa B transcription factor (NF-κB) is an important regulator of apoptosis in inflammatory cells, and evidence has been presented that Zn may regulate NF-κB (see below).

NF-κB was first discovered as a factor regulating the κ-light chain in B-lymphocytes of mice (Siebenlist, 1994). NF-κB is involved in key cellular processes and failure in their regulation may lead to inflammatory disorders and cancer. The expression of mediators was been found to be dependent on NF-κB (Grossmann, 1999). NF-κB is present in most cell types and play an important role in immune and inflammatory response (Barceloux, 1999). NF-κB is composed of two subunits from the REL family of protein (Ghosh and Baltimore, 1990). The Rel family of proteins comprised of ubiquitous transcription factors with a common structural motif for DNA binding and dimerisation (Baldwin, 1996).

The most common form of NF-κB is a heterodimer consisting of two subunits, a 65 kD polypeptide (p65 or Rel A), and a 50 kD polypeptide (p50), but other Rel proteins

are also involved such as Rel-B, v-Rel, p52/NF-κB. These different forms are likely to have different regulatory effects (Barnes and Adcock, 1997). In its inactive form NF-κB is localized in the cytoplasm bound to an inhibitory protein, IκB-α. The inhibitory protein exists in various forms IκB-α, IκB-β, IκB-γ, IκB-δ and IκB-ε (Baldwin, 1996). IκB-α is activated by specific IκB kinases (Thanos and Maniatis, 1995).

### 1.4.1 Activation Of NF-κB

TNF-α and IL-1β are the two most important activators of NF-κB. Expression of TNF-α and IL-1β are increased after the activation of NF-κB, hence indicating a positive feedback mechanism in place (Barnes and Adcock, 1997). Both mechanisms involve members of the TNF receptor associated factor (TRAF), and both converge at the level of the protein kinase NIK (Malinin, 1997). Upon trimerisation of the TNF receptor, the following components are recruited: a) TNF-R associated death domain protein TRADD, b) a receptor interacting protein (RIP), c) a death domain containing serine/threonine kinase, d) TRAF2 and e) IκB kinase (Rahman and MacNee, 1998).

Activation of NF-κB by stimuli is thought to involve several signal transduction pathways (Figure 1.10). Upon activation of NF-κB, IκB undergoes phosphorylation, follow by rapid ubiquitination and proteolysis by non-specific proteases (the proteosome) (Thanos and Maniatis, 1995). Studies have shown a direct and an indirect involvement of a number of kinases in the phosphorylation step. One is the NF-κB inducing kinase (NIK), which has serine/threonine kinase activity (Malinin, 1997). Recent studies have characterized another serine/threonine kinase, CHUK,

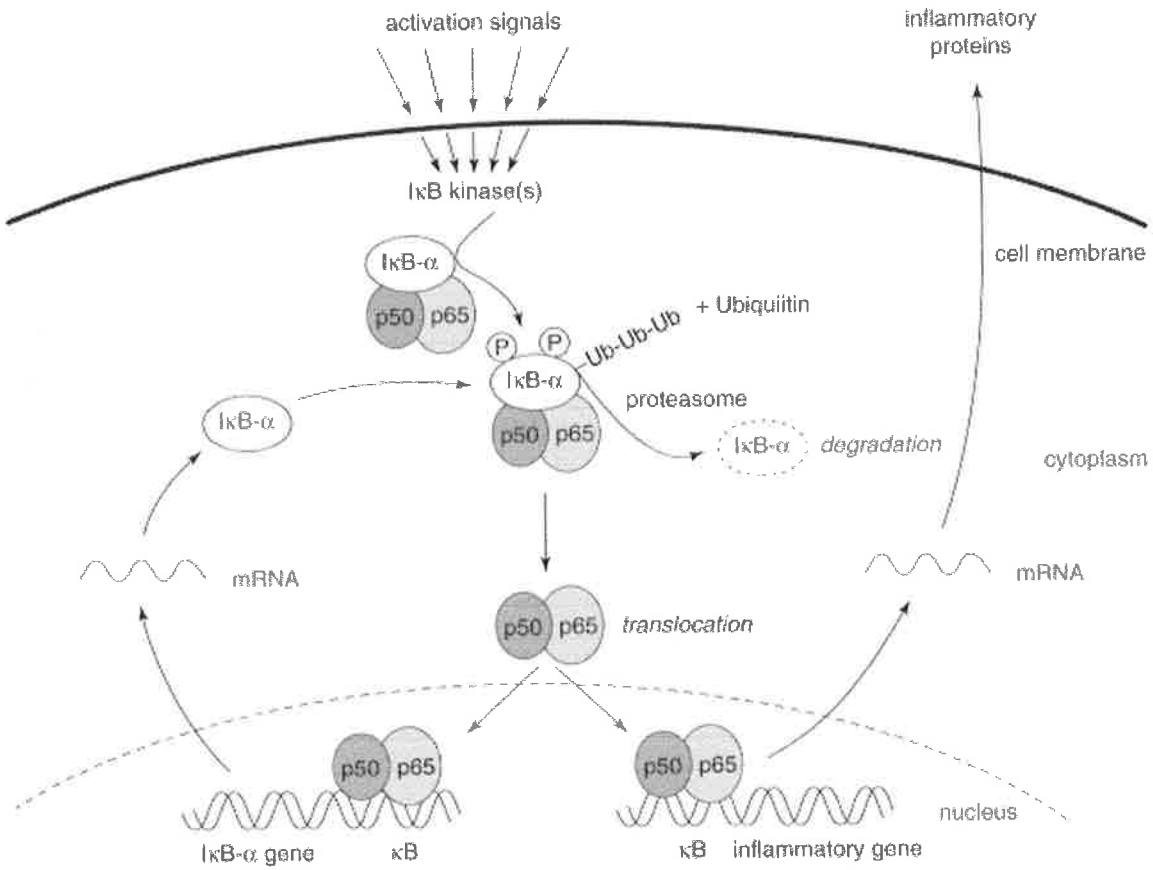


**Figure 1.10: Activation of NF-κB**

Activation of NF-κB involves the following steps. The first step is activation of IκB kinases by stimuli such as TNF-α. This is followed by phosphorylation of the inhibitory protein IκB-α leading to ubiquitination and proteolytic degradation of IκB-α by the proteasome. NF-κB then translocates to the nucleus, where it binds to κB sites in the promoter regions of inflammatory genes. The activation of NF-κB is terminated by an increase in the synthesis of IκB-α following activation of the IκB-α gene. Figure adapted from Barnes and Adcock 1997.

which is downstream of NIK. Similar to CHUK, the IκB kinase (IKK) was also discovered and has been shown to phosphorylate serines 32 aned 36 on IκB-α molecule, leading to activation of NF-κB (Di Donato, 1997). Due to the large number of different signals involved in the activation NF-κB, it is likely that multiple signalling pathways are involved and are integrated to act on a multiprotein IκB-α kinase complex (Rahman and MacNee, 1998).

Following phosphorylation, IκB-α undergoes ubiquitination. This involves covalent attachment of ubiquitin to IκB-α resulting in its recognition by the proteosome. This complex of proteases then degrades IκB-α leading to the release of NF-κB p50 and p65 subunits. This unmasks the nuclear translocation signal leading to the rapid translocation of NF-κB into the nucleus. In the nucleus, NF-κB binds to consensus (κB) sites in promoter sequence of inducible genes (GGGATTTCC), resulting in an increase in transcription and protein synthesis. The p50 subunit within the p50/p65 heterodimer facilitates DNA binding, whereas the p65 subunit is needed for efficient transactivation (Glass, 1997). NF-κB can induce its own termination by binding to the κB site of IκB-α, resulting in the synthesis of IκB-α inhibitory protein (Thompson, 1995). Not every form of the inhibitory protein has a κB site, thus NF-κB is likely to be activated for a longer period in cells where the predominant type of inhibitory protein is other than IκB-α.

### 1.4.2 NF-κB and Zn

Due to its important regulatory roles in inflammation, NF-κB has been suggested an ideal therapeutic target for various inflammatory, degenerative and malignant diseases. Trace elements such as Zn play important regulatory roles in cell signaling via transcription factors and genes (Kudrin, 2000). The potential targets in the NF-κB signaling pathway affected by metals are IkappaB-kinases, IkappaBs, NF-κB, proteosome degradation sites of NF-κB and kappaB sites on DNA (Kudrin, 2000).

The mechanism in which NF-κB binds to thiol-reactive metals has been extensively studied. These metal ions interact with sulfur or nitrogen-containing groups of enzymes such as thiols or imidazole groups (Glusker, 1991). Shumilla and colleagues have demonstrated the inhibition of NF-κB binding to DNA in TNF-α treated A549 human epithelial cell line by various metals including Zn, mercury, cadmium and arsenite in vitro (Shumilla, 1998). This inhibition was dose-dependent and maximum inhibition occurred when metals were pre-incubated with nuclear proteins of the cells. The ability of these metals to inhibit the binding of NF-κB is closely related to their affinity for protein thiols, in particular protein sulfhydryls (Shumilla, 1998). Jeon and colleagues have gone a step further and reported that thiol-reactive metals inhibited NF-κB activation via the blocking of IκB kinase (IKK) (Jeon, 2000). The same study reported that Zn and copper inhibited TNF expression and induction of NF-κB in LPS-stimulated RAW 264.7 murine macrophages.

A study by Connell and colleagues reported a significant increase in the binding of

NF-κB and AP-1in Zn-deficient cultured human endothelial cells exposed to TNF-α. This binding was significantly lowered when the cells were supplemented with physiological levels of Zn (9.2 μM Zn acetate) (Connell, 1997). Another well-known inhibitor of NF-κB, pyrrolidine dithiocarbamate exerts its effects accompanied by an increase in the levels of intracellular Zn (Kim, 1999). In a subsequent study by the same group, pyrithione, a Zn ionophore was found to inhibit NF-κB activity in bovine cerebral endothelial cells in a time dose-dependent manner. Accompanying this was the ability of pyrithione to increase intracellular Zn rapidly. The authors concluded that pyrithione was more potent than PDTC (Kim, 1999).

Dietary supplementation of Zn has been reported to inhibit the activation of NF-κB in the pancreas of Type I diabetic patients. Supplementation of Zn has shown to decrease the severity of alloxan and streptozotocin-induced Type I diabetes animal models (Ho, 2001).

**Zn Finger A20**

The effect of the Zn finger A20 on the regulation of NF-κB activation has also been the focus of many studies. A20 was initially described as an inhibitor of TNF-induced apoptosis (Opipari, 1992). A20 is a TNF and IL-1inducible protein that negatively regulates NF-κB-dependent gene expression (Heyninck, 1999). Over expression of A20 in cultured cells have resulted in the inhibition of NF-κB activation induced by TNF, IL-1, lipopolysaccharide, hydrogen peroxide and phorbol ester in a variety of cells (Beyaert, 2000). It is thought that the C-terminal region of A20 is involved in the

negative feedback regulation of NF-κB activation since A20 itself is under the control of NF-κB (Krikos, 1992).

A20 has been shown to bind to TNF-receptor-mediated factor (TRAF) molecules via its N-terminal domain. A20 interacts with TRAF1 and TRAF2, which are a part of the NF-κB activation cascade initiated by TNF (Song, 1996). The interaction of A20 with TRAF proteins may serve to recruit the inhibitory Zn finger domain to the NF-κB activation cascade (Beyaert, 2000). The mechanism(s) for the effects of A20 is still not clear, however it has been suggested that A20 interferes with the TRAF-IKK pathway, and restricts the availability of IKKs to IKK-activating kinases, leading to inhibition of NF-κB at a step prior to IκB degradation (Heyninck and Beyaert, 1999).

### 1.4.3 NF-κB And Apoptosis

The role of NF-κB in the initiation and execution of apoptosis came from observations that agents that induce apoptosis in cells also activate NF-κB. It has been debatable for a while whether NF-κB functions as a pro-apoptotic or anti-apoptotic agent.

#### Pro-Apoptotic NF-κB Transcription Factor

##### *1. NF-κB Turns On Pro-Apoptotic Genes*

Studies have suggested that NF-κB promotes apoptosis in several models due to its involvement in the expression of several apoptotic genes including TNF-α, c-*myc* and

FasL (Hsu, 1999; Matsui, 1998). For example, activation of NF-κB was shown to mediate TNF-induced apoptosis in murine clonal osteoclasts (Kitajima, 1996). Nakai and colleagues have also shown that NF-κB activation contributes to the induction of c-Myc and p53 and subsequent apoptosis in an excitotoxic model of Huntington's disease (Nakai, 2000).

### *2. Apoptotic Inducers Turn On NF-κB*

NF-κB activation was seen with the inhibition of CD34+ myeloid leukemic cell growth induced by TNF-α (Hu, 1999).

### *3. Activators Of NF-κB Do Not Inhibit Apoptosis*

$H_2O_2$-induced apoptosis of A549 human epithelial cells was not prevented even though activation of NF-κB was induced by hyperoxia (Li, 1997).

### *4. Apoptotic Inducers Require The Action Of NF-κB*

Apoptosis in the human promyelocytic leukemia cell line HL-60 induced by anti-cancer drugs such as etoposide required the activation of NF-κB (Bessho, 1994). The requirement of NF-κB activation for agent-induced apoptosis have been reported in various models including injury-induced cultured astrocytes (Takuma, 1999), alphavirus-induced AT-3 prostate carcinoma and N18 neuroblastoma cells (Lin, 1995), $H_2O_2$-induced T-cells (Dumont, 1999) and in the rat model of focal cerebral ischemia (Schneider, 1999).

*5. Inhibitors Of NF-κB Blocks Apoptosis*

It was also observed that inhibition of NF-κB in these cells by the anti-oxidant pyrrolidine dithiocarbamate also blocked apoptosis (Bessho, 1994).

*6. Some Factors Inhibit Both Apoptosis And NF-κB Activation*

One example of this is the Zn finger A20 which has been shown to inhibit both apoptosis and NF-κB activation in pancreatic islets, induced by cytokines (Grey, 1999), suggesting a role for NF-κB in mediating apoptosis (Grey, 1999).

From the above studies; Lin, Schneider and colleagues have also suggested that NF-κB may have a dual role in that it can be either pro- or anti-apoptotic depending on the time and circumstances in which NF-κB is activated relative to the death stimulus (Lin, 1995; Schneider, 1999).

**Anti-Apoptotic NF-κB Transcription Factor**

*1. Activation Of NF-κB Blocks Apoptosis*

One mechanism by which NF-κB is anti-apoptotic is by increasing expression of survival genes. These include cellular inhibitors of apoptosis {(cIAP)-1, cIAP-2, TRAF-1 and TRAF-2} (Chu, 1997; Stehlik, 1998; Wang, 1998), manganous superoxide dismutase (Manna, 1998), Zn finger protein A20 (Krikos, 1992), cyclin D1 (Guttridge, 1999; Hinz, 1999), Bcl-2 homologue Bfl-1/A1 (Zong, 1999) and Bcl-2 itself (de Moissac, 1998). Some have considered evidence concerning A20 to favour the hypothesis that NF-κB is pro-apoptotic (see above). However, experiments with

A20 have demonstrated that NF-κB is anti-apoptotic. For example, it has been shown that NF-κB up-regulates A20 and this protein prevents TNF-α-induced apoptosis in cells (Krikos, 1992). Further evidence of the anti-apoptotic effect of NF-κB comes from studies of cortical neurons. Elevation of NF-κB activity by pretreatment of cortical neurons with an anti-sense oligonucleotide to IκB-α prevented these cells from undergoing β-amyloid peptide-induced apoptosis (Bales, 1998; Guo, 1998).

The pathway Ras-phosphatidylinositol-3 kinase/Akt, considered to be important for cell survival, has been suggested to protect cells from apoptosis via NF-κB activation. It is thought that this pathway is involved in activation of IKK, the kinase required for the phosphorylation of IκBα and NF-κB activation (Romashkova and Makarov, 1999).

### *2. Knockout Of NF-κB Or Upstream Kinases Induces Apoptosis*

The strongest evidence indicating this came from mouse knockout models in which genes encoding either members of the NF-κB family proteins or upstream kinases were disrupted. It was shown that hepatocytes of RelA (p65)-deficient mice die by apoptosis during embryonic development (Beg, 1995). Another study by Beg and Baltimore also showed a significant reduction in the viability of RelA (p65)-deficient mice macrophages and fibroblasts treated with TNF-α (Beg and Baltimore, 1996). In IKK-β gene knockout and IKK-β/IKK-α double-knockout mice die as embryos showing a significant level of liver cell apoptosis (Li, 2000; Li, 1999).

### *3. Inhibitors Of NF-κB Promotes Apoptosis*

Various studies have showed the inhibitory effect of NF-κB in TNF-induced apoptosis. Wang and colleagues have demonstrated that activation of NF-κB by TNF-α and other agents such as ionizing radiation prevents apoptosis in cells (Wang, 1996). The same study also showed that inhibition of NF-κB promoted apoptosis in cells (Wang, 1996). Van Antwerp and colleagues reported that TNF-α-induced apoptosis was enhanced in a number of cell types expressing a dominant negative IκBα (Van Antwerp, 1996). Another study demonstrated that recruitment of adaptor molecules such as receptor interacting protein (RIP) and TNF receptor-associated factor 2 (TRAF-2) mediates the activation of NF-κB, which results in the protection of cells against TNF-α -induced apoptosis (Liu, 1996). NF-κB blocking of TNF-α-induced apoptosis has been reported in numerous cell types including: keratinocytes (Qin, 1999), endothelial cells (Stehlik, 1998; Zen, 1999), myeloid cells (Liu, 1999), lymphoid cell lines (Jeremias, 1998), hepatocyte cell lines (Xu, 1998), epithelial cells (Soler, 1999), prostate and pancreatic cancer cell lines (McDadẹ, 1999; Sumitomo, 1999), chronic lymphocytic leukemia (Delic, 1998) and fibrosarcoma HT1080 (Wang, 1999).

### *4. Feedback Loop Mechanism*

An alternative mechanism suggested by Aggarwal for the anti-apoptotic effect of NF-κB is via a feedback loop where activation of NF-κB blocks apoptosis while activation of apoptosis also blocks NF-κB activation. Aggarwal used the following examples to

support the feedback loop hypothesis. In endothelial cells undergoing apoptosis due to the lack of growth factors, caspases cleaved the NF-κB p65/RELA subunit, thereby rendering the p65 subunit transcriptionally inactive. This subunit then acts as a dominant negative inhibitor of NF-κB (Levkau, 1999) resulting in the inhibition of NF-κB and thereby inducing apoptosis (Levkau, 1999). By contrast, the surviving cells displayed increased NF-κB activity (Levkau, 1999). It was then proposed that this dominant negative fragment of p65 could act as an efficient pro-apoptotic feedback mechanism between caspase activation and NF-κB inactivation (Levkau, 1999). Consistent with this proposition, an uncleavable caspases-resistant form of p65 prevented cell apoptosis (Aggarwal, 2000).

On the other hand it has been reported that caspases cleaved IκBα thereby activating NF-κB and promoting apoptosis (Reuther and Baldwin, 1999). Cleavage of IκB-α by caspase-3 has been shown in γ-radiation-induced apoptosis and in NF- κB inhibition-induced apoptosis (Jung, 1998; Reuther and Baldwin, 1999). In the human IκB-α, a caspase-3 cleavage site has been identified in the region of amino acids 26 to 32 (Barkett, 1997). Cleavage of IκB-α by caspase-3 produces a N-terminal truncated IκB-α protein that is resistant to degradation by proteosome in response to inducers of NF-κB but it is able to bind to and suppresses NF-κB. If this is correct it suggests a dual role for NF-κB, acting either as a pro- or anti apoptotic agent depending on the type of its inducers and/or inhibitors.

### Pro-Apoptotic Or Anti-Apoptotic?

From the observations above describing the opposing properties of NF-κB or lack of, the role of NF-κB in apoptosis remains a complex issue. It seems that the involvement of NF-κB in the regulation of apoptosis is dependent on several experimental factors (Aggarwal, 2000). It appears that NF-κB alone cannot determine whether cells survive or undergo apoptosis and that proteins important for cell survival are unlikely to be regulated by NF-κB alone. Aggarwal postulated that the outcome for a cell surviving or dying or remaining unaffected by an introduced agent may depend on the pre-determined balance between survival or non-survival proteins. This might explain why NF-κB has a dual role of being pro- and anti-apoptotic. The studies described seem to suggest that NF-κB and apoptosis shares a common upstream signaling pathway but may be involved in different downstream pathways (Aggarwal, 2000). Thus the relationship between NF-κB and apoptosis needs to be further elucidated perhaps through the better understanding of signaling pathways by factors that affect activation of NF-κB in different cellular models. In regards to mast cells, there have been no studies that specifically address the role of NF-κB in mast cell apoptosis and hence the above mechanisms will be tested in mast cell models for reasons described section 1.5.

## 1.5 Types of Cells Studied

Mast cells and neuroblastoma cells were used for the majority of the experiments described in this thesis for several reasons as is apparent below. For the mast cells,

primary cultures from human bone marrow, cord-blood and rat peritoneal were isolated along with the human leukemic cell line HMC-1 and the rat basophilic mast cell line RBL-2H3. The BE(2)-C neuroblastoma cell line was mainly used in studies relating to the role of Zn in apoptosis of neuronal cells (as described in chapter 7). Other cells that were used include: human epithelial cell lines NCI-H292 and A549 and the neuroblastoma cells NIE-115.

### 1.6 Mast Cells

Since their discovery by Paul Erlich nearly a 100 years ago, a vast amount of knowledge has been acquired about the biological functions of these "fattened" cells. They are known for their unique staining characteristics of their proteoglycan and protease-rich cytoplasmic granules. Mast cells are granulated cells localised within organs, particularly within connective tissues and epithelial surfaces (Holgate and Church, 1992). They are an important component of the inflammatory and immune systems. There are no diseases or biological conditions known to exhibit a lack of mast cells from which their role might be determined. It is now widely accepted that they originate from pluripotential haematopoietic cells in the bone marrow (Kitamura and Go, 1978), and differentiate at tissue sites (McNeil, 1996).

There are three main types of mediators in mast cells; 1) granule associated mediators such as histamine, and neutral proteases both preformed in the mast cells, 2) lipid-derived mediators such as leukotrienes, and 3) various cytokines and chemokines, which are newly-formed components (Metcalfe, 1997). Mast cells are long-lived and are strategically located at interfaces with the environment and the vascular network

(McNeil, 1996). Mast cells are often mistaken for are the basophils. However, the two are distinguishable by their location and the contents of their granules. Basophils circulate mainly in the blood whereas mast cells are based in tissues, and mast cells express specific proteases and the c-kit proto-oncogene product, KIT on their surface.

Human mast cells are variable in shape with a round nucleus. The cell membrane consists of multiple folds and projections. The cytoplasm holds a large number of granules along with the mitochondria, ribosomes, rough endoplasmic reticulum and a not so prominent golgi complex (Dvorak, 1988). The granules show heterogenous patterns of scrolls, lattices and whirls, reflecting the way the proteoglycans and proteolytic enzymes are packed. Mast cells exhibit a wide range of adhesion molecules, immune response receptors, and surface molecules that enable them to respond to challenges from specific and non-specific stimuli (Metcalfe, 1997). Their primary functions include phagocytosis, production and release of cytokines and mediators in inflammation (Metcalfe, 1997).

### 1.6.1 Heterogeneity

Mast cells are not homogenous (Holgate and Church, 1992). Hardy and Westbrook first reported that rat mast cells had different morphological and histochemical properties at different tissue sites (Hardy and Westbrook, 1895). It is now recognised that the presence of different types of mast cell is important to the role they play in health and disease. Much of the work performed on the heterogeneity of these cells was done on rats and mouse mast cells (Metcalfe, 1997) but the development of cell cultures from mice and human mast cells has enabled more in depth studies.

Originally mast cells were classified according where they were located. Those situated between connective tissues were called connective tissue mast cells (CTMC), while those located near mucosal areas, were called mucosal mast cells (MCM) (Schwartz, 1993). The most common marker used to distinguish different types of mast cells is the type of protease in the granules. Like rats (Le Trong, 1987) and mice (Miller, 1989), humans have subsets of mast cells that differ in neutral protease content. It has been demonstrated that mast cells at mucosal surfaces such as those in the lung have predominantly tryptase, termed $MC_T$. The granules in these cells have characteristic scroll-like crystal structures seen under electron microscopy (Denburg, 1992), while mast cells in connective tissue of organs such as skin and lymph nodes are enriched with chymase and carboxypeptidase A in addition to tryptase, termed $MC_{TC}$ (Irani, 1986). The granules of these cells have scrolls when observed under electron microscopy (Craig, 1988).

There has been a report of another minor subset of mast cells which only stain with antibodies to chymase but not tryptase, and have been named $MC_C$ (Weidner and Austen, 1991), however their existence remains uncertain. Mast cell subsets also exhibit functional differences. Human skin $MC_{TC}$ are responsive to blood derived activators such as complement components and morphine derivatives as well as neuropeptides, whereas lung or intestinal $MC_T$ are not sensitive to these stimuli (McNeil, 1996). The human $MC_{TC}$ and $MC_T$ cells are comparable to the CTMC and MMC mast cells from mouse and rat tissues respectively, however differences do exist between the human mast cells and those of rats and mice.

Unlike their rodent counterparts, human mast cells have yet to demonstrate the ability to switch from one subset to another following exposure to growth factors (McNeil, 1996). Mice mast cells have the ability to differentiate morphologically, giving them a longer life span and an ability to proliferate extensively, and/or change their phenotype (Takagi, 1992). In humans, it is likely that a common mast cell progenitor has the ability to differentiate into structurally and functionally distinct subsets due to exposure to factors in the microenvironments within which they reside (Ghildyal, 1992).

### 1.6.2 Growth and Maturation

Prior to the identification of interleukin-3 (IL-3) as a mast cell growth factor in the early 1980s, techniques for culturing mast cells were inadequate (Ihle, 1983). In early studies, researchers relied on mast cells isolated from rat peritoneum or from tissues by enzymatic digestion (Metcalfe, 1997). Mast cells have been known to remain differentiated and viable in the presence of IL-3 (Huang, 1990). Research into the biological role of mast cells has been improved through the development of various cell lines such as the human leukemic HMC-1 and rat basophilic RBL-2H3 cells. Primary cultures of mast cells derived from human umbilical cord blood, lung and other tissues, which can be isolated with a high degree of purity are now more accessible to researchers.

The c-kit ligand is also an important growth factor for mast cells, and has been termed c-kit ligand stem cell factor (SCF). Even though IL-3 is a potent growth factor for

mast cells, mature human lung mast cells do not express IL-3 receptors (Valent, 1990), but do express SCF receptors (Okayama and Church, 1992). SCF maintain mast cell viability and promote their differentiation (Mekori, 1997). In addition, SCF also promotes mast cell adhesion to fibroblasts and extracellular matrix (ECM) components, thus playing a role in the migration and distribution of these cells (Mekori, 1997). Stromal cells such as fibroblasts and endothelial cells produce SCF, and often fibroblasts are used as a nutrient layer to maintain mature mast cell cultures (Levi-Schaffer, 1987).

Another agent that has been used experimentally to induce mast cell maturation is sodium butyrate. 1 mM sodium butyrate has been shown to induce growth arrest of immature mast cells and acquisition of abundant cytoplasmic granules similar to those of mature mast cells (Galli, 1982). Butyrate induces markers of differentiation in a wide variety of cell types (Chung, 1985) at this concentration, while higher concentrations induce apoptosis as discussed earlier.

### 1.6.3 Mast Cell Activation

#### IgE-dependent mechanism

Mast cells are activated through IgE receptor ($FcER_I$) dependent or independent mechanism. In the $FcER_I$ dependent mechanism, activation is achieved by cross-linking of IgE molecules bound to the cell surface $FcER_I$ or through interaction of a variety of other agonists such as neuropeptides, basic compounds, complement components and opiates (Metcalfe, 1997), which act directly on the cell surface

(Wasserman, 1994). Mast cells have high affinity IgE receptors in varying numbers, depending on the allergic status of the donor (Warner and Kroegel, 1994). Experimentally, IgE cross-linkage can be induced by the use of anti-IgE antibodies or antibodies against the IgE receptor (Metcalfe, 1997).

$FcER_1$ belongs to a multi-chain immune recognition class of receptors (MIRRs) (Keegan and Paul, 1992). It consists of a tetrameric complex of α-, β- and two γ-chains (Blank, 1989; Kinet, 1988; Kochan, 1988). The α chain has a long extracellular domain, which contains two immunoglobulin-like loops, with the high affinity Fc-IgE binding site. Due to its short cytoplasmic tail, the α chain needs to complex with $B\gamma_2$ for its expression (Kochan, 1988). It has been suggested that $B\gamma_2$ has a role in the coupling of $FcER_1$ to signal transduction mechanisms (Paolini, 1991). The β chain has four membrane spanning regions and shares some homology with CD20, an ion channel (Bubien, 1992).

Cross-linking of the $FcER_1$ receptors induces the tyrosine phosphorylation stimulating one or more bound or newly associated kinases (Metcalfe, 1997). In the RBL-2H3 cell line, src family-activated PTK lyn-$p56^{lyn}$ tyrosine kinase is activated and binds to $FcER_1$ upon receptor aggregation. $p56^{lyn}$ has been shown to phosphorylate the β- and γ- subunits of $FcER_1$ (Jouvin, 1994). Newly phosphorylated tyrosines promote recruitment of more kinase molecules, possibly through their SH2 domains. This type of phosphorylation is restricted to activated receptors and is reversible upon receptor detachment (Metcalfe, 1997). Phosphatidylinositol (PI) 3-kinase is associated with

and activated by proteins containing PTK acitivity or those that are associated to PTKs.

Aggregation of $FcER_1$ on mast cells causes the phosphorylation of tyrosines on phospholipase C-γ1 (PLC-γ1) resulting in the activation of this enzyme (Nishibe, 1990). Translocation of PLC-γ1 from the cytosol to the membrane has two outcomes: 1) it becomes activated; 2) it is relocated near its membrane-associated substrate, phosphatidylinositol 4,5-bisphosphate ($PIP_2$) (Metcalfe, 1997). The breakdown of $PIP_2$ through hydrolysis by phospholipase requires external calcium ions (Beaven, 1984), and result in the formation of two second messengers, inositol 1,4,5-triphosphate ($IP_3$) and diacylglycerol (DAG) (Cunha-Melo, 1987). DAG has been shown to activate protein kinase C (PKC), and two phospholipases; PLD and $PLA_2$ and these have been suggested to support the prolonged activation of PKC at the later stages of cell activation. The activation of $Ca^{2+}$ by $IP_3$ and the PKC signal by DAG interacts synergistically to evoke exocytosis in mast cells (Metcalfe, 1997) (Figure 1.11). This step can be mimicked by addition of the PKC activator phorbol myristate-acetate (PMA) and calcium ionophore A23187.

Signalling events distal to activation of PKC have been termed as late events, and two have been identified. They are the activation of mitogen-activated protein kinase (MAP kinase) and of G proteins (Metcalfe, 1997). The activation of MAP kinase is thought to precede degranulation of mast cells. Two types of G proteins; Gi3 and a small Ras-like G protein are believed to be involved in the late stages of exocytosis of mast cells (Figure 1.11).

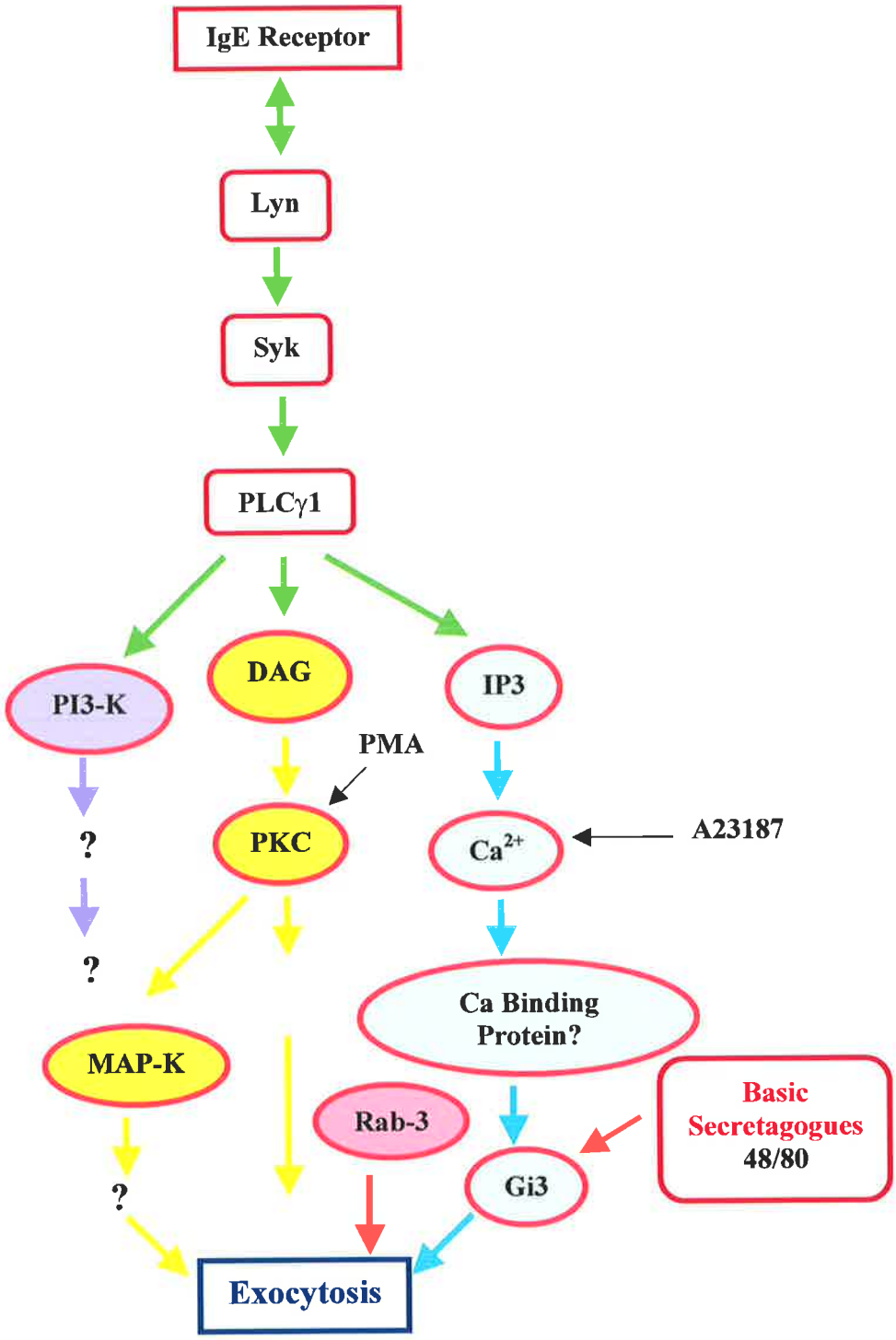


**Figure 1.11: Pathways of Mast Cell Activation.**

Signal transduction pathways in mast cell activation via the aggregation of IgE receptor resulting in exocytosis. Details of this pathway is described in section 1..4.7. Figure adapted from Metcalfe, 1997.

## Non-IgE Dependent Mechanism

As mentioned, exocytosis in mast cells can be induced by a variety of agents other than those interacting with $FcER_1$. One of these is compound 48/80, which was used extensively in this thesis because it is readily available, effective on a wide variety of mast cells and is commonly used for secretory studies. It belongs to a class of polybasic molecules (Lagunoff, 1983). These molecules are thought to release histamine by a common mechanism by interacting on the same site on mast cells in a non-cytotoxic way. However, no specific receptors have been discovered for these molecules (Repke and Beinert, 1987). Since its discovery in 1939, compound 48/80 has been one of the most common substances used to degranulate mast cells (Fasset and Hjort, 1938). Studies of the structure of compound 48/80 have shown that it interacts with membrane proteins and directly activate G proteins. This activation involves insertion of the aromatic rings of compound 48/80 into the membrane and the positively charged domain of the molecule with the COOH-terminal portion of the $\alpha$-subunit of the COOH-terminal portion of G proteins (Mousli, 1990).

Other groups that can induce exocytosis of mast cells include: peptides, cytokines, anaphylatoxins, dextrans and lectins and low affinity receptors

## Exocytosis

There are a number of stages of degranulation involving sequential events that include ATP-dependent processes, movement of vesicles to the actin cytoskeleton matrix beneath the plasma membrane, tethering (loosely attached), then docking at release

sites prior to fusion, release of contents and recycling (Figure 1.12). This process involves a number of docking proteins such as SNAREs (Burgoyne and Morgan, 2003). In mast cells, this process occurs spontaneously by an "all or none" phenomenon (Hide, 1993). However, compound 48/80 appears only to induce a partial degranulation of mast cells (Hide, 1993).

### 1.6.4 Mediators

No other cell produces such a broad range of bioactive molecules like the mast cells. These cells not only release, but also generate (preformed) a heterogenous group of mediators that have different biological functions. Many of the mediators are stored in an active state, allowing for immediate effect upon release. Mast cell mediators are classified into three groups: preformed secretory granules-associated mediators, lipid-derived mediators and cytokines.

#### Granule-associated mediators

#### Histamine

Included in the granule associated mediator group are histamine, proteoglycans and neutral proteases. Along with basophils, mast cells are considered to be the major histamine producing cells of the body. Approximately 3-8 pg of histamine is found in each mast cell from human lung, skin, lymphoid tissue and small intestine (Fox, 1985). Histamine is stored by ionic linkage with carboxyl groups of proteins and proteoglycans of the secretory granules at acidic pH. Histamine dissociates from the

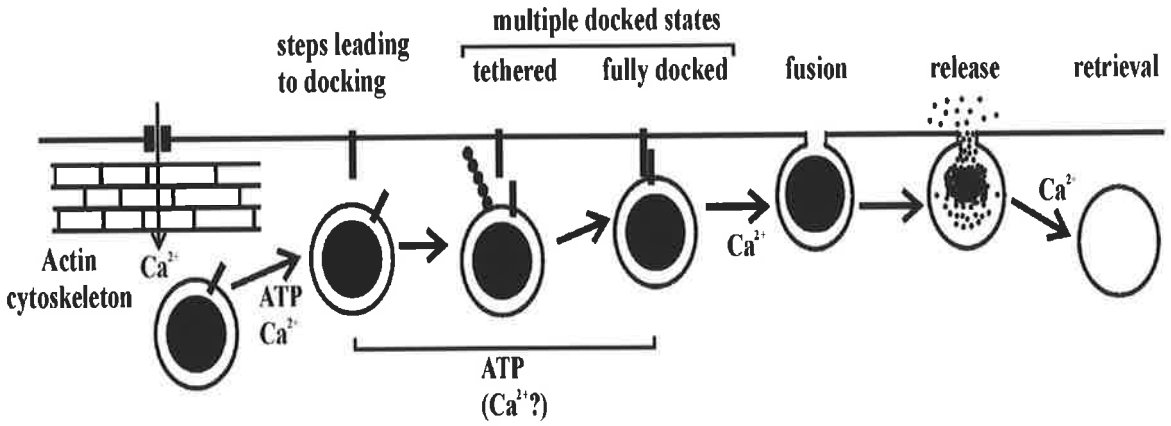


**Figure 1.12: The Exocytosis Pathway**

Figure depicts the sequential events of granule release. These events involve movement of granules to the sub-membranous cytoskeleton, tethering, docking and release of granular contents. Following degranulation, granule contents are recovered by retrieval. Some of these steps are ATP and/or calcium dependent. Figure adapted from Burgoyne and Morgan, 2003.

proteoglycan-protein complex by cationic exchange with extracellular sodium at neutral pH. The wide-ranging biological activities of histamine are then mediated via specific receptors. The release of histamine brings about contraction of airway and gastrointestinal smooth muscle, vasodilation and capillary leakage (Metcalfe, 1997). Histamine is thought to influence events at or near the site of release.

Other granule-associated mediators are proteoglycans, chondroitin sulphate E and neutral proteases such as chymase, tryptase and carboxypeptidase A (Schwartz, 1993).

**Non-granule associated mediators**

There are various non-granular mediators. Activation of mast cells causes the de novo synthesis of lipid-derived substances. Two important metabolites of arachidonic acid are cyclooxygenase and lipoxygenase, both with potent inflammatory effects. Cyclooxygenase products include prostaglandins and thromboxanes. Lipoxygenase generate leukotrienes (LTs), hydroperoxyeicosatetraenoic acids and the reduced forms of HPETEs, hydroxyeicosatetraenoic acids (Metcalfe, 1997). Also generated by mast cells following activation is Prostaglandin (PG) $D_2$. $PGD_2$ is a potent suppressor of platelet aggregation (Lewis and Austen, 1984).

Another group of mediators produced and secreted by mast cells are cytokines and chemokines. Cytokines play a part in cell growth, inflammation, repair and the immune response. These include interleukins (IL-1, IL-3, IL-5, IL-6), GM-CSF and interferons (IFN-γ). The range of chemokines and cytokines that mast cells produce has been extended to include pro-inflammatory molecules. Cytokine induction of

mast cells involves prolonged receptor cross-linkage and extracellular calcium (Metcalfe, 1997), whereas chemokine induction in mast cells is regulated transcriptionally (Oh and Metcalfe, 1994).

### 1.6.5 Zn And Mast Cells

#### Granule Zn

It is well established that mast cells are rich in granule-associated Zn. Gustafson was the first to report this in 1967 using electron microscopy (Gustafson, 1967). The subsequent release of Zn from mast cells following degranulation was reported early on by Bor and colleagues in rat mast cells, where an increase in serum Zn levels was detected (Bor, 1976). Hogberg and Uvnas first reported that Zn prevented the release of histamine in rat peritoneal mast cells (Hogberg and Uvnas, 1960). In a subsequent *in vivo* study demonstrated that Zn inhibited the spontaneous release of histamine from rat lung tissues and tissues induced by low concentration of compound 48/80 (Chvapil, 1976).

Kerp proposed that in the presence of Zn, histamine strongly binds to heparin hence stabilizing the complex, and this could indicate a role for Zn in the storage of granule contents of mast cells (Kerp, 1963). Berqvist and colleagues opposed this theory and reported that there was an insufficient amount of Zn in relation to the amount of histamine in mast cell granules. The authors speculated that the high level of Zn present might be related to enzymes within the granules (Bergqvist, 1971). In a subsequent investigation by Kazimierczak and Maslinski, and Uvnas suggested that

the most likely mechanism is that Zn ions compete with compound 48/80 for receptor binding sites (Kazimierczak and Maslinski, 1974; Uvnas, 1970). Since these studies, we now know more about cellular biology of Zn and this hypothesis seems unlikely. The interactions between Zn and compound 48/80 are studied in relation to apoptosis and NF-κB activation in the result sections of this thesis.

**Effects of Zn on Mediator Secretion**

It has also been proposed that Zn may act via the cell membrane of mast cells to prevent the release of histamine, a property similar to its membrane-stabilizing role. Other stabilizing mechanisms of Zn have also been proposed and these include a) inhibition of membrane enzymes such as phospholipase A by Zn (Karl, 1973), b) inhibiting enzymes that are important for degranulation such as ATP-ases (Donaldson, 1971) and c) blocking of thiol groups (Warren, 1966). Studies by Marone and colleagues have shown that physiological concentrations ($10^{-3} - 3 \times 10^{-2}$ μM) of Zn, in the form of ZnCl inhibit the release of histamine and leukotriene $C_4$ ($TLC_4$) from human lung mast cells (Marone, 1986). It was proposed that Zn act as a competitive antagonist of the calcium-dependent IgE-mediated histamine release from human lung mast cells (Marone, 1986). It is more likely that Zn acts to prevent histamine release by blocking calcium ions, since increase in calcium concentrations in the extracellular medium completely reversed the inhibitory effect of Zn (Marone, 1986).

## Zn Deficiency And Mast Cells

Two studies have looked at the effects of Zn deficiency in animals on mast cell numbers. In the study by Kreavich, weanling male rats were fed either a low Zn diet (0.4 ppm) or a normal Zn diet (40 ppm Zn). The average numbers of mast cells per mm in the subepithelial zone were 15.4 (range 9.2 – 33.1) in the Zn deficient animals compared to 4.0 (range 2.9 – 5.3) in the Zn normal animals (Kreavich, 1981). Cho and colleagues found that Zn deficient diets, decreased the mast cell numbers in gastric glandular mucosa in rats (Cho, 1987).

## Zn In The Granules Of Other Inflammatory Cells

Localization of Zn within the matrix of the crystalloid granules of eosinophils from rats and cattle was first reported in 1967 by Pihl and colleagues (Pihl, 1967). Earlier studies reported that the Charcot-Leyden crystals also contained a significant amount of Zn (Archer and Blackwood, 1965; Buddecke, 1956). Another study found that neutrophil Zn existed in a largely soluble form and was present in small amounts in granules containing alkaline phosphatase (Raja, 1982). Depletion of leukocyte Zn resulted in a reversible decrease in the enzyme's activity (Thorling and Niazy, 1973). Few studies have investigated the distribution of Zn in basophils. These cells are often compared with mast cells, though having distinct characteristics and functions in normal and allergic responses.

### 1.6.6 Mast cell apoptosis

Due to their location in the tissues, the regulation of the number of mast cells is largely dependent upon the local control of proliferation and/or apoptosis (Metcalfe, 1997). External stimuli are also known to induce apoptosis in mast cells; they include drugs, ionizing radiation (Yee, 1994) and hyperthermia (Takano, 1991). These cells undergo apoptosis similar to other cell types in that they display morphological changes accompanied by DNA fragmentation.

#### Growth Factors

Mouse mast cells have been shown to undergo apoptosis as a result of IL-3 withdrawal and this was coincided with a decrease in endogenous bcl-2 mRNA (Yee, 1994). It has been shown that SCF does not induce expression of bcl-2 when added to IL-3 deprived mast cells. This suggests that SCF does not act in association with the induction of bcl-2 RNA (Yee, 1994). The effect of IL-3 deprived apoptosis in mast cells is reversible upon addition of SCF. The discovery of the SCF mediated rescue from apoptosis of IL-3 deprived mast cells have been confirmed in vivo (Inemura, 1994). Several cytokines have been reported to antagonize the SCF-mediated rescue process. One is transforming growth factor (TGF)-β1, which inhibits SCF from preventing apoptosis in IL-3 deprived mast cells without affecting the expression of the SCF receptor, c-*kit* (Mekori and Metcalfe, 1994). IL-4 has been shown to induce apoptosis in human cord blood mast cells in the presence of SCF via a mitochondrial dependent pathway (Oskeritzian, 1999).

Nerve growth factor (NGF) also prevents apoptosis in rat peritoneal mast cells by binding to the high affinity tyrosine kinase receptor for NGF, serine/threonine protein kinase B (PHB or TrkA) (Kawamoto, 1995). NGF also promotes the production of autocrine survival-promoting factors (Bullock and Johnson, 1996). Mast cell heterogeneity has also been the reason for the different effects observed by these and other cytokines on their apoptosis. For example, IL-4 does not induce apoptosis in human lung and fetal liver mast cells (Bischoff, 1999). Interestingly in mature human intestinal mast cells, IL-4 induces proliferation, production of cytokines and release of pro-inflammatory mediators in the presence of SCF (Bischoff, 1999).

**Role of Bax and Bcl-2**

Maurer and colleagues confirmed the role that Bax has in the regulation of mast cell apoptosis. The study reported that Bax-/- mice had increased number of gastric mucosa mast cells compared to Bax+/+ mice. In contrast Bcl-2-/- mice had a decreased number of mast cells. Therefore it was concluded that Bax is important in the promotion of apoptosis in mast cell (Maurer, 2000). Mekori and colleagues extended the mechanistic understanding of SCF mediated survival of human mature mast cells by reporting that SCF-treated mast cells express both Bcl-2 and Bcl-$X_L$ (Mekori, 2001). SCF was hypothesized to regulate these proteins via transcriptional mechanisms and message stabilization (Mekori, 2001). The expression of Bcl-$X_L$ is only limited to human mature mast cells as granulocytes that derived from $CD34^+$ population cultured in the presence of growth factors such as SCF, IL-3, IL-6 and G-SCF did not express this protein (Sanz, 1997). The same study also reported that there was over expression of both Bcl-2 and Bcl-$X_L$ in growth factor-independent mast cell lines HMC-1 and HMC-2 that had activating mutations of c-*kit*. These findings could

explain the excessive accumulation of mast cells in conditions such as mastocytosis (Mekori, 2001).

Other studies have shown the Bcl-2 homologue A1 to be an important agent in the survival of mast cells in allergic reactions (Xiang, 2001). A1 is an early response gene, expressed in tissues such as thymus, spleen and bone marrow and also in T- and B-lymphocytes, macrophages, neutrophils and endothelial cells (Chuang, 1998; Gerber, 1998; Lin, 1993). Activation of mast cells results in the strong induction of A1 mRNA and protein and prolonged mast cell survival (Xiang, 2001). Xiang and colleagues have also shown that FcεRI aggregation induces the expression of A1, required for the mast cell survival during degranulation (Xiang, 2001). Hence A1 has been suggested as a potential target for treatment of allergic diseases.

A study by Asai and colleagues proposed that exposure to monomeric IgE in bone marrow-derived mouse mast cells (BMMC) can render mast cells resistant to growth factor depletion-induced apoptosis (Asai, 2001). In this instance it was observed that the cross-linking of $FcER_I$ was not required and there were no change in the expression of the Bcl-2 family of proteins such as Bcl-$X_L$ and BAD, another pro-apoptotic protein. This result agrees with the hypothesis that interaction of IgE with $FcER_I$ does not induce intracellular signaling (Asai, 2001). The group did not detect any autocrine release of cytokines that affect mast cell survival or proliferation.

## IL-15

Another cytokine that has proven to be anti-apoptotic is IL-15. Masuda and colleagues has reported that IL-15 prevents apoptosis in MC9 mouse mast cells via the expression of bcl-2, mediated by signal transducers and activators of transcription-6 (STAT6) (Masuda, 2001). The group has shown that STAT6 binds directly to the consensus sequence of Bcl-X gene thereby regulating Bcl-$X_L$ expression via IL-15 activation.

## Fas

The Fas/Fas ligand system has been suggested to be a negative controller of murine mast cell numbers (Hartmann, 1997). A study by Yoshikawa and colleagues reported that activation of MC9 mouse mast cells by cross-linking of the $FcER_1$ receptor resulted in the rescue of these cells from apoptosis induced by IL-3-depletion (Yoshikawa, 1999). In a subsequent study by the same group, activation of MC9 mouse mast cells by cross-linking with $FcER_1$ or FcγR was shown to enhance the expression of the Fas-associated death domain-like IL-1 converting enzyme (FLICE) – inhibitory protein (Yoshikawa, 2000). Furthermore, Hartmann and colleagues have shown that resistance to Fas-mediated apoptosis in mouse mast cells was evident even though there was enhanced Fas expression (Hartmann, 1997).

## IgE

Experiments using BMMC have provided another pathway in prolonging mast cell survival. Ishizuka and colleagues have shown that aggregation of $FcER_1$ and ligation

of c-*kit* in BMMC induced the activation of the phosphoinositide 3-kinase pathway (PI3'K) (Ishizuka, 1999).

### 1.6.7 Recovery Of Mast Cells Following Degranulation

Studies by Dvorak and others have shown that mast cells recover following degranulation (Dvorak, 1988) via the re-accumulation of histamine (Dvorak, 1997). Recent studies have suggested that the activation of mast cells contributes to their prolonged survival. The main focus has been on the possible mechanistic effects of IgE induction, with respect to the high affinity $FcER_1$ receptor and its association to Fas-mediated apoptotic pathway. Fas-mediated apoptosis plays an important role in the regulation of the immune system, where the Fas cell surface receptor is expressed on many cell types including T and B cells, granulocytes such as neutrophils, eosinophils and mast cells (Hartmann, 1997). However, there is still controversy as to whether mast cells recover or undergo apoptosis and therefore more studies need to be done the relationship between mast cell degranulation and their survival.

## 1.7 Neuronal Cells

Some of the findings in this thesis are confirmed in neuronal cells, a distinct cell type. Some of these studies preceded the mast cell studies. It was important to determine whether some of the effects of Zn on caspases were specific to a particular cell type or were more general effects. There were less detailed investigations of neuronal cells. This section focuses largely on what is known about Zn and apoptosis in neuronal cells.

### 1.7.1 Zn and Neuronal cells

Significant concentrations of Zn exist in the hippocampus and parts of the cerebral cortex and are important for memory function, cognition and behaviour. These functions are affected in moderate Zn deficiency (Frederickson, 1989; Golub, 1995; Vallee and Falchuk, 1993).

Three main pools of Zn have been proposed to exist in the brain. Firstly a vesicular pool localized in the synaptic vesicles of nerve terminal (Frederickson, 1989; Haug, 1973; Howell and Frederickson, 1989). In mammalian brain cells, vesicular Zn may have a role in modulating various receptors including the α-amino-3-hydroxy-5-methyl-4-isoxazolepropionic acid/kainate receptor, N-methyl-D-aspartate and γ-aminobutyric acid receptor (Harrison and Gibbons, 1994; Huang, 1997; Smart, 1994). The second pool includes, membrane bound, metalloproteins or protein metal complexes involved in both metabolic and non-metabolic reactions (Frederickson, 1989). The third pool consists of free or loosely bound Zn ions in the cytoplasm (Frederickson, 1989). Amongst these pools, the vesicular Zn pool has been considered to be the most significant from a functional point of view (Cuajungco and Lees, 1997; Danscher, 1985; Perez-Clausell and Danscher, 1985). In the central nervous system, labile Zn is mainly detected in the vesicular compartments of the hippocampal mossy fibre terminals (Danscher, 1985; Frederickson, 1989). The neo-Timm's sulphide/silver technique has been used extensively to reveal the Zn-enriched neurons (ZEN).

Zn is released from the hippocampal mossy fibre terminals during neurotransmission into the synaptic clefts where it may reach concentrations up to 300 mM (Assaf and Chung, 1984; Perez-Clausell and Danscher, 1985).

### 1.7.2 Zn and Neuronal cell apoptosis

Alzheimer's disease (AD) and other dementias afflict a significant proportion of the elderly and place a heavy financial burden on health care systems. One area of the cell biology of AD of interest is the cell suicide mechanism of apoptosis, which results in the loss of neurons and glial cells. For example, in AD, cell death in the hippocampus is increased up to 30-fold (Anderson, 1996; Smale, 1995). It has been reported that there is less Zn in the brains of AD patients than those of normal individuals (Constatinidis, 1991; Cuajungco and Lees, 1997). Different neuronal pools of Zn may serve different cellular functions, including nucleic acid synthesis (Vallee and Falchuk, 1993), neurotransmitter storage and secretion in certain presynaptic terminals (Frederickson, 1989) and microtubule polymerization (Oteiza, 1990). Zn is thought to stabilize the microtubule skeleton of neuronal cells and microtubular destabilization has been reported in Zn-deficient rats (Oteiza, 1990).

It has been suggested that deficiency in these labile pools of Zn can trigger apoptosis resulting in neuronal cell loss (Anh, 1998). A study by Anh and colleagues has found that depletion of intracellular Zn by the membrane-permeant Zn chelator TPEN (0.5-3.0 μM) induced protein synthesis-dependent neuronal apoptosis in mouse cortical cell culture (Anh, 1998).

In contrast, other studies have found that rapid and excessive influx of Zn into neurons can result in cell death *in vivo* and *in vitro* (Choi, 1988; Sheline, 2000; Weiss, 1993). The translocation of Zn in presynaptic into postsynaptic neurons has been shown to contribute to neuronal cell death associated with ischemia, seizures and trauma (Frederickson, 1988; Koh, 1996; Sloviter, 1985). Prolonged exposure to 20-80 μM $Zn^{2+}$ has been shown to induce neuronal apoptosis (Fraker and Telford, 1997; Lobner, 2000; Sheline, 2000), while short exposures to higher concentrations of $Zn^{2+}$ (150-600 μM) kill both cortical (Yokoyama, 1986) and cerebellar granule neurons (Manev, 1997). This Zn-mediated cell death has been shown to be dependent on influx of the cation into cells and can be prevented by addition of metal chelators (Koh, 1996).

Various mechanisms have been proposed as to how excessive influx of Zn contributes to neuronal death. The first mechanism involves the entry of Zn into neurons through the same channels as intracellular calcium ($Ca^{2+}$). In order of the most permeable, these channels include 1) $Ca^{2+}$ - permeable AMPA/kainate, 2) voltage-sensitive $Ca^{2+}$ - channels and NMDA channels (Sensi, 1999). The second mechanism involves a change in mitochondrial membrane potential and generation of reactive oxygen species due to Zn influx (Sensi, 1999). A study by Jiang and colleagues reported considerable mitochondria swelling in murine cortical cells associated with increases in cytosolic cytochrome-*c* and apoptosis-inducing factor as a result of induced rapid influx of Zn into these cells via voltage-sensitive $Ca^{2+}$ channels (Jiang, 2001). The same study found that addition of mitochondrial permeability transition pore inhibitors such as cyclosporin A and bongkrekic acid decreased the release Zn-dependent factors from mitochondria of the cortical neuronal cells (Jiang, 2001).

Another mechanism by which high concentration of Zn may induce apoptosis has been proposed by Aizeman and colleagues. They showed that brief exposure of rat cortical cultures to the membrane-permeant oxidizing agent 2,2'- dithiodipyridine induced the release of Zn and triggerrd apoptotic cell death in these neurons (Aizenman, 2000). This was blocked by addition of extracellular potassium, cysteine protease inhibitor butoxy-carbonyl-aspartate-fluoromethylketone, TPEN and other membrane-permeant chelators (Aizenman, 2000). They hypothesized that under oxidative stress, Zn released from intracellular stores can also contribute to the initiation of neuronal apoptosis. In a separate study, Seo and colleagues investigated the role of mitogen-activation protein kinases (MAPKs) such as extracellular signal-regulated kinase (ERK) and reactive oxygen species in Zn-induced neuronal death and found that Zn activates ERK leading to apoptosis of rat pheochromocytoma PC12 cells (Seo, 2001).

Using PC12 cells, Kim and colleagues also found that the Zn transporter $ZnT_1$ has a role in modulating the level of $Zn^{2+}$ neurotoxicity (Kim, 2000). PC12 cells over-expressing wild type forms of rat $ZnT_1$ exhibited enhanced $Zn^{2+}$ efflux and reduced susceptibility to $Zn^{2+}$-induced cell death compared to parental cells, whereas those that were expressing dominant negative $ZnT_1$ had the opposite effect to those containing the wild type (Kim, 2000). The group also reported that L-type $Ca^{2+}$ channels are the main pathways of neurotoxic Zn influx upon depolarization of neurons (Kim, 2000).

Hence, studies seem to suggest that Zn can either be beneficial, in preventing excessive loss of neurons or deleterious, where events triggering its movements in and

out of neuronal cells at excessive levels can lead to apoptosis. The complexities of this are shown in Figure 1.13. Therefore it is important that intracellular Zn concentrations are properly regulated through the process of influx and efflux in order to maintain homeostatic control. The elucidation of the regulatory mechanisms may be important to understanding disease processes and developing therapeutic interventions.

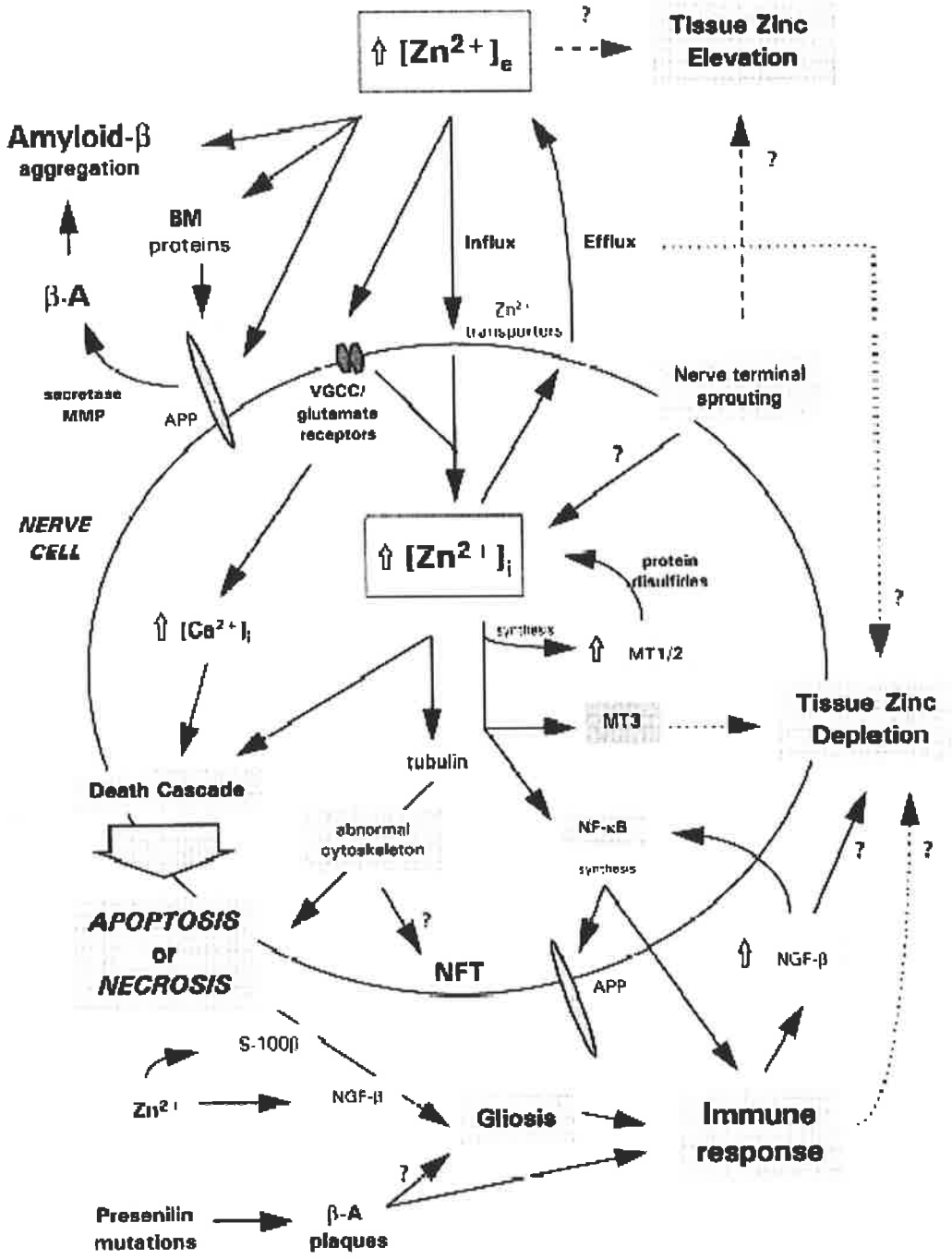


**Figure 1.13: The Complexities of Zn-mediated Signal Transduction Events.**

Figure shows the complex interactions between Zn, apoptosis and NF-κB in neuronal cell apoptosis. Figure adapted from Cuajungco and Lees 1997.

## 1.8 Project Hypotheses And Aims

This project had the following hypotheses: 1) mast cells are rich in labile Zn and that the Zn is released following activation of these cells, 2) the vesicular Zn transporter $ZnT_4$ is expressed and plays a role in mast cell Zn homeostasis, 3) pro-caspase-3 is expressed in mast cells and is associated with mast cell activation, 4) labile Zn depletion either by chelation or degranulation increases the susceptibility of these cells to undergo apoptosis, 5) physiological concentrations of Zn can regulate the activation of NF-κB in mast cells and 6) some of these findings will apply to neuroblastoma cells, a different type of cell.

The aims of the project were to: 1) investigate whether mast cells contain labile pools of Zn inside and outside of the granules and the fate of these pools during activation, 2) determine the subcellular distribution and expression of $ZnT_4$ in mast cells and whether changes in the levels and distribution occurs during mast cell activation, 3) determine the subcellular distribution of pro-caspase-3 in mast cells and relationships to activation, 4) investigate whether Zn chelator and mast cell degranulators affect susceptibility of mast cells to caspase activation, 5) determine whether Zn influences NF-κB nuclear translocation in mast cells and 6) to confirm the relationship between labile Zn and caspase activation in a separate cell type, namely neuroblastoma cells. Therefore the overall intent of this project is to increase understanding of the role of labile Zn in apoptosis including its effects on caspases and NF-κB, especially in relationship to mast cell apoptosis, an area that has not been studied.

# CHAPTER TWO

# MATERIALS AND METHODS

## 2. General Methods

### 2.1 Mast Cell Cultures

Unless otherwise indicated in text, all cells were cultured in RPMI 1640 medium, Hepes-buffered, pH 7.4, supplemented with glutamine (2mM), penicillin (100 IU/ml), streptomycin (100 μg/ml), gentamicin (160 μg/ml) and 10% foetal bovine serum (FBS) in a humidified atmosphere containing 5% $CO_2$.

#### 2.1.1 Isolation Of Human Umbilical Cord Blood Mast Cells

Cord blood mast cells (CBMC) were isolated following a previously described method (Yamaguchi, 1999). The North Western Adelaide Health Service ethics committee granted approval for the collection of human umbilical cord blood. Human umbilical cord blood was collected in sodium heparin blood tubes; diluted 1:1 with phosphate buffered saline (PBS), and overlaid with 8 ml of Ficoll Paque (density 1.077g/ml). Following centrifugation at 1000 g for 20 min at RT, middle layer (containing erythrocytes) was collected and washed twice with PBS (1000 g for 10 min at RT). The cell pellet was resuspended with 10 ml PBS. A second density-dependent centrifugation was performed: the middle layer was collected and washed three times with PBS (1000 g for 10 min at RT). The pellet was resuspended in RPMI-1640 + 10% FBS supplemented with 2 mM $_L$-glutamine, 0.1 mM non-essential amino acids, 200U penicillin/ml, 100 μg/ml streptomycin, 10 mM Hepes and 50 μM 2-mercaptoethanol. Cells were cultured in the presence of 10 ng/ml stem cell factor

(SCF) and 50 ng/ml interleukin-6 (IL-6). Then cells were cultured for 5 weeks and medium was replaced weekly after that with IL-6, non-essential amino acids and SCF.

Mast cells were purified using the following method. Erythrocytes were removed from the suspension by density centrifugation after adding 9.72 ml of Percoll (density 1.128g/ml) to 5.28ml of cell suspension and centrifuged at 1500 g for 20 min at 4°C. The entire Percoll layer above the erythrocyte pellet was collected and washed three times by centrifugation at 1500 g for 10 min at 4°C with 6X volumes of Hank's Balanced Salt Solution (HBSS) + 2% FBS. Nonspecific binding of antibodies was prevented by resuspending the cells in HBSS-protein buffer (HBSS + 2% FBS with 10% horse serum, 1% BSA and 50 μg/ml human IgG) for 30 min with gentle rolling. The suspension was centrifuged at 670 g for 10 min and resuspended in 1ml solution containing anti-*c-Kit* monoclonal antibody YB5.B8 in HBSS-protein buffer for 30 min with gentle rolling. Excess antibody was removed by washing twice in HBSS + 2% FBS (1500 g for 10 min at 4°C).

Cells were incubated with Dynabeads (Appendix 1B) coated with anti-mouse IgG antibody in total volume of 1ml for 1h with gentle rolling [Dynabead: mast cell ratio 3:1]. After the incubation, the suspension was made up to 20 ml with HBSS + 2% FBS and placed in a magnetic particle concentrator (MPC-1) for 1 min. This enabled free beads and beads attached to mast cells to adhere to the side of the MPC-1, while unattached cells and supernatant were discarded. While still attached to the MPC-1, the purified mast cells were washed twice in 20 ml of PBS (1000 g for 5min). The cells were then removed from the MPC-1 and washed three times in HBSS + 2%FBS and resuspended in RPMI-1640 + 10% FBS supplemented with 2 mM $_{L}$-glutamine,

1% non-essential amino acid solution, 100U penicillin/ml, 100 μg/ml streptomycin and 10 ng/ml stem cell factor. The viability of cells was determined by Trypan blue dye (0.2%) exclusion (as described in Morphology and DNA fragmentation below). Cells were cultured in 95% humidified atmosphere containing 5% $CO_2$.

### 2.1.2 Isolation Of Rat Peritoneal Mast Cells (RPMC)

Peritoneal mast cells (RPMC) were isolated from 6-8 wk old female 180g Dark Agouti rats. 20 ml of cold Tyrode's buffer pH 7.4 (Appendix 1A) was injected into the peritoneal cavity and the abdomen massaged for 2 min. A small incision was then made at the lower midline of the peritoneal lining to open the cavity and a sterile pasteur pipette was used to collect the peritoneal wash. RPMC were centrifuged at 150 g for 10 min at RT and the cell pellet was resuspended in 1ml of Tyrode's buffer per rat. RPMC were layered on 2 ml of 22% metrizamide and centrifuged at 280 g for 15 min at RT. The pellet was resuspended in 20 ml of Tyrode's buffer and centrifuged at 150 g for 10 min at RT. The metrizamide step was repeated and the lower third of the gradient containing purified mast cells was collected. Isolated cells were washed once more with Tyrode's buffer. Cells were cultured in RPMI 1640 medium with 10% FBS at 37 °C in a humidified atmosphere containing 5% $CO_2$.

### 2.1.3 HMC-1 Human Mast Cell Line And Its Maturation

The human leukemic mast cell line HMC-1 was obtained from Professor Joseph Butterfield (Division of Allergy and Outpatient Infectious Diseases, Mayo Clinic and Foundation, Rochester, MN). HMC-1 exhibits many characteristics of immature mast

cells and is the only established cell line with a similar phenotype to that of human mast cells (Butterfield, 1988; Nilsson, 1994). These cells have been shown to possess fewer cytoplasmic granules and lower levels of histamine, containing proteases such as chloroacetate esterase and tryptase (Butterfield, 1988). Maturation of HMC-1 cells was achieved in the presence of 1 mM sodium butyrate into culture medium for a period of four days. This has been previously been reported to increase histamine, protease levels and granular contents in HMC-1 cells (DuBuske, 1984; Galli, 1982). Butyrate-treated cells were stained with toluidine blue for comparative purposes against untreated HMC-1. Various experiments were performed on both immature and matured HMC-1 cells.

### 2.1.4 Culturing of Human Bone Marrow Mast cells and RBL-2H3 Basophilic Mast cells

Human bone marrow mast cells were a kind gift of Dr Steven Krilis and were obtained from normal donors according to the protocol described in (Li, 1995). RBL-2H3 rat basophilic mast cell line was a kind gift of Dr Russell Ludowyke (Centre for Immunology, St Vincent's Hospital, University of New South Wales, Sydney, Australia). Both were cultured as described in section 2.1.1 unless stated otherwise in the specific experiments.

### 2.1.5 Toluidine Blue Staining Of Mast Cells

Cytospins of cells were prepared by addition of 80µl of the cell suspension ($0.25x10^6$cells/ml) to the well of each sample chamber (set up includes glass slide,

filter card and chamber cup: Shandon, Appendix 1C). Samples were in spun in a cytocentrifuge for 5 minutes at 500 rpm. Cytospins were stained with toluidine blue (Luna, 1992) to confirm the presence of their granules. Cytospins of the cells were air-dried for 15 min, fixed in acetone followed by 1 min dips in 95%, 70% and 25% ethanol, respectively (in Milli-Q water). Slides were washed in Milli-Q water for 2 min and stained with 0.5% toluidine blue for 5 min at RT. Cells were washed in tap water for 1 min and dehydrated in 95% ethanol for 3 min, followed by 3 min in 100% ethanol. Slides were cleared in Histoclear, blotted dry and mounted in Dako fluorescence mounting medium plus coverslips. Mast cell granules stained purple-red.

### 2.1.6 Degranulation Assays

Mast cells were stimulated to undergo degranulation with various agents, including compound 48/80, calcium ionophore A23187, PMA, and IgE/anti-IgE. Cells ($2x10^6$/ml) were added in 6-well plates and incubated with varying concentrations of the agents for 4 h or 18 h at 37 °C. Adherent cells such as RBL-2H3 cells were grown in 6-well plates until confluence and were stimulated with the above agents with the exception of monoclonal anti-DNP-IgE acting as a rat-specific IgE agent in combination with DNP-BSA.

### 2.1.7 Confirmation Of Mast Cell Degranulation

Degranulation in mast cells was confirmed by morphological characteristics using toluidine blue staining and electron microscopy.

### Toluidine Blue Staining

Air-dried cytosmears of degranulated mast cells in suspension were stained with toluidine blue as described in section 2.1.6. Granular materials in toluidine blue-stained mast cells appear as either reddish or purple-blue. Degranulated mast cells stained a lighter blue compared to a more intense shade in resting cells.

### Electron Microscopy

Untreated and treated cells were processed for electron microscopy; method used was the same for ultra structural visualization of cells described in section 2.5.2.

## 2.1.8 Epithelial Cell Cultures

### A549 and NCI-H292 Epithelial Cells

A549 and NCI-H292 cells were obtained from Dr. D. Knight (QE II Medical Center, University of Western Australia). A549 cells were derived from a human alveolar cell carcinoma; they are epithelial in morphology, hyperdiploid and represent type II alveolar cells (Lieber, 1976). NCI-H292 cells were derived from a cervical node metastasis of a pulmonary mucoepidermoid carcinoma; they are representative of the upper bronchial respiratory airways and are epithelial in morphology containing numerous mucin-secreting granules (Hierholzer, 1993).

### 2.1.9 Neuronal Cell Cultures

#### BE(2)-C and NIE-115 Neuroblastoma Cells

BE (2)-C human neuroblastoma cell line was obtained from European Collection of Cell Cultures (Appendix 1A). These cells were isolated from bone marrow of a 22-month old male with disseminated neuroblastoma in 1972. These cells are multi-potential in regards to neuronal enzyme expression and have a high capacity to convert tyrosine to dopamine. The cells have short neurite-like cell processes and grow in aggregates (Biedler, 1978). NIE-115 mouse neuroblastoma cells were kindly provided by Dr Stephen R. Bolsover, Department of Physiology, University College London, London, UK. These cells have been used as a neuronal model system and can be cultured easily. They have uses in a variety of assays and cellular investigations. N1E-115 cells contain voltage-gated $Na^+$, $K^+$, and $Ca^{2+}$ channels and have been used to investigate $Ca^{2+}$ signaling pathways (Kopper and Adorante, 2002).

## 2.2 Zinc Studies

### 2.2.1 Basal Zinc Measurement

In order to investigate the subcellular distribution of labile Zn in cells, we used the membrane-permeant Zn-specific fluorophore Zinquin. Zinquin has a relatively low affinity for Zn (Kd in the nM range) such that it is unable to compete for tightly chelated Zn in metalloenzymes and can only monitor the more labile pools. Basal Zn levels were visualized and quantified in human umbilical cord blood, rat peritoneal,

immature and mature HMC-1 cells, RBL-2H3 rat mast cells and A549 human lung carcinoma cells. For cells that were in suspension (HMC-1 and human umbilical cord blood), culture medium was removed by centrifugation at 800 g for 5 min, followed by two washes in PBS. The cell pellet was resuspended in 0.5 - 1 ml PBS followed by an incubation with 25 μM Zinquin (section 1.2.8) in PBS for 30min at 37°C. The adherent cells (RBL-2H3 and A549) were grown on glass coverslips and washed twice with PBS prior to addition of 25μM Zinquin for a further 30min at 37°C. Images of Zinquin-stained cells were taken on a fluorescent microscope and were quantified using Video Pro image analysis software (as described in 2.2.3). For greater resolution images were taken on a UV laser confocal microscope (as described in 2.2.3).

### 2.2.2 Zinc Manipulation Assays

Cells were either depleted or supplemented with exogenous Zn in the form of $ZnSO_4$ and the membrane permeable Zn chelator TPEN, respectively. The experiments were performed to determine if Zn was released following mast cell degranulation, the effects of Zn depletion on caspase-3 activation and on activation of the transcription factor NF-κB.

#### Zinc Depletion Assays

TPEN was used at 25 – 100 μM for 3 - 4 h at 37 ° C. Chelation of intracellular Zn was monitored by Zinquin fluorescence. In some experiments TPEN was added in combination with butyrate at 1-4 mM or staurosporine at 1 μM. Detailed description and structure of TPEN is included in section 1.2.9.

**Zinc Supplementation Assays**

$ZnSO_4$ (25 μM) was added to cells along with varying concentrations of pyrithione (stated in specific experiments), a Zn ionophore for 30 min at 37 ° C (Figure 1.4). In NF-κB activation experiments, NCI-H292 human alveolar epithelial carcinoma cells were cultured on glass coverslips and were incubated with or without $ZnSO_4$ and pyrithione for 60 min at 37 ° C. Increase in intracellular Zn was monitored by Zinquin fluorescence.

### 2.2.3 Fluorescence Image Analysis

For fluorescence image analysis, specimens were examined using an Olympus fluorescence microscope, equipped with a UV-B dichroic mirror for low wavelength excitation, and connected to a CCTV video colour camera and computer workstation. Images were captured and fluorescence was quantified using the Video Pro Image Analysis Software Version 4.02 (Leading Edge, South Australia.).

For greater resolution of the subcellular distribution of Zn in the cells, Zinquin-loaded cells were examined using a Bio-Rad MRC-1000 Laser Scanning Confocal Microscope System, equipped with a UV-Argon laser, and in combination with a Nikon Diaphot 300 inverted microscope in fluorescence mode (with excitation at 363/8 nm and emission at 460LP). Untreated or degranulated mast cells in suspension (immature and mature HMC-1) were prepared as cytospins on microscope slides with a drop of Dako fluorescence mounting medium and coverslip on top. Adherent cells cultured on coverslips (25 mm square) were inverted onto microscope slides with a

drop of Dako fluorescence mounting medium with a coverslip on top. The edges of all coverslips in both adherent and non-adherent cells were sealed with nail polish. Images were collected using a 40x water immersion objective lens with NA 1.15. Each image was averaged over 4 scans by Kalman filtering. Fluorescence intensity of cells was quantified using Video Pro analysis software (Version 4.02 Leading Edge, South Australia).

## 2.3 Apoptosis Assays

### 2.3.1 Induction Of Apoptosis By Butyrate And TPEN

Cells were primed with concentrations of sodium butyrate made in culture medium without FBS for 18 h at 37°C. These cells were further treated with TPEN for 4 h at 37°C.

### 2.3.2 Caspase Assay

Caspase-3 was assayed by cleavage of fluorogenic substrate zDEVD-AFC (z-asp-glu-val-asp-7-amino-4-methyl-coumarin) (Figure 2.1). Cells ($5x10^6$-$10^7$ per flask) were cultured with test reagents, washed once with 5 ml PBS and resuspended in 1 ml of NP-40 lysis buffer (5mM Tris-HCL pH 7.5, containing 5mM EDTA and 0.5% NP-40). After 15 min in lysis buffer at 4°C, insoluble material was pelleted at 15,000 g and an aliquot of the lysate was tested for protease activity. 50 µl of cell lysate was added to each assay tube containing 8 µM of substrate in 1 ml of buffer (50 mM Hepes, 10% sucrose, 10mM DTT, 0.1% CHAPS, pH 7.4). After incubation overnight at RT, caspase activity was quantified by fluorescence (Excitation wavelength 400 nm,

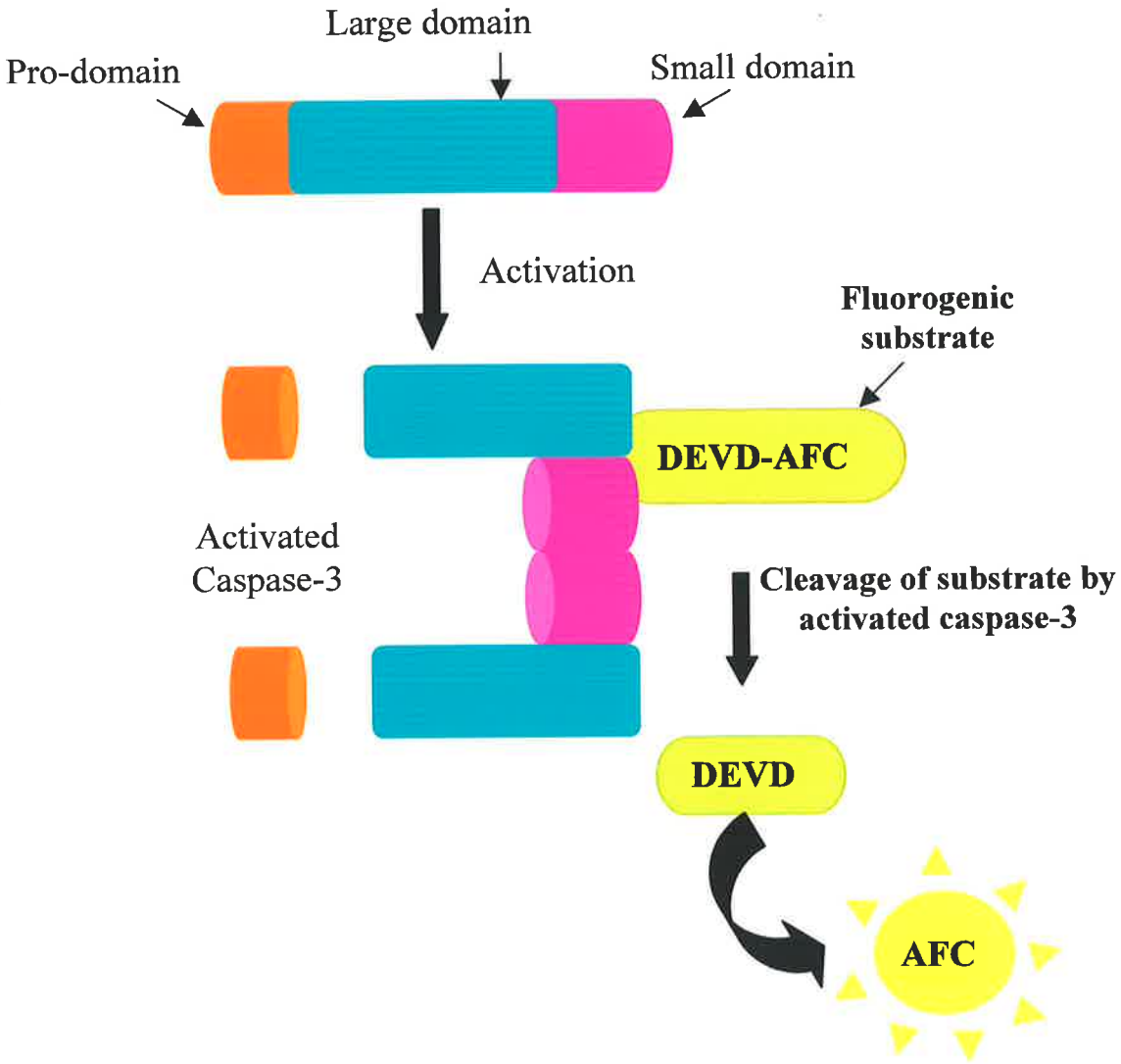


**Figure 2.1: Cleavage Of DEVD-AFC Fluorogenic Substrate By Active Caspase-3.**

Activation of caspase-3 involves the removal of its pro-domain and separation of the large and short domains, reassembling to form a tetramer which is the active caspase-3. Active caspase-3 can cleave DEVD-AFC releasing the coumarin derivative AFC. This is now fluorescent.

Emission wavelength 505 nm) in a Perkin Elmer LS50 spectrofluorimeter. Optimal amounts of added lysate and duration of assay were taken from linear portions of curves determined in preliminary experiments. One unit of caspase activity was taken as one fluorescence unit (with slit width of 5 nm) per h incubation with substrate. Caspase activity was then converted to picomoles of DEVD-AFC cleaved per h calculated from an AFC standard curve (Figure 2.2).

Fluorogenic substrates of caspase-1 (z-VAD-AFC), -2 (z-VDVAD-AFC), -4 (Ac-LEVD-AFC), -5 (Ac-WEHD-AFC), -6 (z-VEID-AFC), and -9 (Ac-LEHD-AFC) were also used as for *z*-DEVD-AFC. The activities of these caspases were also converted to picomoles of DEVD-AFC cleaved per h calculated from an AFC standard curve.

### 2.2.3 Protein Measurements

Protein concentrations of cell lysates used in caspase activity assay were determined using the BioRad Dc protein reagent kit (Appendix 1B). The protein concentration for each treatment was incorporated into units of caspase activity as caspase activity per hour per mg of protein. It was found that the total protein content of cells did not directly relate to the caspase enzyme activity and hence activity was expressed per volume of lysates added.

### 2.2.4 Morphological Criteria And Chromatin Fragmentation

Apoptosis was also confirmed in randomly selected samples by morphological criteria and DNA fragmentation (Medina, 1997). A minimum of 300 cells from replicate tubes were scored. For morphological assessment, cells were examined by phase

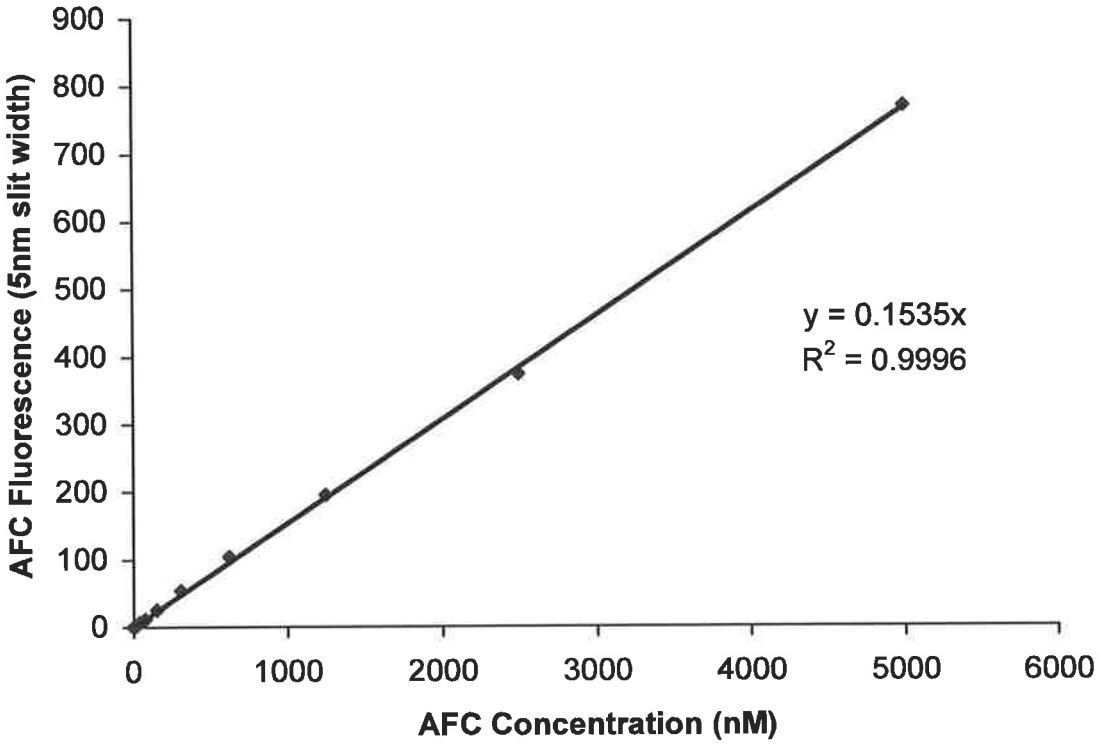


**Figure 2.2: DEVD-AFC Standard Curve.**

contrast microscopy after addition of an equal volume of 0.2% trypan blue in HBSS, pH 7.4. Apoptotic cells were distinguishable from normal cells by their nuclear fragmentation, presence of apoptotic bodies, decreased size and sometimes, intense membrane blebbing. Cells with one or more of these properties were scored as positive. In most cases, they excluded trypan blue. In some experiments, Hoechst dye #33342 was added to a final concentration of 1 μg/ml and cells were analyzed by fluorescence microscopy for chromatin segregation.

## 2.4 Immunofluorescence Labelling

### 2.4.1 Pro-Caspase-3, -4 And $ZnT_4$ Labelling

Immunolabellings for pro-caspase-3 and -4 and $ZnT_4$ were performed based on a previously described method (Menon, 1993), with modifications. For cells in suspension, cytospins were used and for adherent cells, cells were grown on coverslips. Prior to labelling, both cytospin and coverslip grown cells were fixed in 4% paraformaldehyde in PBS for 20 min at RT, followed by three washes in cold 1% BSA + PBS and a further three washes in cold PBS for 3 min each. Cells were permeabilised in 0.2% Triton X-100 in PBS for 10 min at -20°C, followed by three washes in cold PBS for 2 min each. To prevent non-specific binding, cells were incubated with 1% BSA + PBS at RT for 20 min, followed by three washes in PBS for 3 min each. Incubation with respective primary antibodies was done overnight in a moist container. For pro-caspase-3, the primary antibody used was polyclonal rabbit anti-caspase-3; for caspase-4, polyclonal goat anti-caspase-4 and for $ZnT_4$ it was polyclonal rabbit anti-rat $ZnT_4$.

Following overnight incubation, cells had three washes with cold 1% BSA + PBS followed by another 3 washes in cold PBS for 2 min each. Incubation with secondary was at RT for 2 h. For pro-caspase-3, the secondary antibody used was a FITC-conjugated goat anti-rabbit IgG, for pro-caspase-4; FITC-conjugated bovine anti-goat IgG and for $ZnT_4$; FITC-conjugated goat anti-rabbit IgG. After incubation, cells were washed three times with cold 1% BSA + PBS at 3 min each followed by another two washes in cold PBS for 2 min each. Cytospins were mounted with Dako fluorescence mounting medium with a glass coverslip. Adherent cells on coverslips were inverted onto microscope slides with the same fluorescence mounting medium. Labelling was visualized under fluorescence microscopy.

### 2.4.2 NF-κB Labelling

For NF-κB labelling, human epithelial cells (NCI-H292) were either stimulated with 20 ng/ml TNF-α or were untreated. Mast cells were stimulated with degranulators used in degraunlation assays (section 2.1.6). Preparation of cells was the same as in section 2.4.1, except blocking was with 0.05% Tween-20 + 3% BSA in PBS for 20 min at RT, followed by 2 washes in cold PBS for 2 min each. Cells were then incubated with rabbit polyclonal IgG against the p65 subunit of NF-κB at 1:20 dilution, at RT in a humidified container overnight. Cells were washed three times with cold 1% BSA + PBS for 3 min each at RT, followed by two washes with cold PBS for 2 min each at RT. FITC-conjugated goat anti-rabbit IgG was then added for a further 1.5 h at RT. After the incubation, cells were washed with 1% BSA + PBS and cold PBS as described above. A drop of Dako anti-fade fluorescence mounting

medium was added to the cells. Labelling was visualized under fluorescence microscopy.

### 2.5 Electron Microscopy

Electron microscopy was used for ultra-structural analysis of mast cells and labelling of caspase-3, -4 and $ZnT_4$ in mast cells. It was performed with the assistance of the Centre for Electron Microscopy and MicroStructure Analysis (CEMMSA) at the University of Adelaide.

#### 2.5.1 Ultra Structural Visualization Of Cells

Mast cells were washed with PBS (850 g for 5 min); pellet obtained was resuspended in a fixative containing 1.25% glutaraldehyde, 4% paraformaldehyde, and 4% sucrose in PBS, pH 7.2 for 1.5 h at RT. Fixative was discarded (by centrifugation at 850 g for 5 min) and cells were washed twice (850 g for 5 min) with washing buffer (4% sucrose in PBS) and washed two more times with buffer at 10 min each. A rotator was used in the following steps to ensure adequate mixing. The pellet collected was resuspended in 2% osmium tetroxide ($OsO_4$) for 2 h, centrifuged at 2000 g for 10 min and supernatant discarded. Cell pellet was taken through a series of dehydrations using graded ethanol concentrations of: 70%, 90%, 95% and 100% for 20 min on a rotator. After two changes in 100% ethanol, cell pellet was suspended once more in 100% ethanol for 2 h and embedded in a 1:1 mixture of epoxy resin and 100% ethanol overnight. Following overnight incubation, remaining resin and ethanol was discarded, and cells were embedded in 100% of the epoxy resin for 8 h, a fresh

volume of resin was changed followed by incubation overnight. As a final step 100% fresh resin was added to the cells for 4 h and was removed by centrifugation.

Cells were polymerized by the addition of two drops of 100% resin into a gelatin capsule, followed by drop wise addition of the cells into the capsule. The capsule was filled with 100% resin to prevent air form entering and left at RT for 4 h before being placed in a 70°C oven overnight to allow polymerization to a solid block for sectioning. Sections of 60-80 nm were cut, placed on 200 μm mesh nickel grids and viewed using a Philips CM100 transmission electron microscope. Images were captured at various magnifications ranging from 5800x to 100000x using the analySIS software (Soft Imaging Systems, Germany).

### 2.5.2 Immunogold Labelling Of Cells

For immunogold studies, cells were fixed in a gentler fixative made up of 0.25% glutaraldehyde, 4% paraformaldehyde and 4% sucrose in PBS and embedded in LR White resin instead of epoxy. Cells were resuspended in an aqueous solution of 50% ethanol for 10 min on a rotator and centrifuged at 2000 g for 10 min; excess ethanol was removed and cells resuspended in a solution of 70% ethanol for 1 h; this (70% ethanol step) was repeated. Excess ethanol was removed and cells were suspended in a 1:1 mix of 70% ethanol and LR White resin for 1 h on a rotator. Excess resin was removed and cells were resuspended in a 1:2 mix of 70% ethanol and LR White resin for 1 h. This was repeated with cells resuspended in the same mixture of LR White and 70% ethanol for another h, followed by an overnight incubation on a rotator. Cells were incubated for a further 3 h with a fresh volume of LR White resin.

Following polymerization (section 2.5.1) and sectioning, sections were placed on nickel grids.

For immunolabelling, grids were washed twice with glycine, with the dull face of each grid touching drops of glycine for 10 min. Blocking was with 1% ovalbumin solution (1% ovalbumin in PBS with 0.5% Tween 20 and 0.1% Triton-X-100 added) for 20 min; grids were dried by blotting sides with Whatman filter paper.

Incubation with primary antibodies was performed at 1:100 for caspase-3 (polyclonal rabbit anti-caspase-3) and caspase-4 (polyclonal goat anti-caspase-4) and 1:200 for $ZnT_4$ (polyclonal rabbit anti-rat); dilutions were made in 1% ovalbumin in PBS and incubated overnight at 4°C. Following incubation, grids were rinsed six times in 1% ovalbumin in PBS for 5 min each then blotted on filter paper. Incubation with gold-conjugated secondary antibodies made in 1% ovalbumin in PBS for 1.5 h at RT. Secondary immunogold antibodies used were goat anti-rabbit IgG for caspase-3 and caspase-4 for all mast cell types at 1:100 dilution except for RBL-2H3. For RBL-2H3 rabbit anti-goat immunogold antibody (cross reactive with rat) was used at 1:200 dilution. Controls consisted of either grids incubated with either normal rabbit or goat serum (dependent on secondary antibody species) or with 1% ovalbumin in PBS. Grids were rinsed in drops of PBS six times for 5 min each, followed by washes in a series of four small beakers filled with Millipore filtered water and blotted on filter paper.

Counter staining was with uranyl acetate for 10 min, specimens protected from light by covering grids with aluminium foil and rinsed in double distilled water. Grids were

then stained with lead citrate for 10 min in the presence of sodium hydroxide crystals to facilitate carbon dioxide absorption and washed in double distilled water.

Grids were viewed under a Philips CM100 transmission electron microscope with images captured under various magnifications ranging from 5800x to 100000x using the analySIS software (Soft imaging systems, Germany). The number of gold particles in mast cell granules was counted in all control and test samples. The counts were expressed as mean ± SEM gold particles per granule. To allow for variation in granule size, granule area was calculated using the analySIS software (CEMMSA, Adelaide University); counts were expressed as mean ± SEM gold particles per $\mu m^2$ of granule, unless stated otherwise. The data was analysed statistically by ANOVA and Student's *t*-test.

### 2.6 $ZnT_4$ And Pro-caspase-3 mRNA Expression by Northern Hybridization

mRNA expression of both $ZnT_4$ and pro-caspase-3 was determined by northern hybridization. This technique involves: a) isolation of mRNA from cultured cells, b) transfer of RNA to hybridization filter, c) preparation of $ZnT_4$ and pro-caspase-3 probe, d) northern hybridization of transferred RNA using the probe and finally e) stripping of signals from the northern blot.

#### 2.6.1 Isolation Of RNA From Cells

RNA was isolated from confluent flasks of cells using the Qiagen RNeasy mini protocol (Qiagen) and the Trizol method. Following the Qiagen (Appendix 1B) mini protocol, cells were lysed with 300-500 µl of buffer RLT (part of kit with added β-

mercaptoethanol) and homogenized by passing through a 20-G (0.9 mm) needle. The homogenized lysate was mixed with an equal volume of 70% ethanol, and added to a mini spin column (placed in a collecting tube), centrifuged at 8 000 g for 15 sec, flow-through material was discarded. RW1 washing buffer was then added to the mini spin column and re-centrifuged (8 000g for 15 sec) and flow-through was also discarded. 500 µl of buffer RPE was added to the column and centrifuged (8000 g for 15 sec) with flow-through discarded. Excess ethanol was removed from the column by adding 500 µl buffer RPE and centrifuged (10 000 g for 2 min). The mini column was then placed in a new collecting tube and 30 µl of sterile Milli-Q water was added and left to stand for 2 min, followed by centrifugation for 1 min at 10 000 g. Another volume of sterile Milli-Q water was added to the column and left to stand for 5 min, before centrifugation for 2 min at 10 000g. Eluates obtained from both spin were kept as they contained pure RNA. The RNA was stored at -80°C.

**Trizol Method**

Isolation of mRNA from cells using Trizol (Appendix 1B) involved lysing cells with 1 ml of Trizol for 5 min at 15- 30°C. 0.2 ml chloroform was added for each 1 ml Trizol and mixture shook vigorously for 15 sec, incubated at RT for 15 min and centrifuged at 12, 000 g for 15 min at 4°C. This facilitated the separation of layers consisting of a bottom red phenol-chloroform layer, middle layer and a colourless layer at the top of the tube. RNA exists exclusively in the top layer; and this was transferred to a fresh tube. 0.5 ml isopropyl alcohol was added per 1 ml of Trizol and mixture incubated for 10 min at RT, centrifuged at 12, 000 g for 15 min at 4°C. RNA precipitate was seen as a gel-like pellet on the side of the tube. The supernatant was

discarded. RNA pellet was washed once with 1 ml 75% ethanol (7500 g for 5 min at 4°C), and supernatant was discarded. RNA pellet was washed with sterile Milli-Q water and pellet was air-dried at RT for 1 h. Once dried, pellet was resuspended in 30 µl of sterile Milli-Q water and incubated at 60°C for 10 min. RNA was stored at -20°C.

To confirm that isolated RNA was not degraded, a mini-gel was prepared; 0.5 g DNA grade agarose was dissolved in 37 ml of diethyl pyrocarbonate (DEPC)-treated water by heating. Once dissolved, 5 ml of 10X MOPS buffer was added and the solution cooled to 60°C. 8 ml of 40% formaldehyde was added prior to the gel being poured. 3 µl of RNA was mixed with 3 µl RNA loading buffer, heated for 5 min at 65°C, followed by 5 min on ice. Gel was run for 20 min at 90V. RNA integrity was visualized with Kodak gel imaging software.

### 2.6.2 RNA Transfer To Hybridization Filter

10 µg of RNA was mixed with an equal volume of RNA loading buffer, heated for 5 min at 68°C and then put on ice for 5 min. RNA was loaded on a 1% agarose gel containing 1x MOPS and 17% formaldehyde with a total volume of 300 ml. RNA was run on a 1% agarose gel with a total volume of 150 ml for 2 h at 80V. Excess formaldehyde was removed by soaking in Milli-Q water (rocking platform) for 15 min and viewed under the UV transilluminator. Gel was further soaked in 10x saline sodium citrate buffer (SSC) for 10 min and a downward stack was set up consisting of pre-soaked thin towellings as the top layer in the same dimensions as the gel, 3 pieces

of pre-soaked 3mm Whatman paper the shape of the gel, followed by the nylon membrane filter cut out to the dimensions of the gel, another 3 pieces of pre-soaked 3mm Whatman filter paper the shape of the gel and at the bottom, two thick layers of teri-wipes toweling and normal paper toweling (Figure 2.3).

Volumes of 10x SSC transfer solution were dribbled onto the top of the stack every 15 min for 4 h. After transfer, the RNA was UV cross-linked to the filter and photographed. The positions of the 18S and 28S rRNA bands were marked on the filter paper with pencil; the filter was then air dried and stored between two sheets of 3 mm Whatman filter paper.

### 2.6.3 Preparation Of $ZnT_4$ DNA Probe For Northern Hybridization

$ZnT_4$ probe was prepared by isolating a 1.4 kb fragment containing the open reading frame for this Zn transporter from two expression vectors; pc-DNA3 and pGEFP-N3.

### Isolation Of $ZnT_4$ Fragment From pc-DNA3

A restriction digest was performed to cut the 1.4 kb fragment from the 5.4 kb pcDNA3 (Figure 2.4) containing the open reading frame of the Zn transporter $ZnT_4$. For the digest, 3 μg of the vector was used with 50 units of the following restriction enzymes: BamH I, Not I and Xba I, enzyme buffer 2 and Milli-Q water was used to make up the total volume of the reaction. The digest reaction was incubated at 37°C for 1.5 h. Restriction by BamH I and Not I excised the 1.4 kb fragment (Figure 2.5); hence a larger digest using 15 μg of plasmid with BamH I and Not I was performed for 1.5 h at 37°C followed by incubation at 4°C. The fragment was visualized by

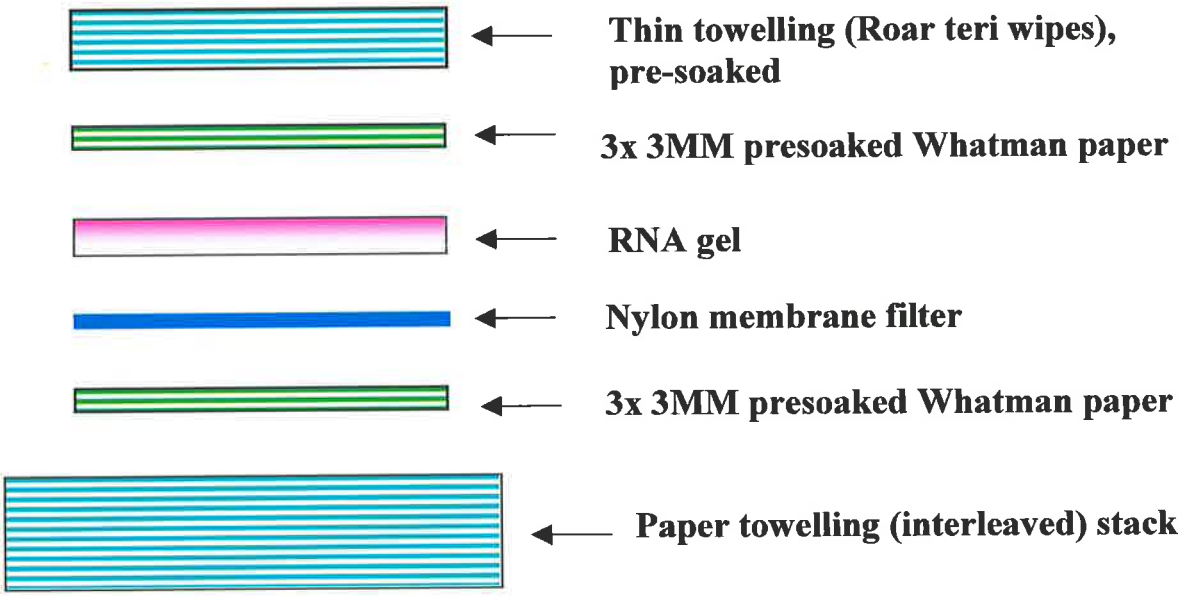


**Figure 2.3: Northern Blot Transfer Stack.**

Stacking order of towels, filter papers, nylon membrane and RNA gel for transfer.

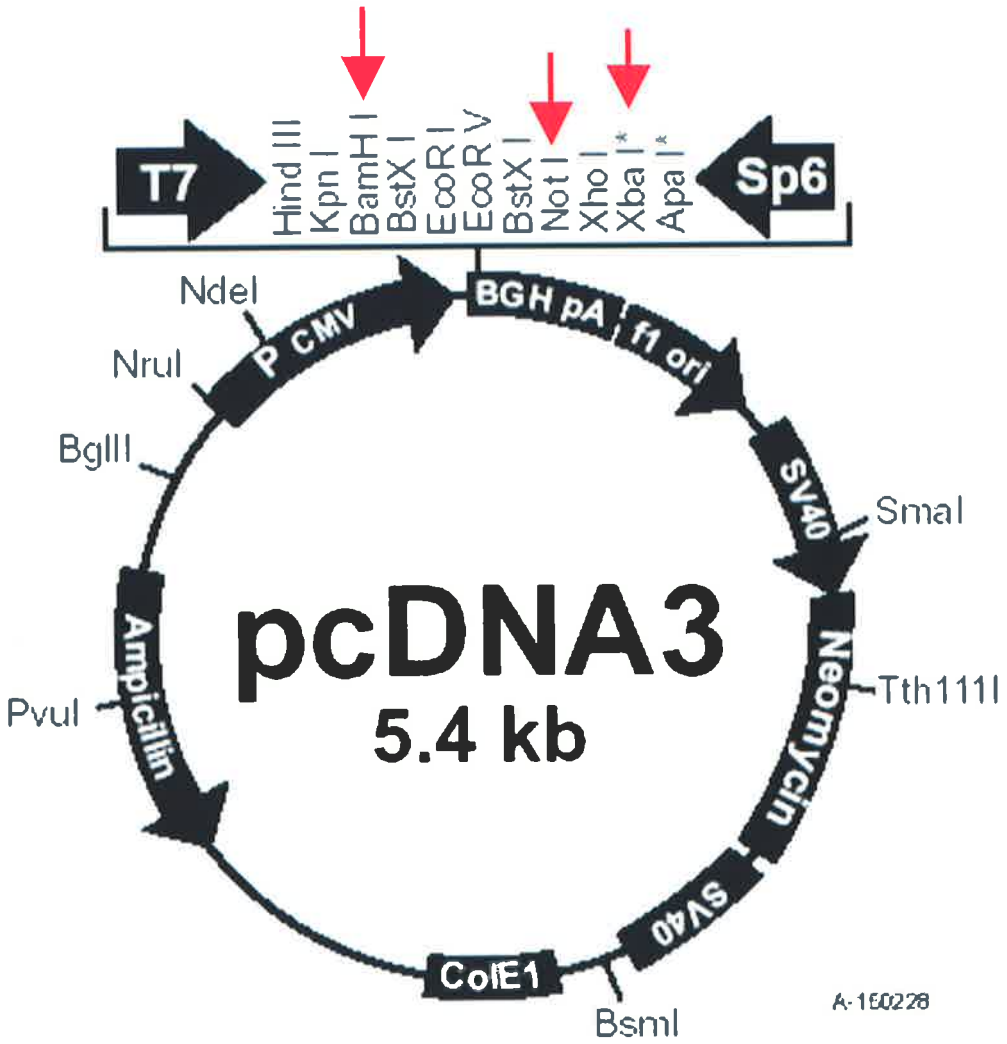


**Figure 2.4: Expression Vector pcDNA3**

pcDNA3 vector containing 1.4 kb fragment that has the open reading frame for the Zn transporter $ZnT_4$. Red arrows indicate sites of excision.

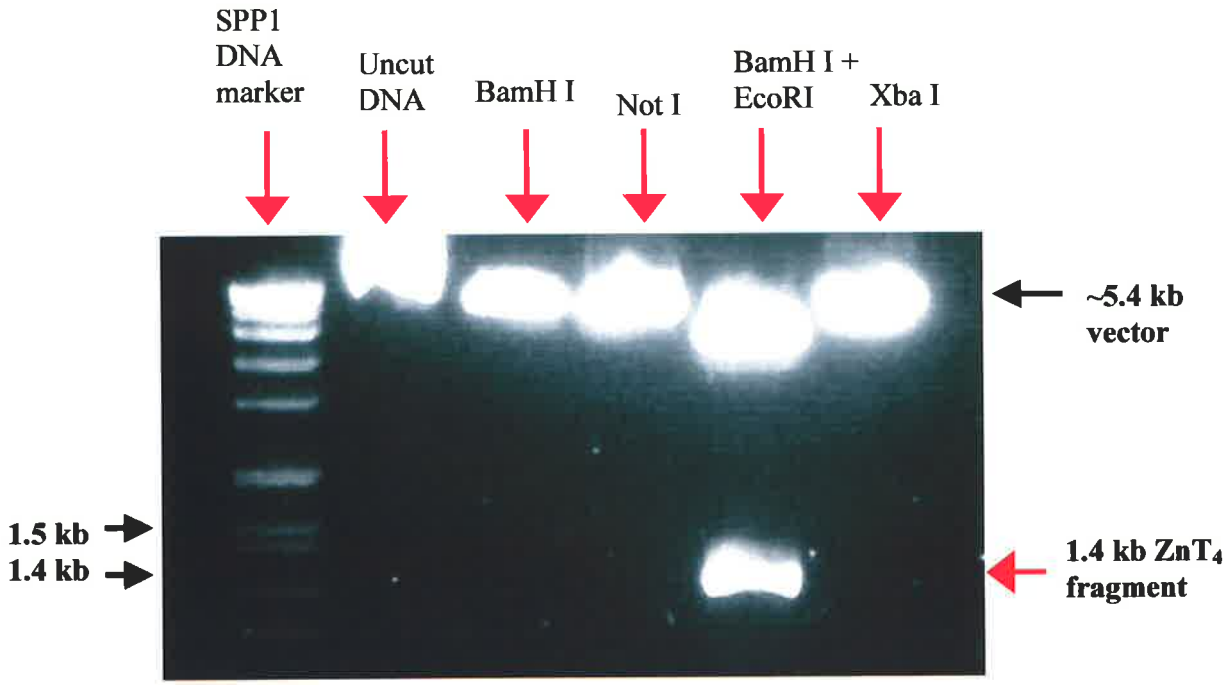


**Figure 2.5: Restriction Digest of pcDNA3 by BamH I, Not I, BamH I + EcoR I for $ZnT_4$ Fragment.**

1.4 kb fragment containing the open reading frame for the Zn transporter $ZnT_4$ was excised by several restriction enzymes indicated above with red arrows. It was found that restriction digest with a combination of BamH I and Not I resulted in the 1.4 kb fragment.

electrophoresis on a 1% low melting point agarose gel in 1x TAE buffer (1 g low melting point agarose dissolved into 100 ml of 1x TAE buffer, cooled for 10 min and 15 µl of 1mg/ml ethidium bromide) for 2.5 h at 65V. SPP1/*EcoRI* DNA molecular weight marker was included in the agarose gel for identification of fragment size (Figure 2.5).

**Isolation Of $ZnT_4$ DNA Fragment From pGEFP-N3 Vector**

The $ZnT_4$ DNA fragment was also isolated from a restriction digest using both BamH I and EcoR I restriction enzymes from the pGEFP-N3 vector (Figure 2.6). The resulting digest showed a fragment of 1.4 kb size (Figure 2.7). The same protocol was followed as described in 2.6.4.

**Purification Of $ZnT_4$ DNA Fragment**

The 1.4 kb fragment was cut out of the gel and DNA extracted using the Qiagen quick gel extraction kit. Briefly, the excised DNA fragment was melted and for each 100 µl of gel volume, 300 µl of buffer QG was added. One gel volume of isopropanol was added to the mixture. To bind the DNA, 800 µl of sample mixture was added to a QIAquick spin column placed inside a 2 ml eppendorf and this was centrifuged at 8 000 g for 1 min; flow-through was discarded. This was repeated until all of the sample volume was added to the spin column. DNA was washed with buffer PE and column left to stand for 5 min, then centrifuged for 1 min at 8 000 g and flow-through was again discarded. The spin column was then placed in a new 1.5 ml eppendorf and DNA was eluted with slight modifications to the kit instructions. 20 µl of sterile

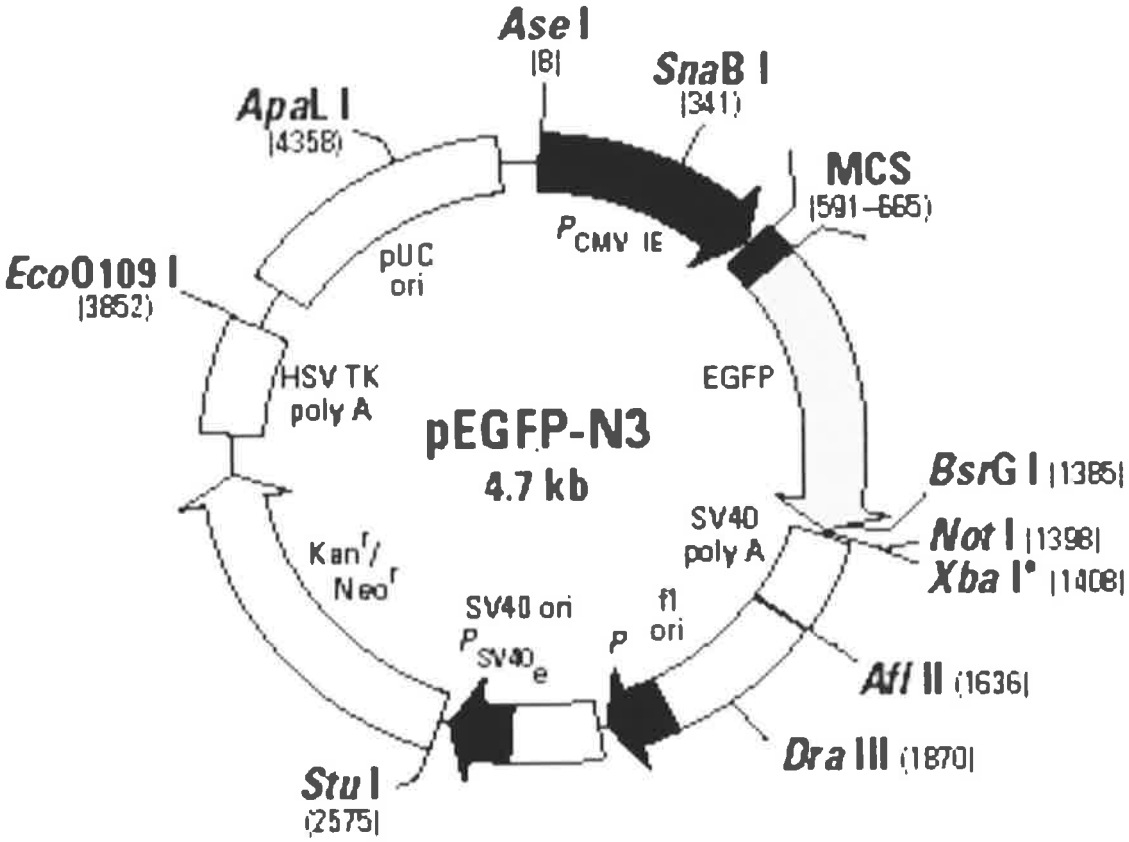


**Figure 2.6: pGEFP-N3 Mammalian Expression Vector**

1.4 kb fragment containing the open reading frame for the Zn transporter $ZnT_4$ was excised within the insert with a combination of BamH I and EcoR I (not shown) which resulted in the 1.4 kb fragment.

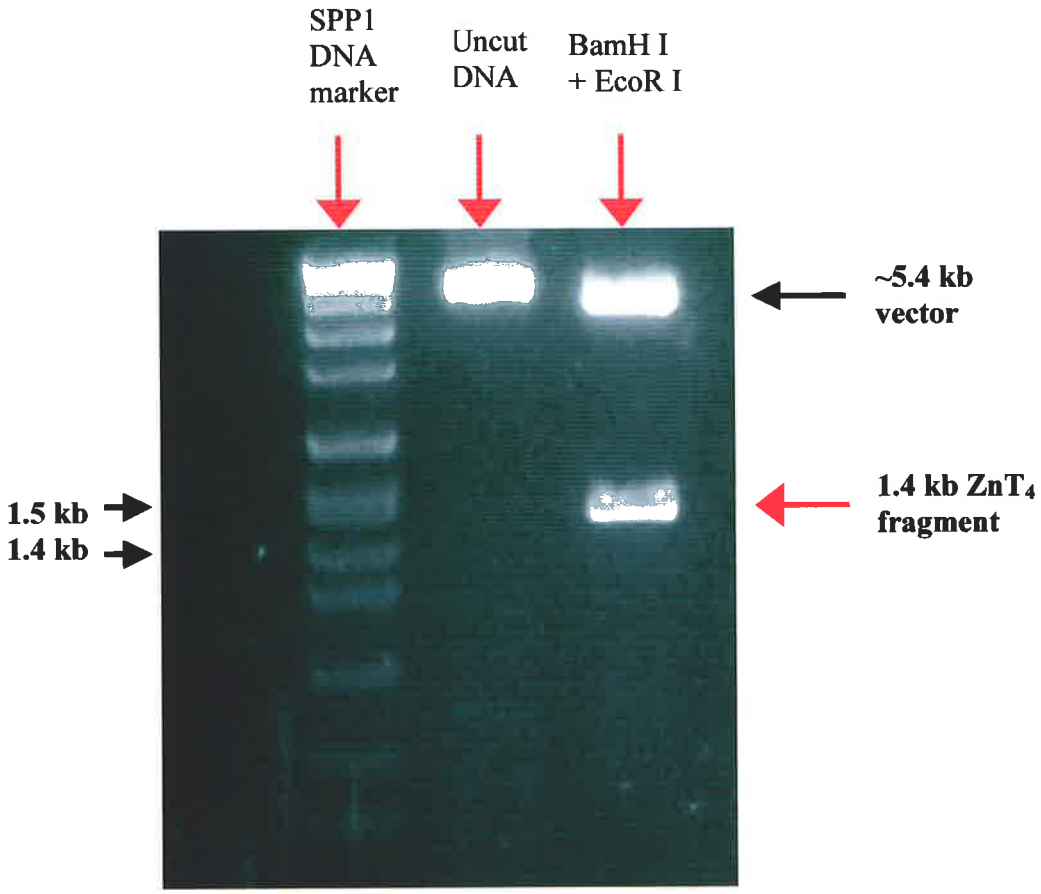


**Figure 2.7: Restriction Digest of pGEFP-N3 by BamH I and EcoR I for $ZnT_4$ Fragment.**

1.4 kb fragment containing the open reading frame for the Zn transporter $ZnT_4$ was excised by several restriction enzymes indicated above with red arrows. It was found that a combination of BamH I and EcoR I resulted in the 1.4 kb fragment.

Milli-Q water was added to the spin column; this was left for 5 min and then centrifuged for 1 min at 8 000 g; flow-through was kept. Another volume of sterile Milli-Q water was added to the column and left for 5 min and then centrifuged as before. The volumes accumulated from both spins were kept and stored at -20°C until pure DNA was confirmed on a gel.

A small volume of isolated DNA added to loading buffer was visualized on a 1% DNA grade agarose gel made in 1x TAE buffer (with ethidium bromide); SPP1 DNA molecular weight marker was included. In cases where DNA was not pure, it was precipitated by ethanol. Two DNA sample volumes of 100% ethanol and 1/10 sample volume of sodium acetate (pH 5.2) were added to the sample. The mixture was centrifuged at 8 000 g for 30 min at 4°C and supernatant discarded. The pellet was dissolved with 500 µl of 70% ethanol and centrifuged for 30 min at 8 000 g at 4°C and the supernatant was again discarded. The pellet was air dried for 1 h to a semi-transparent appearance and dissolved in 50 µl of sterile Milli-Q water.

**Controls For $ZnT_4$ Northern Hybridization**

Expression of $ZnT_4$ was determined by northern hybridization with positive control as the Madin-Darby canine kidney II cells (MDCK II) transfected with the full length of rat $ZnT_4$-myc cDNA and cultured in medium lacking doxycycline (MDCK II Dox -). The negative control was transfected MDCK II cells cultured in medium in the presence of doxycycline (MDCK II Dox +). MDCK II Dox + expresses little or no $ZnT_4$.

### 2.6.4 Preparation of Pro-caspase-3 DNA Probe For Northern Hybridization

mRNA expression of pro-caspase-3 in mast cells was determined by northern hybridization. Pro-caspase-3 probe was prepared by isolating DNA insert from pGEM-T-Easy plasmid, amplified and further purified for probing.

#### Isolation Of Pro-caspase-3 Insert From pGEM-T-Easy Plasmid

Human pro-caspase-3 insert was isolated from pGEM-T-Easy plasmid (Figure 2.8) collected from *E. coli* JM109 bacteria (kind gift of Dr Prue Cowled, Department of Surgery, QEH) using the Qiagen plasmid midi kit. Briefly, bacterial cells were harvested (centrifugation at 6000 g for 15 min at 4°C), and cell pellet was resuspended in buffer P1 and buffer P2 at RT for 5 min. Buffer P3 was added to the suspension, mixed and incubated on ice for 20 min. Suspension was centrifuged at 20 000 g for 30 min at 4°C and supernatant containing the plasmid DNA was removed. The supernatant was re-centrifuged at 20 000 g for 15 min at 4°C and supernatant was collected and was allowed to flow through a resin column via gravity flow then washed with 2 volumes of buffer QC. DNA was eluted with 5 ml of buffer QF and precipitated with 3.5 ml isopropanol, mixed and centrifuged immediately at 15 000 g for 30 min at 4°C; supernatant was carefully decanted afterwards. The remaining DNA pellet was washed with 70% ethanol and centrifuged at 15 000 g for 10 min, supernatant was decanted without disturbing the pellet. The pellet was air dried for 10 min and redissolved in 50 µl Milli-Q water and stored at 4°C.

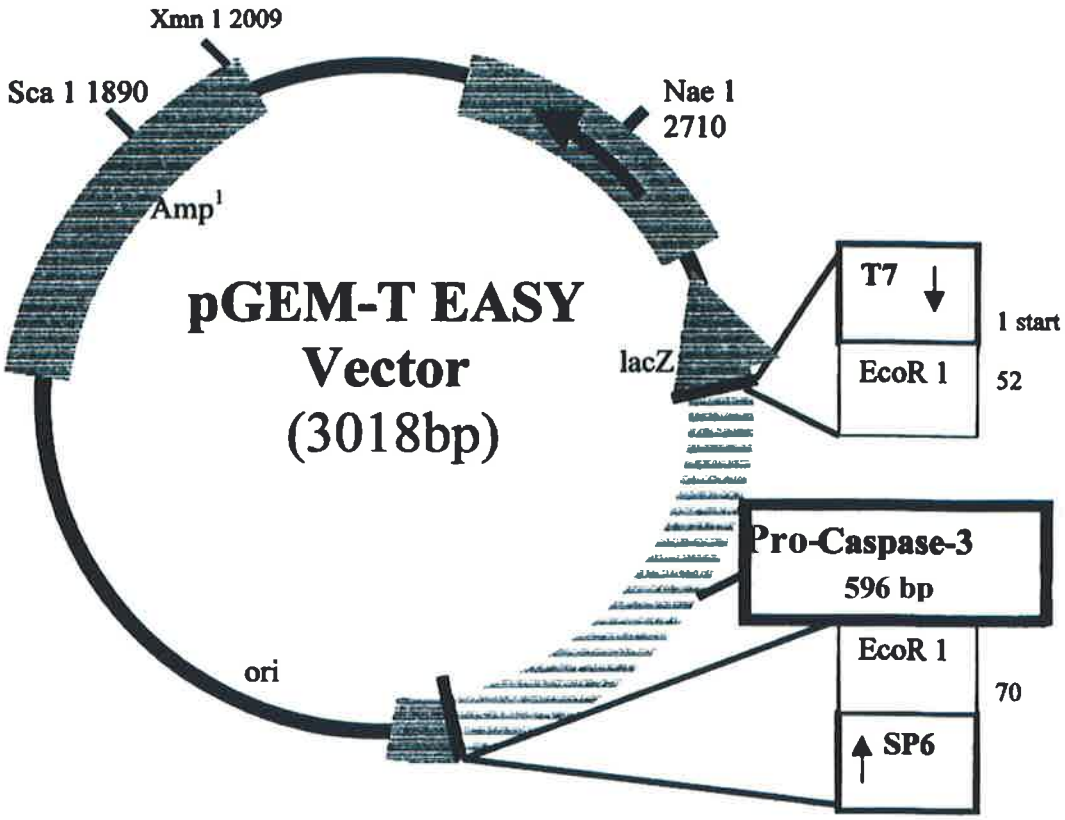


**Figure 2.8: pGEMT-EASY containing Pro-caspase-3 DNA insert**

pGEMT-EASY circular map containing the pro-caspase-3 insert.

**PCR Amplification Of Pro-caspase-3 DNA Insert**

To confirm the presence of the 596 bp pro-caspase-3 insert, PCR amplification was performed with primers SP6 and T7 (kind gift of Dr Prue Cowled, Department of Surgery, QEH). PCR amplification was carried out with 0.1 µl Taq polymerase, 10x reaction buffer, 50 ng of each primer, 0.4 mM dNTPs and 1 mM $MgCl_2$ and template cDNA in a final volume of 25 µl. In each PCR reaction, a positive and a negative control was included, one where sterile water replaced template cDNA and the other with 100 ng of UPIUB dam-DNA (provided by Department of Surgery, QEH). PCR reactions were carried out in a PTC DNA Engine Peltier Thermal cycler. Cycle conditions began with 5 min at 94°C, to denature template DNA, followed by 35 cycles of denaturation for pro-caspase-3 PCR, 1 min at 94°C, 1 min at annealing temperature of 51°C for caspase-3 primers {the annealing temperature was determined using the formula Tm (melting temperature) = 2(A+T) + 4(G+C)}, followed by 1 min elongation at 72°C. A final elongation step of 5 min at 72°C was added to the end of each amplification program and product was incubated at 4°C. 10 µl aliquot of each PCR product of the reaction was visualised by 1% TAE agarose gel electrophoresis along with 10 µl aliquot of DNA markers; SPP1 and 1 kb DNA Ladder Plus (Figure 2.9).

**Purification Of Pro-caspase-3 DNA Insert**

A restriction digest was performed using EcoR I to excise the pro-caspase-3 insert from the plasmid. For a single reaction, 5 µg of plasmid DNA was added to 5 µl of EcoR I restriction enzyme (20 000 units/ml), 10 µl EcoR I buffer and 82 µl sterile

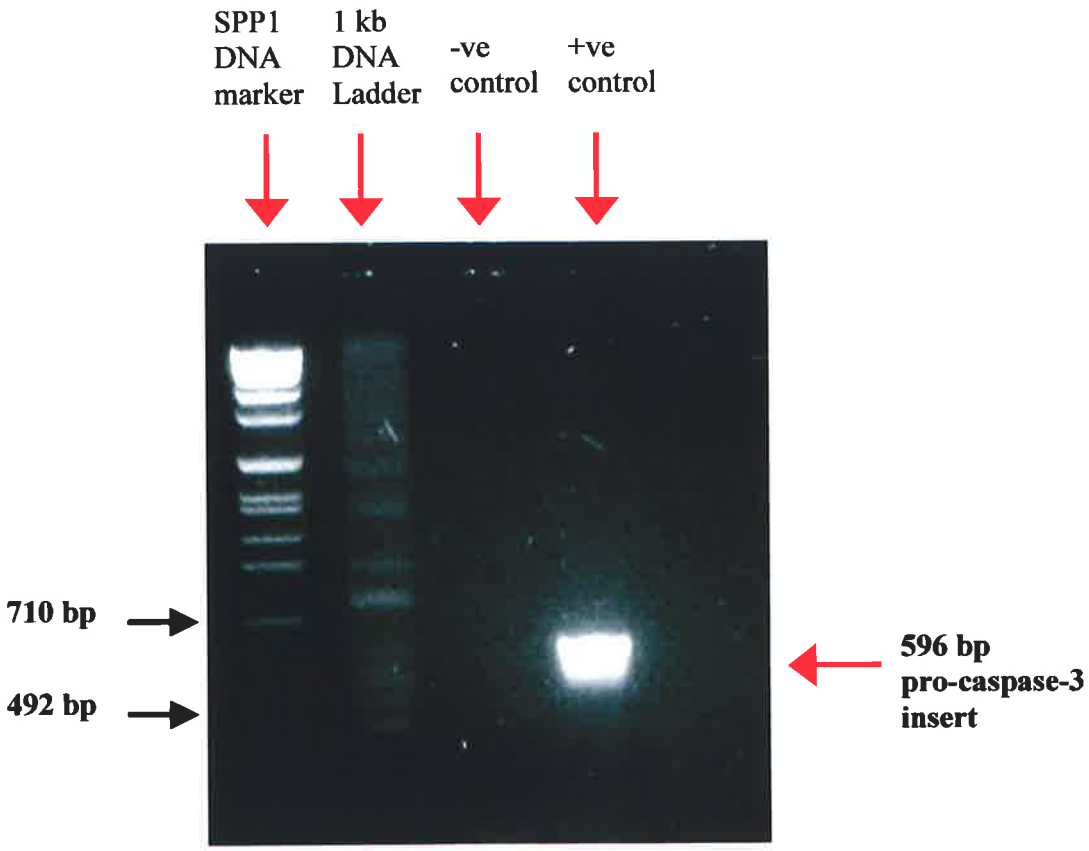


**Figure 2.9: PCR amplification of Pro-caspase-3 DNA insert.**

PCR amplification of pro-caspase-3 digest using SP6 and T7 primers with SPP1 and 1 kb DNA Ladder Plus markers. Negative (-ve) control contains no DNA and positive (+ve) control contains the 596 bp pro-caspase-3 DNA insert.

Milli-Q water. The reaction was incubated at 37°C for exactly 1.5 h, followed by incubation on ice. A 5 µl aliquot of the digested product mixed with DNA loading buffer and 10 µl aliquot of SPP1 DNA marker was visualised on 1% low melting point agarose gel. The remaining product of the digestion was also visualised in another 1% low melting point agarose gel. The gel was then viewed under UV transilluminator and the 596 bp band was excised using a sterile scalpel blade. The gel slice was placed in a 1.5 ml eppendorf tube, heated to 70°C and the melted gel was purified using the QIAquick gel extraction kit. The purified DNA was stored at –20 °C until it was probed.

**Expression Of Pro-caspase-3 mRNA By Northern Hybridization**

Expression of pro-caspase-3 was determined in various mast cell types by northern hybridization with positive controls (described below).

**Controls For Pro-caspase-3 Northern Hybridization**

Positive controls used in pro-caspase-3 northern hybridization procedure were mRNA of SW480 and SW620 human colon cancer cells. These cells were kindly provided by Dr Prue Cowled, Department of Surgery, QEH.

### 2.6.5 Northern Hybridization/Blotting

This step involves the hybridization of RNA transferred filters, preparing $ZnT_4$ and pro-caspase-3 probe from their excised inserts and labelling with $\alpha$-$^{32}P$ radionucleotide, followed addition of probe to hybridized filters. Hybridization of

filters was carried out in glass bottles in a Hybaid Micro-4 hybridization oven. Filters were incubated with 10 ml of pre-hybridization mixture consisting of 1M NaCl, 10% dextran sulfate, 1% SDS, 50% deionised formamide and approximately 4 mg of boiled ssDNA at 42°C with continuous rotation for 4 h.

**Labelling of Probe**

The DNA probe was labelled with $\alpha$-$^{32}$P-dATP (Appendix 1B) using random primers from the Giga-prime DNA labelling kit (or Deca-prime kit), following the manufacturer's instructions (Appendix 1B). 100 ng of the DNA probe ($ZnT_4$ or pro-caspase-3 purified inserts) was denatured at 100 °C for 5 min in 1.5 ml eppendorf tube. The sample was placed on ice for 5 min followed by the addition of 6 µl of the decanucleotide primer solution and reaction buffer. 50 µCi of $\alpha$-$^{32}$P-dATP was added to the mixture along with 1µl (5 units) of Klenow enzyme. The labelled-mixture was incubated for 1 h at 37°C.

A purification column was prepared by placing a small amount of cotton wool into the base of 2 ml sterile syringe. The syringe was filled with 2 ml of Sephadex G-50 solution. The column was then eluted with 200 µl of 2 mM β-mercaptoethanol and 100 µg of herring sperm DNA and centrifuged at 300 g for 6 min.

180 µl of 2 mM β-mercaptoethanol was added to the heated labelled-DNA mixture, passed through the Sephadex G-50 column and centrifuged at 650 g for 8 min. The eluate containing the labelled-probe was collected in a sterile 10 ml tube, denatured at 100°C for 5 min and incubated on ice for 5 min. The probe mixture was added to the

bottle containing the filter and pre-hybridization mix, and incubated overnight at 42°C with constant rotation in a Hybaid oven.

Filters were taken out of the bottle and washed in 2xSSC for 30 min at 42°C, 1xSSC/0.1% SDS for 30 min, 60°C and finally 0.1xSSC/0.1%SDS for 30 min at 65°C to remove background radiation on the membranes of filters. The radioactivity was monitored after each wash with a hand-held β-counter, and washings were ceased when readings of 10-15 cpm were registered. The hybridized filters were blot dried, covered with cling wrap and exposed to Hyperfilm in film cassettes with intensifying screens at -70°C. The film was developed in an automatic developer at the Department of Radiology, QEH.

**Stripping Of Northern Blots**

Hybridised northern blots were stripped of radiolablled probe by washing three times in a boiling solution of 0.1xSSC with 1% SDS for 15 min with gentle rocking. Following the washing steps, blots were rinsed in 2xSSC for 5 min at RT and air-dried.

### 2.6.6 Quantification Of Northern Bands

Northern bands on filters were scanned into the computer using the Fuji Bas Reader analysis program. Quantification of bands was performed using the Scion Image software.

### 2.7. Expression of $ZnT_4$ By RT-PCR

Expression of $ZnT_4$ was also determined by RT-PCR. Complementary DNA was prepared from 1 µg of total RNA using reverse transcriptase (Appendix 1B) and random hexamer primers. First strand cDNA was PCR amplified with polyTaq enzyme, using the following oligonucleotides as primers.

$ZnT_4$- sense: ATGGGCAGGGACGCGCCGGCCTG

$ZnT_4$- antisense: GTACTGGAACTTTGACAATTTGCACA

hGAPDH- sense: AAACCCATCACCATCTTCCAG

hGAPDH- antisense: AGGGGCCATCCACAGTCTTCT

ratGAPDH- sense: GCCATCAACGACCCCTTCAT

ratGAPDH- antisense: CGCCTGCTTCACCACCTTCT

Reverse Transcriptase reaction was set out as follows:

| | Volume | Final concentration |
|---|---|---|
| RNA total (1µg) | 1µl | |
| Buffer 5X | 4µl | |
| DDT 0.1M | 2µl | 10 mM |

| | | |
|---|---|---|
| dNTPs 2.5 mM | 4µl | 0.5 mM |
| Random hexamer primers | 1µl | 2.5 µM |
| MMLV-RT 200U/µl (Life Technology) | 1µl | |
| RNAse inhibitor 40 U/µl (Promega) | 1µl | |
| dd-$H_2O$ to | 20µl | |

Reaction was incubated for 10 min at 23 °C, then 45 min at 42°C and reaction was stopped by incubating for 5 min at 95 °C. Samples were then kept at -20 °C.

PCR reaction was set out as follows:

| | Volume | Concentration |
|---|---|---|
| RT aliquot | 4µl | |
| Buffer 10X | 5µl | |
| $MgCl_2$ 50mM | 2µl | 2mM |
| dNTPs 10 mM | 1 µl | 0.2mM |
| Primer sense 5 µM (50 pmol/µl) | 0.5-1.5 µl | 0.1-0.3 µM |
| Primer anti-sense 5 µM (50 pmol/µl) | 0.5-1.5 µl | 0.1-0.3 µM |
| Taq | 0.5µl | |
| dd- $H_2O$ to | 50µl | |

PCR reactions were carried out in a Perkin Elmer Gene Amp PCR system 9700. Cycle conditions began with 3 min at 95°C. This step was followed by 25 cycles of 45 min at 95°C, 45 min at 51°C, 45 min at 72°C and followed by 1cycle of 7 min at 72°C.

Positive controls were RNA from rat kidney and intestine, tissues that express high levels of this transporter and the anti-sense primer derived from the coding sequences

of $ZnT_4$. Primers specific for the housekeeping enzyme GAPDH were included as internal control. A negative control was used to exclude contamination of genomic DNA in the samples.

### 2.8 Statistical Analysis

All experiments were repeated at least three times. The results of typical experiments are described or data were pooled, as indicated in text. Unless indicated, results are expressed as mean of triplicates ± SEM. Statistical significance was determined by the student *t*-test, ANOVA analysis using the Tukey-Gramer multiple comparisons test where appropriate and is indicated in text or legends to Figures.

# CHAPTER THREE

# ZINC AND $ZnT_4$ IN MAST CELLS PRIOR TO AND FOLLOWING ACTIVATION

## 3.1 Introduction

Electron microscopic studies by several groups between the 1960s and 1980s demonstrated that rat mast cell granules were rich in Zn (Angyal and Archer, 1968; Danscher, 1980; Gustafson, 1967; Uvnas, 1975). However, little is known about the role of Zn in mast cell biology, especially human mast cells. In particular it is not clear whether the Zn is in the labile pools, what happens to it during mast cell activation and degranulation and its relationship to the newly discovered family of Zn transporters.

In an early investigation in rat mast cells, Zn was found to inhibit histamine release most effectively at certain concentrations of compound 48/80 (Hogberg and Uvnas, 1960). Several hypotheses have been proposed for this inhibitory action of Zn, ranging from its membrane stabilization effects to its competition with compound 48/80 for receptor binding sites on mast cells (Kazimierczak and Maslinski, 1974; Kerp, 1963; Uvnas, 1970). In later studies Marone and colleagues reported inhibition of histamine and leukotriene $C_4$ release from human lung mast cells at physiological concentrations of Zn (Marone, 1986). These findings suggest that Zn is involved at the activation stage of mast cells. Due to the lack of ongoing investigations in this area, the exact mechanism(s) by which Zn acts in its inhibitory effect on histamine release remain unclear.

In order to understand more about the involvement of Zn in the activation of mast cells, changes in the levels and localization of Zn following activation were investigated. In recent years, developments of Zn-specific fluorophores, in particular Zinquin, have facilitated the studies of intracellular Zn in cells. Zinquin is a membrane-permeant Zn-specific fluorophore with a relatively low affinity for Zn (Kd

in the nM range) such that it is unable to compete for tightly chelated Zn in metalloenzymes and can only monitor the more labile pools (Zalewski, 1993).

The other important aspect of the investigation was to determine the distribution of $ZnT_4$ in mast cells. The transportation of Zn is facilitated by two families of Zn transporters, the hZIP and cation diffusion facilitator (CTF). Members of the hZIP family mediate uptake of Zn across the plasma membrane, whereas members of the CTF are involved in Zn efflux or intracellular sequestration in vesicles (Cousins and McMahon, 2000; Gaither and Eide, 2001). There has been no investigation of Zn transporters in mast cells. This study focused on the fourth member of the CTF family of Zn transporters (namely $ZnT_4$) since antibody and cDNA probes for $ZnT_4$ were available and this transporter is thought to be localized in cell vesicles (Cousins and McMahon, 2000; Murgia, 1999). A point mutation in the $ZnT_4$ gene represents the molecular basis of the murine syndrome *lethal milk,* that determines a defect in Zn secretion in milk (Huang and Gitschier, 1997); the corresponding wild type gene is widely expressed suggesting a potential role for this protein in the homeostasis of Zn in other cell systems, including mast cells. Hence, the experiments performed were to determine whether $ZnT_4$ was expressed in rat and human mast cells and its relationship to labile Zn prior to and following their activation.

Using Zinquin and antibodies to $ZnT_4$, fluorescence images were obtained detailing the distribution of intracellular labile Zn and $ZnT_4$ in rat and human mast cells before and after activation. Mast cells were activated with commonly used agents such as compound 48/80, IgE and PMA.

## 3.2 Methods

### 3.2.1 Distribution Of Intracellular Labile Zn

Intracellular labile Zn was visualized in primary cord blood mast cells (CBMC) and bone marrow mast cells (BMMC), immature and mature HMC-1 cells, RBL-2H3 and rat peritoneal mast cells (RPMC). Adherent cells (RBL-2H3) were grown on coverslips and stained with Zinquin. All treatments with Zinquin (25 μM) were for 30 min at 37°C. Zinquin fluorescence was also determined in mast cells activated with various agents: A23187, compound 48/80 IgE/anti IgE or PMA for 18 h at 37°C. Mast cells were also treated with the Zn chelator, TPEN at 50μM for 4 h at 37°C.

Zn was visualized using Zinquin by both epi- fluorescence and confocal microscopy as discussed in 2.3.1.

### 3.2.2 Distribution And Expression Of $ZnT_4$

#### Immunofluorescence

$ZnT_4$ distribution was determined by immunofluorescence using rabbit anti-$ZnT_4$ antibody and goat anti-rabbit Ig FITC-conjugated. Cells were cyto-centrifuged on microscope slides and fixed with 4% paraformaldehyde before staining with $ZnT_4$ antibody. Distribution of $ZnT_4$ was visualized by fluorescence microscopy and intensity quantified using Video Pro Image Analysis software.

**Immunogold Labelling**

$ZnT_4$ distribution was also determined by immunogold labelling as described in section 2.5. In brief, mast cells were processed and labelled for $ZnT_4$ using primary antibodies for this transporter and secondary antibodies conjugated to gold particles of diameter size 10 nm (section 2.5.2). Labelling was visualized on a Philips CM100 transmission electron microscope. Images were captured under various magnifications ranging from 5800x to 100, 000x using the analySIS software (Soft imaging systems, Germany). For a quantitative analysis, the numbers of gold particles in the granules of mast cells were counted in all control and test samples. The counts were expressed as mean ± SEM gold particles per granule. To allow for variation in granule size, granule area was calculated using the analySIS software (CEMMSA, Adelaide University). Counts were expressed as mean ± SEM gold particles per $\mu m^2$ of granule. The data were analysed statistically by ANOVA and Student's *t*-test.

**Northern Hybridization and RT-PCR**

The expression of $ZnT_4$ was determined by Northern hybridization (sections 2.7 and 2.9) and RT-PCR (section 2.7.4) in immature and mature HMC-1 and RBL-2H3 cells. Quantification of northern bands was performed as described in section 2.9.5.

### 3.2.3 Statistical Analysis

The results of typical experiments are described or data were pooled, as indicated in text. Statistical significance was determined by ANOVA, student *t*-test and the Tukey-Kramer multiple comparisons test where appropriate and is indicated in text or legends to Figures.

## 3.3 Results

### 3.3.1 Basal Zinquin Fluorescence Of Mast Cells

Mast cells fluoresced intensely when labeled with Zinquin, suggesting high levels of labile Zn compared to most other cell types studied previously in this laboratory. The level of labile Zn was compared between different mast cell types and for comparison the human lung epithelial cell line A549 (typical of many other cell types). At the same microscope and lamp settings, A549 cells had a weak fluorescence, of 10.1 ± 0.6 gray scale units (GSU) of fluorescence intensity, human CBMC had 80.5 ± 4.5 GSU, immature HMC-1 had 132.4 ± 11.1 GSU and RBL-2H3 had 60.4 ± 3.0 GSU (Figure 3.1A). In a separate experiment, similar intense Zinquin fluorescence was seen with RPMC and BMMC (Figure 3.1B). Zinquin fluorescence was quenched by the Zn chelator TPEN confirming that the fluorescence is due to Zn. For example 50 μM TPEN decreased Zinquin fluorescence of immature HMC-1 cells by 60.6 ± 7.6 % ($P<0.005$). It has not yet been possible to convert Zinquin fluorescence into a real Zn concentration (see section 3.4).

### 3.3.2 Morphology And Zinquin Fluorescence In Immature And Mature HMC-1 Cells

The next step was to determine whether Zn levels change with maturation with mast cells. A comparison was made between immature and mature HMC-1 cells. HMC-1 cells were induced to mature by treatment with 1 mM butyrate for 4 days under normal culture conditions. This is a common method used to induce HMC-1

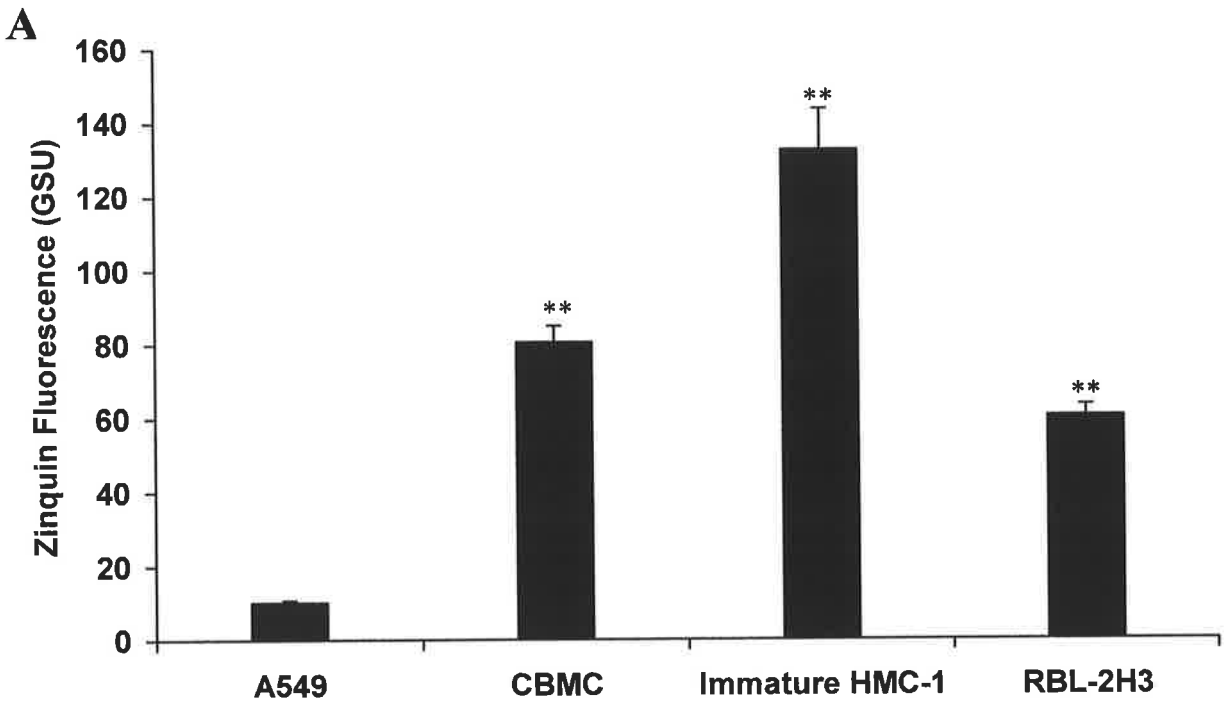
A
160
140
120
100
80
60
40
20
0
Zinquin Fluorescence (GSU)
**
**
**
A549
CBMC
Immature HMC-1
RBL-2H3

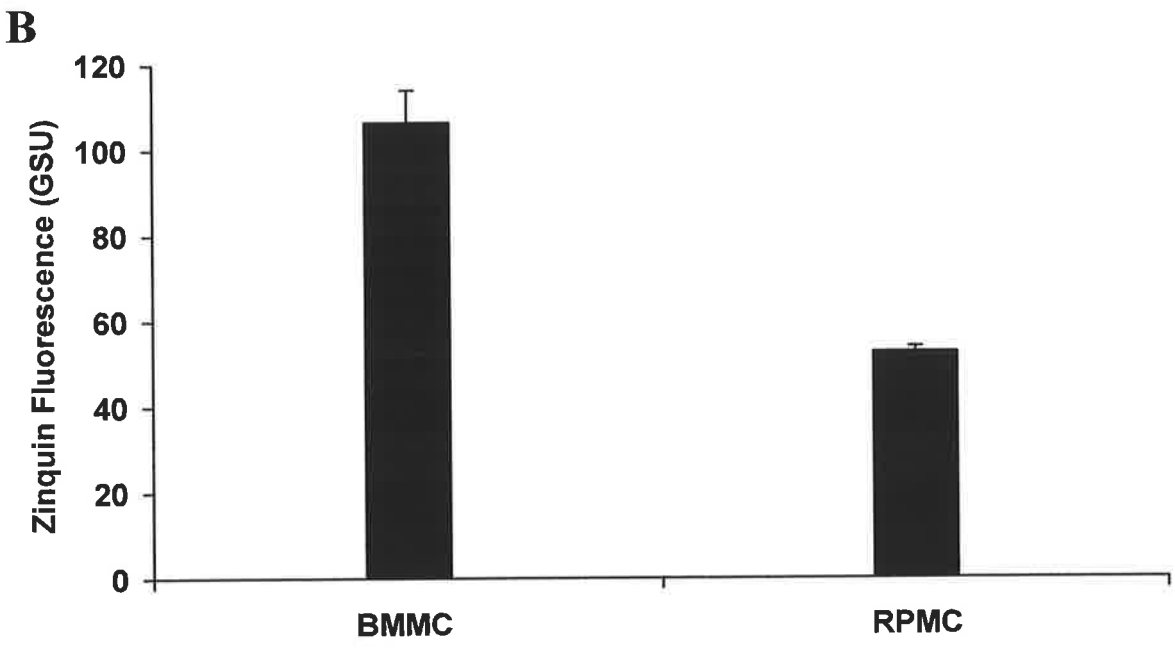
B
120
100
80
60
40
20
0
Zinquin Fluorescence (GSU)
BMMC
RPMC

**Figure 3.1**

**Figure 3.1: Basal Zinquin Fluorescence of Mast Cells and A549 Cells.**

Experiments shown in A and B were performed under similar but not identical conditions on separate days. In order to factor in for variations due to experimental conditions, results are shown on separate graphs. The scales of the two graphs are therefore not identical.

**A:** Basal Zinquin fluorescence of A549 human epithelial cells, CBMC, Immature HMC-1 and RBL-2H3 showing abundant Zn in mast cells. Fluorescence intensity expressed as Mean ± SEM. Statistical significances are indicated as ** $P<0.005$ for comparisons with A549 cells.

**B:** Basal Zn fluorescence of BMMC and RPMC. Fluorescence intensity expressed as Mean ± SEM.

maturation (see 2.1.3). This concentration of butyrate does not affect the viability of mast cells although higher concentrations cause apoptosis (see chapter 5). The criteria for maturation were increased granularity assessed by staining of granules with toluidine blue and by electron microscopy (Galli, 1982). Figure 3.2 shows a limited number of granules in untreated immature HMC-1 cells (Figure 3.2A) whilst butyrate-treated HMC-1 cells had abundance of granules causing the cells to stain more darkly (Figure 3.2B). Electron microscopy confirmed these observations (Figure 3.2 C and D). Different types of granules can been seen at higher magnification in the mature HMC-1 cells. These include granules with the scroll like pattern (thin yellow arrow- Figure 3.2E) and amorphous granules with various amounts of electron dense material in them (yellow arrow heads- Figure 3.2F).

Zinquin fluorescence of immature and mature HMC-1 cells was determined under identical conditions. There was no significant difference in Zinquin fluorescence between immature HMC-1 (59.8 ± 4.2) and mature HMC-1 (65.7 ± 3.2, P=0.13) pixels suggesting that Zn levels do not change with butyrate-induced maturation. These values were different than those reported in Figure 3.1 because the gain settings on the fluorescence imaging camera were different.

### 3.3.3 Effect Of Activation On Morphology And Zinquin Fluorescence

Activation was induced by treatment with 1μg/ml of compound 48/80 for 18 h at 37°C. Figure 3.3B and D show typical ultrastructural morphological changes of activated mast cells including vacuolated cytoplasm and membrane projections

A

B

C

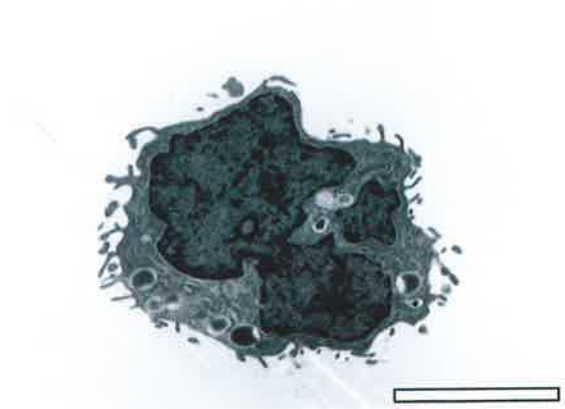

D

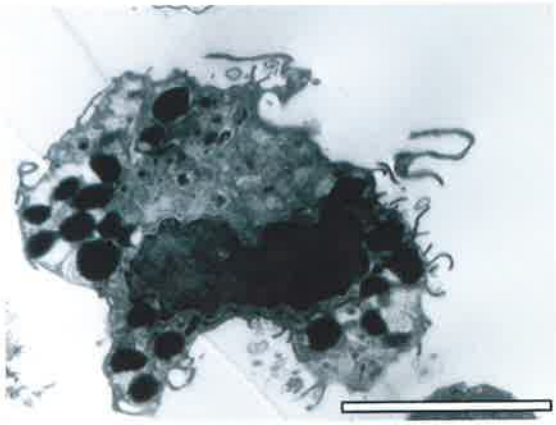

E

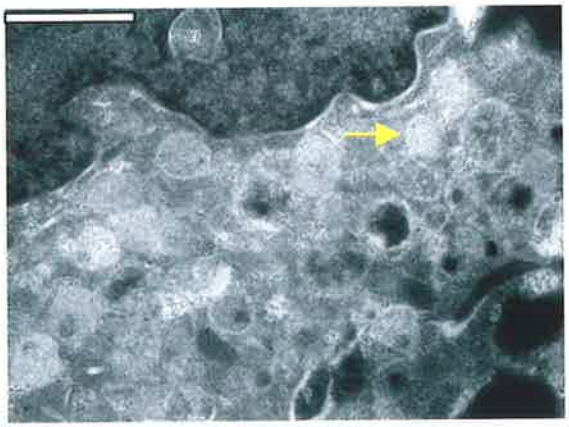

F

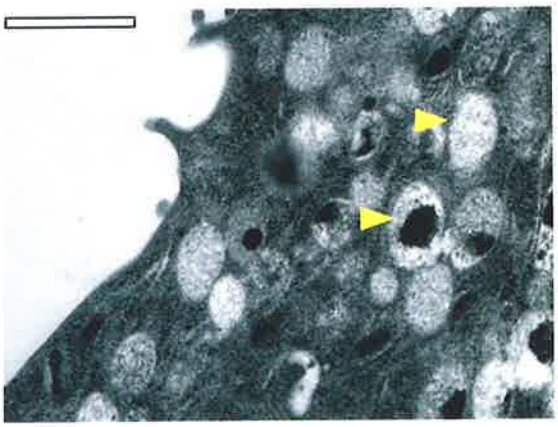

**Figure 3.2**

**Figure 3.2: Maturation of HMC-1 cells by 1 mM butyrate.**

**A:** Immature HMC-1 cell stained with toluidine blue showing pale staining and little granularity. Scale bar indicates 12 μm.

**B:** Mature HMC-1 stained with toluidine blue showing darker staining and abundant granules. Scale bar indicates 14 μm.

**C:** Typical electron micrograph of an immature HMC-1 cell showing large nucleus and few electron dense granular components. Scale bar indicates 4 μm.

**D:** Typical electron micrograph of a mature HMC-1 cell showing smaller nucleus and numerous electron dense granules. Scale bar indicates 5 μm.

**E:** Higher magnification of a mature HMC-1 cell showing a type of granule with scroll-like pattern (thin yellow arrow). Scale bar indicates 1μm.

**F:** Higher magnification of mature HMC-1 cell showing an amorphous type of granule (yellow thick arrow heads). Scale bar indicates 1μm.

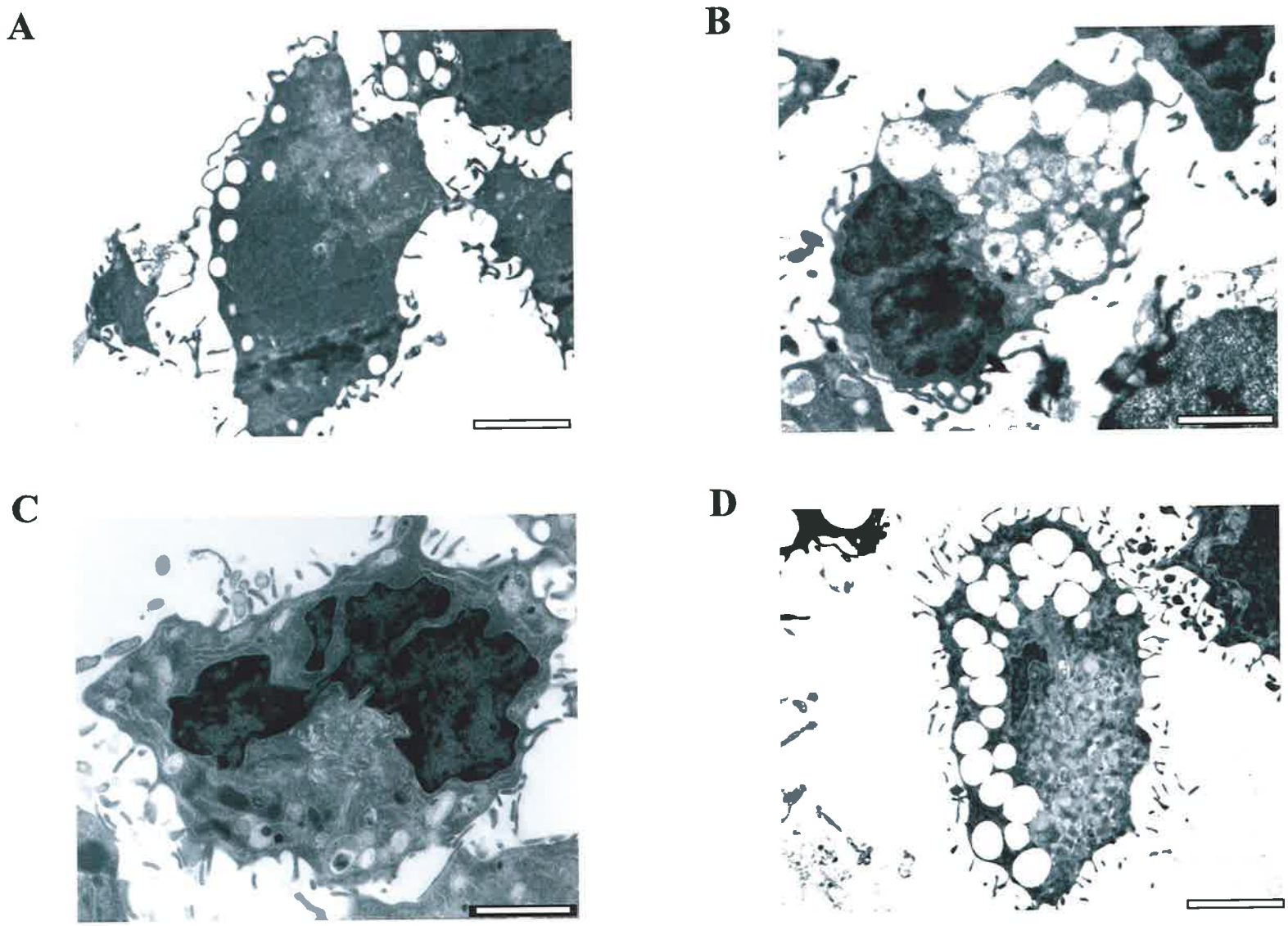


**Figure 3.3**

**Figure 3.3: Electron micrographs of HMC-1 cells before and after activation.**

**A:** Non-activated immature HMC-1 cell showing typical features of a resting mast cell.

**B:** Immature HMC-1 cell treated with compound 48/80 to induce activation. Note the swollen granules and membrane projections.

**C:** Non-activated mature HMC-1.

**D:** Mature HMC-1 cell treated with compound 48/80. Similar features as in B.

Scale bars on A, B, C, and D indicate 2 μm.

compared to the non-activated cells (Figure 3.3A and C). Figure 3.4B and D shows similar pale vacuolated cytoplasm in toluidine blue stained cells after activation.

To determine whether intracellular labile Zn changes with activation, the cells were labelled with Zinquin. Firstly, the pattern of Zinquin fluorescence was vesicular like suggesting a granular distribution of Zn. Activation resulted in a significant decrease in Zinquin labelling in the immature (Figure 3.4F) and mature (Figure 3.4H) HMC-1 cells compared with the intense fluorescence in non-activated immature (Figure 3.4E) and mature (Figure 3.4G) HMC-1 cells. Zinquin staining was also observed to decrease in RBL-2H3 and CBMC cells treated for 18 h at 37°C with 0.5μM of calcium ionophore or 1μg/ml compound 48/80 respectively (Figure 3.5).

A similar loss of Zn was seen RPMC undergoing spontaneous activation during exposure to UV light for 10 minutes. This was achieved by letting them sit on a microscope slide with continuous exposure to UV light. There was an increase in surface area of the cell due to swelling of granules and a marked reduction in Zinquin fluorescence. This typically occurred over a time period of 10 min (Figure 3.6).

Reductions ($P<0.005$) of Zinquin fluorescence were seen in various types of mast cells (CBMC, BMMC, RPMC, immature and mature HMC-1 cells) treated with a variety of agents {compound 48/80 (1 μg/ml), PMA (100 nM) + A23187 (0.5 μM) or IgE (0.5 μg/ml) + anti-IgE (0.2 μM)}; these reductions in Zinquin fluorescence were of a similar magnitude to the decreases induced by Zn chelator TPEN (Table 3.1).

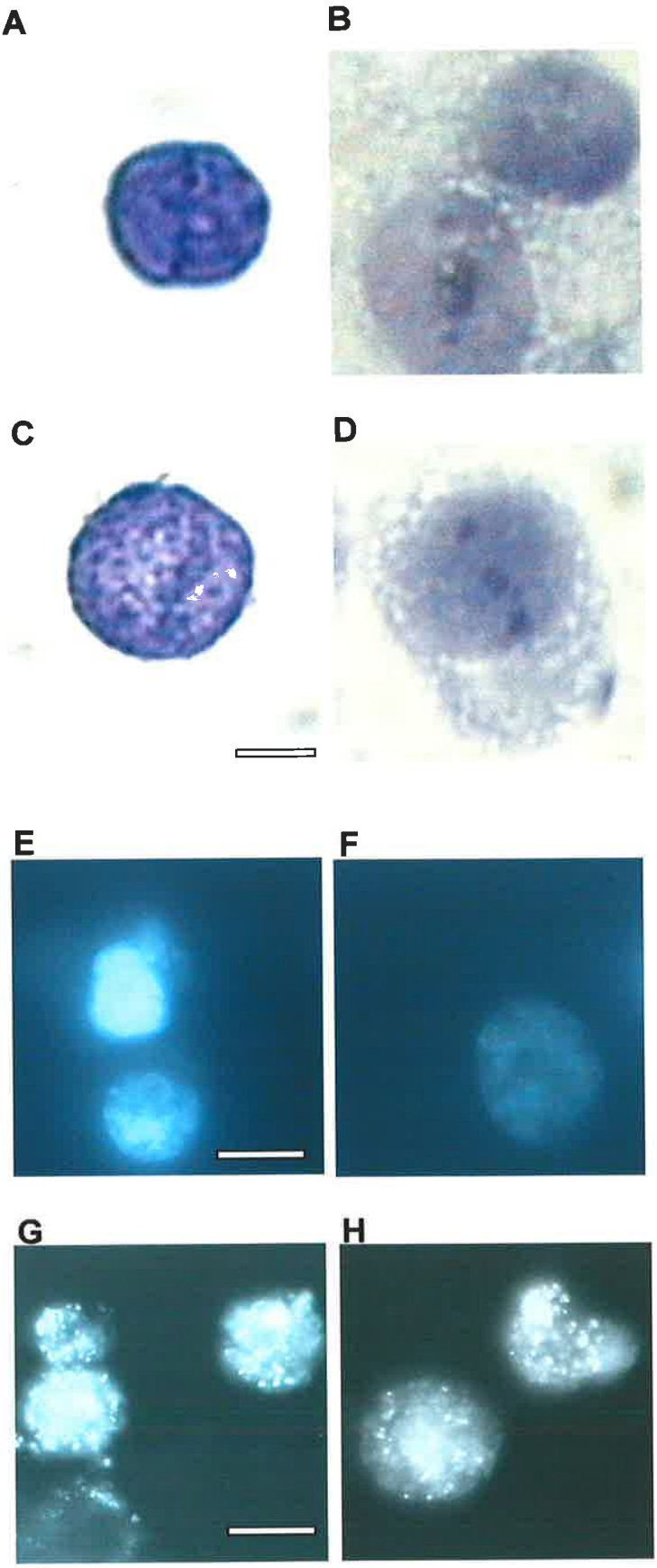


**Figure 3.4**

**Figure 3.4: Effects of activation on toluidine blue staining and Zinquin fluorescence.**

**A-D:** Toluidine blue images of immature (A and B) and mature (C and D) HMC-1 mast cells untreated (A and C) and treated (B and D) with 1μg/ml of compound 48/80 for 18 h at 37°C respectively. Figure shows swollen, pale vacuolated cytoplasm in the activated cells. Scale bar indicates 6μm in C and D and 8μm in A and B.

**E-H:** Zinquin fluorescence images of immature (E and F) and mature (G and H) HMC-1 mast cells untreated (E and G) and treated (F and H) with 1μg/ml of compound 48/80 for 18 h at 37°C respectively. Figure shows granular like fluorescence staining pattern and decreased intensity following activation. Scale bars indicate 14 μm.

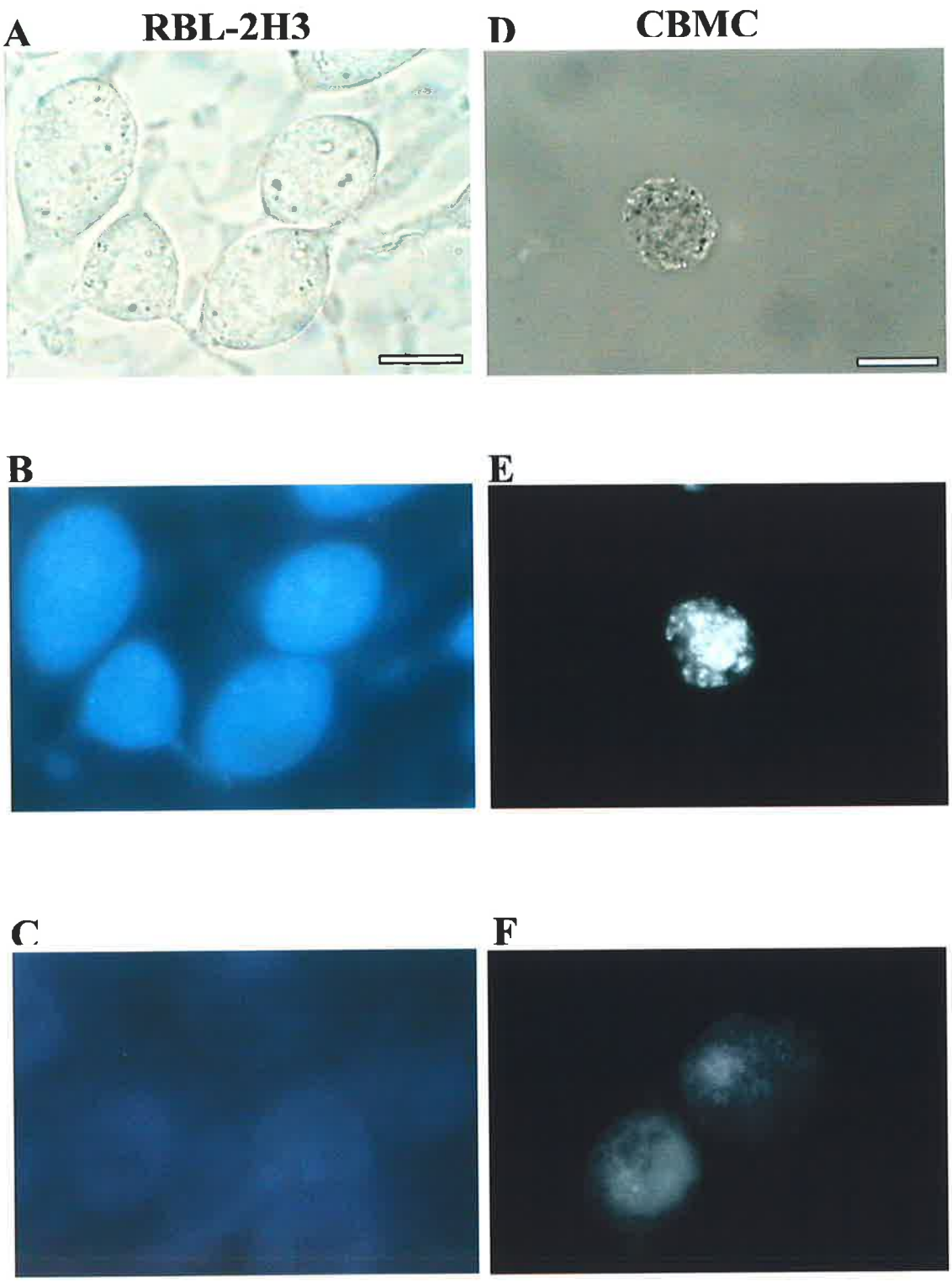


**Figure 3.5**

**Figure 3.5: Effects of activation on Zinquin fluorescence in RBL-2H3 and CBMC cells.**

Left hand panel of images show RBL-2H3 cells, while the right hand panel of images show CBMC cells.

**A-C:** Panel A shows bright field image of untreated RBL-2H3 cells and panel B is the corresponding Zinquin fluorescence. Panel C show Zinquin fluorescence of RBL-2H3 cells treated with activator calcium ionophore A23187 (0.5 μM) for 18 h at 37°C. Note the decrease in Zinquin fluorescence with activation of cells. Scale bar for A, B and C indicates 14 μm.

**D-F:** Panel D shows bright field image of untreated CBMC cells and panel E is the corresponding Zinquin fluorescence. Panel F show Zinquin fluorescence of CBMC cells treated with 1μg/ml of compound 48/80 for 18 h at 37°C. Similarly Zinquin fluorescence decreased with activation of cells. Scale bar for D, E and F indicates 12μm.

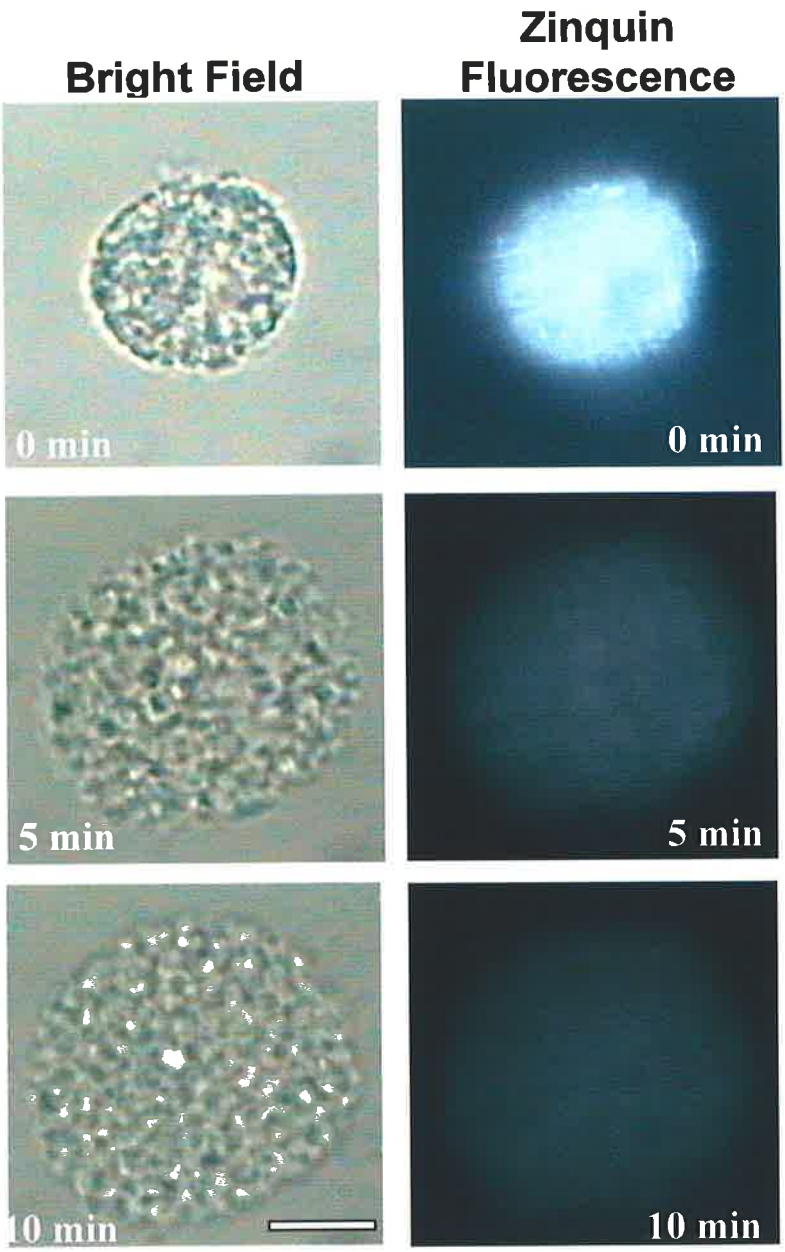
Bright Field
Zinquin
Fluorescence
0 min
0 min
5 min
5 min
10 min
10 min

**Figure 3.6**

**Figure 3.6: Changes in Zinquin fluorescence during spontaneous degranulation of RPMC cells.**

Left hand panel shows bright field images of RPMC cells, while the right hand panel of images show the corresponding Zinquin fluorescence. During UV fluorescence microscopy some RPMC cells underwent spontaneous degranulation. A series of images were captured at different time points by both bright field and Zinquin fluorescence. Note the increase in surface area due to swelling of granules and the marked reduction in Zn dependent Zinquin fluorescence. Scale bar indicates 7μm in left and right panels.

**Table 3.1. Effects of Treatment with Activators or TPEN on Zinquin Fluorescence of Mast Cells.**

| Mast Cell Type | Treatment[a] | Zinquin fluorescence[b] (% of control, ± SEM) |
|---|---|---|
| Immature HMC-1 | 48/80 (1 μg/ml) | 59.5 ± 6.1** |
| | IgE (5 μg/ml) + Anti-IgE (0.2 μM) | 58.4 ± 7.1* |
| | TPEN (50 μM) | 39.4 ± 7.6** |
| Mature HMC-1 | 48/80 (1 μg/ml) | 55.9± 2.8** |
| RPMC | 48/80 (1 μg/ml) | 35.2 ± 1.5** |
| Bone-marrow derived | IgE (5 μg/ml) + Anti-IgE (0.2 μM) | 65.8 ± 9.4* |
| | PMA (100 nM) + A23187 (0.5 μM) | 41.4 ± 27.7* |
| | TPEN (100 μM) | 53.7 ± 6.8** |
| CBMC | 48/80 (1 μg/ml) | 49.1 ± 2.5** |

a. Cells were treated for 18h at 37°C with reagents in culture medium, except for TPEN, which was added for 2 h.

b. Zinquin fluorescence of cells expressed as % of fluorescence of control cells

At least 20 cells were quantified by image analysis from replicate tubes.

* $P<0.05$ ** $P<0.005$

### 3.3.4 Repletion Of Zn After Degranulation

In order to investigate whether mast cells can replete their Zn stores following degranulation, mature HMC-1 cells were degranulated with 1 μg/ml compound 48/80 for 18 h, then washed, cultured in fresh medium for 24 h and Zinquin fluorescence again measured. Zinquin fluorescence decreased from 79.9 ± 4.1 gray scale units in control cells to 38.5 ± 4.2 in cells treated with compound 48/80 ($P<0.005$). After re-culture, Zinquin fluorescence was 73.8 ± 3.7 gray scale units, not significantly different from the initial Zinquin fluorescence of the untreated mast cells (Figure 3.7).

### 3.3.5 Expression of $ZnT_4$ mRNA in mast cells

Figure 3.8 shows the expression by RT-PCR of $ZnT_4$ mRNA in untreated mature HMC-1, immature HMC-1 and RBL-2H3 cells. These were compared with rat kidney and rat intestine (kindly provided by Dr Murgia), tissues that express high levels of this transporter and which served as positive controls; another positive control ($ZnT_4$ +ve Figure 3.8) was the anti-sense primer derived from the coding sequences of $ZnT_4$ (see section 3.2). Primers specific for the housekeeping enzyme GAPDH were included as internal control. The no DNA track is a control containing RNA from intestine not exposed to Reverse Transcriptase enzyme. This negative control is used to exclude contamination of genomic DNA in the samples.

In order to compare quantitatively the levels of $ZnT_4$ mRNA, expression in the various mast cell types was determined by northern blotting. Figure 3.9 shows the expression

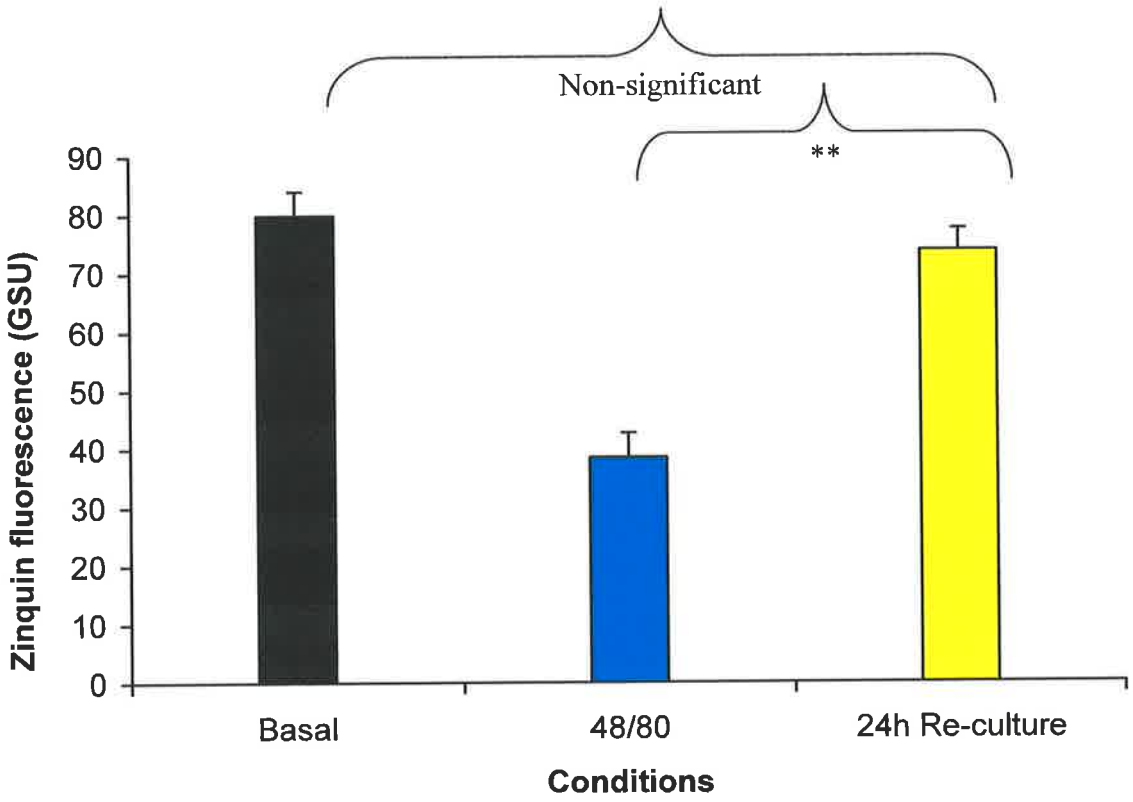
Non-significant
**
Zinquin fluorescence (GSU)
90
80
70
60
50
40
30
20
10
0
Basal
48/80
24h Re-culture
Conditions

**Figure 3.7**

**Figure 3.7: Repletion of Zn after degranulation.**

Mature HMC-1 cells were degranulated with 1 μg/ml compound 48/80 for 18 h and Zinquin fluorescence measured (blue column). They were then washed, re-cultured in fresh medium for 24 h and Zinquin fluorescence again measured (yellow column). Basal Zinquin fluorescence of untreated cells is indicated by the black columns. Bars indicate SEM for means of triplicates. Statistical significances are indicated as ** $P<0.005$ for comparisons by brackets.

**Figure 3.8: Expression of $ZnT_4$ in mast cells and other cell types.**

RT-PCR showing abundance of $ZnT_4$ mRNA (1.3 Kb fragment) in immature and mature HMC-1 and RBL-2H3 mast cells, compared with rat kidney and intestine. GAPDH band (0.25 Kb - human primers) and 0.5 Kb (rat primers) mRNA) serves as a loading control. The positive control ($ZnT_4$ +ve) was anti-sense primer derived from the coding sequences of $ZnT_4$. The no DNA track is a control containing RNA from intestine that has not been exposed to reverse transcriptase.

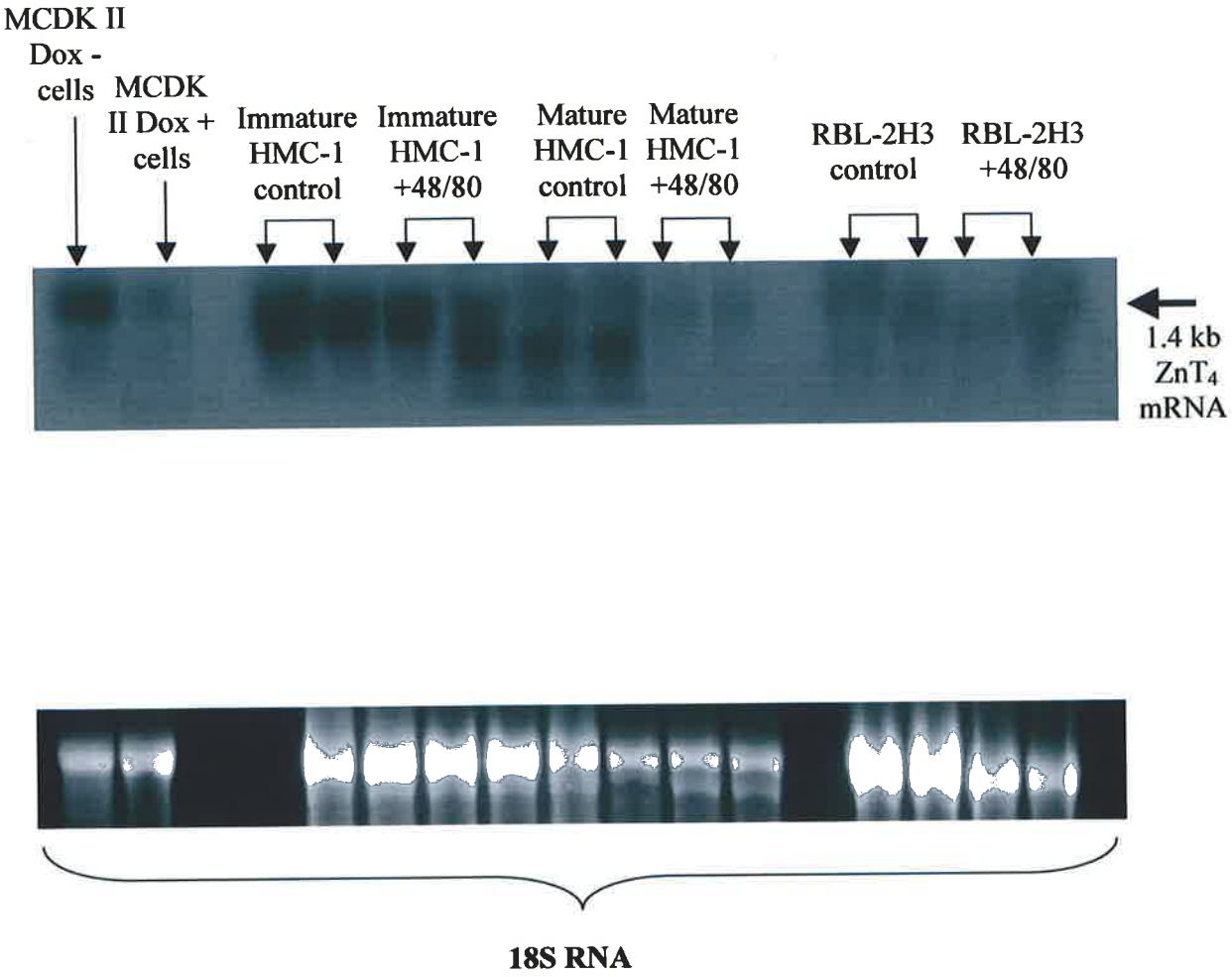
MCDK II Dox - cells
MCDK II Dox + cells
Immature HMC-1 control
Immature HMC-1 +48/80
Mature HMC-1 control
Mature HMC-1 +48/80
RBL-2H3 control
RBL-2H3 +48/80
1.4 kb ZnT4 mRNA
18S RNA

**Figure 3.9**

**Figure 3.9: $ZnT_4$ mRNA expression in immature and mature HMC-1 and RBL-2H3 mast cells by Northern Hybridization.**

Northern blot analysis using a $ZnT_4$ probe is shown in the upper panel and parallel ethidium bromide staining pattern of control 18S rRNA on the lower panel. Figure shows high expression of $ZnT_4$ mRNA in immature and mature HMC-1 mast cells and RBL-2H3 mast cells compared to MDCK II Dox + cells, which serve as a negative control.

of $ZnT_4$ mRNA in both untreated and compound 48/80 treated immature and mature HMC-1 mast cells and RBL-2H3 mast cells by northern hybridization. The positive control for these experiments was mRNA prepared from MCDK II cells transfected with $ZnT_4$ under control of doxycycline-sensitive promoter (gift of Dr Chiara Murgia, INRAN, Rome). In the absence of doxycycline, $ZnT_4$ mRNA was transcribed (Figure 3.9 - left hand lane). In the presence of doxyclycine, $ZnT_4$ expression was suppressed (Figure 3.9 - lane 2) and this served as a negative control. Levels of 18S mRNA served as loading controls.

Levels of $ZnT_4$ expression in various mast cell types were significantly higher than that of the negative control (Figure 3.10, MCDK II Dox +ve) (Figure 3.10, $P<0.005$). Lanes 3 and 4 show $ZnT_4$ mRNA (in duplicate tracks) for untreated immature HMC-1 cells (Figure 3.9). Lanes 5 and 6 show $ZnT_4$ mRNA in compound 48/80 treated immature HMC-1 cells (Figure 3.9). There was no apparent difference between untreated and compound 48/80 treated cells and this was confirmed by quantification of the intensity of the bands using a phosphoimager (Figure 3.10). However, in mature HMC-1 cells, mRNA expression was higher in untreated compared to compound 48/80 treated cells (Figure 3.10, $P<0.005$). Finally the pattern in RBL-2H3 cells was similar to that of immature HMC-1 cells, where there was no significant difference between untreated and compound 48/80 treated cells (Figure 3.9 and Figure 3.10).

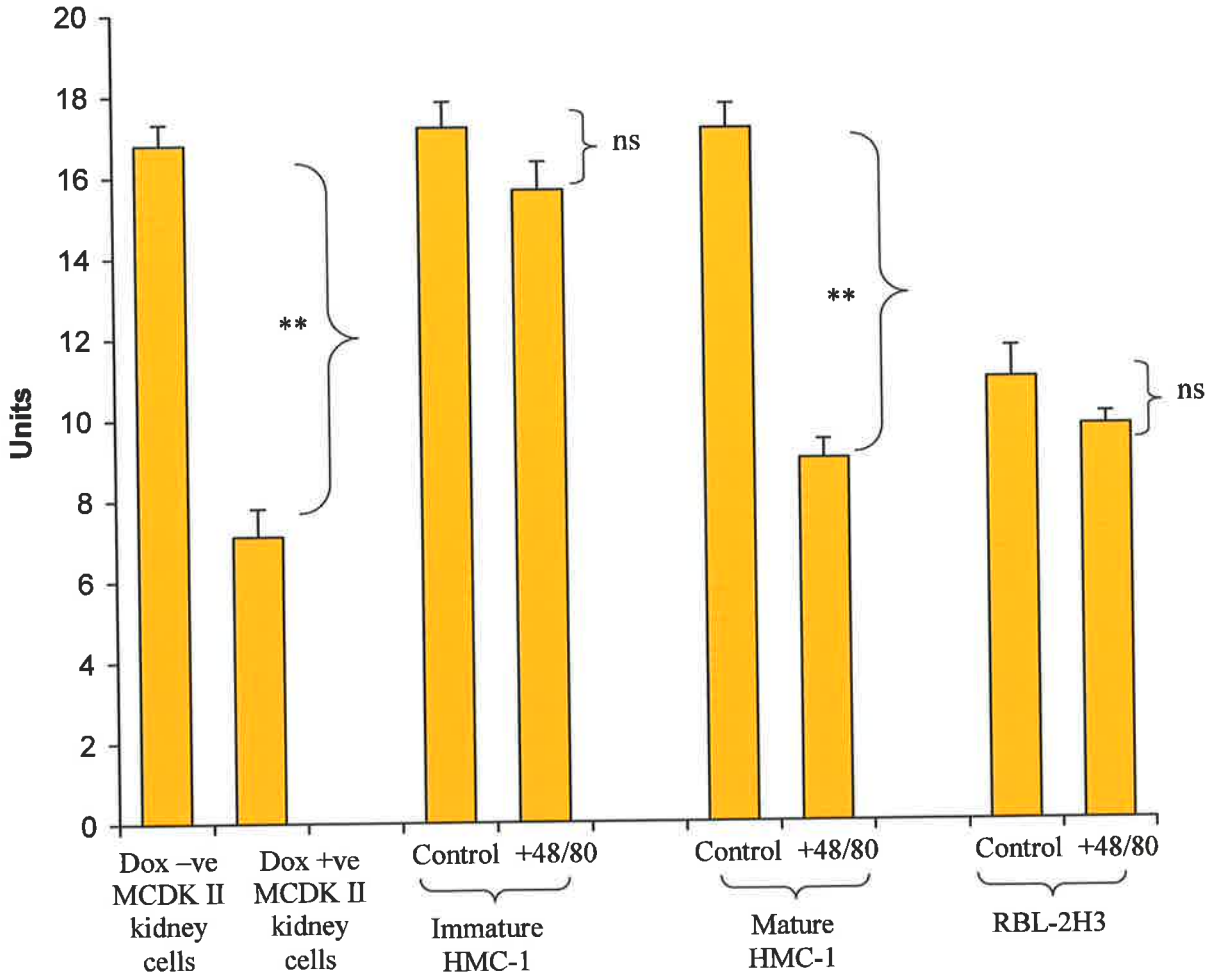
Units
20
18
16
14
12
10
8
6
4
2
0
**
ns
**
ns
Dox –ve MCDK II kidney cells
Dox +ve MCDK II kidney cells
Control
+48/80
Immature HMC-1
Control
+48/80
Mature HMC-1
Control
+48/80
RBL-2H3

**Figure 3.10**

**Figure 3.10: Quantification of northern bands showing $ZnT_4$ mRNA expression in immature and mature HMC-1 and RBL-2H3 mast cells.**

Northern bands were quantified for immature and mature HMC-1 mast cells and RBL-2H3 mast cells. Figure shows high levels of $ZnT_4$ mRNA expression in all mast cell types particularly immature HMC-1 cells. There was no difference between levels of $ZnT_4$ mRNA in untreated and treated cells (except for mature HMC-1).

Bars indicate SEM for means of triplicate measurements from each of the duplicate tracks. Statistical significances are indicated as ** $P<0.005$.

### 3.3.6 Localization And Levels Of $ZnT_4$ In Mast Cells

These results show that $ZnT_4$ mRNA is abundant in mast cells; the protein expression was then assayed by immunofluorescence.

High levels of $ZnT_4$ protein in RBL-2H3 mast cells were shown by strong labelling with rabbit anti-$ZnT_4$. $ZnT_4$ had a vesicular-like pattern of fluorescence both in the cytoplasm and around the nucleus (Figure 3.11). Perinuclear staining was particularly evident (panel F). It was also observed that $ZnT_4$ staining was concentrated in the main body of the cell and labelling was absent in the dendritic-like protuberances of the cells (Figure 3.11E and F). Bright staining for $ZnT_4$ was also seen in other types of mast cells including immature and mature HMC-1 cells and RPMC cells (Figure 3.12A, C and E). As for RBL-2H3 cells, a similar perinuclear and vesicular-like staining pattern was observed. An interesting pattern of distribution was observed in some RPMC cells, where $ZnT_4$ labeling surrounded the outer region of the cytoplasm and the center of the cell, likely to be the nucleus (Figure 3.12E).

The effects of activation on $ZnT_4$ were determined by treatment with 1μg/ml compound 48/80 for 18 h 37°C. There were no changes in the levels or distribution of $ZnT_4$ in immature and mature HMC-1 cells as a result of activation (Figure 3.12B and D). This is also shown quantitatively in Figure 3.13 where 300-500 cells were analysed. However, there was a significant decrease in $ZnT_4$ levels in RPMC cells (Figure 3.12E & F and Figure 3.13).

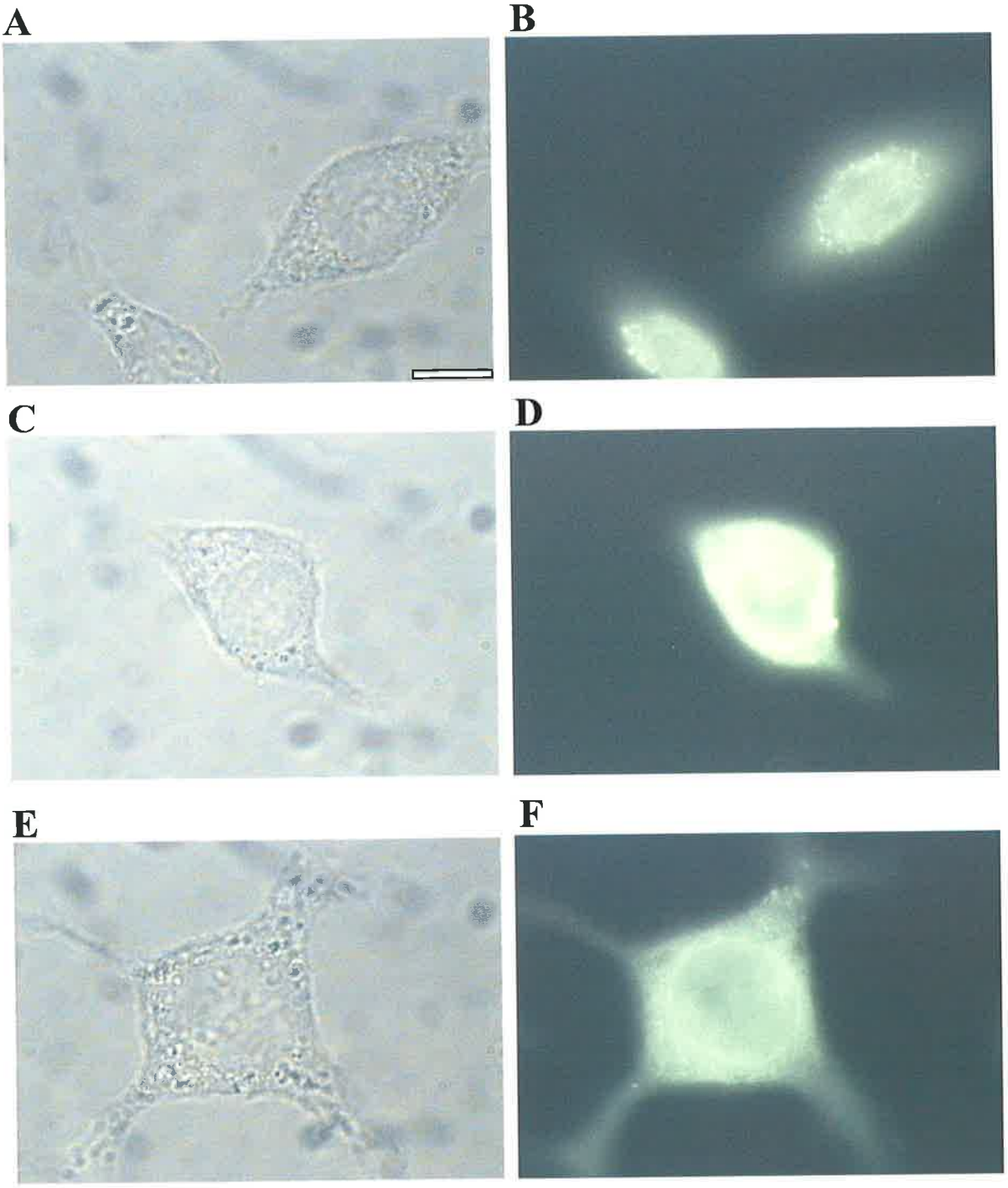


**Figure 3.11**

**Figure 3.11: $ZnT_4$ immunofluorescence labelling of RBL-2H3 cells.**

Figure shows bright field images (A, C and E) and corresponding $ZnT_4$ immunofluorescence images (B, D and F) of RBL-2H3 cells. Note the granular-like pattern of labelling and peri-nuclear localisation (F). Scale bar indicates 10 μm for all panels.

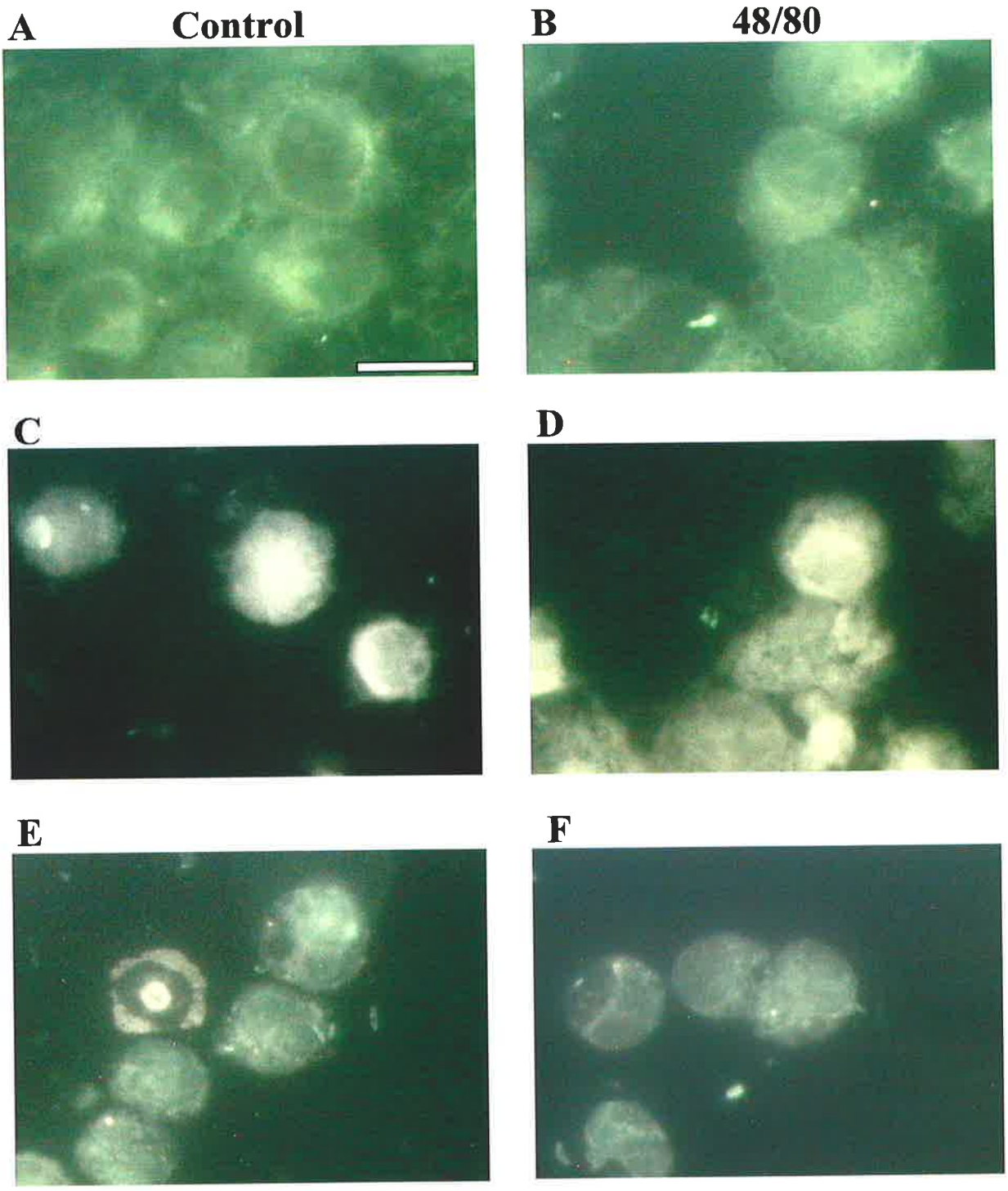


**Figure 3.12**

**Figure 3.12: Effects of activation on $ZnT_4$ immunofluorescence labelling in mast cells.**

**A and B:** $ZnT_4$ immunofluorescence in immature HMC-1 cells before (A) and following activation (B) with 1μg/ml compound 48/80 for 18 h at 37°C.

**C and D:** $ZnT_4$ immunofluorescence in mature HMC-1 cells before (C) and following activation (D) with 1μg/ml compound 48/80 under similar conditions.

**E and F:** $ZnT_4$ immunofluorescence in RPMC cells before (E) and following activation (F) with 1μg/ml compound 48/80 under similar conditions. Note the interesting nuclear staining pattern in some of the cells.

Figure shows no overall major change in $ZnT_4$ fluorescence due to activation. Scale bar indicates 16 μm for all panels.

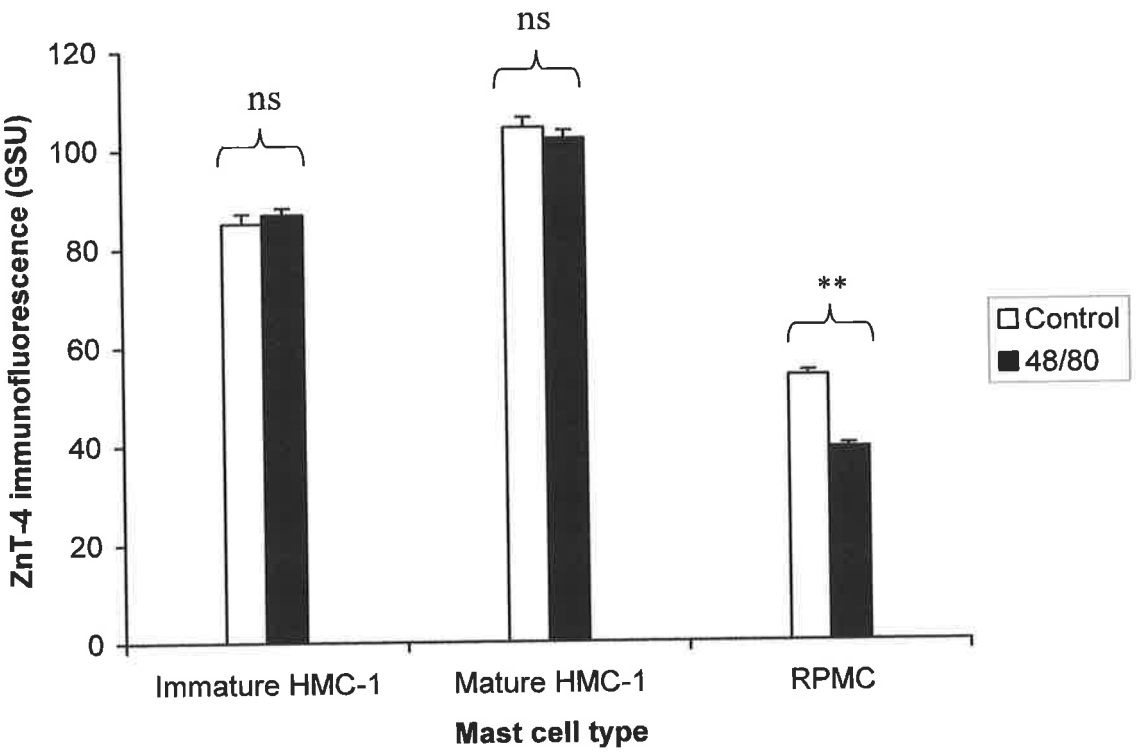
ns
ns
**
120
100
80
60
40
20
0
ZnT-4 immunofluorescence (GSU)
Control
48/80
Immature HMC-1
Mature HMC-1
RPMC
Mast cell type

**Figure 3.13**

**Figure 3.13: Quantitative effects of activation on $ZnT_4$ immunofluorescence in mast cells.**

Immature and mature HMC-1 and RPMC cells were treated with 1μg/ml compound 48/80 for 18 h 37°C. Immunofluorescence was quantified from images of 300-500 cells each. Bars indicate SEM for means of triplicates. Statistical significances are indicated as ** $P<0.005$ for comparisons between 48/80 treated and control cells. Comparisons can only be made within each cell type since experiments were performed on separate days under different fluorescence settings and therefore are not directly comparable. The experiment was repeated three times and a typical experiment is shown.

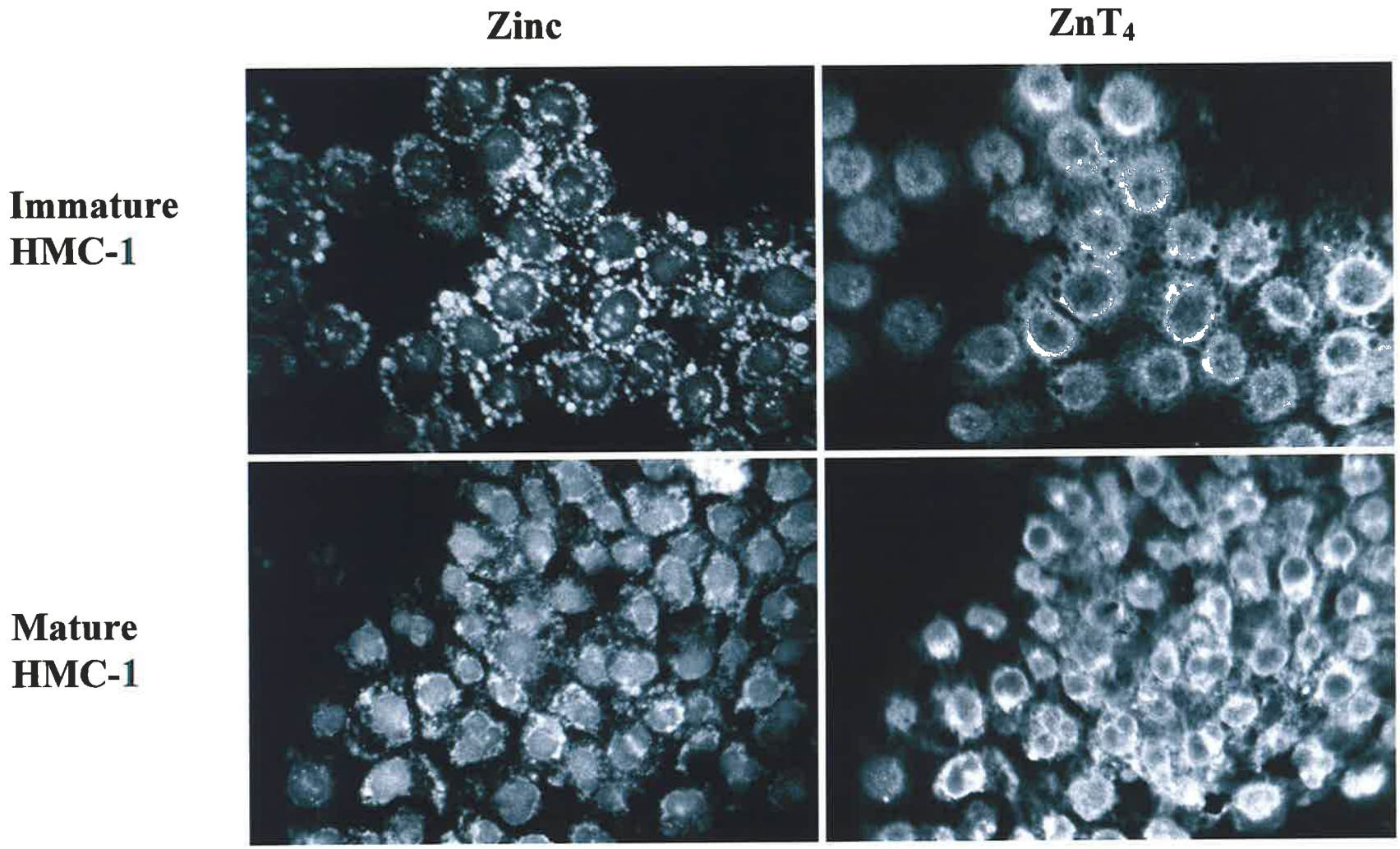


Figure 3.14

**Figure 3.14: Confocal Images of Zn and $ZnT_4$ in Immature and Mature HMC-1.**

Fluorescence labelling of Zn using Zinquin and corresponding $ZnT_4$ by immunofluorescence in dual labelled cells by confocal fluorescence microscopy. Each image is a composite image of a Z-series of 12 focal planes in the Z-axis. Note the vesicular-like fluoresence of both Zn and $ZnT_4$.

### 3.3.7 Dual Labelling Of $ZnT_4$ And Zn In Mast Cells

Dual labeling analysed by confocal studies in immature and mature HMC-1 mast cells showed a granular distribution of both Zn (by Zinquin fluorescence) and $ZnT_4$ (by immunofluorescence) (Figure 3.14). These images were merged and pseudocoloured and a typical example is shown for mature HMC-1 cells in Figure 3.15. There was only partial co-localisation of $ZnT_4$ (green) and Zn (blue), suggesting that they are contained in different subsets of vesicles. In particular, $ZnT_4$ positive vesicles were often found to be more peripherally located than the Zinquin-labeled vesicles.

### 3.3.8 Immunogold Labelling Of $ZnT_4$ In Mast Cells

The localization of $ZnT_4$ in immature and mature HMC-1 was also examined by electron microscopy using immunogold labelling. In immature HMC-1 cells (Figure 3.16 A-D), gold particles labelling $ZnT_4$ were observed inside the granules (orange arrows), lining the granules (red arrows) and in surrounding cytoplasmic areas (yellow arrows). There was little labelling in the cells not treated with primary antibody (panel E). A similar pattern of distribution for $ZnT_4$ was seen in mature HMC-1 cells (Figure 3.17 A-D).

Gold particles per granules were also counted. In immature HMC-1 cells treated with secondary antibody alone there was negligible labelling ($0.13 \pm 0.1$ particles per granule) compared to $7.9 \pm 0.6$ particles per granule in $ZnT_4$ labelled cells (Table 3.2, $P<0.005$). Similarly, with mature HMC-1 cells there were $0.91 \pm 0.5$ particles per

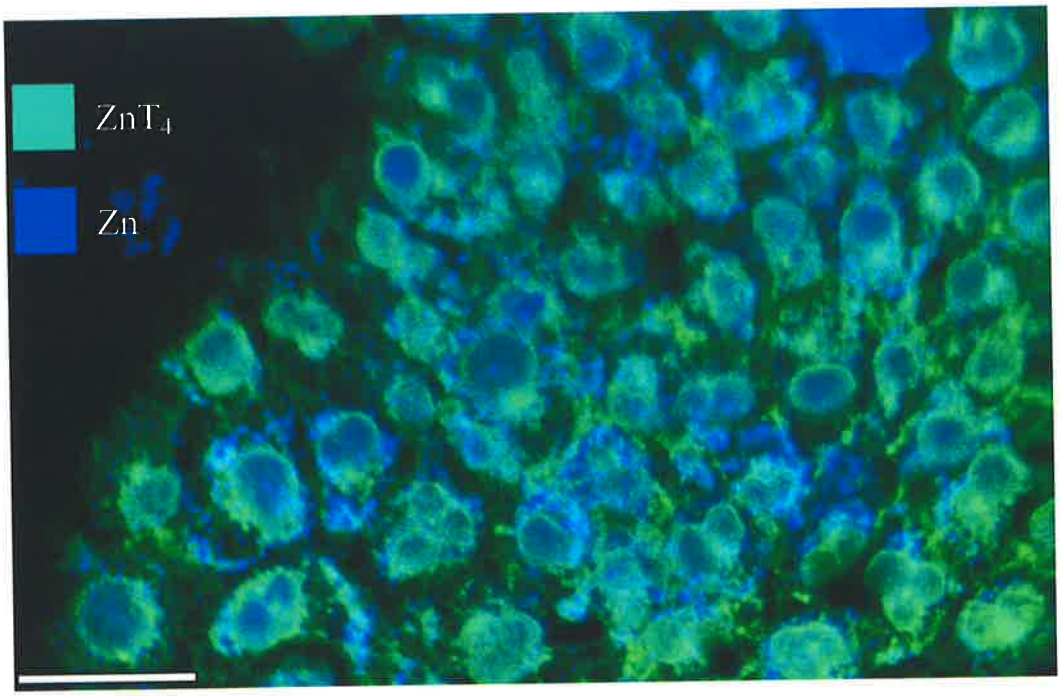


**Figure 3.15**

**Figure 3.15: Different Localization of $ZnT_4$ and Zn in Mature HMC-1.**

Images from figure 3.14 were merged for mature HMC-1 cells using a confocal software program. Green represents $ZnT_4$ and blue represents Zn. Figure shows a more peripheral localization of $ZnT_4$ and more perinuclear localization of Zn-containing vesicles. Scale bar indicates 24 μm.

A

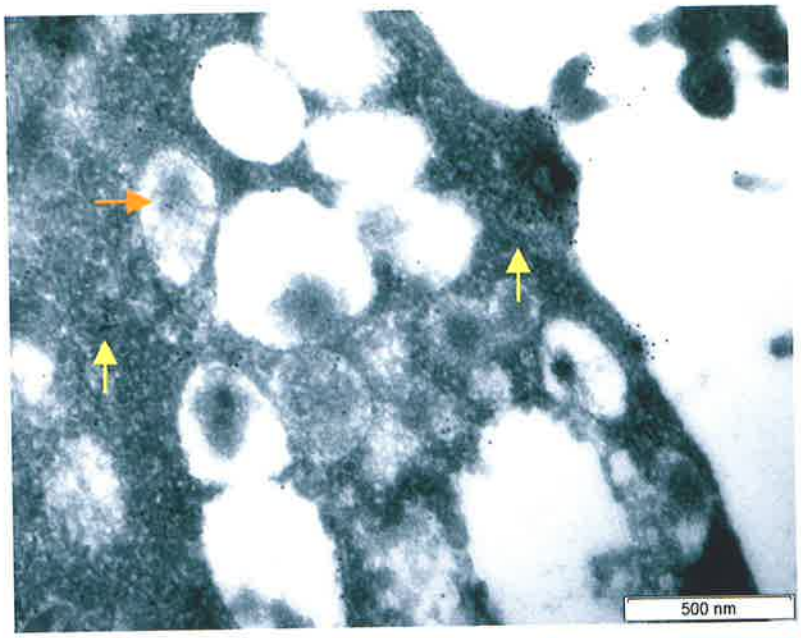


B

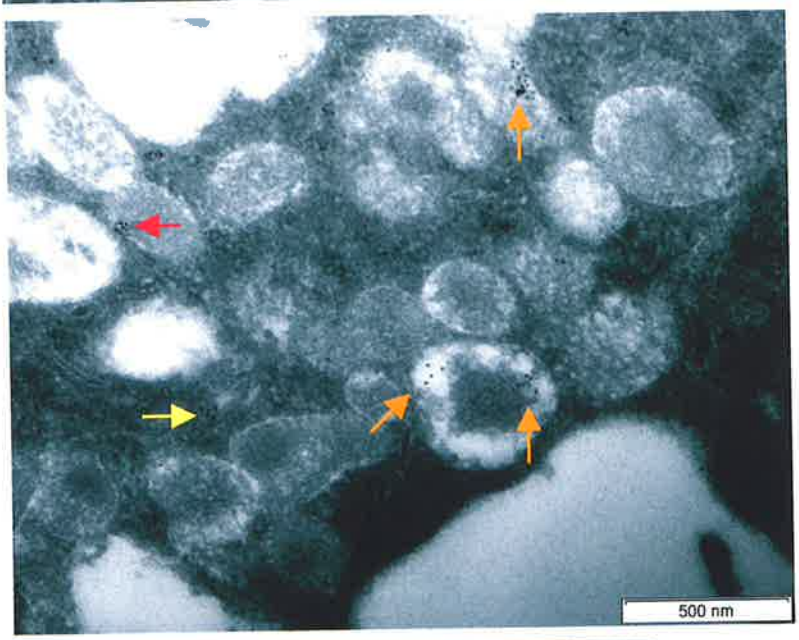


C

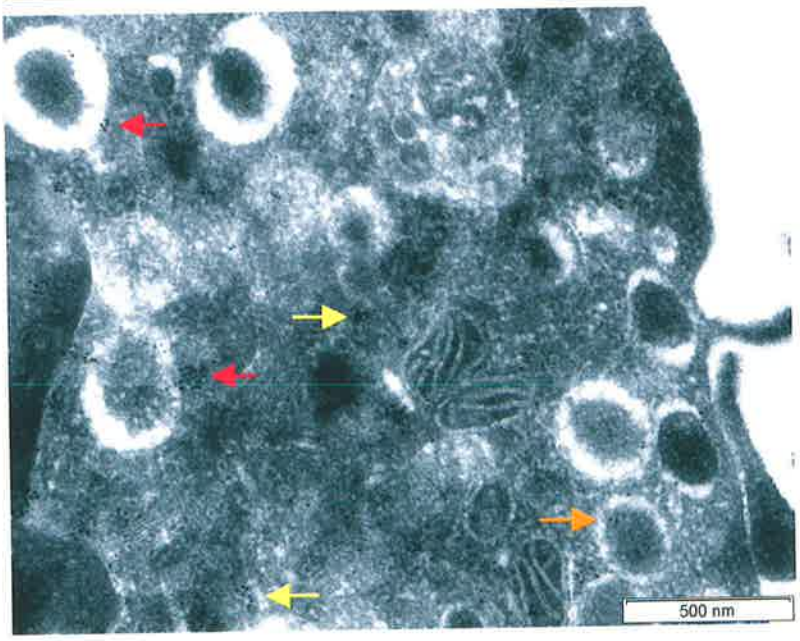

**D**

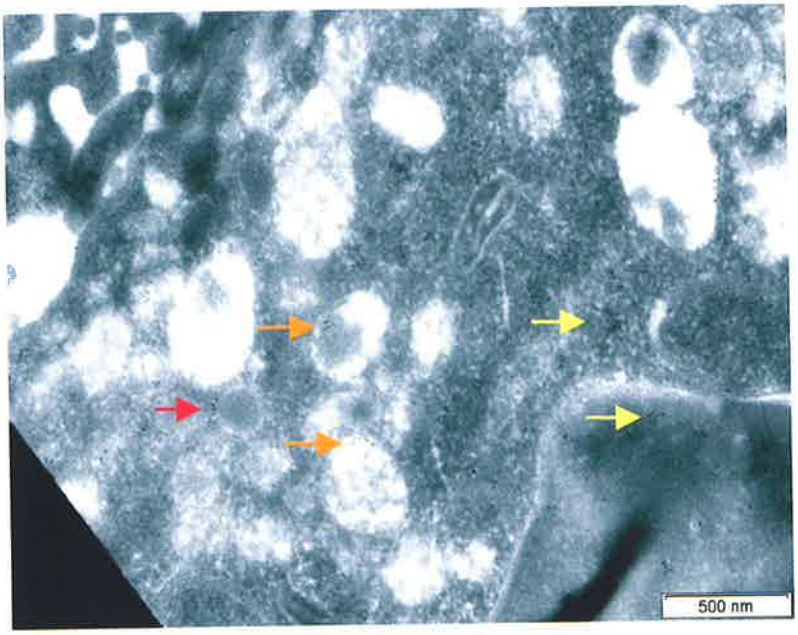


**E**

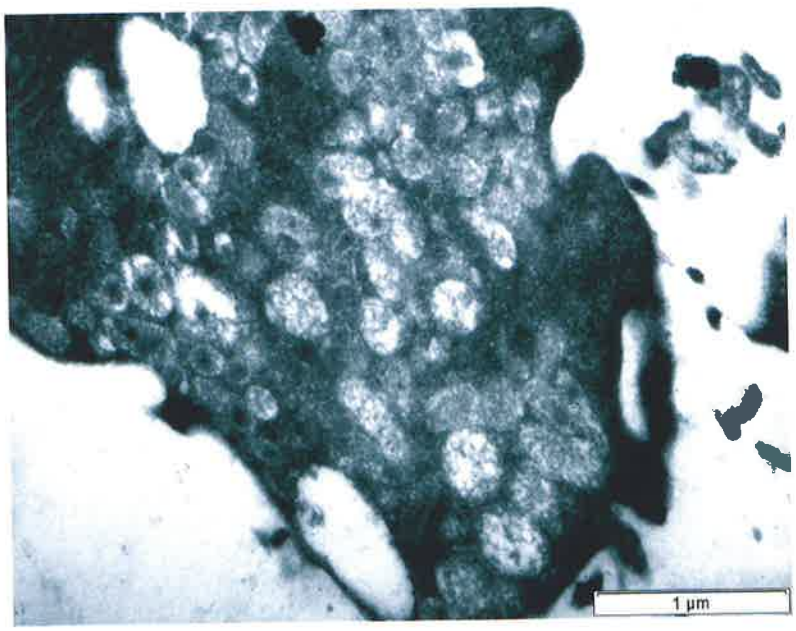


**Figure 3.16**

**Figure 3.16: Localisation of $ZnT_4$ in immature HMC-1 cells by immunogold labelling.**

**A-D:** Immunogold labelling $ZnT_4$ in immature HMC-1 mast cells. Scale bars are as shown in images.

**E:** Control (lacks the primary antibody) showing little gold labelling. Scale bar as shown in image.

Figure shows $ZnT_4$ labelling inside of granules (orange arrows), lining the granules (red arrows) and in the surrounding cytoplasm (yellow arrows).

A

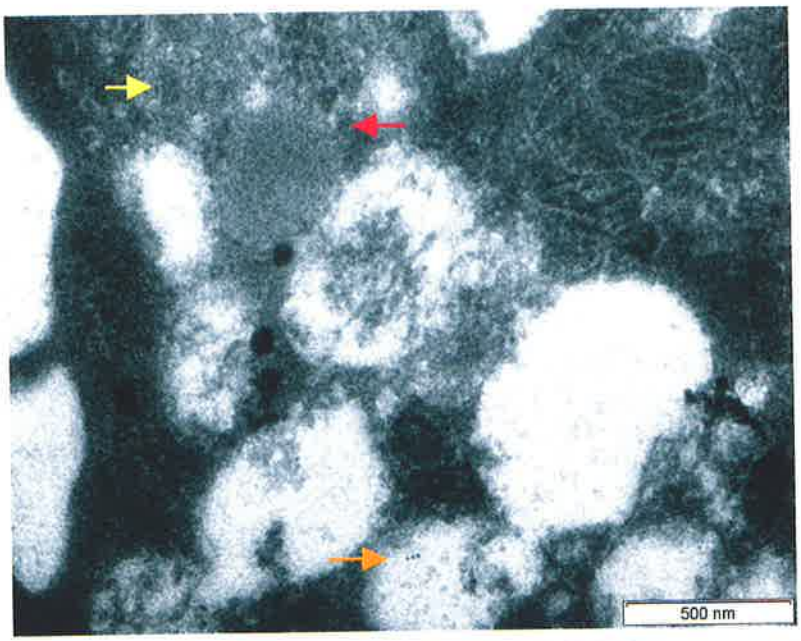


B

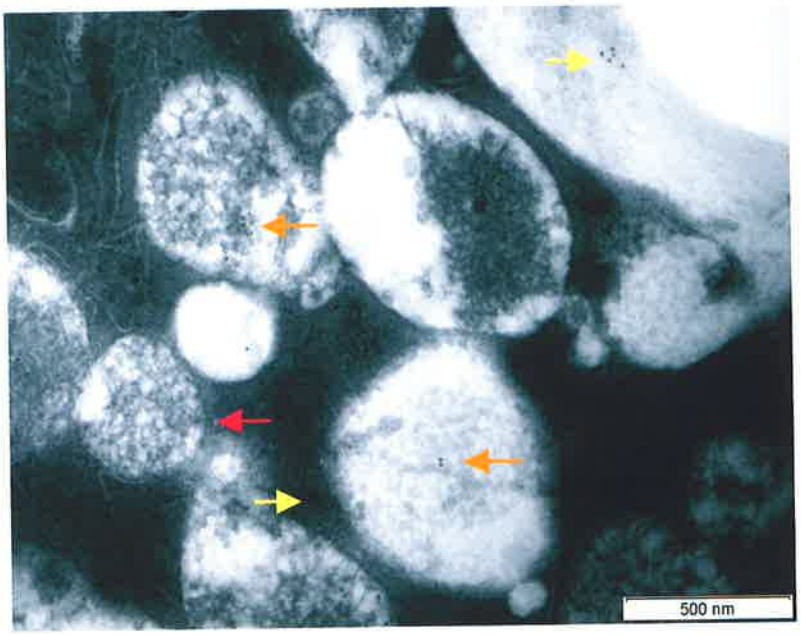


C

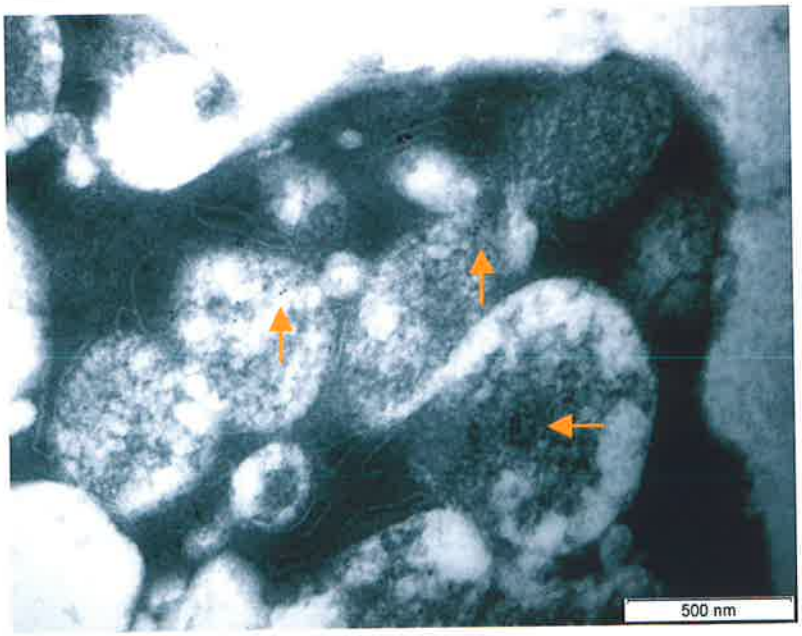

D


E

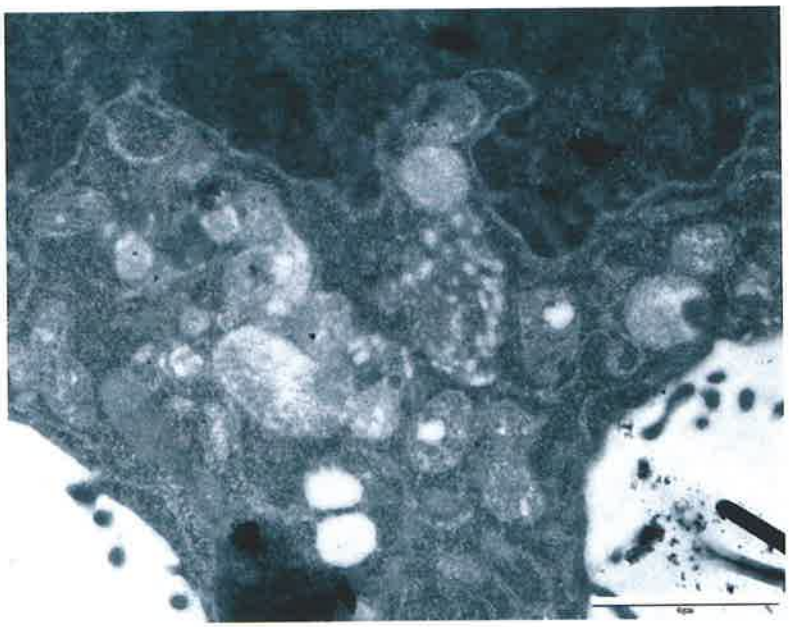

**Figure 3.17**

**Table 3.2: Number of $ZnT_4$-labelled gold particles per granule and per $\mu m^2$ granule in immature HMC-1 and mature HMC-1 cells.**

| | Immature HMC-1 | | Mature HMC-1 | |
|---|---|---|---|---|
| | **Gold particles per granule** (Mean±SEM) | **Gold particles per $\mu m^2$ granule** (Mean±SEM) | **Gold particles per granule** (Mean±SEM) | **Gold particles per $\mu m^2$ granule** (Mean±SEM) |
| **Control[a]** | 0.13 ± 0.1 | 5.1 ± 1.5 | 0.91 ± 0.2 | 8.3 ± 2.3 |
| **$ZnT_4$-labelled[b]** | 7.9 ± 0.6** | 69.5 ± 8.0** | 6.0 ± 0.5** | 98.8 ± 8.6** |

**a** = Mean gold particles per granule and per $\mu m^2$ granule of unlabelled cells ± SEM.
**b** = Mean gold particles per granule and per $\mu m^2$ granule of $ZnT_4$-labelled cells ± SEM.
**n** = A total of 80 granules were sampled for control and $ZnT_4$-labelled for all experiments.
** = $P<0.005$

granule counted in control cells compared to 6.0 ± 0.5 particles per granule (Table 3.2, $P<0.005$) in $ZnT_4$ labelled cells.

To allow for variation in the granule size, these data we corrected for granule area and expressed as mean ± SEM gold particles per $\mu m^2$ of granule in both immature and mature HMC-1 cells (Table 3.2). When data was corrected for granular area, significant differences were seen between the counts for $ZnT_4$ labelled immature HMC-1 cells with 69.5 ± 8.0 gold particles per $\mu m^2$ of granule compared to 98.8 ± 8.6 gold particles per $\mu m^2$ of granule (Table 3.2, $P<0.05$).

### 3.4 Discussion

The findings of these experiments are: 1) large amounts of labile Zn in granules of immature and mature HMC-1 mast cells, 2) release of this Zn during mast cell activation, 3) repletion of Zn in fresh medium after a further 24 h culture, 4) abundant $ZnT_4$ mRNA in mast cells, 5) $ZnT_4$ distributed either in the plasma membrane or in a subset of peripherally-located vesicles, distinct from localization of Zn and 6) no loss of $ZnT_4$ protein with activation (except with RPMC).

This study confirms previous findings using electron microscopy (Gustafson, 1967) that mast cell granules are rich in Zn and shows that the Zn can be depleted during mast cell degranulation and repleted in subsequent culture. The observation that mast cell lines like HMC-1 and RBL-2H3 and primary cord and bone-marrow derived mast cells can be cultured for long periods in the same low Zn-containing medium as other cells (e.g. A549 cells) and yet contain much more Zn, implies that mast cells have a well-developed mechanism for uptake of this metal ion as well as intracellular mechanisms to concentrate Zn into secretory granules. Recent studies in pancreatic islet cells suggests that the high content of Zn in their secretory granules is due to expression of the Zn transporter $ZnT_5$ in the membranes of these granules (Kambe, 2002). Another Zn transporter involved in secretion is $ZnT_4$, which is highly expressed in mammary epithelium (Michalczyk, 2002) and intestine (Murgia, 1999). $ZnT_4$ plays a critical role in secretion of Zn into breast milk (Murgia, 1999). At least in MDCK cells, this transporter is expressed on the membrane of intracellular vesicles of different cell types. The studies here report high expression of $ZnT_4$ mRNA by

northern blotting and RT-PCR in at least two different types of mast cells, HMC-1 and RBL-2H3. These levels were of a similar magnitude to those found in rat intestine.

Figure 3.18 shows a schema of the proposed distribution of Zn and $ZnT_4$ in mast cells before (A) and after (B) activation. Immunostaining experiments showed that $ZnT_4$ had a vesicular distribution like that of Zinquin labeling and suggestive of localization in the mast cell granule membrane. Indeed, the primary sequence of $ZnT_4$ includes 6 putative membrane-spanning domains; between domains IV and V is a His-rich loop which binds Zn and is thought to be involved in uptake of this metal across lipid membranes (Murgia, 1999). In addition, immunogold labelling experiments also showed $ZnT_4$ inside the granules, lining outside of granules and in surrounding cytoplasmic area. Some of the cytoplasmic labelling appeared to be in the plasma membrane (Figure 3.16A). It was observed that the density of $ZnT_4$ immunogold particles within granules was modestly but significantly increased in the mature HMC-1 cells compared with the immature HMC-1 cells. Although there was no obvious difference between Zinquin staining of immature and mature HMC-1 cells, this increase might relate in some way to granule maturation in mast cells.

While Zn was lost with mast cell activation, $ZnT_4$ was retained further supporting the hypothesis that Zn vesicles and $ZnT_4$-contaning vesicles are distinct. However, in RPMC a loss of $ZnT_4$ was observed following activation. Since RPMC are primary mast cells, localization of $ZnT_4$ may be different from that of malignant mast cells. It would be interesting to look at the electron microscopic localization of $ZnT_4$ in primary mast cells but there were an insufficient number of cells to perform the immunogold experiments.

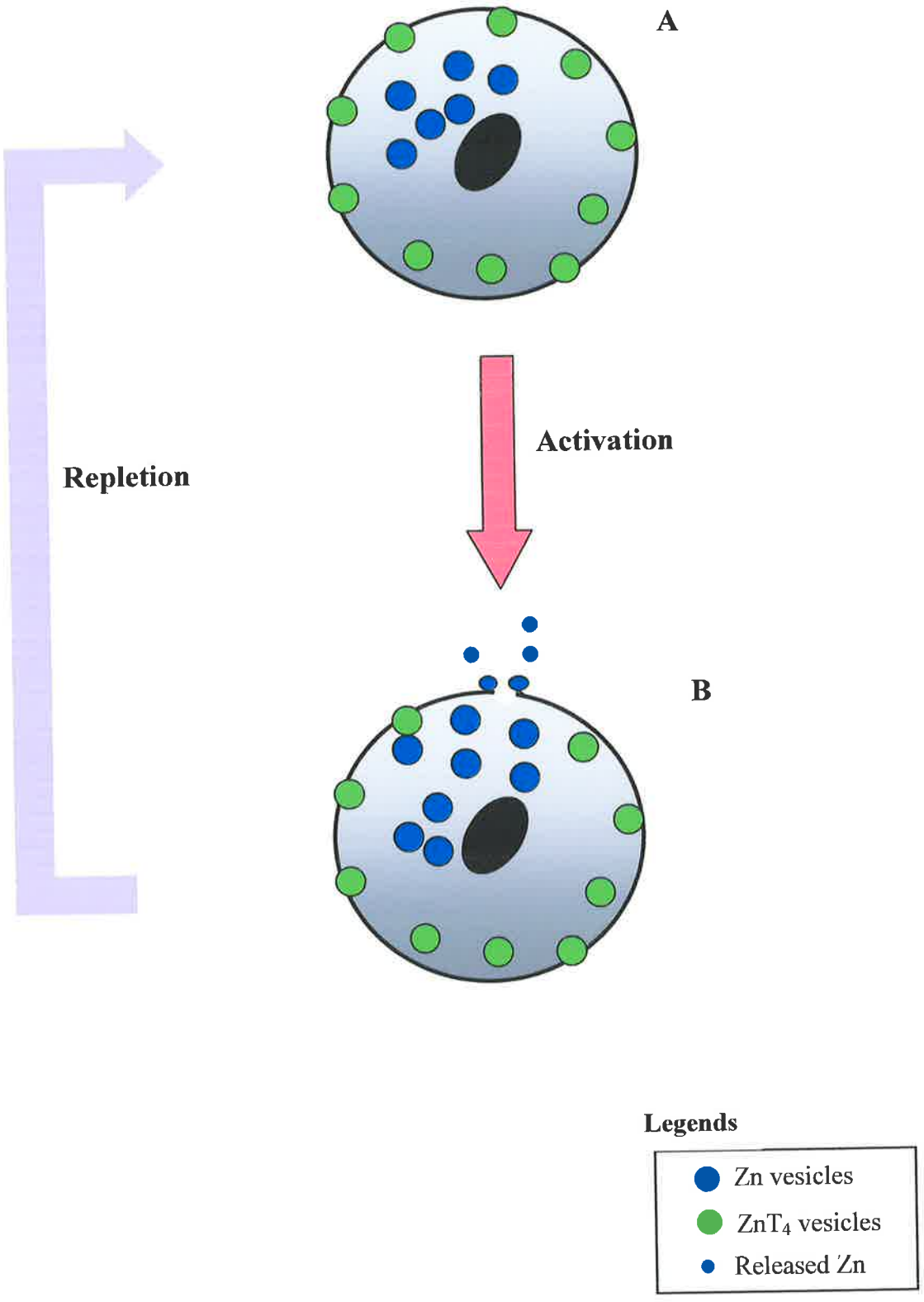
A
Repletion
Activation
B
Legends
Zn vesicles
ZnT4 vesicles
Released Zn

**Figure 3.18**

**Figure 3.18: Schema of Zn and $ZnT_4$ distribution in untreated and activated mast cells.**

**A:** A resting mast cell showing perinuclear localization of Zn (blue circles) and more apical localization of $ZnT_4$ (green circles). It is not clear whether the $ZnT_4$ is within the plasma membrane nor is it clear what relationship there is between two types of vesicles.

**B:** Activated mast cell undergoing degranulation with release of Zn but not $ZnT_4$. Activated mast cells can recover their Zn by taking up Zn from their environment (repletion).

Dual labeling confocal studies in mast cells showed only partial co-localization of Zn and $ZnT_4$+ve vesicles, with the latter more peripherally located in the cell. This may indicate that $ZnT_4$ is expressed in more apically-located granules or that it preferentially mediates uptake of Zn from the extracellular environment of the cell. This may indicate that the main function of $ZnT_4$ is not directly involved in the transport of Zn into vesicles. Similar conclusions were reached by Ranaldi and colleagues in kidney derived cells with a $ZnT_4$ specific antibody and Zinquin labeling. They also showed that this transporter does not localize to the same set of vesicles that contain Zn (Ranaldi, 2002). This was also reported in human breast epithelial cell where there was an absence of overlap between Zn and $ZnT_4$ (Michalczyk, 2002).

Zn and $ZnT_4$ levels did not appear to change with maturation at least in HMC-1 cells. A number of possible functions for $ZnT_4$ can be proposed. Firstly, it may be involved in uptake of Zn by mast cells. The high level of $ZnT_4$ in these cells may enable mast cells to scavenge extra Zn from their environment more readily than other cells, particularly after activation and degranulation. Secondly, it may be involved in packaging of Zn into secretory granules. This seems unlikely since the $ZnT_4$ vesicles were more apical than the Zn vesicles. If $ZnT_4$ were involved in incorporation of Zn into vesicles, then one would expect that the $ZnT_4$ would be concentrated in the region of the golgi where secretory granules are formed. Thirdly, $ZnT_4$ may be involved in mast cell secretion. It was not possible to address this issue here but further experiments could be done looking at mast cell secretion in the $ZnT_4$ defective lethal milk mice.

# CHAPTER FOUR

# LOCALISATION OF PRO-CASPASE-3 AND -4 IN MAST CELLS AND EFFECTS OF ACTIVATION

## 4.1 Introduction

The main focus of this thesis is the potential of Zn as a regulator of caspase-3. There have been no published studies on the localization and levels of caspases in mast cells and their effects on the function and survival of these cells. This chapter describes the localisation and levels of pro-caspases-3 and -4 in mast cells under normal and activated conditions. As shown in chapter three, mast cells are rich in Zn. Since Zn is an inhibitor of pro-caspase-3 activation, it was interesting to determine whether there was a spatial relationship between Zn and pro-caspase-3. The relationship between Zn and mast cell apoptosis, particularly the activation of pro-caspase-3, has not been defined. The release of Zn following mast cell degranulation, shown in the previous chapter has led to the hypothesis that activation of mast cells results in changes in susceptibility of these cells to undergo caspase activation and apoptosis.

Another interesting question concerns the fate of mast cells following degranulation; they may be removed by apoptosis or they may recover. Some evidence has been obtained showing that mast cells do recover following activation (Dvorak, 1991), but this needs further confirmation. Studies of mast cell apoptosis have mainly focused on the importance of growth factors such as stem cell factor (SCF) and IL-3 in preventing apoptosis.

Caspases are critical for apoptosis, a highly conserved and regulated form of cell death important in maintaining cellular homeostasis (Kerr, 1987). The caspase family consists of at least 14 members that are expressed in almost all cell types as inactive pro-caspases (Creagh and Martin, 2001). Pro-caspases are found in several

intracellular compartments including: mitochondria, golgi apparatus, cytosol, endoplasmic reticulum and nucleus (Porter, 1999; Susin, 1999; Zhivotovsky, 1999). Caspase-3 is a wellknown executioner enzyme in the process of apoptosis (Slee, 2001). It is responsible for the proteolytic cleavage of critical protein regulators such as DNA repair enzymes and mediators of protein synthesis (Cohen, 1997; Thornberry and Lazebnik, 1998).

Pro-caspase-3 is activated by initiator caspases, which include caspases-8 and -9 through two main intracellular pathways; 1) ligation of death receptor such as Fas/Apop-1/CD95 receptors and 2) release of apoptogenic factors from mitochondria such as cytochrome *c* (Hengartner, 2000). Activation of caspase-3 involves the proteolytic processing of the 32KDa cytosolic proenzyme to a tetrameric heterodimer of 17KDa subunits and can be quantified by the capacity of cell cytosol to cleave the fluorogenic substrate DEVD-AFC (Talanian, 1997).

Activation of caspase-3 leads to downstream events of apoptosis, which include characteristic morphological changes of DNA fragmentation, chromatin condensation, membrane blebbing and formation of apoptotic bodies (Sahara, 1999; Sebbagh, 2001; Song and Steller, 1999). Pro-caspase-3 is widely distributed with high expression in human cell lines of lymphocytic origin (Fernandes-Alnemri, 1994) but it has not yet been studied in mast cells.

Pro-caspase-4 was also studied for comparison in this thesis since it is thought to be largely a pro-inflammatory caspase rather than a pro-apoptotic caspase. The role of caspase-4 is elusive, although most studies have suggested that its main role is in the

processing of pro-inflammatory cytokines (Earnshaw, 1999), and the maturation of caspase-1, a known pro-inflammatory caspase (Wang and Lenardo, 2000). However, other studies have also shown that over expression of caspase-4 resulted in apoptosis, including involvement in Fas-mediated apoptosis; (Kamada, 1997; O'Connell, 2000; Ossina, 1997). Pro-caspase-4 is found in most tissues excluding the brain, with significant amounts in lung and liver, ovary and placenta (Munday, 1995).

The experiments in this chapter demonstrate the localisation of pro-caspases-3 and -4 within immature and mature HMC-1 human mast cells, RBL-2H3 and rat peritoneal mast cells. Immunofluorescence and immungold labelling were used to determine the localisation of these pro-caspases before and after degranulation.

## 4.2 Methods

### 4.2.1 Expression Of Pro-Caspase-3 By Northern Hybridization

The expression of pro-caspase-3 was determined by Northern hybridization (section 2.6.7 onwards) in immature and mature HMC-1 and RBL-2H3 cells. Quantification of northern bands was performed as described in section 2.6.13 using pro-caspase-3 cDNA insert excised from pGEM-T-Easy plasmid (gift of Dr Prue Cowled, Department of Surgery, QEH) and amplified and purified for probing.

### 4.2.2 Activation Of Mast Cells

Immature and mature HMC-1and RBL-2H3 mast cells were activated with 1μg/ml compound 48/80 for 18 h at 37°C.

### 4.2.3 Localization Of Pro-Caspase-3 And -4 By Immunofluorescence

Distribution of pro-caspase-3 and -4 were determined by immunofluorescence using primary rabbit anti-pro-caspase-3 and -4 antibodies and secondary FITC-conjugated goat anti-rabbit antibody. Cells were cyto-centrifuged on microscope slides and paraformaldehyde fixed before staining with antibodies (sections 2.1.5 and 2.4). Distributions of pro-caspase-3 and -4 were visualized by epi-fluorescence microscopy and confocal UV fluorescence microscopy. Epi-fluorescence was quantified using Video Pro Image Analysis software.

### 4.2.4 Localization Of Pro-Caspase-3 And -4 By Electron Microscopy

The localizations of pro-caspase-3 and -4 were also determined by immunogold labelling. Mast cells were processed and labelled for the pro-caspases using the same method as described for $ZnT_4$ (Chapter 3.2.2). Quantitation of gold particles was performed using the analySIS software. Levels of pro-caspases were expressed as number of gold particles per granule. To allow for variation of granule size, levels were also expressed as the number of gold particles per $\mu m^2$ of granule.

### 4.2.5 Statistical Analysis

The results of typical experiments are described or data were pooled, as indicated in text. Statistical significance was determined by the student *t*-test and the Tukey-Kramer multiple comparisons test where appropriate and is indicated in text or legends to Figures.

## 4.3 Results

### 4.3.1 Expression Of Pro-Caspase-3 mRNA In Mast Cells

The expression of pro-caspase-3 mRNA was determined by northern hybridization in immature and mature HMC-1 and RBL-2H3 mast cells untreated and compound 48/80 treated (Figure 4.1). Positive controls were included: SW480 (lane 1) and SW620 (lane 2). Pro-caspase-3 was expressed in all untreated and treated mast cells. Northern bands were quantified and levels of pro-caspase-3 expression were found to be high in the various mast cell types (Figure 4.2). High levels of pro-caspase-3 were seen in RBL-2H3 mast cells and immature HMC-1, compared to those of mature HMC-1 mast cells (Figure 4.2 $P<0.005$). For each mast cell type, there were no significant differences between untreated and compound 48/80 treated cells (Figure 4.2).

### 4.3.2 Expression Of Pro-Caspase-3 And -4 In Mast Cells By Immunofluorescence

Epi- fluorescence labelling of pro-caspase-3 was studied in three different types of mast cells: immature HMC-1 (Figure 4.3), mature HMC-1 (Figure 4.4) and RPMC (Figure 4.5). Images are shown using both 20x and 100x objective lenses. Secondary antibody alone (FITC-conjugated goat anti-rabbit) did not label the cells as shown in the bottom panel in each figure. By contrast, cells treated with both primary and secondary antibodies were fluorescent suggesting that pro-caspase-3 is expressed by mast cells. The 100x images for immature and mature HMC-1 cells show largely cytoplasmic distribution of pro-caspase-3. This is particularly evident in Figure 4.4 where the shadow of the nucleus can be seen. In RPMC, pro-caspase-3 was also

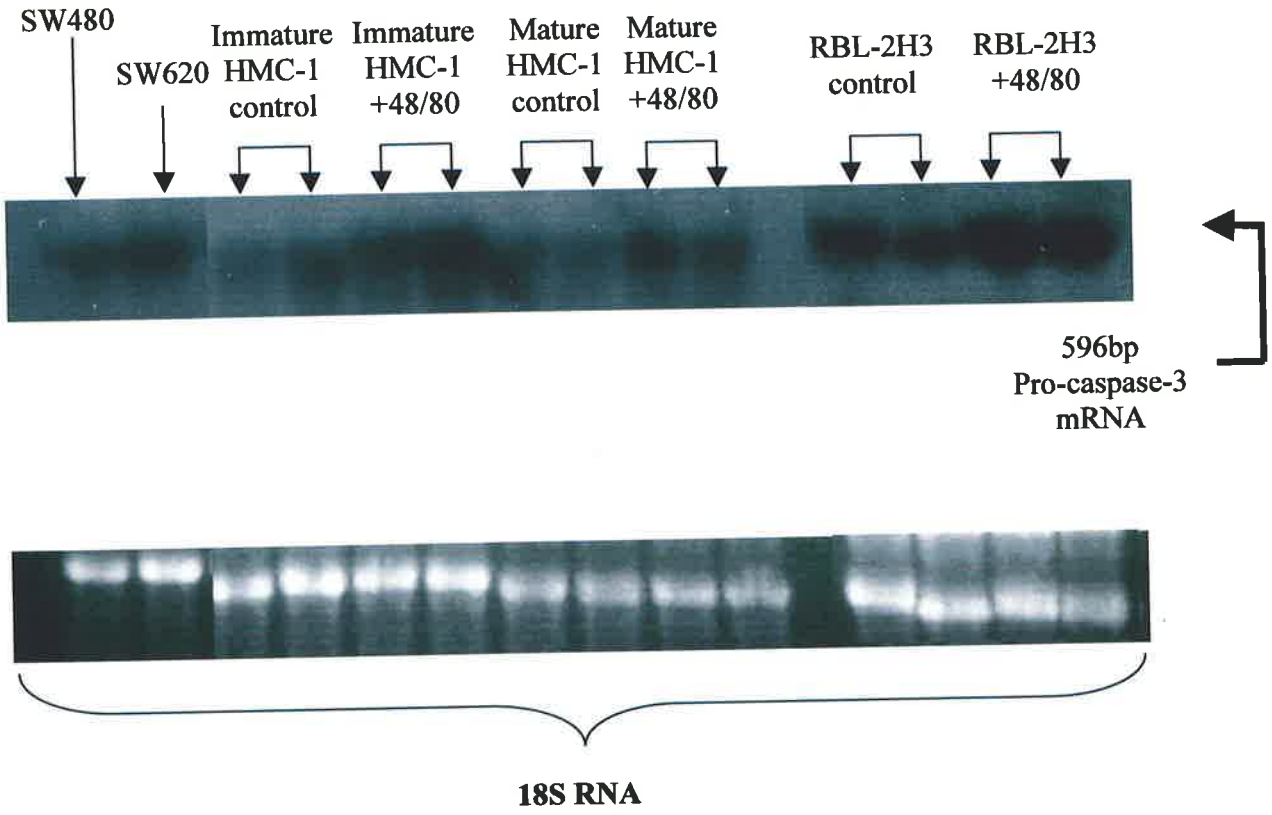
SW480
SW620
Immature HMC-1 control
Immature HMC-1 +48/80
Mature HMC-1 control
Mature HMC-1 +48/80
RBL-2H3 control
RBL-2H3 +48/80
596bp Pro-caspase-3 mRNA
18S RNA

**Figure 4.1**

**Figure 4.1: Pro-caspase-3 mRNA expression in immature and mature HMC-1 and RBL-2H3 mast cells by Northern Hybridization.**

Northern blot analysis using a pro-caspase-3 probe is shown in the upper panel and parallel ethidium bromide staining pattern of control 18S rRNA on the lower panel. Figure shows high expression of pro-caspase-3 mRNA in immature and mature HMC-1 mast cells and RBL-2H3 mast cells. Positive controls were mRNA from SW480 and SW620 cells.

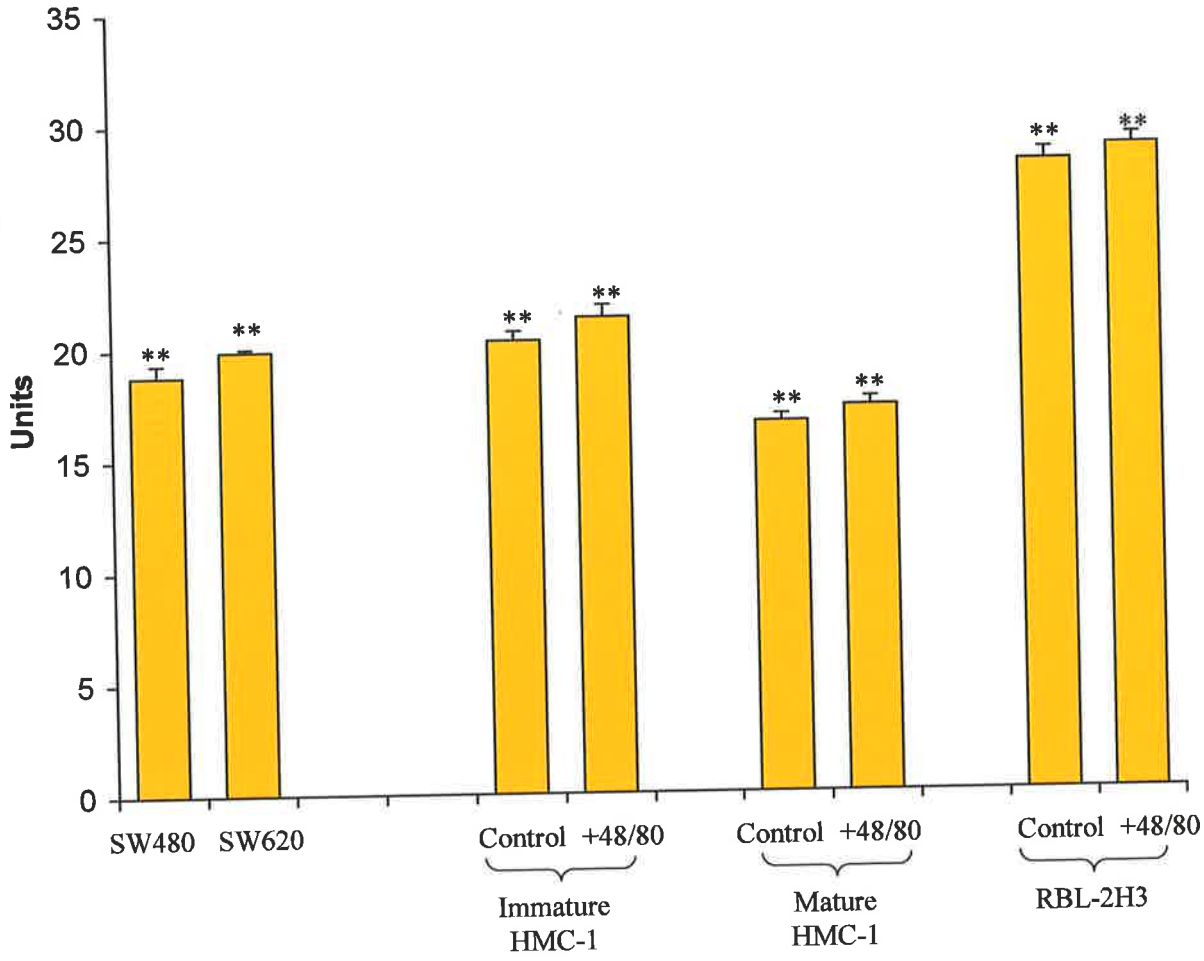
35
30
25
20
15
10
5
0
Units
**
SW480
SW620
Control
+48/80
Immature HMC-1
Mature HMC-1
RBL-2H3

**Figure 4.2**

**Figure 4.2: Quantification of northern bands showing pro-caspase-3 mRNA expression in immature and mature HMC-1 and RBL-2H3 mast cells.**

Northern bands were quantified for immature and mature HMC-1 mast cells and RBL-2H3 mast cells. Figure shows high levels of pro-caspase-3 mRNA expression in all mast cell types studied. There was no difference between levels of pro-caspase-3 mRNA in untreated and treated cells.

Bars indicate SEM for means of triplicate measurements from each of the duplicate tracks. Statistical significances are indicated as ** $P<0.005$.

## Immature HMC-1 Pro-caspase-3

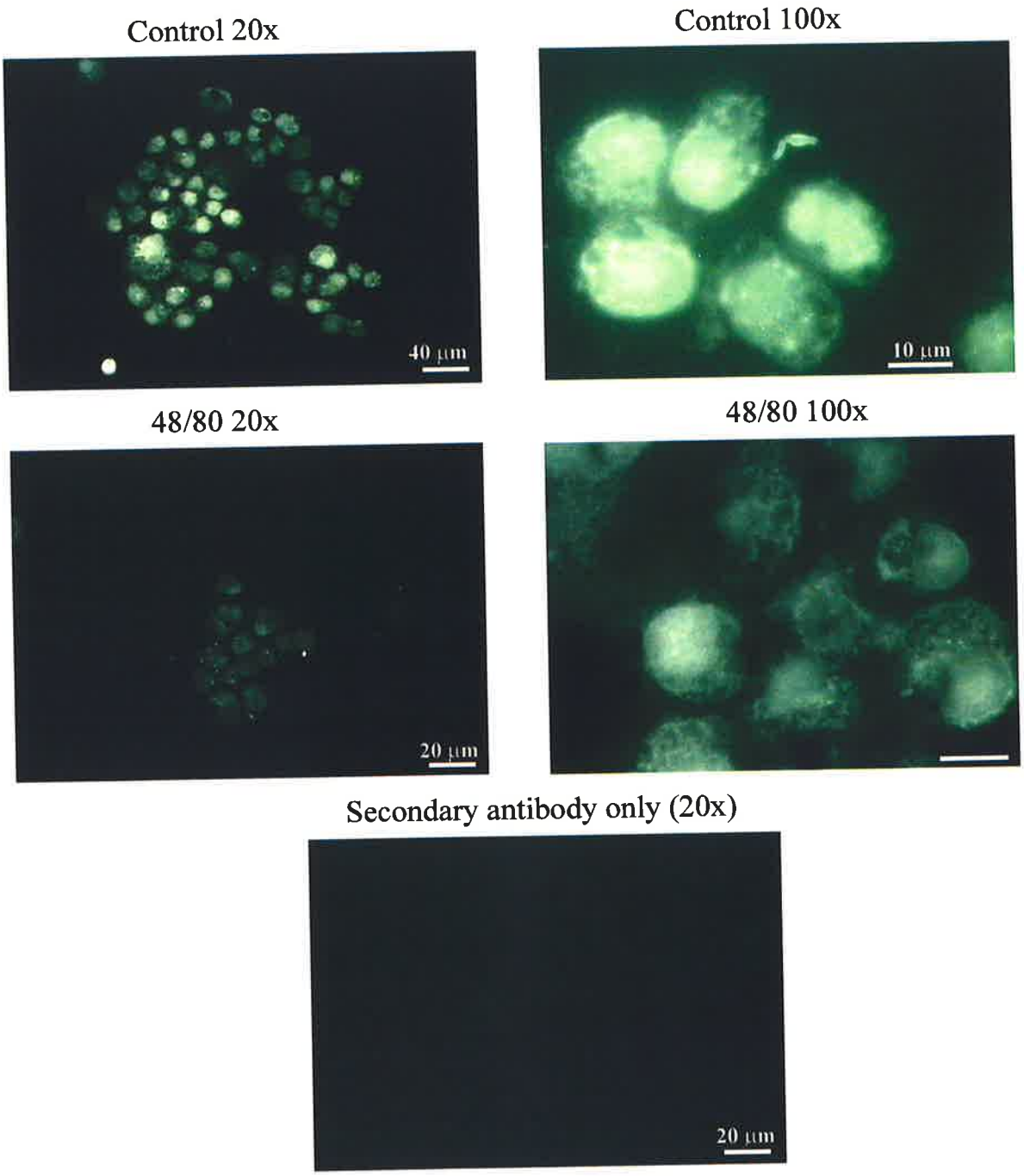


**Figure 4.3**

**Figure 4.3: Subcellular localization of pro-caspase-3 in immature HMC-1 mast cells treated with compound 48/80.**

Figure shows typical immunofluorescence images of pro-caspase-3 localization in control (top panels) and 1 μg/ml compound 48/80 (bottom panels) treated immature HMC-1 captured under 20x lens (LHS panels) and 100x lens (RHS panels). Images captured under 20x show the overall distribution of fluorescence in the cell population. While images captured under 100x show the cytoplasmic distribution of pro-caspase-3.

## Mature HMC-1 Pro-Caspase-3

Control 20x

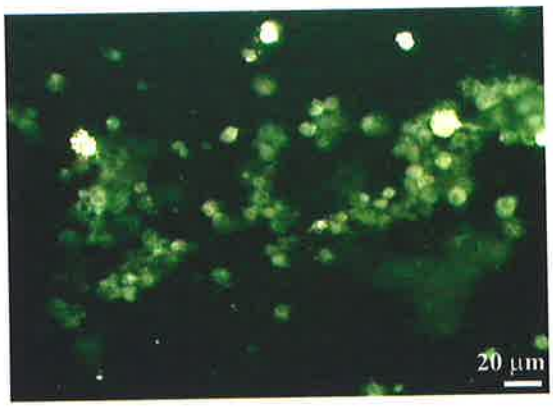


Control 100x

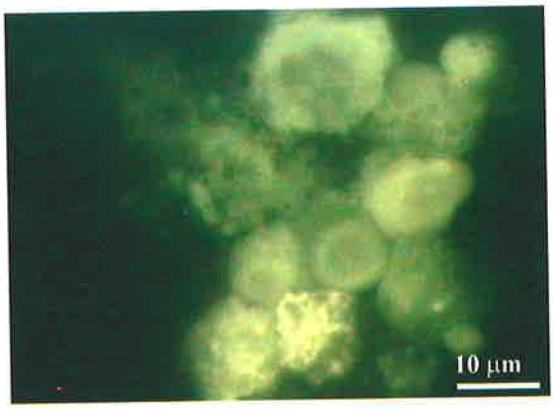


48/80 20x

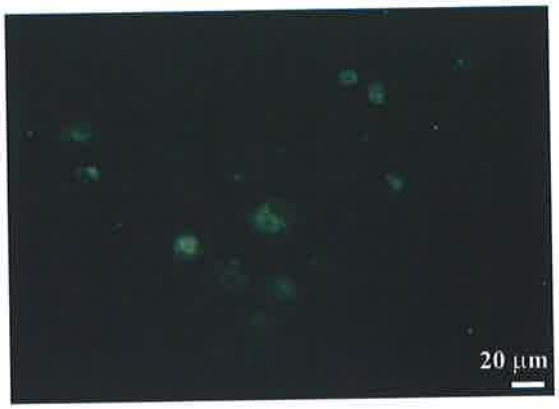


48/80 100x


Secondary Ab only (20x)


**Figure: 4.4**

**Figure 4.4: Subcellular localization of pro-caspase-3 in mature HMC-1 mast cells treated with compound 48/80.**

Figure shows typical immunofluorescence images of pro-caspase-3 localization in control (top panels) and 1 μg/ml compound 48/80 (bottom panels) treated mature HMC-1 captured under 20x lens (LHS panels) and 100x lens (RHS panels). Images captured under 100x show cytoplasmic distribution of pro-caspase-3.

## RPMC Pro-caspase-3

Control 20x

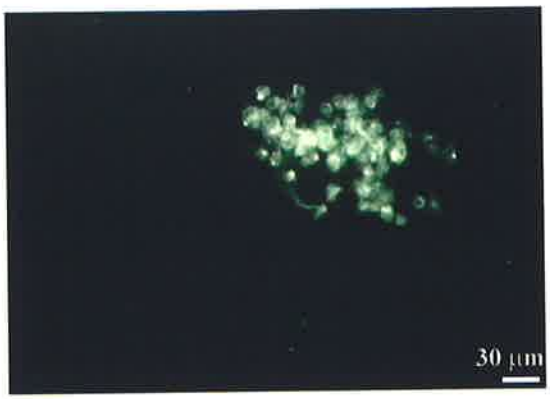


Control 100x

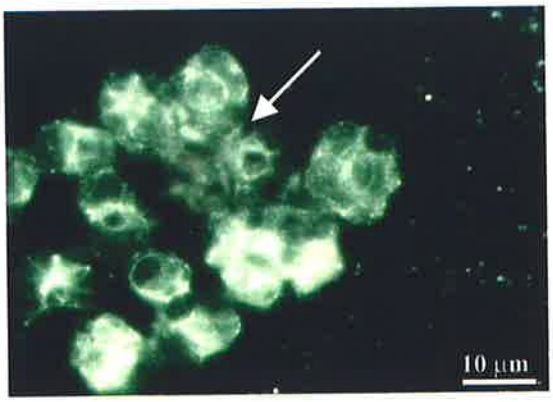


48/80 20x

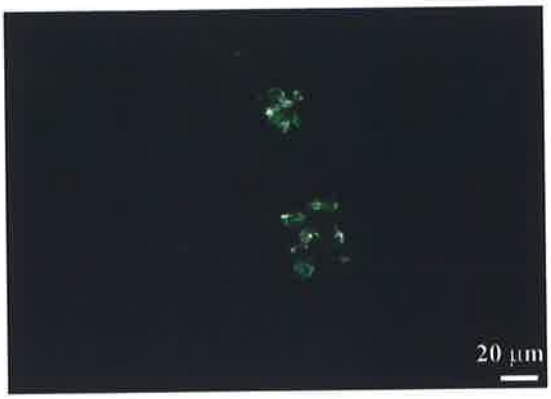


48/80 100x


Secondary Antibody only (20x)


**Figure 4.5**

**Figure 4.5: Subcellular localization of pro-caspase-3 in RPMC treated with compound 48/80.**

Figure shows typical immunofluorescence images of pro-caspase-3 localization in control (top panels) and 1 μg/ml compound 48/80 (bottom panels) treated RPMC captured under 20x lens (LHS panels) and 100x lens (RHS panels). Images captured under 100x show cytoplasmic distribution with occasional cells (white arrow) showing a perinuclear pattern of pro-caspase-3.

cytoplasmic but occasional cells showed a perinuclear pattern (Figure 4.5, white arrow).

To achieve a higher resolution, pro-caspase-3 distribution was determined by immunofluorescence confocal microscopy in immature and mature HMC-1 cells (Figure 4.6 left hand panels). This figure shows pro-caspase-3 with a cytoplasmic and vesicular-like distribution, similar to that of Zn and may indicate that pro-caspase-3 is in the secretory granules.

Similar patterns were seen for pro-caspase-4 in epi-fluorescence labelling for immature HMC-1 (Figures 4.7), mature HMC-1 (Figure 4.8) and RPMC (Figure 4.9). Figure 4.10 shows images obtained by confocal microscopy. As for pro-caspase-3, the distribution of pro-caspase-4 appeared to be cytoplasmic and vesicular.

### 4.3.3 Effects Of Mast Cell Activators On Pro-Caspase-3 And -4 In Immature And Mature HMC-1 Cells And RPMC

Since the distribution of pro-caspase-3 and -4 appears to be vesicular, the next step was to determine whether degranulation of mast cells would decrease levels of both pro-caspases. To induce degranulation, mast cells were treated with 1μg/ml compound 48/80 for 18 h. Pro-caspase-3 levels in compound 48/80 treated cells are shown for immature HMC-1 (Figure 4.3, middle panels), mature HMC-1 (Figure 4.4, middle panels) and RPMC (Figure 4.5, middle panels). These were examined by epi-fluorescence microscopy. For each cell type there was a substantial decrease in pro-caspase-3 fluorescence. Similar decreases were seen in images obtained by confocal

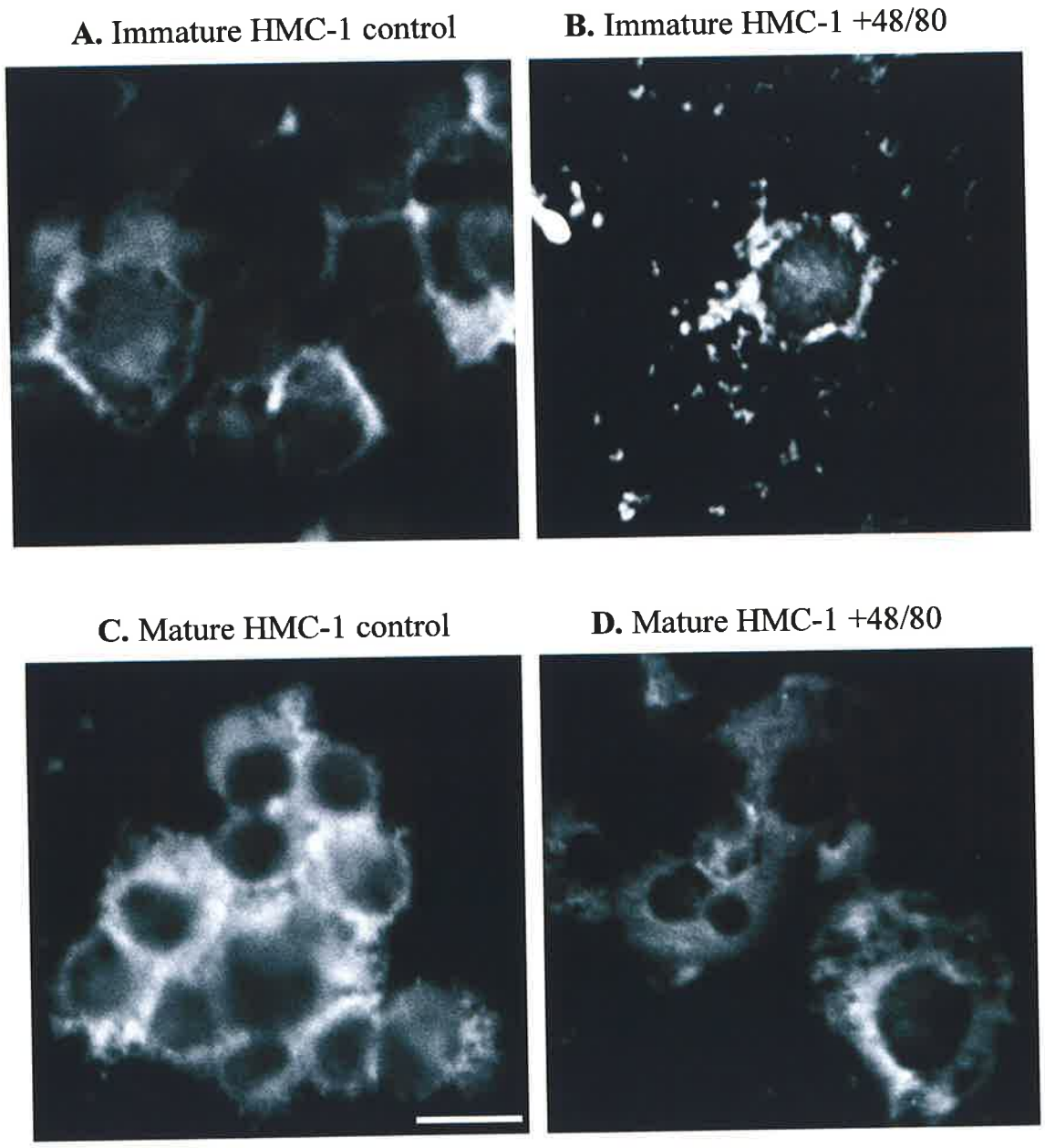
A. Immature HMC-1 control
B. Immature HMC-1 +48/80
C. Mature HMC-1 control
D. Mature HMC-1 +48/80

**Figure 4.6**

**Figure 4.6: Localization of pro-caspase-3 in immature and mature HMC-1mast cells treated with compound 48/80 by confocal immunofluorescence.**

Figure 4.6 A-D shows four typical confocal images of pro-caspase-3 localization in immature (A and B) and mature (C and D) HMC-1 cells before (A and C) and after (B and D) treatment with 1μg/ml compound 48/80. Scale bar indicates 20 μm. Figure shows cytoplasmic and vesicular-like distribution of pro-caspase-3.

microscopy (Figure 4.6, B and D). Also note the presence of pro-caspase-3 in granular material being released from the mast cell shown in Figure 4.6B. There were also decreases in pro-caspase-4 levels in compound 48/80 treated immature HMC-1 (Figure 4.7, middle panels), mature HMC-1 (Figure 4.8, middle panels) and RPMC (Figure 4.9, middle panels). This decrease was also seen by confocal microscopy (Figure 4.10, RHS panels).

To further validate the effects of degranulation on pro-caspase-3, fluorescence intensity was quantified in a minimum of 120 cells before and after treatment with compound 48/80. The data are summarised in Table 4.1 for three separate experiments for each mast cell type. For example, in experiment one immature HMC-1 cells had a mean fluorescence intensity ± SEM for pro-caspase-3 of 39.9 ± 0.8 GSUand this decreased to 11.6 ± 0.3 ($P<0.005$) after treatment with compound 48/80. Significant decreases were seen in all three experiments. Similar decreases were seen in mature HMC-1 cells and RPMC treated with compound 48/80 (Table 4.1). Significant decreases were also seen for pro-caspase-4 for each mast cell type (Table 4.1).

### 4.3.4 Localization Of Pro-Caspase-3 And -4 In Mast Cells By Electron Microscopy

The decrease in fluorescence of pro-caspase-3 and -4 with mast cell activation is consistent with the hypothesis that pro-caspases are contained within secretory granules and released following degranulation. Therefore the distribution of pro-caspase-3 and -4 in resting mast cells was studied at the electron microscopy level

## Immature HMC-1 Pro-caspase-4

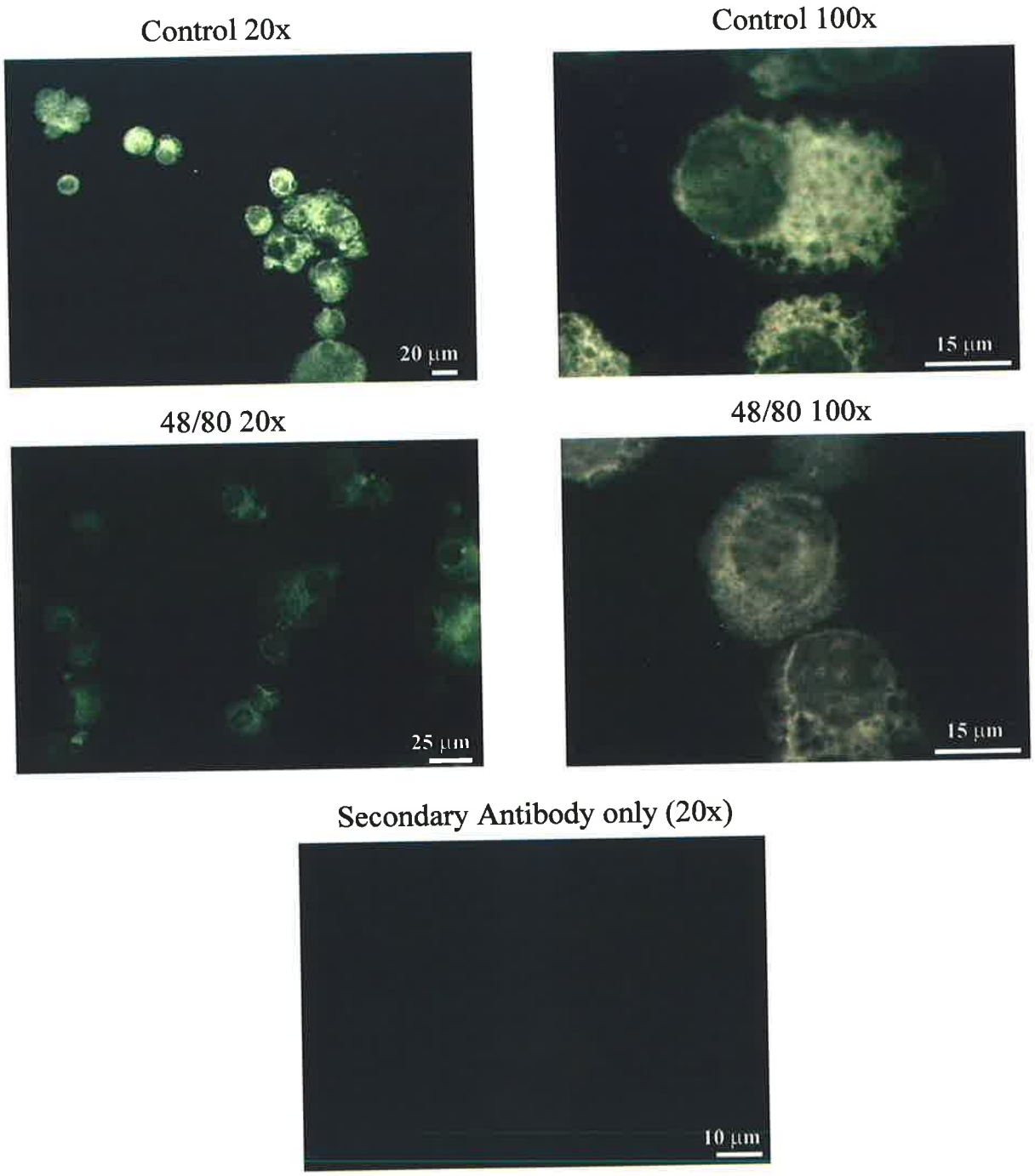


**Figure 4.7**

**Figure 4.7: Subcellular localization of pro-caspase-4 in immature HMC-1 mast cells treated with compound 48/80.**

Figure shows typical immunofluorescence images of pro-caspase-4 localization in control (top panels) and 1 μg/ml compound 48/80 (bottom panels) treated immature HMC-1 captured under 20x lens (LHS panels) and 100x lens (RHS panels). Images captured under 100x show cytoplasmic distribution of pro-caspase-3.

## Mature HMC-1 Pro-caspase-4

Control 20x


Control 100x


48/80 20x


48/80 100x


Secondary Antibody only (20x)


**Figure 4.8**

**Figure 4.8: Subcellular localization of pro-caspase-4 in mature HMC-1 mast cells treated with compound 48/80.**

Figure shows typical immunofluorescence images of pro-caspase-4 localization in control (top panels) and 1 μg/ml compound 48/80 (bottom panels) treated mature HMC-1 captured under 20x lens (LHS panels) and 100x lens (RHS panels). Images captured under 100x show cytoplasmic distribution of pro-caspase-3.

## RPMC Pro-caspase-4

Control 20x

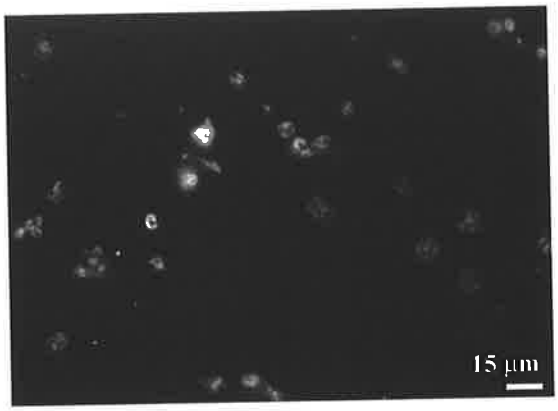


Control 100x

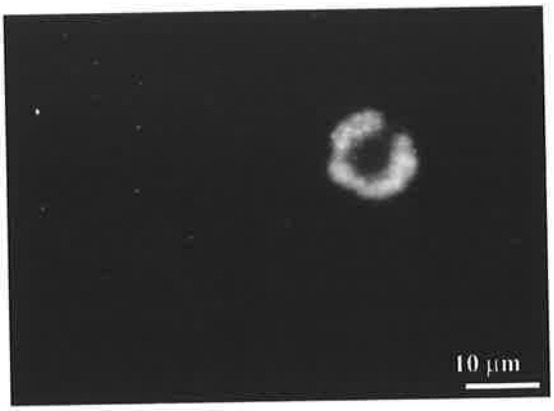


48/80 20x


48/80 100x

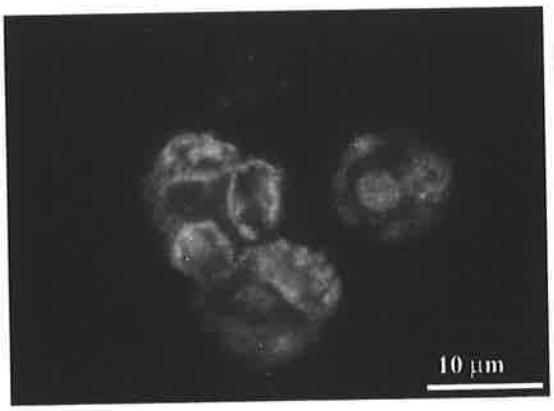


Secondary Antibody only (20x)


**Figure 4.9**

**Figure 4.9: Subcellular localization of pro-caspase-4 in RPMC treated with compound 48/80.**

Figure shows typical immunofluorescence images of pro-caspase-4 localization in control (top panels) and 1 μg/ml compound 48/80 (bottom panels) treated RPMC captured under 20x lens (LHS panels) and 100x lens (RHS panels). Images captured under 100x show cytoplasmic and occasional perinuclear distribution of pro-caspase-3.

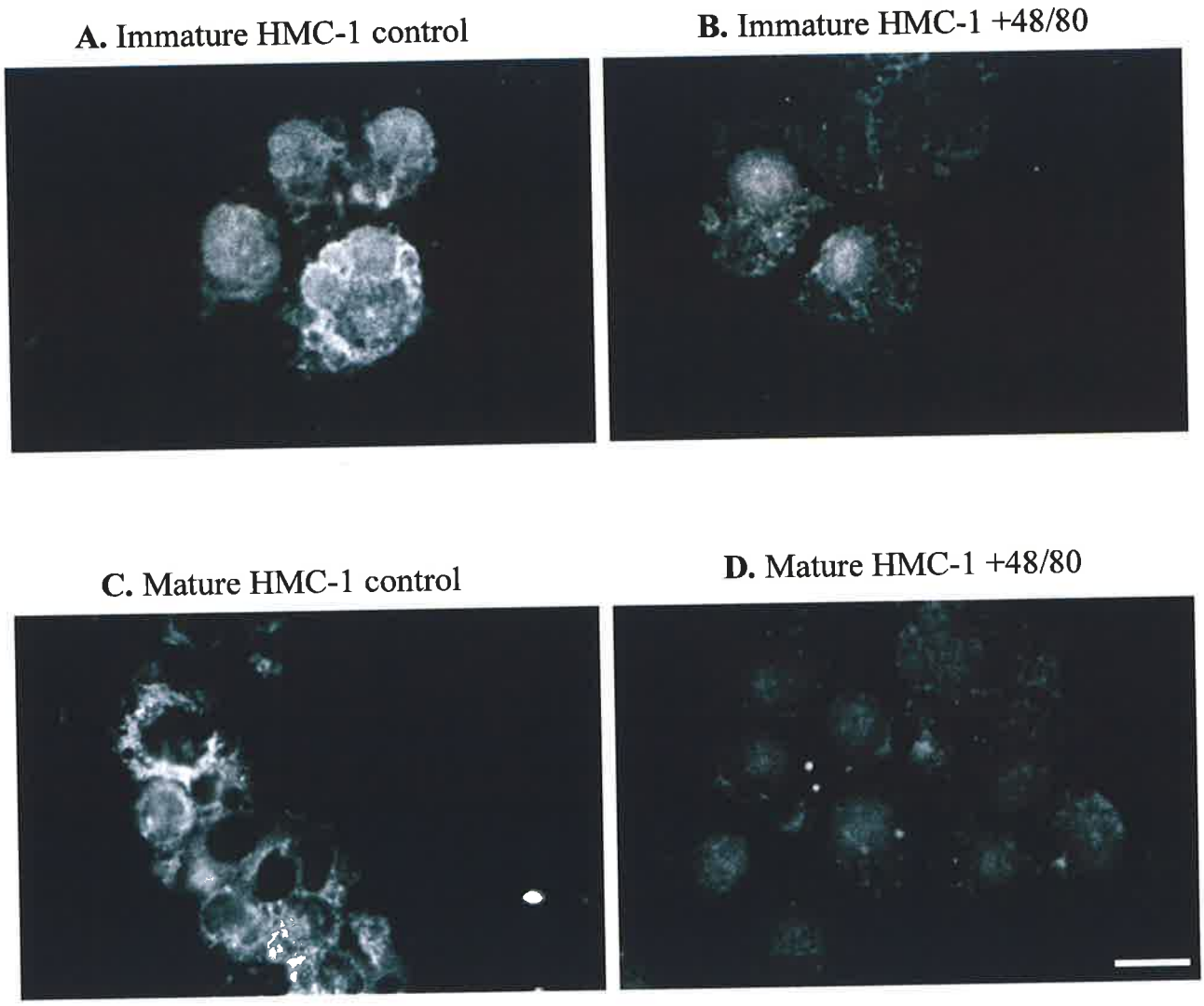
A. Immature HMC-1 control
B. Immature HMC-1 +48/80
C. Mature HMC-1 control
D. Mature HMC-1 +48/80

**Figure 4.10**

**Figure 4.10: Localization of pro-caspase-4 in immature and mature HMC-1 mast cells treated with compound 48/80 by confocal immunofluorescence.**

Figure 4.10 A-D shows four typical confocal images of pro-caspase-4 localization in immature (A and B) and mature (C and D) HMC-1 cells before (A and C) and after (B and D) treatment with 1μg/ml compound 48/80. Scale bar indicates 20 μm. Figure shows cytoplasmic and vesicular-like distribution pro-caspase-4.

**Table 4.1. Effect of Degranulation on pro-caspase-3 and pro-caspase-4 levels**

| | Pro-caspase-3 | | | | Pro-caspase-4 | | | |
|---|---|---|---|---|---|---|---|---|
| Cells | Expt 1 | Expt 2 | Expt 3 | Mean[d] | Expt 1 | Expt 2 | Expt 3 | Mean[d] |
| Immature HMC-1 | | | | | | | | |
| Control[a] | 39.9 ± 0.8 | 23.6 ± 0.5 | 39.9 ± 0.4 | 34.5 | 34.3 ± 0.8 | 26.4 ± 0.7 | 30.2 ± 0.6 | 30.3 |
| +48/80[b] | 11.6 ± 0.3** | 15.5 ± 0.3** | 14.8 ± 0.3** | 14.0 | 25.8 ± 0.7** | 6.5 ± 0.2** | 16.4 ± 0.6** | 16.2 |
| n[c] | 355 | 347 | 321 | | 340 | 273 | 219 | |
| Mature HMC-1 | | | | | | | | |
| Control[a] | 20.2 ± 0.3 | 46.4 ± 1.2 | 52.0 ± 0.9 | 39.6 | 36.3 ± 1.2 | 37.0 ± 1.4 | 46.4 ± 1.1 | 39.9 |
| +48/80[b] | 15.8 ± 0.2** | 17.1 ± 0.5** | 17.7 ± 0.9** | 16.8 | 7.6 ± 0.4** | 17.0 ± 0.5** | 14.7 ± 0.5** | 13.1 |
| n[c] | 484 | 283 | 109 | | 272 | 121 | 213 | |
| RPMC | | | | | | | | |
| Control[a] | 42.0 ± 1.5 | 38.3 ± 1.1 | 41.6 ± 0.7 | 40.6 | 28.1 ± 0.7 | 12.5 ± 0.5 | | 20.3 |
| +48/80[b] | 27.9 ± 1.6** | 27.1 ± 1.6** | 14.2 ± 0.4** | 23.1 | 6.0 ± 0.3** | 10.4 ± 0.5** | | 8.2 |
| n[c] | 144 | 190 | 224 | | 233 | 128 | | |

**a** = Pro-caspase fluorescence of untreated cells; Mean ± SEM, (GSU) for each individual experiment.
**b** = Pro-caspase fluorescence of cells treated for 18hr with 1μg/ml compound 48/80; Mean ± SEM, (GSU) for each individual experiment.
**c** = Total number of cells used for quantification of fluorescence.
**d** = Mean of three experiments
** = $P<0.005$

using the immunogold technique. Figure 4.11; panel A shows the ultrastructural features of an immature HMC-1 mast cell. Note the large nucleus and granules represented by electron dense areas. As expected, mast cells incubated with secondary gold-labelled antibody (lacking primary antibody) were not stained (panel B, high magnification). Panels C-F shows immunogold labelling of pro-caspase-3 in immature HMC-1 cells, which was especially prominent in the amorphous material (yellow arrows), scroll like structures (orange arrows) of mast cell granules and in exocytosed materials (red arrow).

Panel A in Figure 4.12 shows ultra structural features of a mature HMC-1 cells, notice the smaller nucleus and abundant granular vesicles. Control lacking primary antibody was not stained (Figure 4.12, panel B). A similar pattern of pro-caspase-3 labelling was seen for mature HMC-1 cells in Figure 4.12, panels C-F.

Panel A of Figure 4.13 shows the ultrastructural features of an RBL-2H3 mast cell, with prominent nucleus and various shaped granules. As for the other mast cell types there was no labelling with secondary antibody alone (panel B). Pro-caspase-3 was localized in both amorphous (yellow arrows) and scroll like granular structures (orange arrows) in RBL-2H3 rat mast cells (Figure 4.13, panels C-F). Some labelling was seen in intra-granular spaces (blue arrows).

Immunogold labelling for pro-caspase-4 was localized in amorphous material (yellow arrows), and intra-granular spaces (blue arrows) of immature HMC-1 mast cells (Figure 4.14, panels A-D). Control section lacking primary antibody shows little particle labelling in both granules and surrounding areas (panel E). A similar pattern

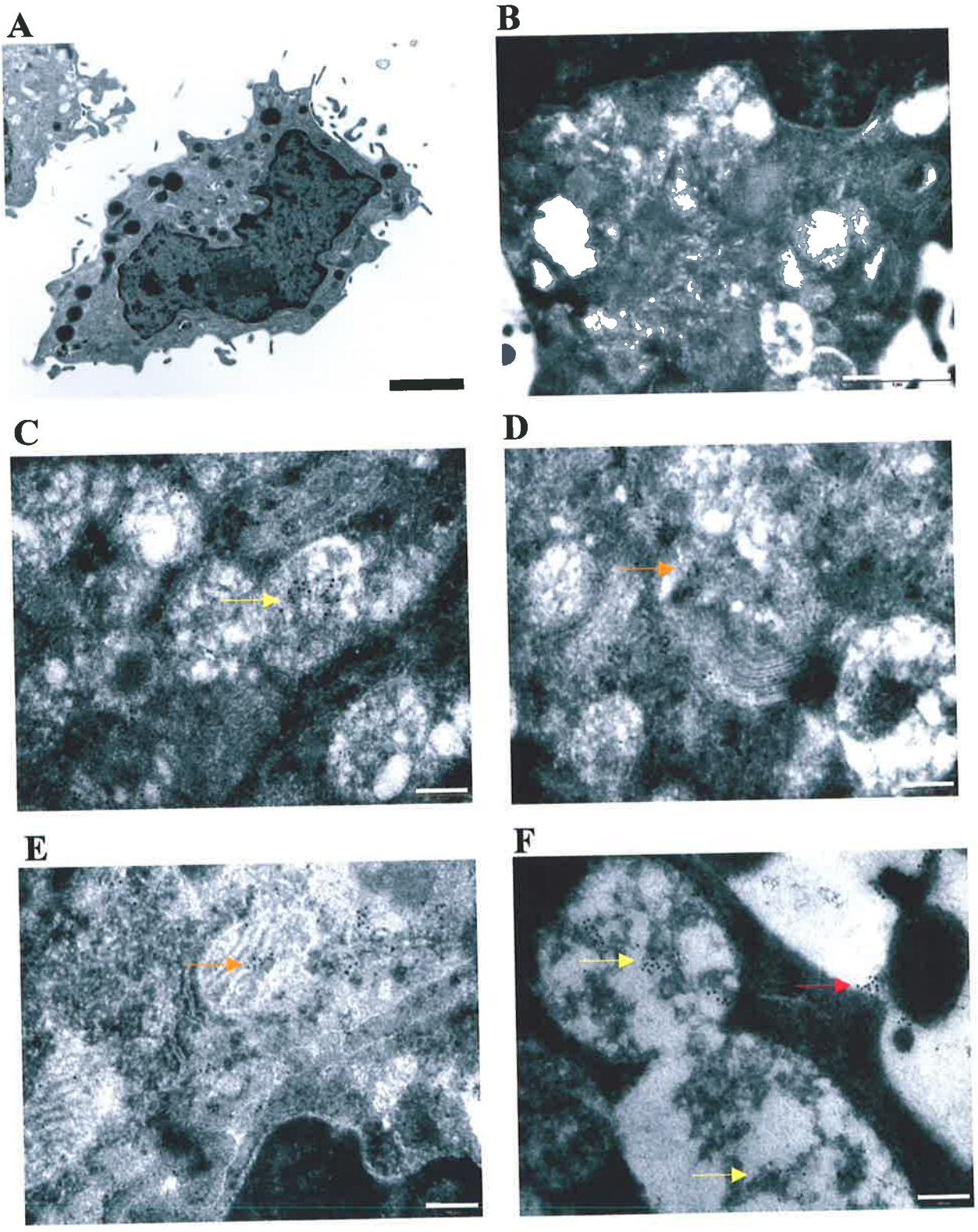


**Figure 4.11**

**Figure 4.11: Subcellular localization of pro-caspase-3 in immature HMC-1 mast cells by immunogold labelling.**

**A:** Ultra-structural features of an immature HMC-1 with large nucleus and few granules. Scale bar indicates 2 μm.

**B:** Control lacking primary antibody was absent of gold particles. Scale bar indicates 1 μm.

**C-F:** Shows four typical images of pro-caspase-3 localization in immature HMC-1 cells. Panels show clusters of gold-labelled pro-caspase-3 associated with amorphous material within granules (yellow arrows), scroll like structures (orange arrows) and exocytosed materials (red arrow). Scale bars indicate 200 nm.

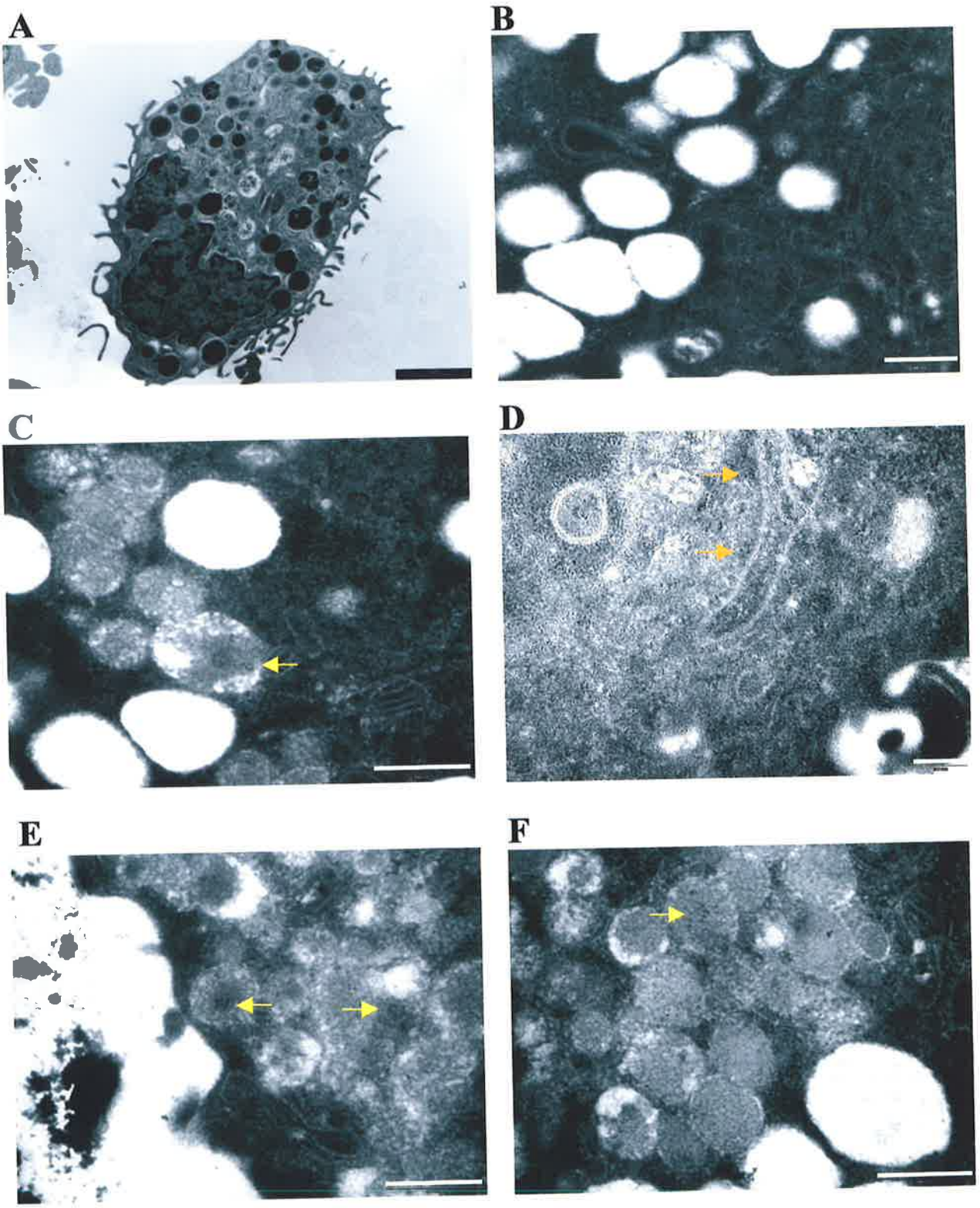


**Figure 4.12**

**Figure 4.12: Subcellular localization of pro-caspase-3 in mature HMC-1 mast cells by immunogold labelling.**

**A:** Ultra-structural features of a mature HMC-1 with smaller nucleus and a large number of granules. Scale bar indicates 2 μm.

**B:** Control lacking primary antibody was absent of gold particles. Scale bar indicates 500 nm.

**C-F:** Shows four typical images of pro-caspase-3 localization in mature HMC-1 cells. Panels show clusters of gold-labelled pro-caspase-3 associated with amorphous material within granules (yellow arrows) and scroll like structures (orange arrows). Scale bars for C, E and F indicate 500 nm and D indicates 200 nm

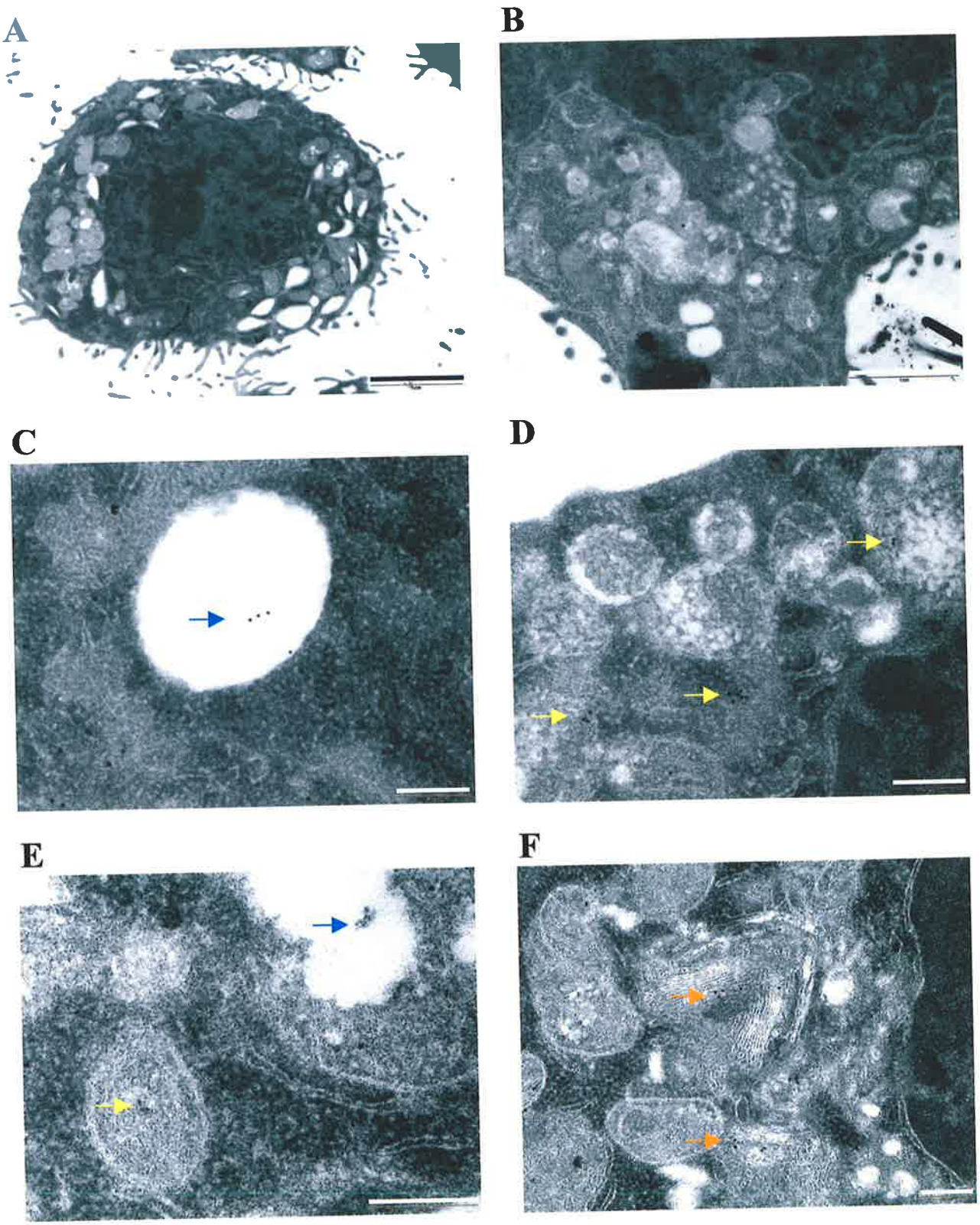


**Figure 4.13**

**Figure 4.13: Subcellular localization of pro-caspase-3 in RBL-2H3 mast cells by immunogold labelling.**

**A:** Ultra-structural features of an RBL-2H3 mast cell with prominent nucleus and a large number of granules. Scale bar indicates 2 μm.

**B:** Control lacking primary antibody was absent of gold particles. Scale bar indicates 1 μm.

**C-F:** Shows four typical images of pro-caspase-3 localization in RBL-2H3 mast cells. Panels show clusters of gold-labelled pro-caspase-3 associated with amorphous material within granules (yellow arrows), scroll like structures (orange arrows) and in granular spaces (blue arrows). Scale bars indicate 0.2 μm.

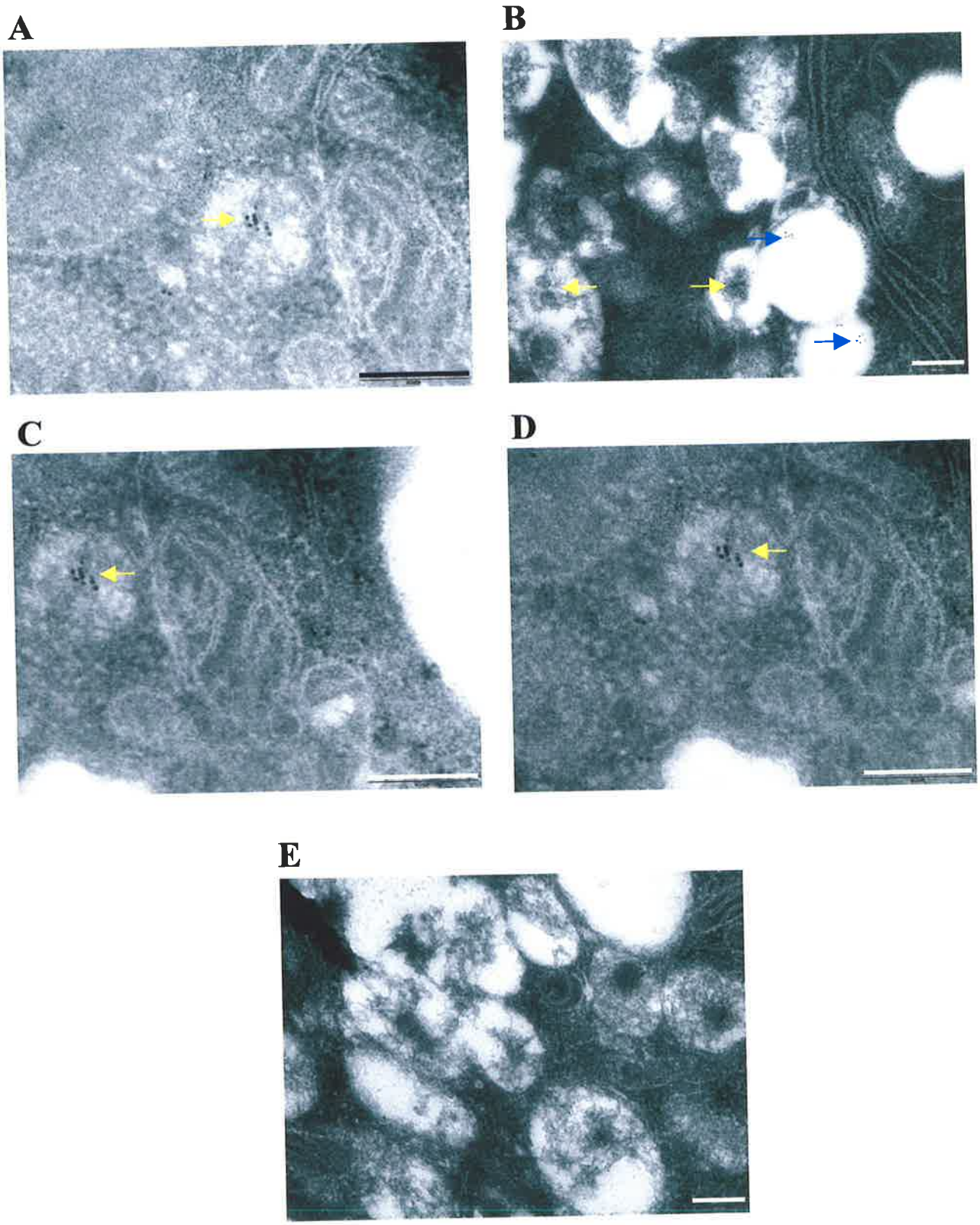


**Figure 4.14**

**Figure 4.14: Subcellular localization of pro-caspase-4 in immature HMC-1 mast cells by immunogold labelling.**

**A-D:** Shows four typical images of pro-caspase-4 localization in immature HMC-1 mast cells. Panels show clusters of gold-labelled pro-caspase-4 associated with amorphous material within granules (yellow arrows) and in extragranular spaces (blue arrows). Scale bars indicate 200 nm.

**E:** Control lacking primary antibody had few gold particles. Scale bar indicates 200 nm.

was seen in mature HMC-1 mast cells with pro-caspase-4 labelling also in areas surrounding granules (Figure 4.15, panels A-D pink arrows), as well as in amorphous materials of granules (Figure 4.15, yellow arrows). Particle labelling in control section was absent (Figure 4.14 and 4.15, panel E). Pro-caspase-4 distribution in RBL-2H3 rat mast cells was also observed in amorphous granular materials (Figure 4.16, panels A-D yellow arrows) and in surrounding areas of granules (Figure 4.16 pink arrows).

### 4.3.5 Quantification Of Gold Labelling

Gold particles in granules were counted and expressed first as gold particles per granule (Table 4.2). In cells lacking primary antibody, the number of gold particles per granule were 0.49 ± 0.1 for pro-caspase-3 and 0.28 ± 0.1 for pro-caspase-4. Significantly higher numbers of gold particles per granule were observed in cells labelled with both primary and secondary antibodies. Pro-caspase-3-labelled cells had 9.7 ± 0.1particles per granule while pro-caspase-4 labelled cells had 4.8 ± 0.1 particles per granule. To allow for variation in the granule size, granule area was calculated and expressed as mean ± SEM gold particles per $\mu m^2$ of granule for immature HMC-1 cells (Table 4.2). The number of gold particles per $\mu m^2$ of granule was significantly higher ($P<0.005$) for both pro-caspase-3 (110.9 ± 17.2) and -4 labelled cells (50.5 ± 5.2) compared to controls.

A similar trend was seen for mature HMC-1 where the number of gold particles in pro-caspase-labelled cells was significantly higher than that of cells stained with secondary antibody alone (Table 4.3). The number of gold particles per granule were

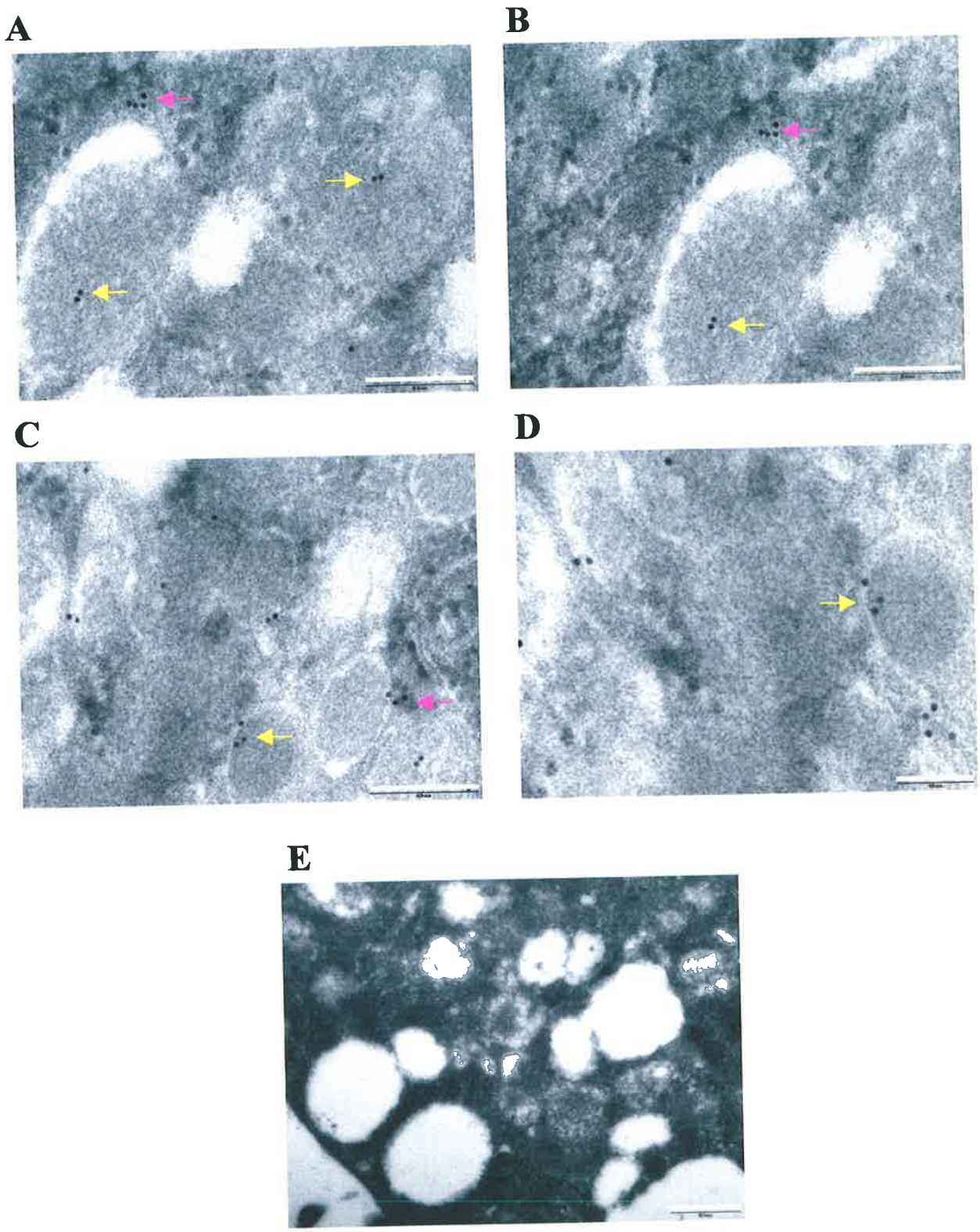


**Figure 4.15**

**Figure 4.15: Subcellular localization of pro-caspase-4 in mature HMC-1 mast cells by immunogold labelling.**

**A-D:** Shows four typical images of pro-caspase-4 localization in mature HMC-1 mast cells. Panels show clusters of gold-labelled pro-caspase-4 associated with amorphous material within granules (yellow arrows) and in surrounding areas (pink arrows). Scale bars for A-C indicate 200 nm and D indicates 100 nm.

**E:** Control lacking primary antibody was absent of gold particles. Scale bar indicates 500 nm.

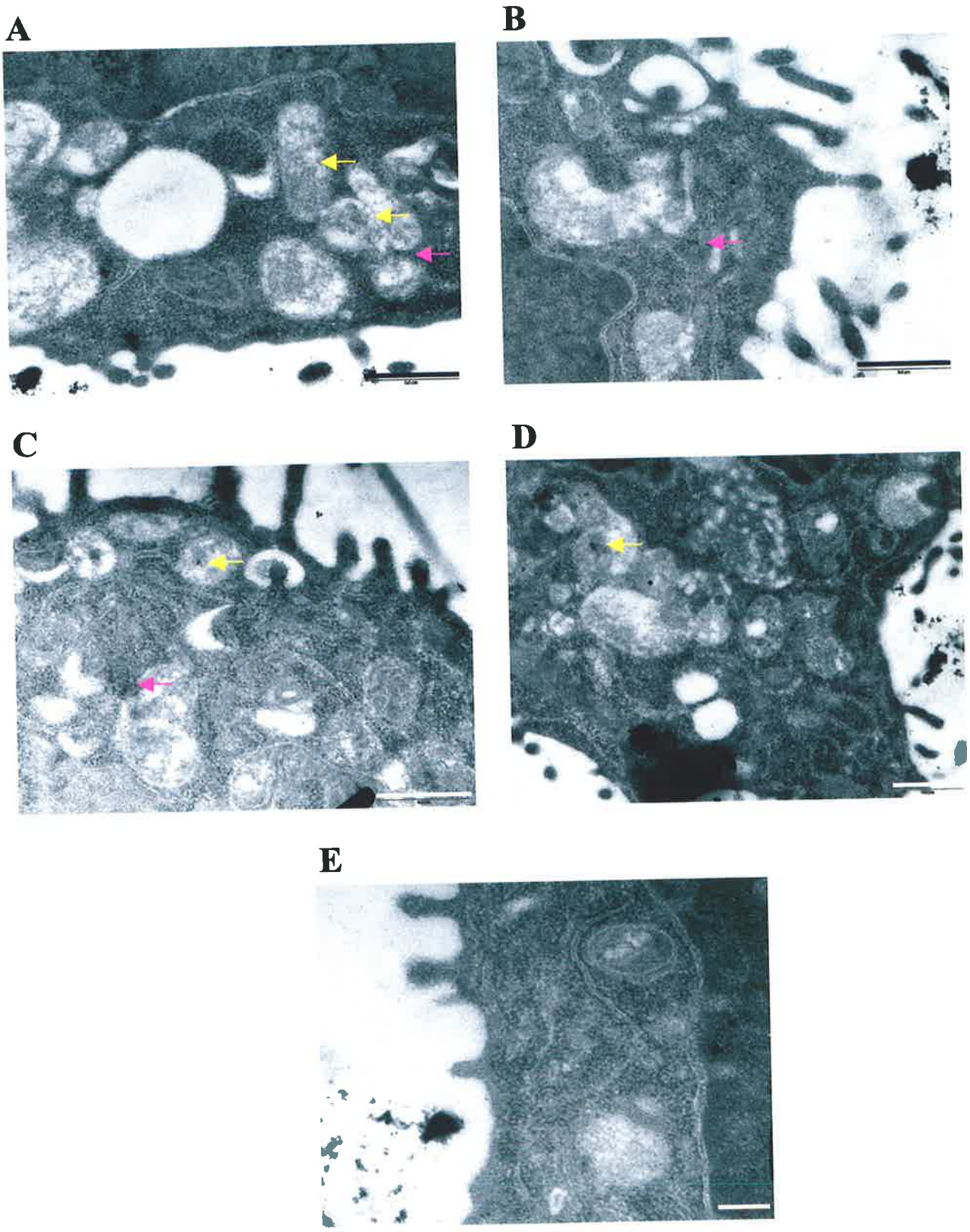


**Figure 4.16**

**Figure 4.16: Subcellular localization of pro-caspase-4 in RBL-2H3 mast cells by immunogold labelling.**

**A-D:** Shows four typical images of pro-caspase-4 localization in RBL-2H3 mast cells. Panels show clusters of gold-labelled pro-caspase-4 associated with amorphous material within granules (yellow arrows) and in surrounding areas (pink arrows). Scale bars for A-D indicate 0.5 μm.

**E:** Control lacking primary antibody was absent of gold particles. Scale bar indicates 0.2 μm.

**Table 4.2: Number of pro-caspase-3 and -4-labelled gold particles per granule and per $\mu m^2$ granule in immature HMC-1 cells.**

| | Pro-caspase-3 | | Pro-caspase-4 | |
|---|---|---|---|---|
| | **Gold particles per granule** (Mean ± SEM) | **Gold particles per $\mu m^2$ granule** (Mean ± SEM) | **Gold particles per granule** (Mean ± SEM) | **Gold particles per $\mu m^2$ granule** (Mean ± SEM) |
| **Secondary Antibody alone[a]** | 0.49 ± 0.1 | 4.1 ± 1.1 | 0.28 ± 0.1 | 2.3 ± 0.7 |
| **Caspase-labelled[b]** | 9.7 ± 0.7** | 110.9 ± 17.3** | 4.8 ± 0.4** | 50.5 ± 5.2** |

**a** = Gold particles per granule and per $\mu m^2$ granule of cells treated with secondary antibody alone; Mean ± SEM.
**b** = Gold particles per granule and per $\mu m^2$ granule of caspase-labelled cells; Mean ± SEM.
A total of 80 granules were sampled for control and caspase-labelled cells for all experiments.
** = $P<0.005$

**Table 4.3: Number of pro-caspase-3 and -4-labelled gold particles per granule and per $\mu m^2$ granule in mature HMC-1 cells.**

| | Pro-caspase-3 | | Pro-caspase-4 | |
|---|---|---|---|---|
| | **Gold particles per granule** (Mean ± SEM) | **Gold particles per $\mu m^2$ granule** (Mean ± SEM) | **Gold particles per granule** (Mean ± SEM) | **Gold particles per $\mu m^2$ granule** (Mean ± SEM) |
| **Secondary Antibody alone[a]** | 0.91 ± 0.2 | 13.8 ± 2.4 | 0.62 ± 0.1 | 7.6 ± 1.8 |
| **Caspase-labelled[b]** | 8.5 ± 0.8** | 79.6 ± 7.1** | 2.9 ± 0.2** | 36.1 ± 3.9** |

**a** = Mean gold particles per granule and per $\mu m^2$ granule of unlabelled cells ± SEM.
**b** = Mean gold particles per granule and per $\mu m^2$ granule of caspase-labelled cells ± SEM.
A total of 80 granules were sampled for control and caspase-labelled for all experiments.
** = $P<0.005$

0.91 ± 0.2 for pro-caspase-3 in cells lacking primary antibody and 8.5 ± 0.8 ($P<0.005$) for cells labelled with primary and secondary antibodies. For pro-caspase-4 these were 0.62 ± 0.1 and 2.9 ± 0.2 particles per granule ($P<0.005$), respectively. The numbers of gold particles per $\mu m^2$ granule were also significantly increased where pro-caspase-3-labelled cells had 79.6 ± 7.1 and pro-caspase-4-labelled cells had 36.1 ± 3.9 (Table 4.3 $P<0.005$).

Although a greater density of gold particles was seen for pro-caspase-3 when compared with pro-caspase-4, this does not necessarily mean that the levels of pro-caspase-3 are higher than pro-caspase-4, since labelling is dependent on many factors such as the affinity of the primary antibody and the effect of fixation on antigen availability.

## 4.4 Discussion

The findings of these experiments are: 1) pro-caspase-3 mRNA expression in various mast cell types, 2) cytoplasmic and vesicular distribution of pro-caspase-3 and -4 proteins in immature and mature HMC-1, as well as perinuclear localization of both pro-caspases in RPMC, 3) decreased levels of pro-caspase-3 and -4 in mast cells activated by compound 48/80 and 4) distribution of pro-caspase-3 and -4 within granules of immature and mature HMC-1 and RBL-2H3 mast cells, observed by electron microscopy.

Our studies here report high expression of pro-caspase-3 messenger RNA in at least two different types of mast cell, HMC-1 and RBL-2H3, untreated and treated with compound 48/80. The levels found in both immature and mature HMC-1 cells and RBL-2H3 cells were similar to those found in the positive controls (colon cancer cell lines) and higher than the levels found in mature HMC-1 cells. It is not clear why mature HMC-1 cells had less pro-caspase-3 mRNA then the immature cells. This may be a loading problem since the 18S RNA bands were also less intense for mature HMC-1 cells than for the immature cells. There was insufficient time to explore this further but future studies should look at the effects of maturation on expression of pro-caspase-3 in more detail. In addition, there was no effect of activation on the levels of pro-caspase-3 mRNA.

The vesicular distribution of both pro-caspases is similar to that of the distribution of Zn, suggesting the pro-caspases are within the granules. This was confirmed by immunogold labelling experiments where gold particles labelling for both pro-

caspases were observed mainly among granular materials. However some labelling was also seen in surrounding areas, mostly just outside of the granules. By immunofluorescence, an interesting perinuclear pattern was seen in RPMC. It could be that pro-caspases-3 and -4 are highly concentrated in this region, possibly due to high numbers of secretory vesicles close to the nucleus, unique to this type of mast cell. There were no significant differences between the localisation of the pro-caspases between immature and mature HMC-1, suggesting that expression of these pro-caspases do not change during development of mast cells. However, this observation needs confirmation with primary mast cells at defined stages of maturation. Nor was there a difference between the mean pro-caspase-3 fluorescence of the two mast cell types studied, human HMC-1 and rat RPMC. This may indicate that the development of pro-caspase-3 in both human and rat mast cells is similar.

A difference was seen between pro-caspase-4 expression in HMC-1 versus RPMC but the implications of this are not clear. However, only two mast cell types were studied and other cell types needed to be included such as human cord blood and lung mast cells. It is also not known whether the expression of both pro-caspases in mast cells is comparable to other cell types such as lymphocytes and other granulocytes.

Similarly to Zn, pro-caspase-3 and -4 were decreased following degranulation of mast cells further consistent with their localisation within secretory granules. This observation was confirmed by immunogold labelling showing pro-caspases not only within granules but also released with exocytosed materials. This is an unusual finding as caspases are usually considered to act within the cells whereas components of secretory granules are normally released to the extracellular environment. One

possibility is that these caspases play a role in cleavage of extracellular substrates such as matrix proteins. This has not previously been shown but could be an area for further studies. Another explanation is that the caspases are needed for cleavage of granular components during apoptosis of mast cells. It is interesting that electron microscopy studies showed pro-caspase labelling both outside and inside of granules. Pro-caspase-3 within the granules may cleave substrates that are not accessible to caspases outside of the granules. A third possibility is that by having the pro-caspases within the mast cell granules, the survival of the cells can be prolonged by release of these caspases during activation. This is further discussed in chapter 8.

The results of the experiments in this chapter demonstrate for the first time that pro-caspases-3 and -4 are expressed at both the transcriptional and translational levels in mast cells and that they are localized within vesicular structures particularly the granules. The relevance of these findings to apoptosis of mast cells is described in chapter 5.

# CHAPTER FIVE

# INTERACTIONS BETWEEN ZINC DEPLETION AND APOPTOTIC INDUCERS ON CASPASE ACTIVATION IN MAST CELLS

## 5.1 Introduction

Localization of pro-caspases-3 and -4 in mast cells, as described in the previous chapter led to further investigation into the relevance of these and other caspases in mast cell apoptosis. This chapter describes the levels and effects of various active caspases in mast cells under normal and activated conditions. These cells were treated with an agent that functionally depletes Zn alone and in combination with apoptotic inducers. One of the aims being investigated here is whether intracellular Zn depletion by degranulators (e.g. compound 48/80) or chelators (TPEN) influence caspase activation.

Regulation of mast cell numbers is largely dependent upon proliferative and/or apoptotic signals (Metcalfe, 1997). It has been shown that mouse mast cells undergo apoptosis as a result of IL-3 withdrawal and this coincides with a decrease in endogenous *bcl*-2 mRNA (Metcalfe, 1997). This effect is reversible upon addition of stem SCF. External stimuli are also known to induce apoptosis in mast cells, including drugs, ionizing radiation (Yee, 1994) and hyperthermia (Takano, 1991). It has been suggested that activation of mast cells by IgE may prolong their survival (Shalit and Levi-Schaffer, 1995). Alternatively degranulation may make them more susceptible to apoptosis, since *in vivo* it may be more efficient to remove degranulated mast cells by apoptosis and replace them by newly formed mast cells from the bone marrow.

As discussed in chapter three, the role of granular Zn in mast cells is unclear, but its presence in a range of mast cells indicates some highly conserved function. It is conceivable that mast cell granule Zn is involved in regulation of pro-caspases,

especially since these were also present in the granules. Zinc is a potent inhibitor of apoptosis and depletion of Zn by Zn chelator has been shown to induce apoptosis in various cell lines (McCabe, 1993; Sunderman, 1995).

Various active caspases were assayed because of their specific functions in apoptotic and non-apoptotic processes. The experiments in this chapter primarily concern active caspase-3 but other active caspases (-1, -2, -4, -5, -6 and -9) were also studied. Out of the caspases chosen, caspases-2 and -9 are initiator caspases, caspases-1, and -4 and -5 are pro-inflammatory caspases and caspases-3 and -6 are effector caspases. Levels of these caspases were determined by assaying cleavage of fluorogenic substrates.

Two major questions being addressed in this chapter are: 1) does functional depletion of Zn in mast cells by Zn chelator increase their susceptibility to caspase-3 activation and apoptosis and 2) does depletion of Zn in mast cells induced by activation increase their susceptibility to apoptosis? If both answers are yes this must imply a role for granular Zn in regulation of caspase-3 activation. The apoptotic inducers used in this study were butyrate and staurosporine. Previous studies from this laboratory have shown that butyrate is an inducer of apoptosis in a variety of cancer cell lines. In addition low concentrations of butyrate, which cause little apoptosis were able to synergise with other apoptotic inducers (e.g. staurosporine) in activation of caspase-3. In particular, cell primed overnight with a low concentration of butyrate were much more susceptible to induction of apoptosis by staurosporine (Medina, 1997). This low concentration of butyrate does not induce maturation of the cells over the 24 h period since four days are required for this to occur.

## 5.2 Methods

### 5.2.1 Activation Of Mast Cells

Mast cells were activated with the following stimuli: compound 48/80, calcium ionophore A23187 or phorbol myristate acetate (PMA). Cells were incubated with the stimuli for 18 h at 37°C.

### 5.2.2 Treatment With Apoptotic Inducers (Butyrate, Staurosporine) Or TPEN

Mast cells were incubated with apoptotic inducers butyrate (concentrations of 1- 10 mM) or staurosporine (0.1-1 μM) for 18 h at 37 °C, followed by a further 4 h with or without Zn chelator TPEN. Cells were treated with TPEN at concentrations of 25, 50 or 100 μM.

### 5.2.3 Fluorogenic Substrate Assay For Active Caspases

Levels of active caspases-1, -2, -3, -4, -5, -6 and -9 were determined in mast cell lysates. This fluorometric assay involves cleavage of AFC conjugated substrates relatively specific for each caspase measured (see section 2.3.2). However, there is some overlap between caspase specificities. In particular, caspase-7 can cleave the fluorogenic substrate z-asp-glu-val-asp-7-amino-4-methyl-coumarin (z-DEVD-AFC) that is used for assay of caspase-3. For simplicity and clarity the caspase activities are referred to by their caspase names and the substrate specificities are given in section 2.3.2. Caspase-3 and DEVD-caspase activity are used interchangeably.

Release of AFC from the substrate results in an increase in fluorescence, which is measured in a fluorescence spectrophotometer. Caspase activity was derived from fluorescence units (with slit width of 5 nm) and then converted to picomoles of substrate cleaved per hour calculated from an AFC standard curve (Figure 2.2). Caspase activity is expressed in the results as Units, where one Unit of caspase activity is taken as one picomole of substrate cleaved per h, per 50 μl of cell lysates.

### 5.2.4 Statistical Analysis

The results of typical experiments are described or data were pooled, as indicated in text. Statistical significance was determined by the student *t*-test and the Tukey-Kramer multiple comparisons test where appropriate and is indicated in text or legends to Figures.

## 5.3 Results

### 5.3.1 Basal Levels Of Active Caspases In Mast Cells

Basal levels of the active form of caspases-1, -2, -3, -4, -5, -6 and -9 were measured in immature HMC-1 mast cells (lysate of 4 x $10^5$ cells per cuvette) and for comparison in the same number of A549 human epithelial cells (Figure 5.1). The figure shows that caspases-1, -3 and -6 are the most abundant caspase activities in the untreated HMC-1 mast cells with very little caspases-2, -4, -5 and 9 (blue columns). A somewhat similar profile was seen for A549 cells with caspases-1, -3 and -6 also being the most abundant (pink). Overall A549 cells had higher basal caspases levels than immature HMC-1 cells. These were significantly different for caspases-1, -3 and -6 ($P<0.005$). Basal levels of caspases in mature HMC-1 cells and other types of mast cells were comparable with those of immature HMC-1 cells as is evident from subsequent figures.

### 5.3.2 Concentration-Dependent Induction Of Caspase-3 (DEVD-Caspase) Activity By Butyrate In Mast Cells

To determine whether basal levels of caspase-3 increases in mast cells treated with an apoptotic inducer, immature HMC-1 cells were treated with 0, 1, 2, 4, 8 and 10 mM butyrate for 18 h. Active caspases-3 levels were assayed by cleavage of DEVD-AFC. Levels were expressed as % of that in untreated cells (figure 5.2A). Data were pooled from three separate experiments each in triplicate. Figure shows a concentration-

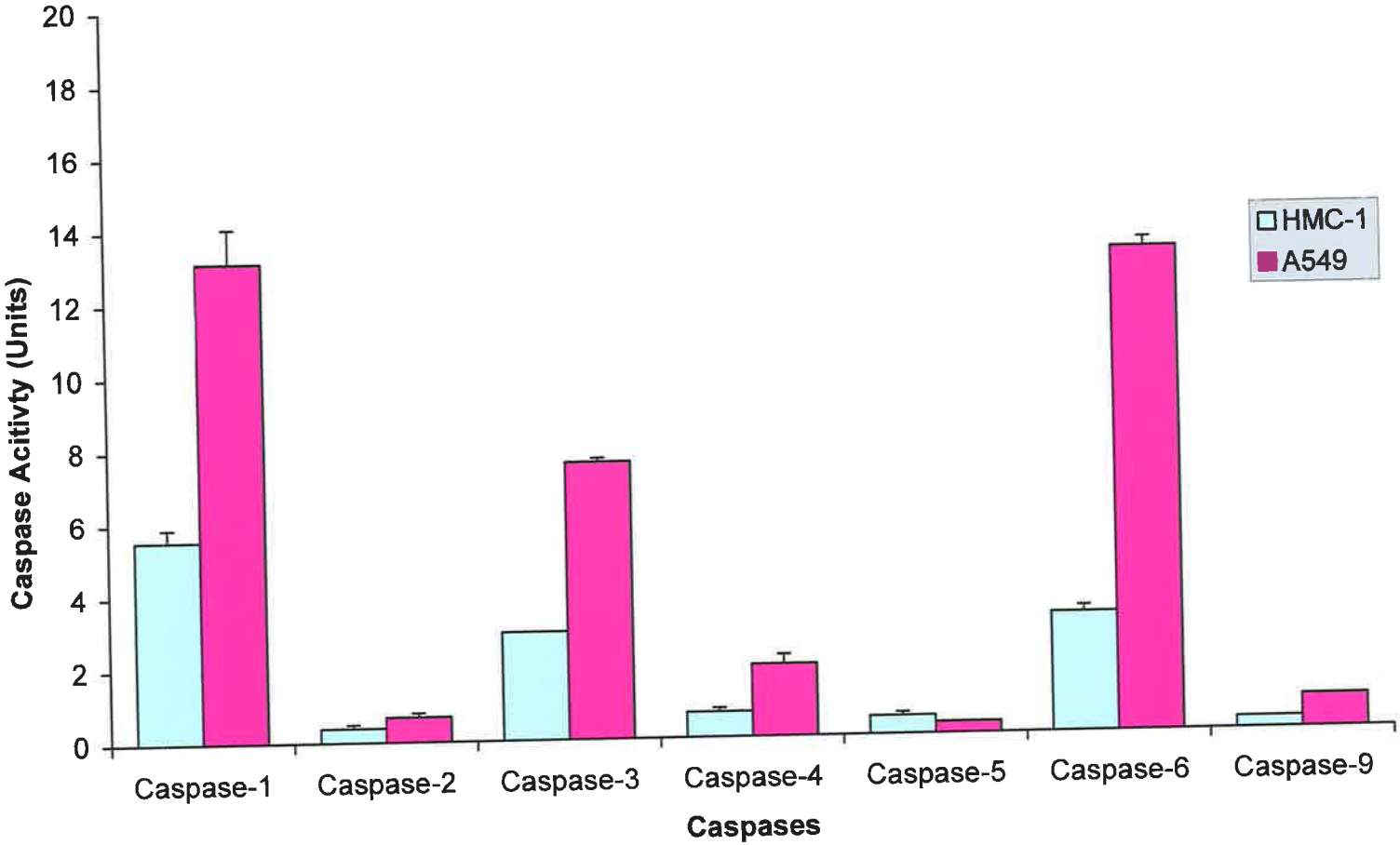
20
18
16
14
12
10
8
6
4
2
0
Caspase Acitivty (Units)
HMC-1
A549
Caspase-1
Caspase-2
Caspase-3
Caspase-4
Caspase-5
Caspase-6
Caspase-9
Caspases

**Figure 5.1**

**Figure 5.1: Basal levels of caspases in immature HMC-1, RBL-2H3 mast cells and A549 epithelial cells.**

Basal levels of active caspases-1, -2, -3, -4, -5, -6 and –9 as determined by cleavage of fluorogenic substrates (section 2.3.2) in immature HMC-1, RBL-2H3 mast cells and A549 human epithelial cells. Figure shows that caspase-1, -3 and –6 are the most abundant caspases in the mast cells, similar to the profile in A549 epithelial cells. Data are expressed as Units of activity per 50 µl of lysates ($4 \times 10^5$ cells).

Data are means of triplicates ± SEM for a typical experiment. Protein level of control immature HMC-1 cells was 0.05 mg/50 µl of lysates, 0.1 mg/50 µl of lysates for RBL-2H3 and 0.09 mg/ 50 µl of lysates for A549 epithelial cells.

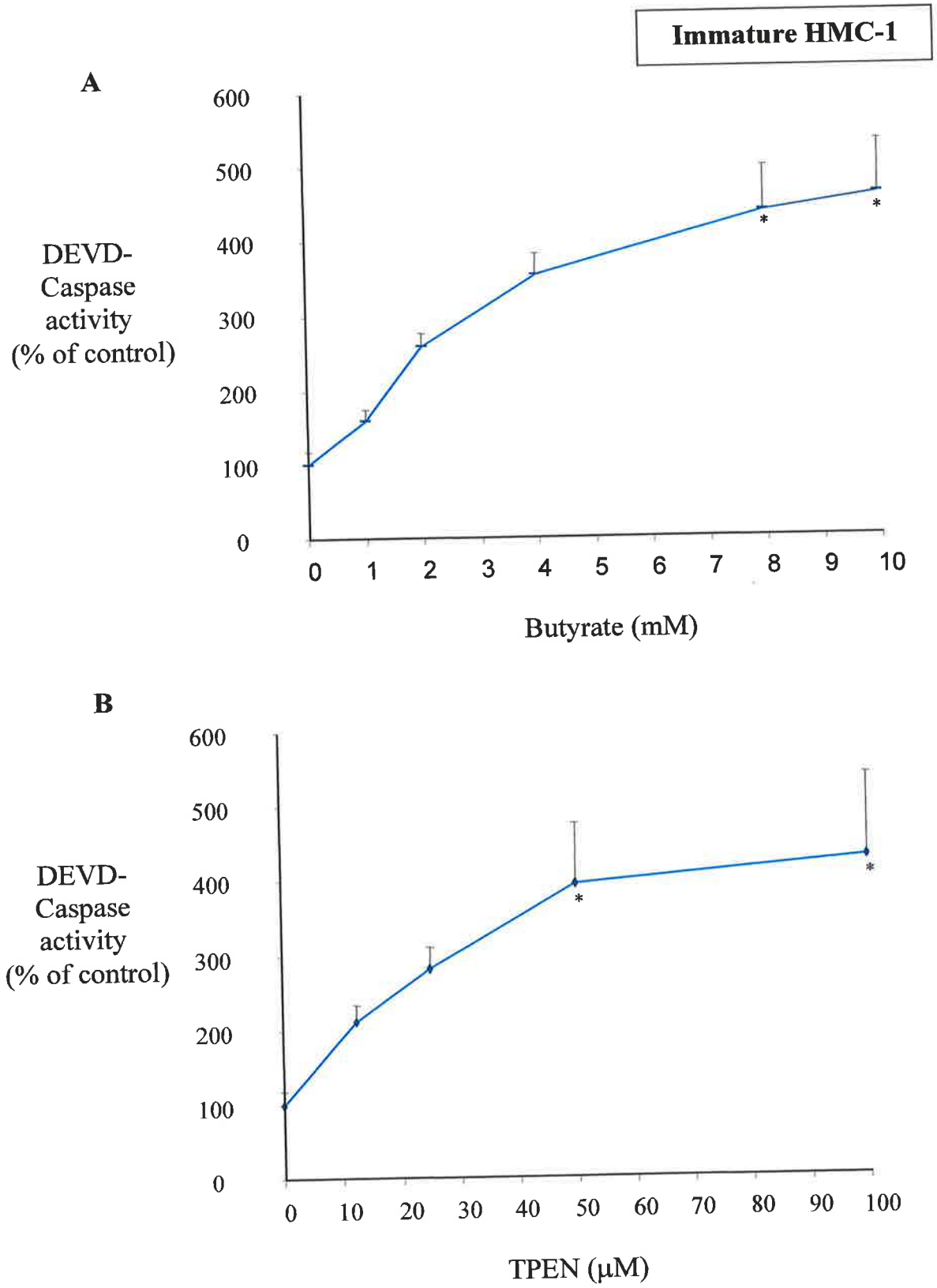
Immature HMC-1
A
DEVD-Caspase activity (% of control)
600
500
400
300
200
100
0
0 1 2 3 4 5 6 7 8 9 10
Butyrate (mM)
B
DEVD-Caspase activity (% of control)
600
500
400
300
200
100
0
0 10 20 30 40 50 60 70 80 90 100
TPEN (μM)

**Figure 5.2**

**Figure 5.2: Concentration-dependent induction of caspase-3 (DEVD-caspase) by butyrate and TPEN in immature HMC-1 mast cells.**

Immature HMC-1 cells were treated with varying concentrations of butyrate for 18 h (A) or TPEN for 4 h (B). Levels of active caspase-3 were measured and expressed as % of that in control cells. Figure shows that both butyrate and TPEN induce significant increases in caspase-3 activity, which plateau out at 8 mM butyrate and 50 μM TPEN.

Statistical significances were between treated and control cells and are indicated as * $P<0.05$.

dependent increase in caspase-3 levels, which was significant at 8 and 10 mM butyrate ($P<0.05$).

Similar results were obtained with mature HMC-1 cells. Figure 5.3 shows the concentration-dependent increases in caspase-3 activity in cells treated with varying concentrations of butyrate (Figure 5.3A). Some of these experiments were repeated in human primary cord blood mast cells (CBMC). Butyrate alone induced significant caspase-3 activity in a concentration-dependent manner (Figure 5.4A, $P<0.005$).

### 5.3.3 Concentration-Dependent Induction Of Caspase-3 (DEVD-Caspase) Activity By TPEN In Mast Cells

To determine whether Zn depletion also increases caspase-3 activity in mast cells, immature HMC-1 cells were treated with varying concentrations of TPEN (12.5, 25, 50 or 100 μM) for 4 h, before lysing the cells and assaying for caspase activity (Figure 5.2B). There was an increase in caspase-3 levels with increasing concentration of TPEN up to 50 μM. Significances were seen at 50 and 100 μM TPEN ($P<0.05$). Similar results were seen for mature HMC-1 cells (Figure 5.3B) and CBMC (Figure 5.4B).

### 5.3.4 Interaction Between Butyrate And TPEN In Induction Of Caspase-3 (DEVD-Caspase) And -6 (VEID-Caspase) Activity In Mast Cells

Immature HMC-1 cells were treated overnight with 2mM butyrate (blue columns) or no addition (yellow columns) before treatment with TPEN or DMSO (solvent for TPEN) (Figure 5.5A). The first set of columns (DMSO) show a modest significant

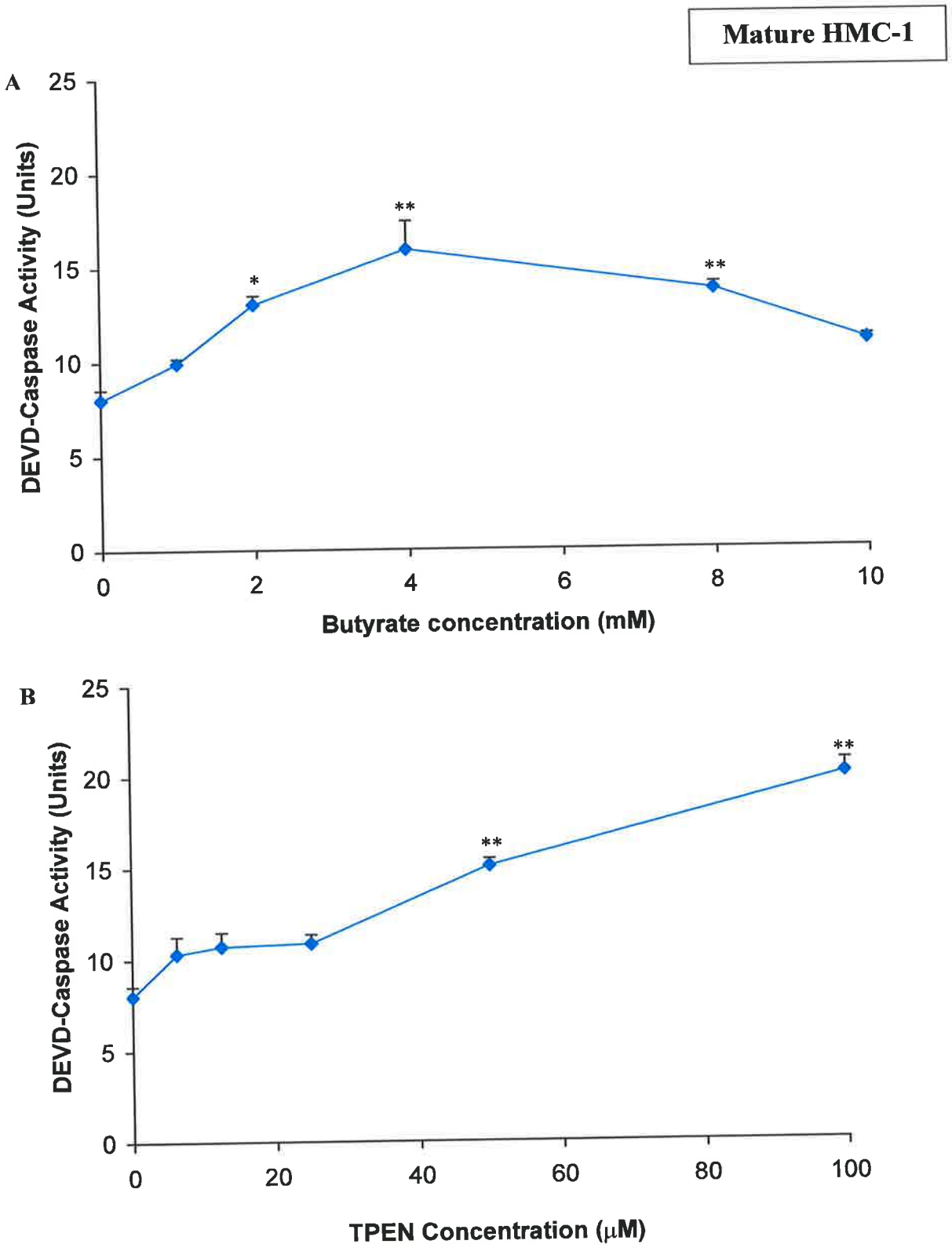
Mature HMC-1
A
DEVD-Caspase Activity (Units)
Butyrate concentration (mM)
B
DEVD-Caspase Activity (Units)
TPEN Concentration (μM)

**Figure 5.3**

**Figure 5.3: Concentration-dependent induction of caspase-3 (DEVD-caspase) activity by butyrate and TPEN in mature HMC-1 mast cells.**

Mature HMC-1 mast cells were treated with butyrate for 18 h (A) or TPEN for 4 h (B) at 37°C. Figure shows increases in caspase-3 activity of cells treated with butyrate or TPEN. Note maximum increase in caspase-3 activity in cells treated with butyrate was seen at 4 mM.

Data are expressed as Units of activity per 50 µl of lysates ($4 \times 10^5$ cells). Bars indicate SEM for means of triplicates. Protein level of control cells was 0.06 mg/50 µl of lysates. Statistical significances for comparison between treated and control cells are indicated as *$P<0.05$ and **$P<0.005$.

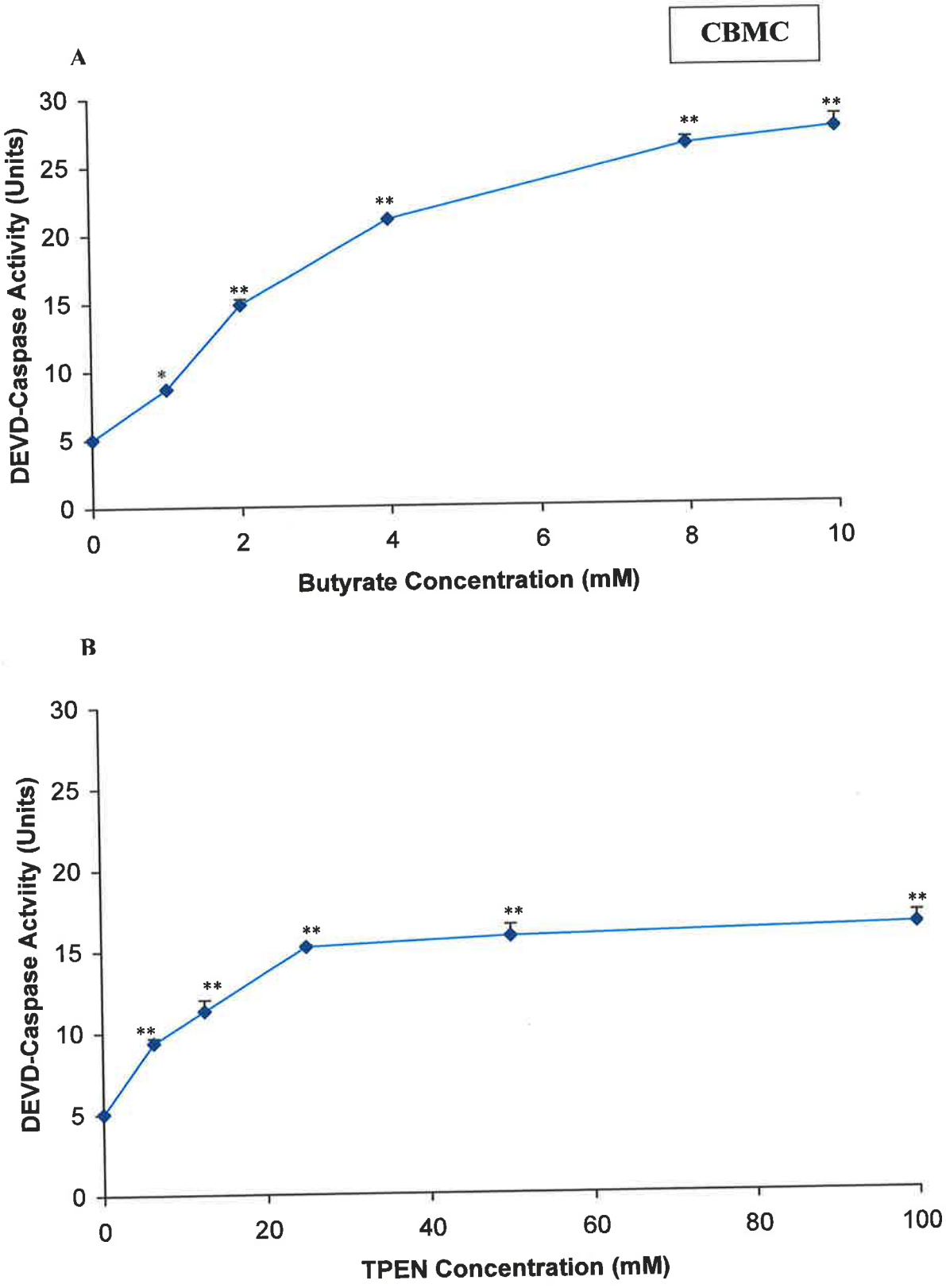
CBMC
A
DEVD-Caspase Activity (Units)
Butyrate Concentration (mM)
B
DEVD-Caspase Actviity (Units)
TPEN Concentration (mM)

**Figure 5.4**

**Figure 5.4: Concentration-dependent induction of caspase-3 (DEVD-caspase) activity by butyrate or TPEN in CBMC.**

CBMC were treated with butyrate (1, 2, 4, 8 and 10 mM) for 18 h (A) or 6.25, 12.5, 25, 50 or 100 μM TPEN for 4 h (B). Cells were then assayed for caspase-3 activity and data are expressed as Units of activity per 50 μl of lysates ($4 \times 10^5$ cells). Figure shows significant increases in caspase-3 activity by butyrate (A) or TPEN (B) in CBMC.

Data are means of triplicates ± SEM for a typical experiment. Protein level of control lung mast cells was 0.003 mg/50 μl of lysates. Statistical significances for comparison between treated and control cells are indicated as *$P<0.05$ and **$P<0.005$.

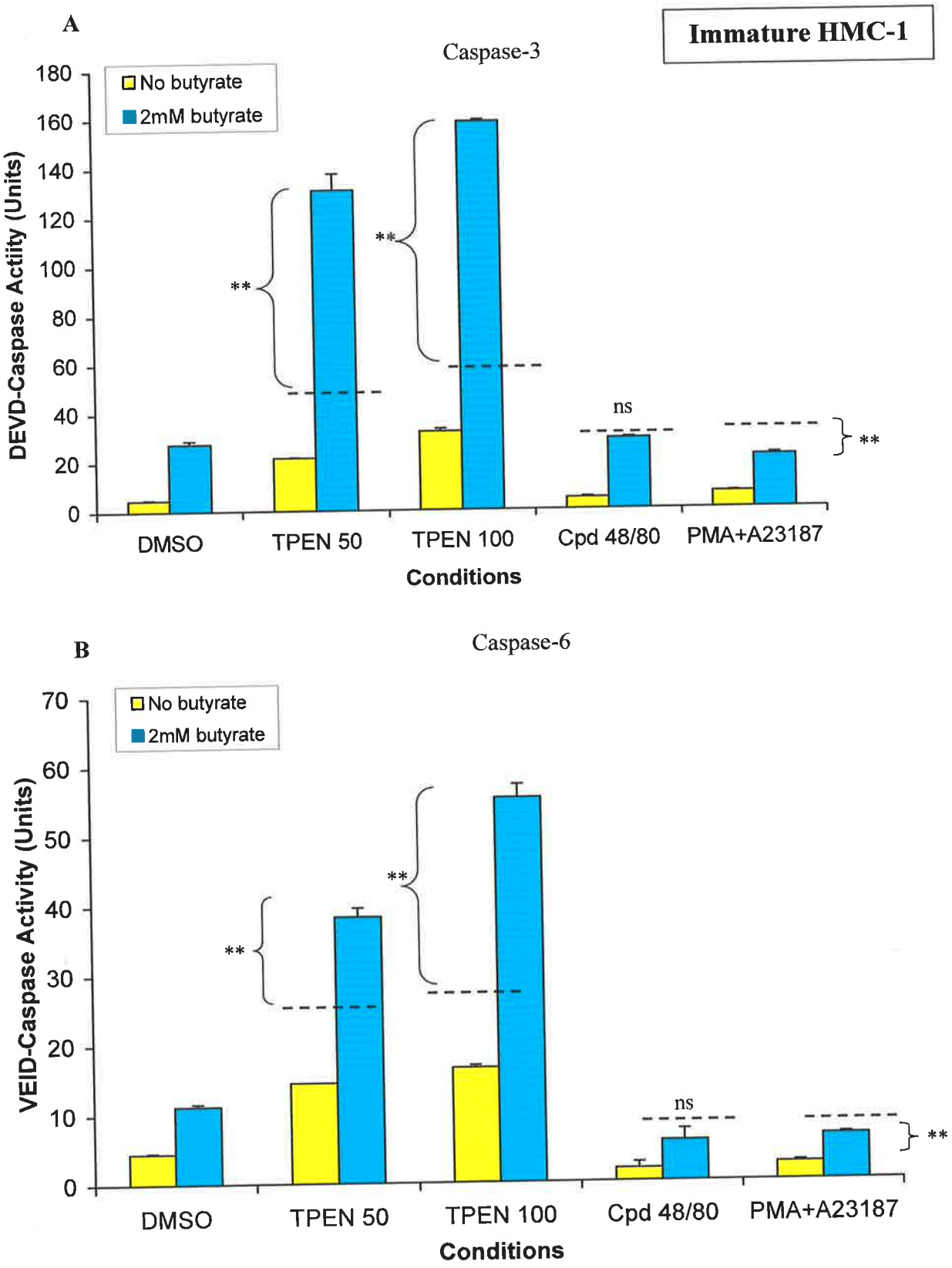
A
Caspase-3
Immature HMC-1
No butyrate
2mM butyrate
DEVD-Caspase Actiity (Units)
180
160
140
120
100
80
60
40
20
0
**
**
ns
**
DMSO
TPEN 50
TPEN 100
Cpd 48/80
PMA+A23187
Conditions
B
Caspase-6
No butyrate
2mM butyrate
VEID-Caspase Activity (Units)
70
60
50
40
30
20
10
0
**
**
ns
**
DMSO
TPEN 50
TPEN 100
Cpd 48/80
PMA+A23187
Conditions

**Figure 5.5**

**Figure 5.5: Interactions between butyrate and degranulators or TPEN in induction of caspase-3 (DEVD-caspase) and -6 (VEID-caspase) activity in immature HMC-1 cells.**

Immature HMC-1 cells were primed overnight in the absence of (yellow columns) or presence of (blue columns) 2 mM butyrate. Other additions were as follows. For TPEN treatment, cells were incubated for the final 4 h of culture with 50 or 100 μM TPEN. Cells lacking TPEN received the same concentration of DMSO (solvent for TPEN- final concentration 0.5%). DMSO alone did not have an effect. For treatment with degranulators, cells were treated with 1 μg/ml compound 48/80, 100 ng PMA + 0.5 μM A23187 for 18 h.

Cells were then assayed for caspase-3 activity (A) or caspase-6 activity (B) and data are expressed as Units of activity per 50 μl of lysates (4 x $10^5$ cells). Dotted lines show expected values if interactions were additive. Note the synergistic interaction between TPEN and butyrate but lack of synergy between degranulators and butyrate.

Data are means of triplicates ± SEM for a typical experiment. Protein content of lysates were 0.05 mg/50 μl for A and B. Statistical significances were between the values obtained for a combination of butyrate and TPEN or degranulators and the predicted additive values as indicated by the dashed lines.

increase in caspase-3 activity due to 2 mM butyrate alone (blue columns, $P<0.005$) compared to untreated cells (yellow columns). The second and third sets of columns show moderate but significant increases in caspase-3 activity due to TPEN treatment alone (yellow columns, $P<0.005$). Large increases were seen when cells were treated with a combination of butyrate and TPEN (blue columns). These increases were significantly greater than the predicted additive effect of butyrate and TPEN alone as indicated by dashed lines ($P<0.005$). A similar pattern was observed for caspase-6 levels in immature HMC-1 cells treated with the same agents (Figure 5.5B).

Figure 5.6 shows the interactions between 2mM butyrate and TPEN on caspase-3 and -6 in mature HMC-1 cells. As for immature HMC-1 cells, TPEN and butyrate alone induced small significant increases in caspase-3 activity and were synergistic in combination (Figure 5.6A). Similar trends were also seen for caspase-6 activity (Figure 5.6B). Some of these experiments were repeated with primary CBMC. Again a synergistic interaction was seen between butyrate and TPEN at several concentrations of TPEN (Figure 5.7A) and butyrate (Figure 5.7B). The lack of synergy between 2 mM butyrate and 100 μM TPEN (Figure 5.7A) may be due to the commitment of cells to the necrotic pathway rather than apoptosis. At this high concentration, TPEN may damage primary mast cells in a non-apoptotic way. As can be seen in Figure 5.7A, the optimal concentration of TPEN was 25 μM and at higher concentrations there was a progressive decrease in caspase-3 activity.

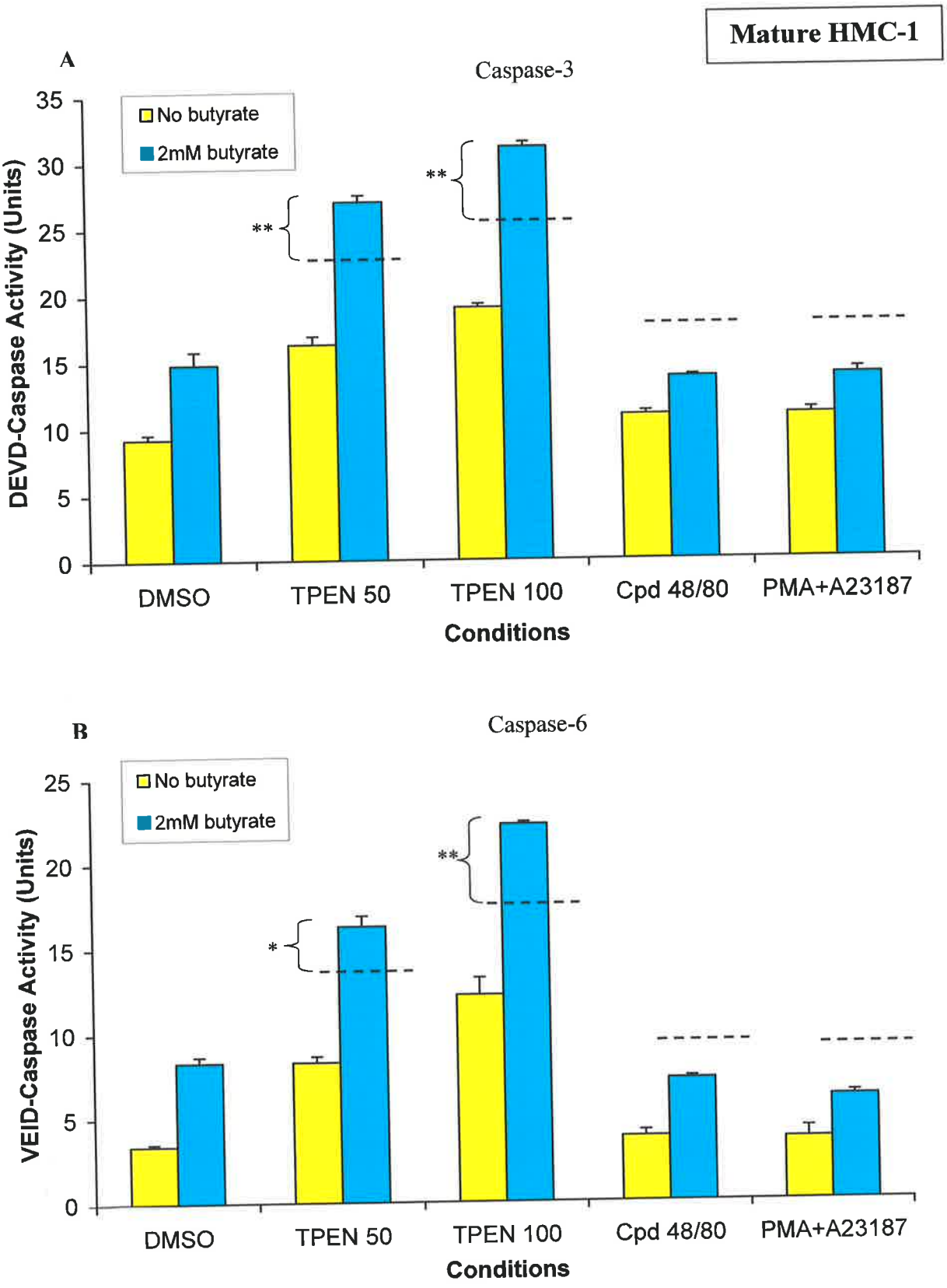
Mature HMC-1
A
Caspase-3
No butyrate
2mM butyrate
DEVD-Caspase Activity (Units)
35
30
25
20
15
10
5
0
**
**
DMSO
TPEN 50
TPEN 100
Cpd 48/80
PMA+A23187
Conditions
B
Caspase-6
No butyrate
2mM butyrate
VEID-Caspase Activity (Units)
25
20
15
10
5
0
*
**
DMSO
TPEN 50
TPEN 100
Cpd 48/80
PMA+A23187
Conditions

**Figure 5.6**

**Figure 5.6: Interactions between butyrate and degranulators or TPEN in induction of caspase-3 (DEVD-caspase) and -6 (VEID-caspase) activity in mature HMC-1 cells.**

Same legend as in Figure 5.5 except that the protein content of lysates were 0.06 mg/50 µl for A and B. Figure shows synergy between TPEN and butyrate.

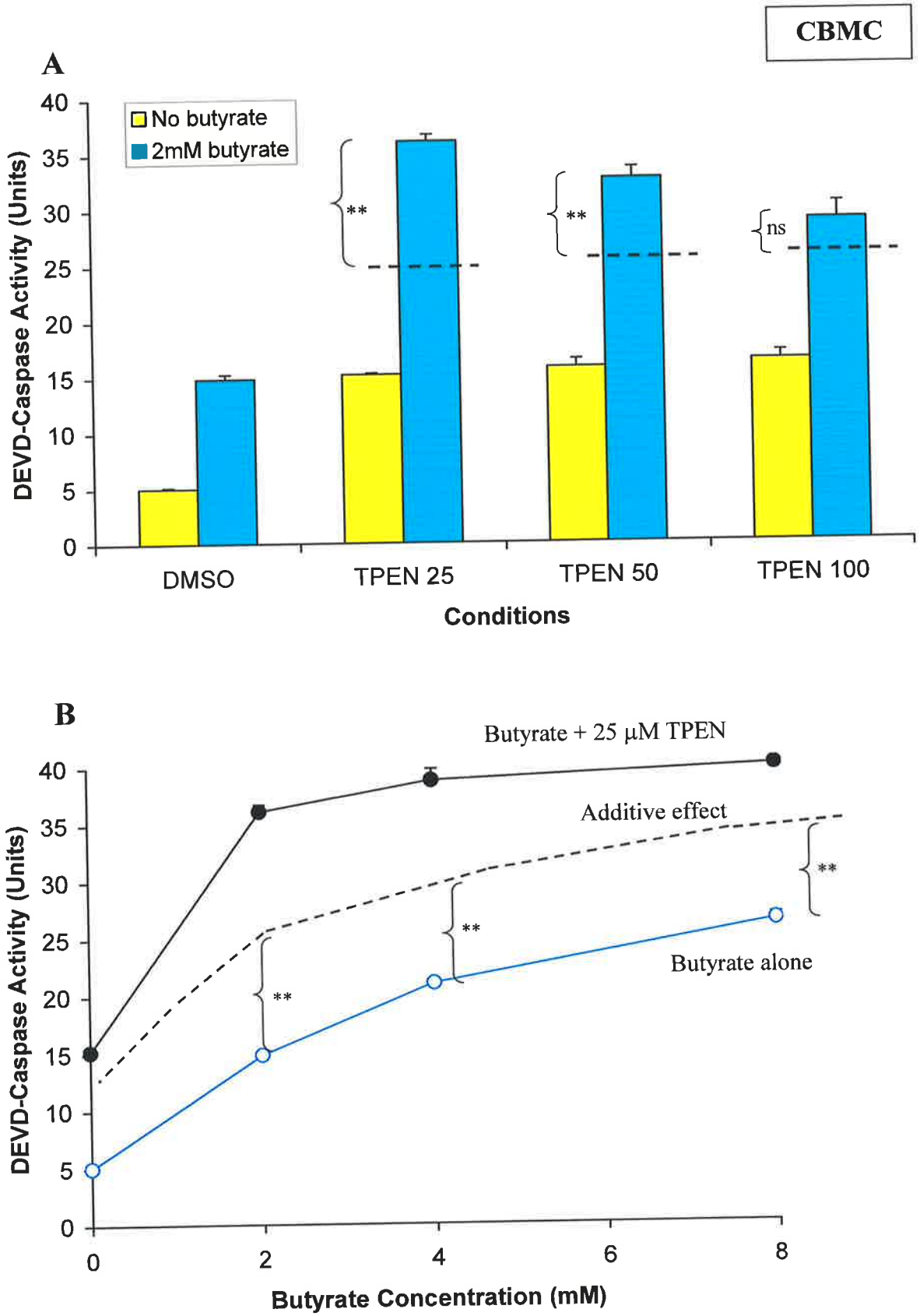
CBMC
A
No butyrate
2mM butyrate
DEVD-Caspase Activity (Units)
40
35
30
25
20
15
10
5
0
**
**
ns
DMSO
TPEN 25
TPEN 50
TPEN 100
Conditions
B
Butyrate + 25 μM TPEN
Additive effect
Butyrate alone
**
**
**
DEVD-Caspase Activity (Units)
0
2
4
6
8
Butyrate Concentration (mM)

**Figure 5.7**

**Figure 5.7: Interaction between butyrate TPEN on caspase-3 (DEVD) activity in CBMC.**

**A**: Same legend as in Figure 5.5A except that CBMC were used and there was no treatment with degranulators. Figure shows synergy between TPEN and butyrate at 25 and 50 μM TPEN but no synergy at 100 μM TPEN.

**B**: CBMC were treated with butyrate (2, 4 or 8 mM) for 18 h with or without 25 μM TPEN for 4 h. Cells were then assayed for caspase-3 activity and data are expressed as Units of activity per 50 μl of lysates ($4 \times 10^5$ cells). Figure shows synergistic increases in caspase-3 activity in CBMC treated with varying concentrations of butyrate and TPEN.

Data are means of triplicates ± SEM for a typical experiment. Protein level of control lung mast cells was 0.003 mg/50 μl of lysates.

### 5.3.5 The Effect Of Zn Depletion By Degranulator On Caspase Activity In Mast Cells

Having established that Zn depletion by chelator induces caspase activation it was next determined whether Zn depletion by degranulators had the same effect. As shown in chapter three, degranulators caused a large reduction of intracellular Zn in mast cells. Therefore it was interesting to determine whether degranulators would also synergise with butyrate in inducing caspase-3 activity. The fourth sets of columns in figure 5.5A show that compound 48/80 alone did not induce caspase-3 activity (yellow columns). In addition, a combination of butyrate and compound 48/80 did not synergise with each other (blue columns). There was also no synergy between butyrate and another degranulator (PMA+A23187). This is despite the level of Zinquin-stainable Zn decreasing to similar extent in the cells treated with TPEN or degranulators (Table 3.1). In fact, the level of caspase-3 and –6 activities for the combination of butyrate and PMA +A23187 was significantly less than the predicted additive effects of butyrate alone and PMA+A23187 alone ($P<0.005$).

Degranulators also did not induce caspase-3 or caspase-6 activity and did not synergise with butyrate in mature HMC-1 cells (Figure 5.6A). Again, the level of caspase-3 and –6 activities for the combination of butyrate and PMA +A23187 was significantly less than the predicted additive effects of butyrate alone and PMA+A23187 alone ($P<0.05$). This was also found for combination of butyrate and compound 48/80 (Table 5.6A, $P<0.005$). With CBMC, because of the low number of cells available, only the effect of degranulators alone was tested. These did not increase caspase-3 activity in CBMC. For example the caspase-3 activity for

compound 48/80 treated CBMC increased by 0.31 Units over the control (not significant).

### 5.3.6 Interaction Between Staurosporine And Compound 48/80 On Levels Of Active Caspases In Mast Cells

As shown in previous sections there was no synergy between butyrate and Zn depletion by degranulators in activated caspase-3. To see whether this result holds for another apoptotic inducer, butyrate was replaced by staurosporine. Immature HMC-1 cells were treated with varying concentrations of staurosporine (0.1, 0.5 and 1 μM) in the presence (blue columns) or absence (purple columns) of 1 μg/ml compound 48/80. Treatment of cells with compound 48/80 alone did not induce caspase-3 activity (first set of columns in Figure 5.8A) as shown previously. Staurosporine alone caused significant increases in caspase-3 activity with optimal effect seen at the lowest concentration assayed 0.1 μM. The decreases seen at higher concentrations of staurosporine may be due cell death by necrosis as well as apoptosis. This was not investigated further. There were no further increases in caspase-3 activity in the presence of both compound 48/80 and staurosporine. As for interactions between butyrate and degranulators, the level of caspase-3 activity for the combination of staurosporine and compound 48/80 tended to be less (although in this case not significantly) than the predicted additive effects of staurosporine alone and compound 48/80 alone (Figure 5.8A).

Staurosporine alone also induced caspase-3 activity in mature HMC-1 cells (Figure 5.9A, $P<0.005$). Compound 48/80 alone did not induce significant caspase-3 activity

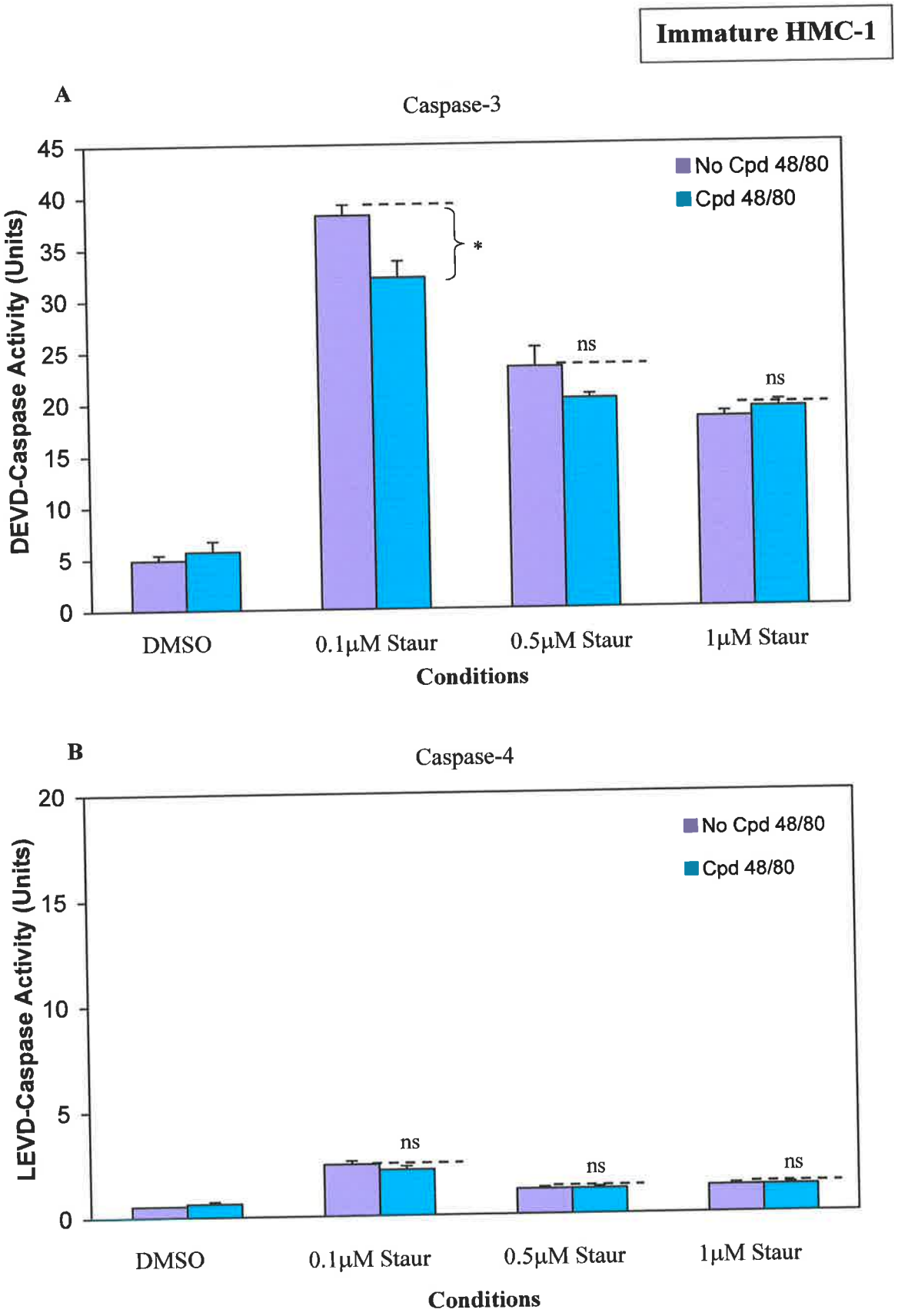
Immature HMC-1
A
Caspase-3
DEVD-Caspase Activity (Units)
45
40
35
30
25
20
15
10
5
0
No Cpd 48/80
Cpd 48/80
*
ns
ns
DMSO
0.1μM Staur
0.5μM Staur
1μM Staur
Conditions
B
Caspase-4
LEVD-Caspase Activity (Units)
20
15
10
5
0
No Cpd 48/80
Cpd 48/80
ns
ns
ns
DMSO
0.1μM Staur
0.5μM Staur
1μM Staur
Conditions

**Figure 5.8**

**Figure 5.8: Effects of activation and apoptotic inducer on the levels of active caspase-3 (DEVD-caspase) and -4 (LEVD-caspase) in immature HMC-1 mast cells.**

Immature HMC-1 cells were treated overnight in the absence of (purple columns) or presence of (blue columns) 1 μg/ml compound 48/80 and the indicated concentrations of staurosporine. Figure 5.8 shows no synergy between staurosporine and compound 48/80 for either caspase-3 activity (A) or caspase-4 activity (B).

Data are expressed as Units of activity per 50 μl of lysates ($4 \times 10^5$ cells). Bars indicate SEM for means of triplicates. Dotted lines show the predicted additive effect between staurosporine and compound 48/80 (A and B). Protein level of control immature HMC-1 cells was 0.06mg/50 μl of lysates. Different scale bars are presented for caspase-3 (A) and -4 (B).

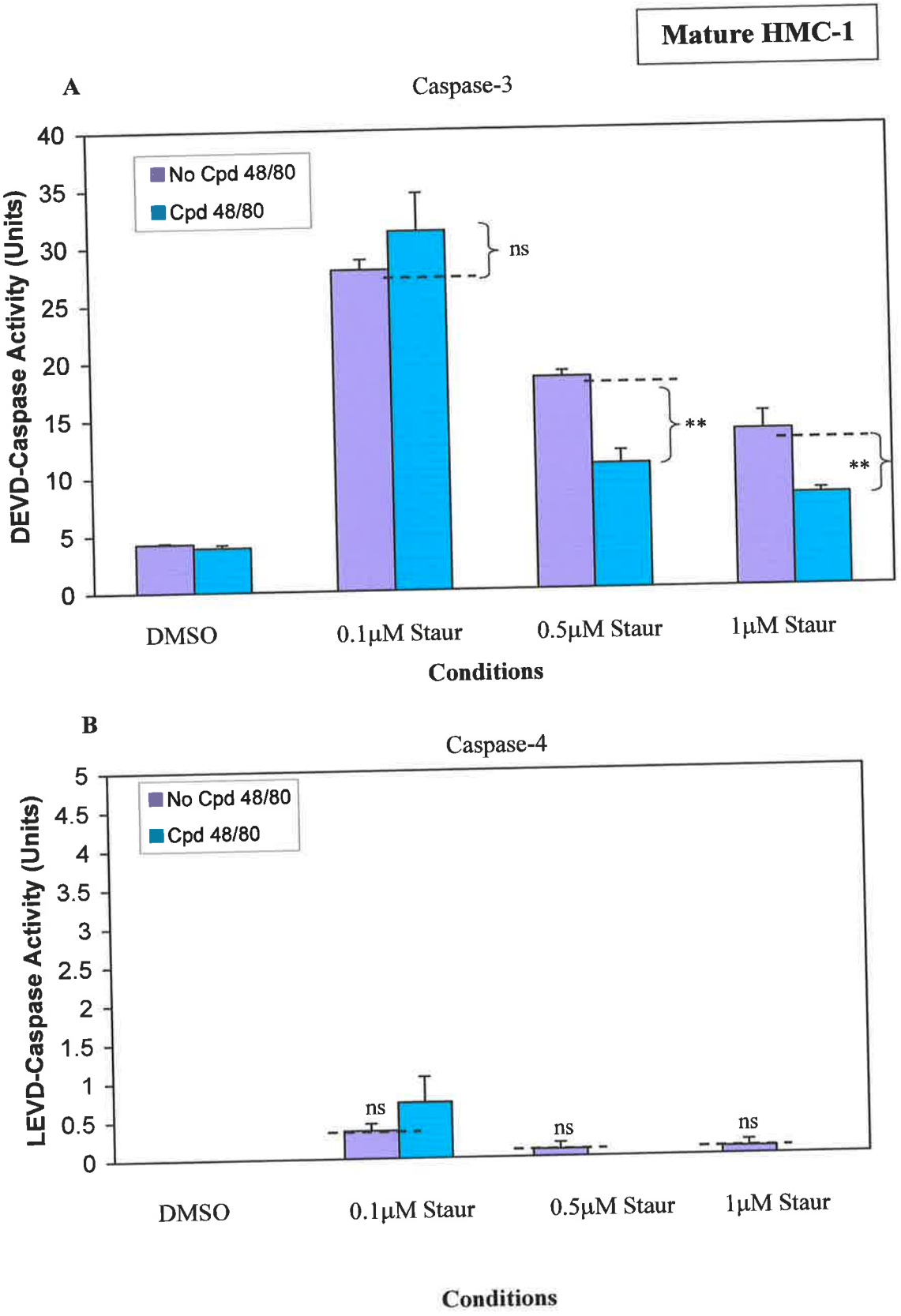
Mature HMC-1
A
Caspase-3
DEVD-Caspase Activity (Units)
40
35
30
25
20
15
10
5
0
No Cpd 48/80
Cpd 48/80
ns
**
**
DMSO
0.1μM Staur
0.5μM Staur
1μM Staur
Conditions
B
Caspase-4
LEVD-Caspase Activity (Units)
5
4.5
4
3.5
3
2.5
2
1.5
1
0.5
0
No Cpd 48/80
Cpd 48/80
ns
ns
ns
DMSO
0.1μM Staur
0.5μM Staur
1μM Staur
Conditions

**Figure 5.9**

**Figure 5.9: Effects of activation and apoptotic inducer on the levels of active caspase-3 (DEVD-caspase) and -4 (LEVD-caspase) in mature HMC-1 mast cells.**

Same legend as Figure 5.8, figure shows no synergy between staurosporine and compound 48/80.

Data are expressed as Units of activity per 50 μl of lysates ($4 \times 10^5$ cells). Bars indicate SEM for means of triplicates. Dotted lines show additive effect between staurosporine and compound 48/80 (A and B). Protein level of control mature HMC-1 cells was 0.04 mg/50 μl of lysates. Different scale bars are presented for caspase-3 (A) and -4 (B).

and did not synergise with staurosporine (Figure 5.9A). The level of caspase-3 activity for the combination of staurosporine and compound 48/80 was significantly less than the predicted additive effects of staurosporine alone and compound 48/80 alone (Figure 5.9A).

Another caspase, caspase-4 was also studied using the same cell lysates. There were minimal increases in caspase-4 in these cells (Figure 5.8B and 5.9B). Caspase-4 was not induced by staurosporine or compound 48/80 alone in either immature (Figure 5.8B) or mature (Figure 5.9B) HMC-1 cells. There was also no synergy between staurosporine and compound 48/80 at any concentrations tested (Figure 5.8B and 5.9B).

### 5.3.7 Effects Of Degranulator And TPEN On Chromatin Fragmentation In Immature HMC-1 Cells

To confirm that the caspase activation due to Zn depletion was associated with apoptotic cell death, immature HMC-1 cells were treated with 50 μM TPEN for 4 h and stained with Hoechst dye 33342. Figure 5.10A shows the normal intact chromatin of the untreated cells while figure 5.10B shows the characteristic chromatin fragmentation (thin arrow) and condensation of chromatin around the nucleus (thick arrow). By contrast, compound 48/80 did not result in any chromatin changes characteristic of apoptosis (Figure 5.10C). This agrees with the lack of induction of caspase activity.

**Hoechst Dye 33342**

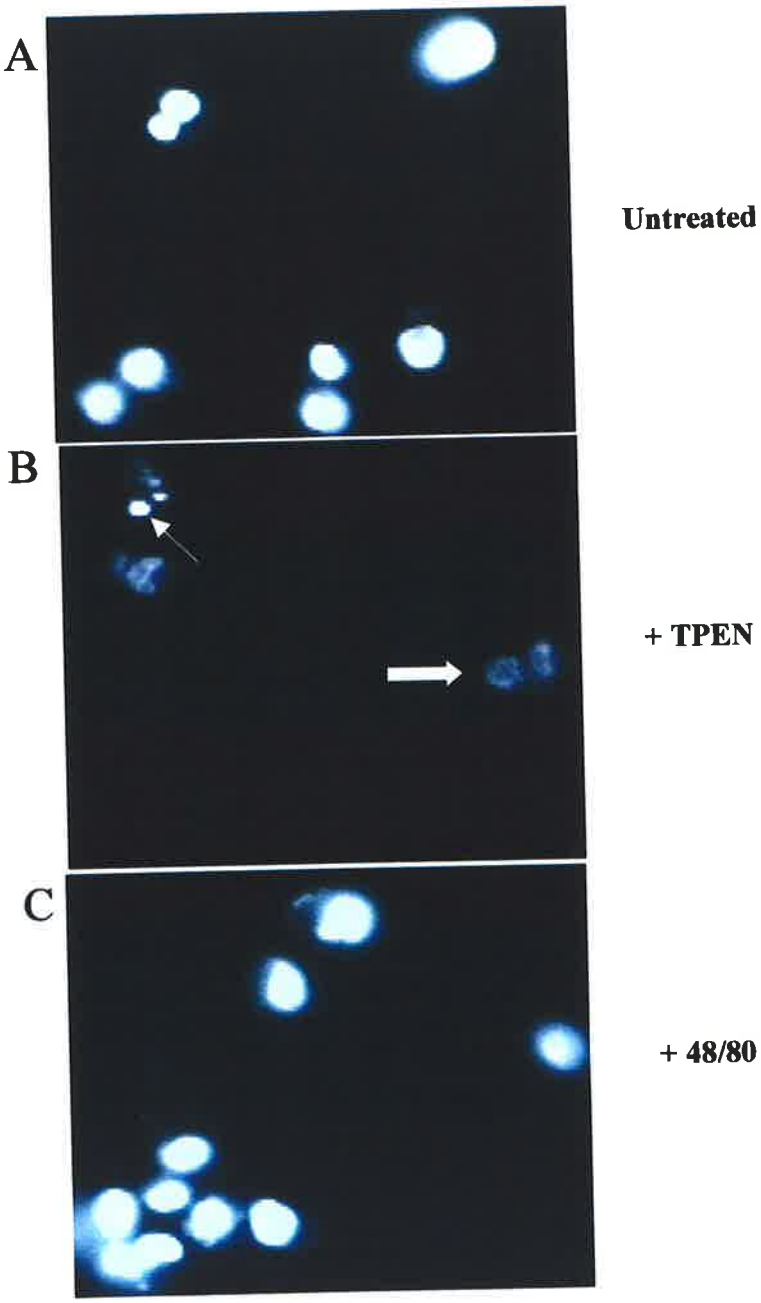


**Figure 5.10**

**Figure 5.10: Effects of degranulator and TPEN on chromatin fragmentation in immature HMC-1 cells.**

**A-C:** Typical images of Hoechst dye 33342 stained untreated immature HMC-1 mast cells showing minimal apoptosis in control (A), while TPEN treated cells (B) showed typical fragmentation of chromatin (thin arrow) and condensation of chromatin around the nucleus (thick arrow). Compound 48/80 treated cells showed minimal apoptosis similar to untreated cells .

## 5.4 Discussion

The findings of these experiments are: 1) mast cells contain various active caspases, 2) activation of these caspases is increased in response to apoptotic stimuli (e.g. butyrate), 3) depletion of Zn by TPEN alone causes a modest increase in caspase activity whereas depletion of Zn by degranulators did not, and 4) depletion of Zn by TPEN synergises with butyrate whereas there was no synergy in cells where Zn was depleted by degranulators.

In the previous chapter, it was demonstrated that pre-cursor forms of caspase-3 and -4 were present in mast cells, particularly within the granules. It was important next to determine whether active forms of these and other caspases exist in mast cells and can be induced by apoptotic stimuli. Some basal caspase activity (especially caspase-1, -3 and -6) were detected in untreated HMC-1 mast cells; these were no greater than in A549 human epithelial cells, an unrelated cell type. One possible reason for the presence of basal caspases is that they play other regulatory roles aside from apoptosis, for example both caspases-1 and -4 have been implicated in inflammation (Wang and Lenardo, 2000). Another possibility is that they are involved in the regulation of mast cell numbers where a small percentage of the population is undergoing apoptosis. In this case, the basal caspase levels reflect the proportion of apoptotic cells in the culture.

There have been little studies of mast cell apoptosis in response to physiological stimuli. In one study, mast cells of *Bax*-deficient mice had prolonged survival following withdrawal of the growth factor IL-3 *in vitro* and after application of the

glucocorticoid fluocinonide to the ear skin *in vivo* (Maurer, 2000). The studies reported in this chapter begin to elucidate these pathways. They show that caspases can be activated in response to common apoptotic stimuli. Thus both butyrate and staurosporine caused a concentration-dependent increase in caspase-3 acitivty in immature and mature HMC-1 mast cells and primary human cord blood mast cells. Butyrate is thought to act by inhibition of histone deacetylase and hyperacetylation of histones resulting in unpacking of the chromatin and new gene expression that may include pro-apoptotic genes (Medina, 1997). Staurosporine acts by a distinct mechanism by inhibiting protein kinases and causing mitochondrial changes such as cytochrome *c* release that lead to apoptosis (Kluck, 1997). Therefore mast cells are responsive to a broad range of apoptotic stimuli.

Whether the high levels of labile Zn in mast cells granules play a role in regulation of caspases is not clear. Since some of the pre-cursor forms of caspases were in mast cell granules, there may be a relationship between granule Zn and granule caspase activity. To investigate this further, the effects of depletion of Zn were studied first by chelation with TPEN and secondly by degranulation with mast cell activators. There was a difference between these two sets of results. While TPEN was potently synergistic with butyrate, degranulators were not synergistic. This was despite the fact that Zinquin-stainable Zn decreased to the same extent in mast cells treated with degranulators as it did in mast cells treated with TPEN. Thus granule Zn cannot be an important regulator of caspase activity.

If pro-caspases are located in the granules of mast cells and are released during degranulation, one would predict that the apoptotic response of degranulated cells to a

toxin would be diminished. To some extent this was observed, since cells treated with a combination of degranulator and either butyrate or staurosporine often had less caspase activity than would be predicted if these agents were having a simple additive effect. An alternative explanation is that the cells were undergoing necrosis rather than apoptosis when cells were treated with a combination of degranulator and apoptotic inducer. This was difficult to test due to the lack of a sensitive and reliable indicator of necrosis in mast cells.

Caspase activation by TPEN was associated with apoptosis of mast cells as was shown by the fragmentation of chromatin in these cells using a chromatin dye. Degranulators did not induce chromatin fragmentation consistent with their lack of effect on caspase-3 activation. These results suggest that TPEN depletes a pool of labile Zn that regulates caspase activation and this pool of Zn is not the same as the pool of Zn contained in the granules. However, it needs to be determined whether more physiological activators such as IgE / antiIgE have similar effects *in vitro* and *in vivo*.

These results need to be considered in the context of whether mast cells die *in* situ after degranulation or whether they recover their granule contents and remain functional. One example of this is the studies showing the recovery of mast cells following FcεRI-mediated degranulation (Dvorak, 1988). There is a possibility that a number of mast cells do undergo apoptosis following degranulation *in vivo* by mechanisms that bypass the normal survival signals of mast cells.

There may be a compromise between the two hypotheses. Thus there is a need to have both recovery and apoptosis in order to maintain the balance between the generation of

mast cells and their removal. If all mast cells were to recover following degranulation, the consequences of over-crowding might result in aberrations in both immune and inflammatory processes. My results have shown that following degranulation, cultured mast cells can recover their Zn and do not directly undergo apoptosis. However, the conditions in which the experiments were performed may not resemble the exact *in vivo* conditions to which mast cells are normally exposed.

In conclusions the main finding in these studies was that Zn depletion by TPEN but not by degranulators increases the susceptibility of mast cells to undergo caspase activation by an apoptotic inducer.

# CHAPTER SIX

# EFFECTS OF ZINC DEPLETION AND SUPPLEMENTATION ON ACTIVATION OF NF-κB

## 6.1 Introduction

The experiments described in this chapter explore the possible role of NF-κB in mediating the effects of intracellular Zn on apoptosis and inflammatory processes in mast cells. Suppression of apoptosis of inflammatory cells prolongs their survival *in vitro* and *in vivo* and is a factor in maintaining the chronic inflammatory process (Simon, 2001). An important factor mediating the suppression of apoptosis in inflammatory cells is the transcription factor NF-κB. NF-κB plays an important role in the expression of a broad range of genes involved in inflammatory diseases (Lee and Burckart, 1998), as well as regulating the apoptosis process (Ward, 1999). NF-κB has been suggested as an ideal therapeutic target for various inflammatory, degenerative and malignant diseases (Baichwal and Baeuerle, 1997; Barnes and Karin, 1997). While some evidence has been presented indicating that NF-κB is pro-apoptotic (that is, it is important for apoptosis to occur as discussed in literature review), the bulk of evidence supports the hypothesis that NF-κB is anti-apoptotic and prolongs the survival of inflammatory cells (Castro-Alcaraz, 2002; Karin, 1998).

Therefore it was of interest to determine whether Zn influences activation of NF-κB in mast cells. One would predict that if a) Zn blocks apoptosis and if b) NF-κB blocks apoptosis, and if c) Zn acts via NF-κB, then Zn should *promote* the activation of NF-κB in mast cells. However, a recent study by Connell and colleagues reported that Zn supplementation in Zn-deficient endothelial cells *prevented* cytokine-mediated activation of NF-κB (Connell, 1997).

Stimuli that activate NF-κB are: pro-inflammatory cytokines (TNF-α and IL-1β), oxidants (hydrogen peroxide), viruses (Rhinovirus), activators of protein kinase C (phorbol esters), and immune stimuli such as allergens (Baldwin, 1996). TNF-α and IL-1β are the two most important inducers of NF- κB and both contribute to the positive feedback loop for NF-κB activation (Lee and Burckart, 1998). In its resting phase, NF-κB is suppressed by binding of the inhibitory protein IκB in the cytoplasm of the cells.

Activation of NF-κB involves several complex signal transduction pathways. These include direct and indirect involvements of a number of kinases in the phosphorylation process (Figure 1.10). Due to the large number of different signals involved in the activation of NF-κB, it is likely that multiple signalling pathways are involved and are integrated to act on a multiprotein IκB-α kinase complex (Rahman and MacNee, 1998). Once activated, NF-κB translocates into the nucleus and binds to specific target sequences in the regulatory elements of genes.

Trace elements such as Zn play important regulatory roles in cell signaling via transcription factors and genes. The potential targets in the NF-κB signaling pathway affected by metals are IκB-kinases, IκBs, NF-κB, proteosome degradation sites of NF-κB and κB binding sites on DNA (Kudrin, 2000). Various metals including Zn, mercury, cadmium and arsenite *in vitro* inhibit NF-κB binding to DNA in TNF-α treated A549 human epithelial cell line (Shumilla, 1998). Over expression of the Zn-finger protein A20 has also resulted in the inhibition of NF-κB activation induced by

TNF, IL-1, lipopolysaccharide, hydrogen peroxide and phorbol ester in a variety of cells (Beyaert, 2000).

The main aim of the experiments was to determine whether changes in intracellular Zn levels induced by Zn chelator TPEN, Zn ionophore pyrithione or degranulators, influence NF-κB activation in mast cells. The effects of changes in intracellular Zn on increase in cell size, another parameter of mast cell activation were also studied. Activation of NF- κB was determined by translocation of NF- κB to the nucleus in immunofluorescence experiments. NF- κB has been mostly studied in epithelial cells; therefore prior to the experiments on mast cells, initial studies were conducted on NCI-H292 human epithelial cells.

## 6.2 Methods

### 6.2.1 Activation Of NF-κB By TNF-α In Mast Cells And NCI-H292 Human Epithelial Cells

NCI-H292 mucoepidermoid carcinoma cells from human lungs were obtained from Dr Darryl Knight (University of WA). These are a model of bronchial epithelial cells (Hierholzer, 1993). NCI-H292 and RBL-2H3 cells were grown on coverslips and treated with 20ng/ml of TNF-α for 4 h at 37°C. Immature and mature HMC-1 mast cells were treated with 20ng/ml of TNF-α for up to 4 h at 37°C.

### 6.2.2 Activation Of Immature And Mature HMC-1 And RBL-2H3 Mast Cells By Degranulators

Mast cells were treated with 1μg/ml compound 48/80 overnight, 5 μg/ml IgE overnight /anti-IgE (1:5000, 2 h) for HMC-1 cells and 35ng/ml DNP-IgE (overnight)-50ng/ml DNP-BSA for 30 min for RBL-2H3 mast cells. Following incubation with various degranulators, NF-κB was assayed in these cells.

### 6.2.3 Detection And Quantification Of NF-κB By Immunofluorescence Labelling

Adherent cells were grown on coverslips and cells in suspension were spun onto microscope slides by cytocentrifugation. The same protocol was followed for both mast and epithelial cells. The protocol has been described in details in section 2.4.2. Cells were fixed in 4% paraformaldehyde. Primary antibody was a rabbit polyclonal antibody (IgG) against the p65 subunit of NF-κB. This was used at 1:20 dilution.

Secondary antibody was an FITC-conjugated goat anti-rabbit (IgG) secondary antibody used at 1:50 dilution. NF-κB was visualized and fluorescence was quantified using the Video Pro image analysis software. Localisation of NF-κB was also classified into three cellular areas: cytoplasmic indicating inactive NF-κB, perinuclear and nuclear indicating active NF-κB. Fluorescence intensity was expressed as grayscale units (GSU).

### 6.2.4 Measurement Of Cell Size By Image Analysis

In addition, the area of the cells was quantified using the same software. In brief a line was drawn around the cell perimeter and the area measured by Video Pro and expressed as pixels squared.

### 6.2.5 Depletion And Supplementation Of Zn In Mast Cells

Depletion of Zn in mast cells was induced by treatment with 25 μM of TPEN for 4 h at 37 °C. Supplementation of Zn was with 25 μM $ZnSO_4$ and 0.1 μM Zn pyrithione for 30 min at 37 °C. Both agents were added to cells prior to treatment with degranulators or TNF-α.

### 6.2.6 Statistical Analysis

The results of typical experiments are described or data were pooled, as indicated in text. Statistical significance was determined by the student *t*-test and the Tukey-Kramer multiple comparisons test where appropriate and is indicated in text or legends to Figures.

## 6.3 Results

### 6.3.1 Activation Of NF-κB In NCI-H292 Human Epithelial Cells

Untreated NCI-H292 cells had a moderate fluorescence labelling for NF-κB and this was significantly increased by TNF-α treatment ($P<0.005$, Figure 6.1). This increase was almost completely suppressed by Zn supplementation using $ZnSO_4$ and pyrithione ($P<0.005$). The increase in total cellular fluorescence for NF-κB with activation was an unexpected finding and is further discussed in section 6.4. Figure 6.2 shows that the increase in fluorescence by TNF-α was accompanied by a change in subcellular distribution of NF-κB from cytoplasm to nucleus. Zn supplementation suppressed the translocation of NF-κB into the nucleus (Figure 6.2). Specificity of labelling was confirmed in cells labelled with only secondary antibody, showing absence of fluorescence.

### 6.3.2 Activation Of NF-κB In Immature And Mature HMC-1 And RBL-2H3 Mast Cells

These experiments were repeated and extended in immature HMC-1 mast cells. Increase in NF-κB total cellular fluorescence intensity was seen with 20 ng/ml TNF-α ($P<0.005$, Figure 6.3). This was associated with a redistribution of fluorescence to the nucleus from the cytoplasm in 92.8% of the cells (Figure 6.4, Table 6.1). There was also a small percentage (3.6%) of cells in the TNF-α treated population displaying a perinuclear localization of NF-κB. Zn supplementation prevented both the increase in

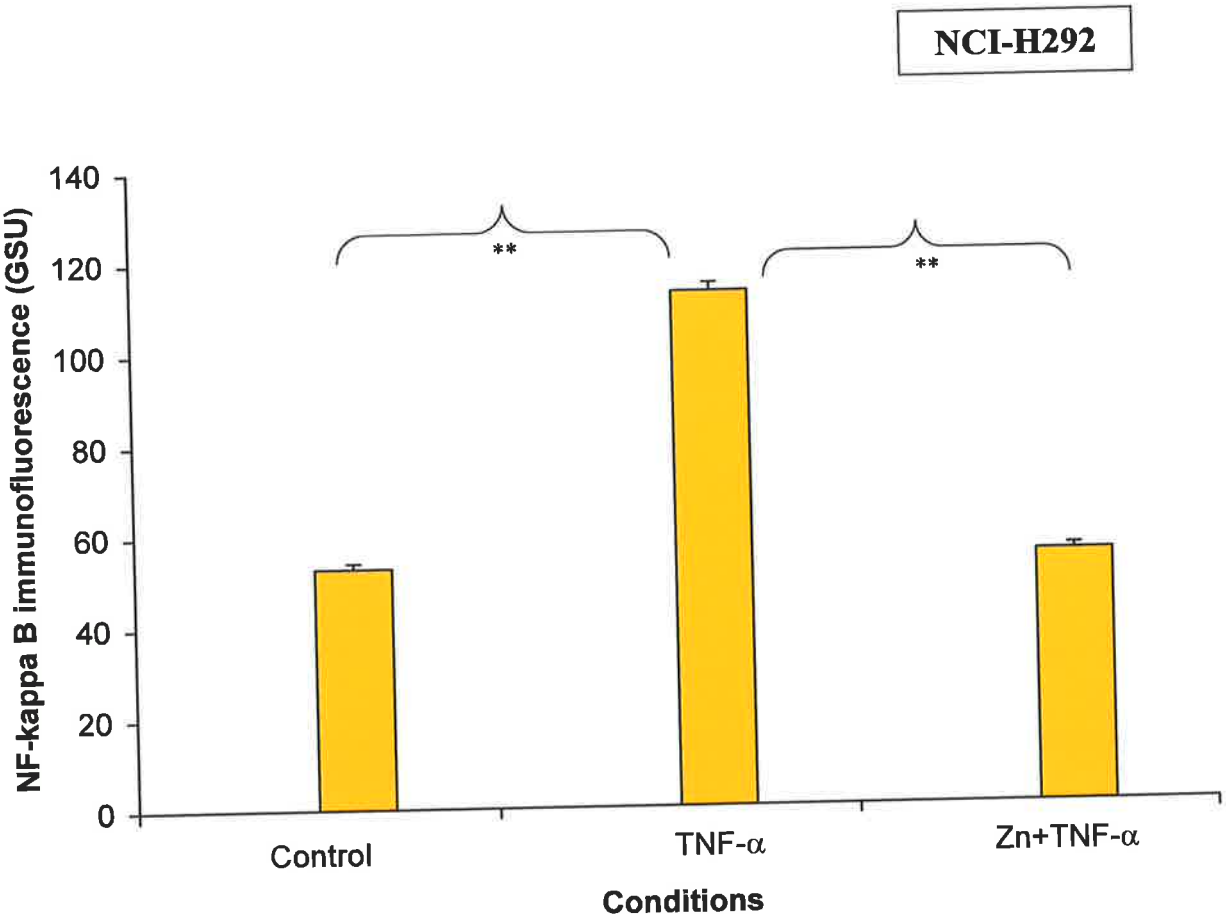
NCI-H292
NF-kappa B immunofluorescence (GSU)
140
120
100
80
60
40
20
0
**
**
Control
TNF-α
Zn+TNF-α
Conditions

**Figure 6.1**

**Figure 6.1: Total cellular immunofluorescence for NF-κB in NCI-H292 human epithelial cells.**

NCI-H292 human epithelial cells were treated with 25 μM $ZnSO_4$ and 0.1μM pyrithione for 30 min to increase intracellular Zn. Other cells did not receive Zn pyrithione. Cells were treated for 4 h with 20 ng/ml of TNF-α to induce NF-κB activation. Figure shows an increase in total cellular NF-κB immunofluorescence in TNF-α treated cells and almost complete suppression following treatment with Zn pyrithione.

Data are means of triplicates ± SEM for a typical experiment. Statistical significances are indicated as **P<0.005.

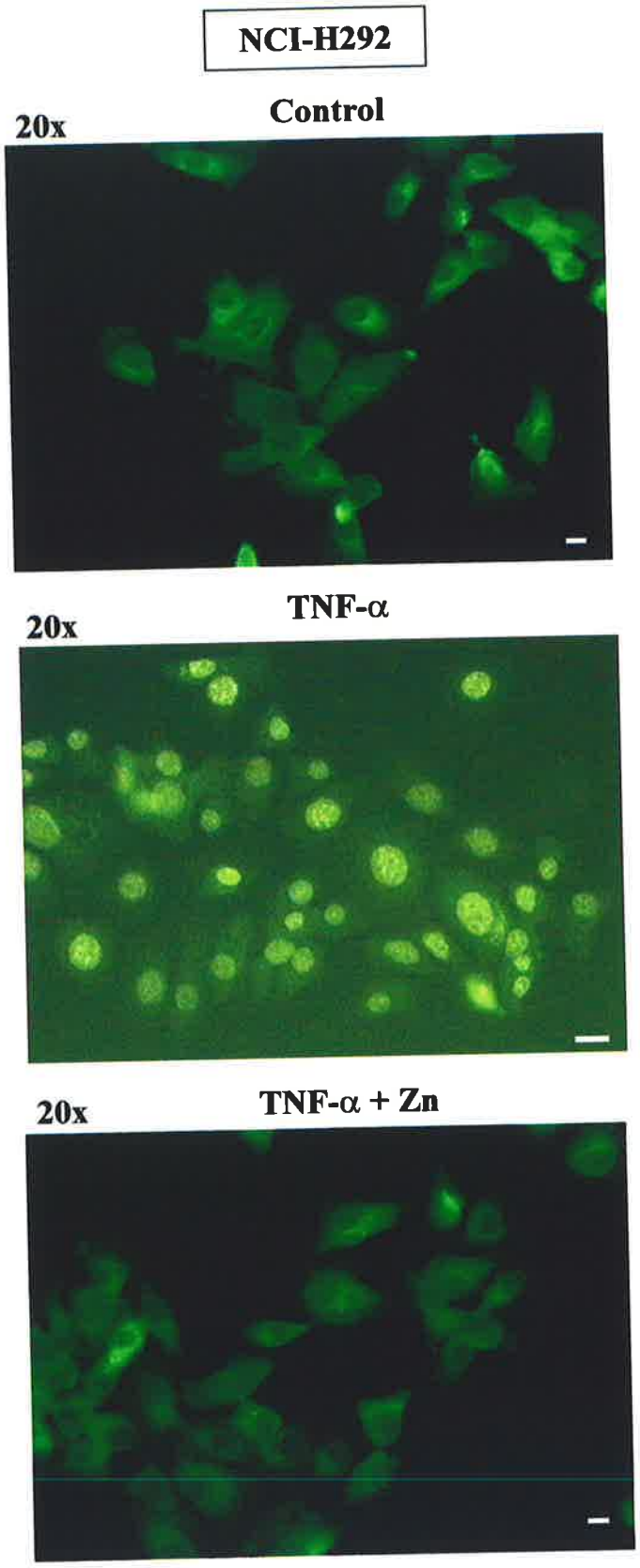


**Figure 6.2**

**Figure 6.2: Effect of exogenous Zn supplementation on TNF-α-induced activation of NF-κB in NCI-H292 human epithelial cells.**

Cells were treated as described in Figure 6.1 legend and representative images are shown here. Top panel shows cytoplasmic immunofluorescence of inactive NF-κB in untreated NCI-H292 human epithelial cells. Middle panel shows nuclear immunofluorescence of active NF-κB in cells treated with 20 ng/ml of TNF-α for 4 h. Bottom panel shows cytoplasmic labelling of NF-κB in cells treated with TNF-α and 25 μM $ZnSO_4$ and 0.1μM Zn pyrithione for 30 min. Figure shows significant decreases in nuclear fluorescence of NF-κB following Zn supplementation.

Scale bar indicates 20 μm for all panels.

total cellular fluorescence (Figure 6.3) and the redistribution to the nucleus (Figure 6.4, Table 6.1).

As for immature HMC-1 cells, mature HMC-1 cells treated with TNF-α had a prominent perinuclear and nuclear translocation of NF-κB (Figure 6.6, Table 6.2). Zn supplementation completely prevented this redistribution ($P<0.005$). The same results were obtained for RBL-2H3 mast cells (Figure 6.8 and 6.9) with the exception of a higher perinuclear distribution in TNF-α treated cells (Table 6.3). Again Zn suppressed this translocation.

In order to ensure that pyrithione itself is not having a direct effect on NF-κB or being cytotoxic for the mast cells, an experiment was performed with various concentrations of pyrithione (0.1, 0.5, 1, 2 and 4 μM) in the absence of exogenous Zn on TNF-α in immature HMC-1 cells. There was no effect on either activation of NF-κB or viability of cells at 0.1 μM pyrithione, which was the concentration used in the Zn supplementation studies. However, there was toxicity at concentrations greater than 1 μM pyrithione.

### 6.3.3 Effect Of Zn Depletion By TPEN On The Activation Of NF-κB In Mast Cells

These experiments were then repeated to determine whether Zn depletion by TPEN would influence activation of NF-κB. Increase in NF-κB total cellular fluorescence intensity in immature HMC-1 cells was seen with 25 μM TPEN ($P<0.005$, Figure 6.3). This was associated with a redistribution of NF-κB fluorescence to the nucleus from

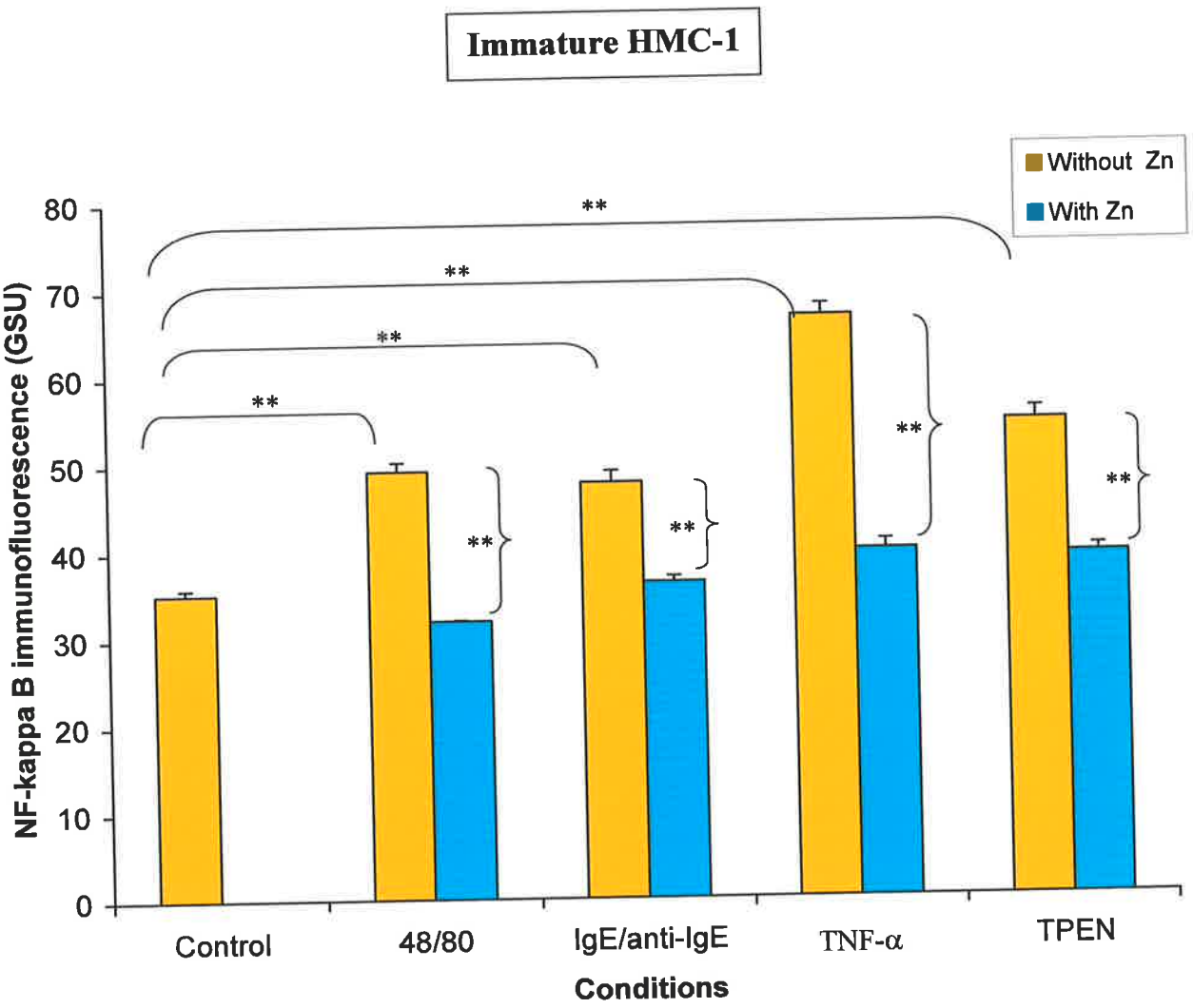
Immature HMC-1
Without Zn
With Zn
NF-kappa B immunofluorescence (GSU)
80
70
60
50
40
30
20
10
0
**
**
**
**
**
**
**
Control
48/80
IgE/anti-IgE
TNF-α
TPEN
Conditions

**Figure 6.3**

**Figure 6.3: Effect of TNF-α, TPEN or degranulators on NF-κB immunofluorescence in immature HMC-1 mast cells with and without Zn supplementation.**

Immature HMC-1 mast cells were treated with 25 μM $ZnSO_4$ and 0.1μM pyrithione for 30 min to increase intracellular Zn (blue columns). Cells were then treated with 20 ng/ml of TNF-α for 2 h, or 25 μM TPEN for 4 h or degranulators for 18 h. Some cells were treated with these agents without Zn supplementation (yellow columns). Figure shows an increase in total cellular NF-κB immunofluorescence in cells treated with all agents and significant decreases in fluorescence of NF-κB following Zn supplementation.

Data are means of triplicates ± SEM for a typical experiment. Statistical significances are indicated as **P<0.005.

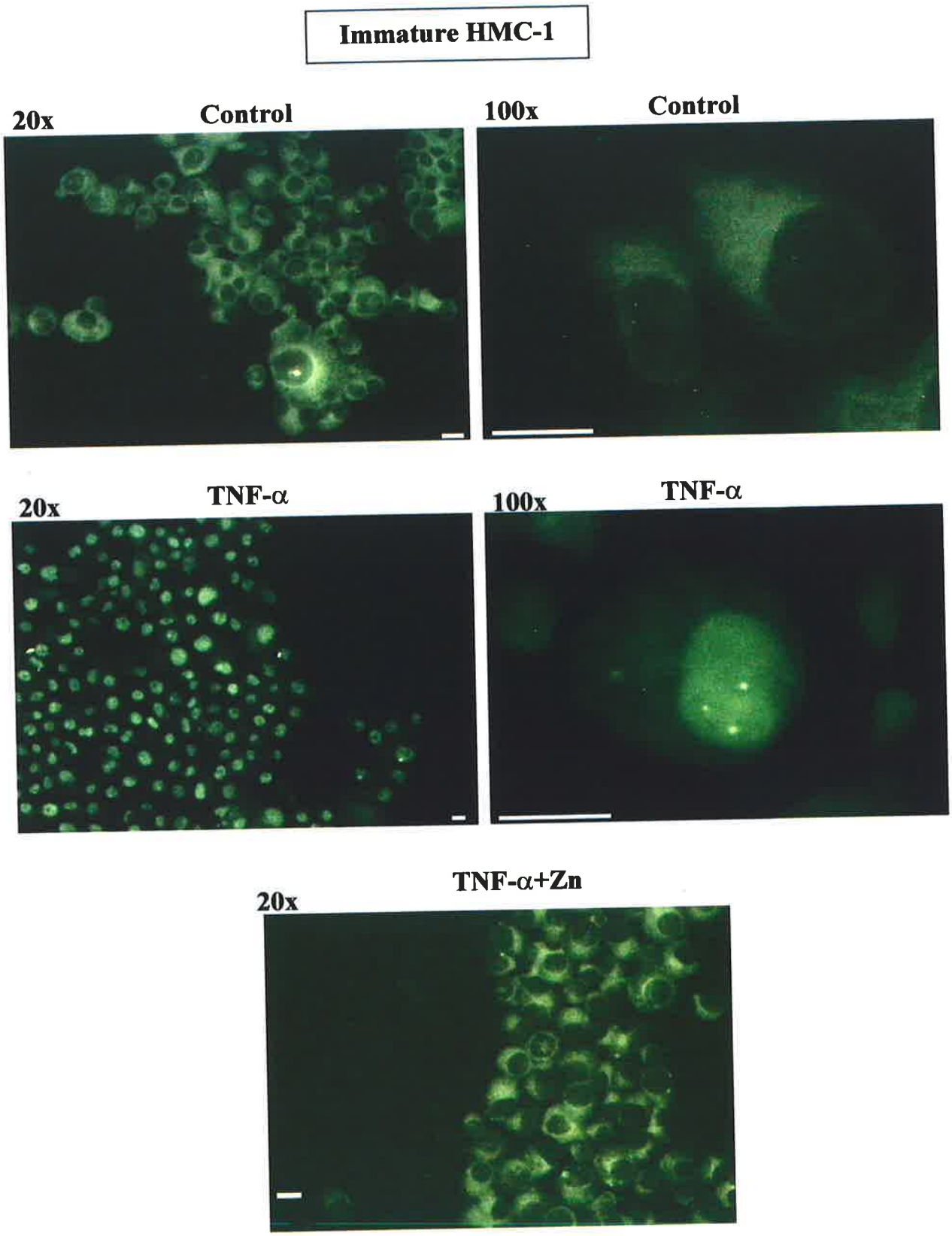
Immature HMC-1
20x
Control
100x
Control
20x
TNF-α
100x
TNF-α
TNF-α+Zn
20x

**Figure 6.4**

**Figure 6.4: Translocation of NF-κB to the nucleus in TNF-α treated immature HMC-1 mast cells and its suppression by Zn**

Cells were treated as in Figure 6.3 and representative images are shown. Figure shows cytoplasmic fluorescence labelling in untreated cells (top LHS and RHS panels) and nuclear fluorescence labelling (NF-κB activation) following treatment with TNF-α (middle LHS and RHS panels). Bottom panel shows cytoplasmic fluorescence labelling in cells treated with TNF-α and $ZnSO_4$. Scale bars indicate 20 μm for all panels.

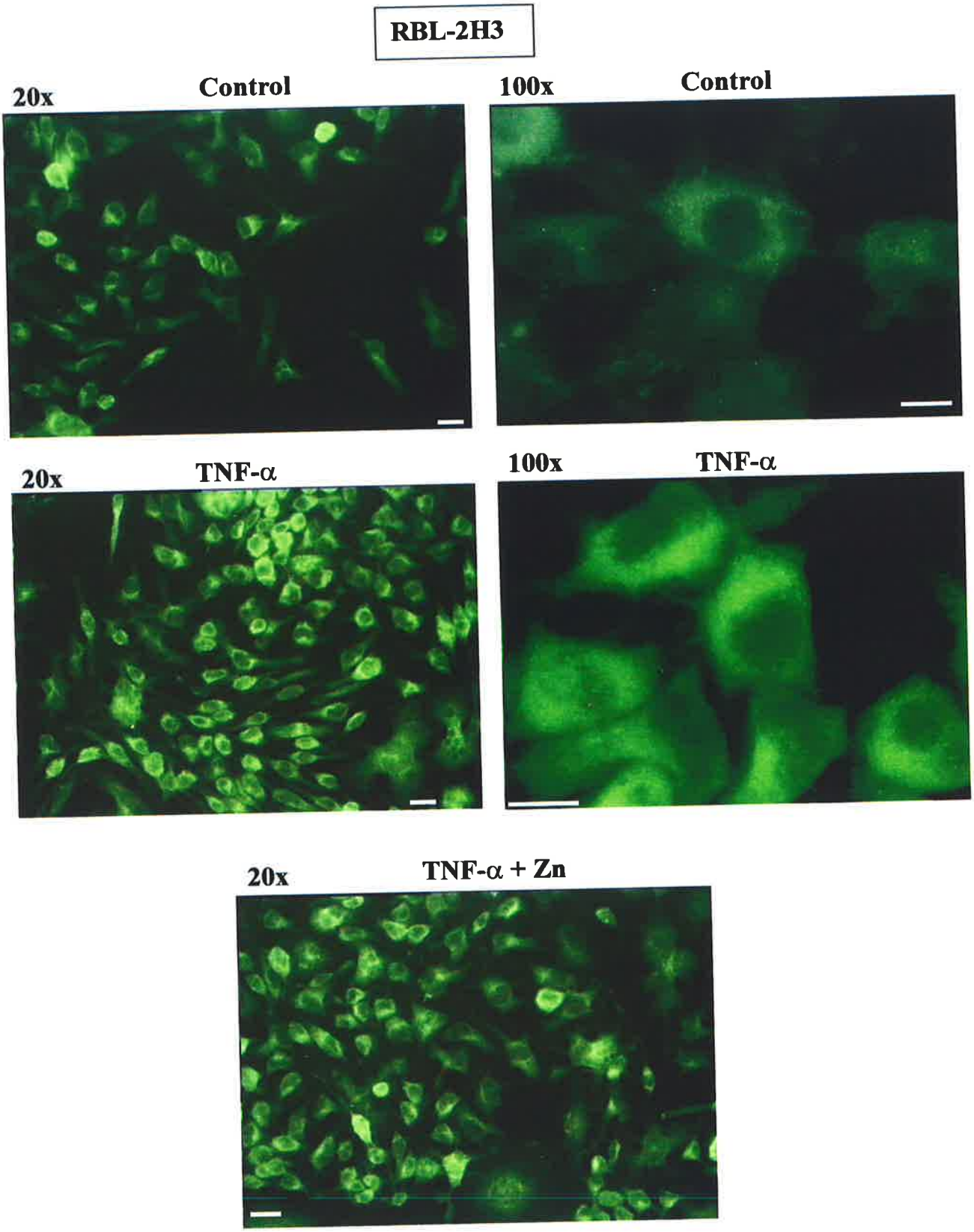
RBL-2H3
20x
Control
100x
Control
20x
TNF-α
100x
TNF-α
20x
TNF-α + Zn

**Figure 6.9**

**Figure 6.9: Translocation of NF-κB to the perinucleus in TNF-α treated RBL-2H3 mast cells and its suppression by Zn**

RBL-2H3 mast cells were treated as in Figure 6.3 and representative images are shown. Figure shows cytoplasmic fluorescence labelling in untreated cells (top panels) and perinuclear fluorescence labelling following treatment with TNF-α (middle LHS and RHS panels). Bottom panel shows mainly cytoplasmic fluorescence labelling in cells treated with TNF-α and $ZnSO_4$.

Scale bar indicates 20 μm for all panels except for middle LHS panel where scale bar indicates 30 μm.

**Table 6.1 Localisation of NF-κB in immature HMC-1 cells**

| Conditions | n | %Cytoplasmic (out of total) | %Perinuclear (out of total) | %Nuclear (out of total) | %Nuclear+ %Perinuclear (out of total) |
|---|---|---|---|---|---|
| **Untreated** | 361 | 100 ± 0.0 | 0.0 ± 0.0 | 0.0 ± 0.0 | 0.0 ± 0.0 |
| **48/80** | 350 | 92.0 ± 2.3 | 8.0 ± 2.3 | 0.0 ± 0.0 | 8.0 ± 2.3 |
| **48/80+Zn** | 342 | 95.9 ± 0.6 | 4.1 ± 0.6 | 0.0 ± 0.0 | 4.1 ± 0.6 |
| **IgE/anti-IgE** | 217 | 92.1± 3.1 | 6.0 ± 3.3 | 2.0 ± 2.0 | 7.9 ± 3.1 |
| **IgE/anti-IgE +Zn** | 329 | 97.3 ± 0.4 | 2.7± 0.4 | 0.0 ± 0.0 | 2.7 ± 0.4 |
| **TNF-α** | 391 | 3.6 ± 3.6** | 3.6 ± 0.7 | 92.8 ± 2.9** | 96.4 ± 3.6** |
| **TNF-α+Zn** | 318 | 97.4 ± 2.6 ** | 2.6 ± 2.6 | 0.0 ± 0.0 ** | 2.6 ± 2.6 ** |
| **TPEN** | 372 | 6.8 ± 0.3** | 22.3 ± 0.9** | 70.9 ± 1.1** | 93.2 ± 0.3** |
| **TPEN+Zn** | 345 | 87.1 ± 5.4 ** | 5.8 ± 3.6 * | 7.2 ± 3.0 ** | 12.9 ± 5.4 ** |

Data are expressed as Mean ± SEM

Cells were classified according to:

**a:** Cytoplasmic; diffused cytoplasmic labelling

**b:** Perinuclear; labelling around rim of the nucleus

**c:** Nuclear; labelling within nucleus

* P<0.05 and ** P<0.005: comparison between untreated and corresponding treated cells for each pattern of labelling.

* P<0.05 and ** P<0.005: comparison between with and without Zn treatment.

the cytoplasm in 70.9% of the cells and perinuclear redistribution in 22.3% of the cells (Figure 6.5, Table 6.1). Zn supplementation prevented both the increase in total cellular fluorescence (Figure 6.3) and the redistribution to the nucleus (Figure 6.5, Table 6.1).

Similar results were obtained for TPEN-treated mature HMC-1 mast cells (Figure 6.6 and 6.7, Table 6.2) and TPEN-treated RBL-2H3 mast cells (Figure 6.8 and 6.10, Table 6.3). However, TPEN-treated cells had a much higher nuclear translocation of NF-κB than cells treated with TNF-α where it was largely perinuclear. Zn supplementation produced the same suppressive effect as in HMC-1 cells.

### 6.3.4 Effect Of Degranulators On The Activation Of NF-κB In Mast Cells

In order to determine whether Zn depletion by degranulation had similar effects to that of TPEN, mast cells were treated with compound 48/80, IgE/anti-IgE or for rat mast cells DNP-IgE/DNP-BSA, the equivalent of IgE/anti-IgE for human mast cells. There was an increase in total cellular NF-κB fluorescence for each of the mast cell types and for each of the degranulators used (Figure 6.3, 6.6. and 6.8, $P<0.005$). Overall there was an increase in perinuclear staining for mature HMC-1 and a moderate increase in nuclear staining (Tables 6.1, 6.2 and 6.3). The one major difference between the mast cell types was that for mature HMC-1 cells, degranulators gave an equivalent effect to treatment with TNF-α and TPEN whereas, with the other mast cell types, degranulators had significantly less effect. Interestingly, mature HMC-1 cells treated with degranulators had a higher nuclear translocation of NF-κB than seen in

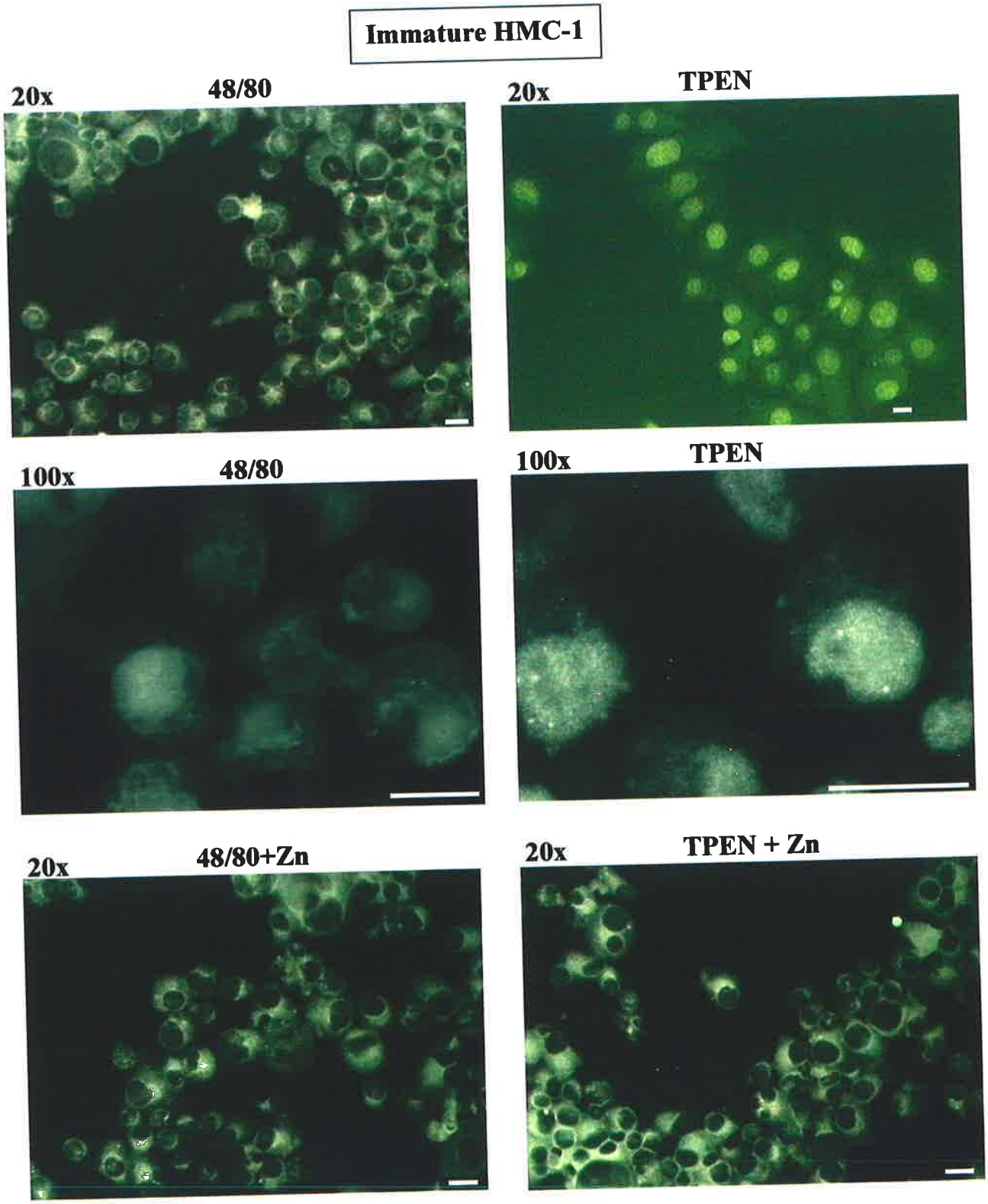
Immature HMC-1
20x
48/80
20x
TPEN
100x
48/80
100x
TPEN
20x
48/80+Zn
20x
TPEN + Zn

**Figure 6.5**

**Figure 6.5: Translocation of NF-κB to the nucleus in immature HMC-1 mast cells treated with TPEN or compound 48/80 and effects of Zn.**

Cells were treated as in Figure 6.3 and representative images are shown. For the control untreated cells, see Figure 6.4. Figure shows cytoplasmic fluorescence labelling in compound 48/80 treated cells (LHS panels) and nuclear fluorescence labelling following treatment with TPEN (RHS panels). Zinc suppressed nuclear translocation in TPEN treated cells (bottom RHS panel).

Scale bar indicates 20 μm for all panels except for middle LHS panel where scale bar indicates 10 μm.

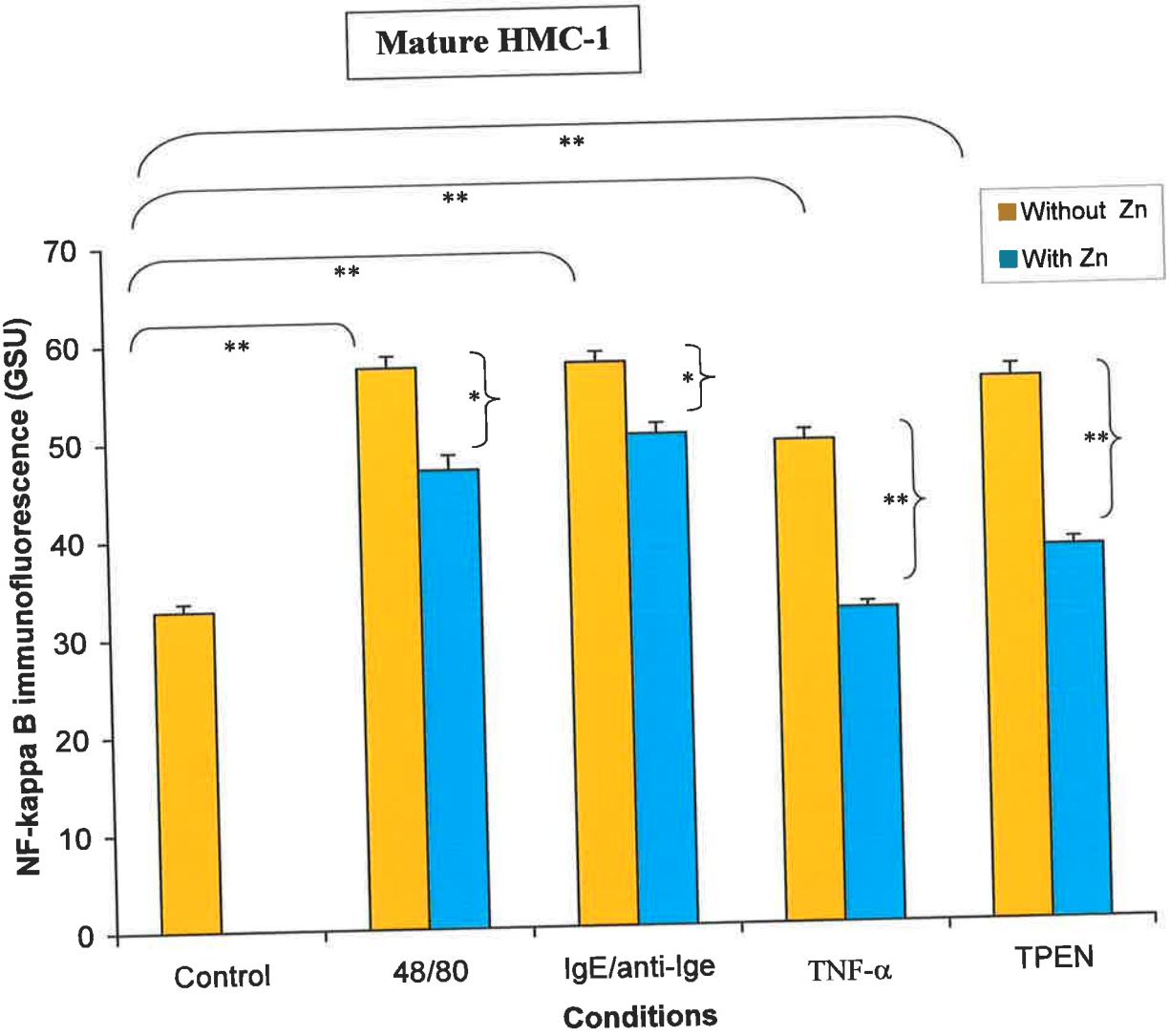
Mature HMC-1
Without Zn
With Zn
NF-kappa B immunofluorescence (GSU)
70
60
50
40
30
20
10
0
**
**
**
**
*
*
**
**
Control
48/80
IgE/anti-Ige
TNF-α
TPEN
Conditions

**Figure 6.6**

**Figure 6.6: Effect of TNF-α, TPEN or degranulators on NF-κB immunofluorescence in mature HMC-1 mast cells with and without Zn supplementation.**

Mature HMC-1 mast cells were treated with 25 μM $ZnSO_4$ and 0.1μM pyrithione for 30 min to increase intracellular Zn (blue columns). Cells were then treated with 20 ng/ml of TNF-α for 2 h, or 25 μM TPEN for 4 h or degranulators for 18 h. Some cells were treated with these agents without Zn supplementation (yellow columns). Figure shows an increase in total cellular NF-κB immunofluorescence in cells treated with all agents and significant decreases in fluorescence of NF-κB following Zn supplementation.

Data are means of triplicates ± SEM for a typical experiment. Statistical significances are indicated as * $P<0.05$ and ** $P<0.005$.

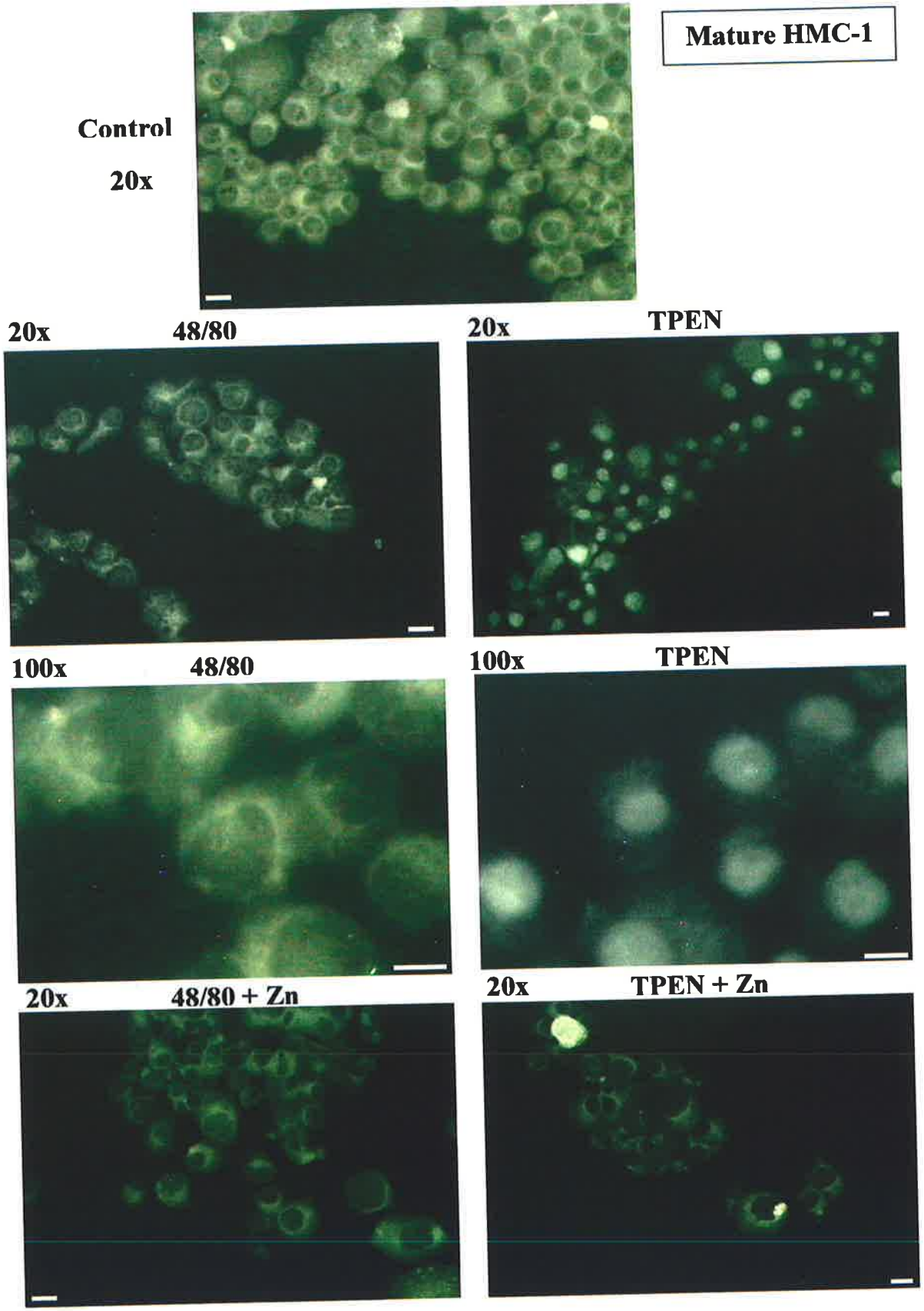
Mature HMC-1
Control
20x
20x
48/80
20x
TPEN
100x
48/80
100x
TPEN
20x
48/80 + Zn
20x
TPEN + Zn

Figure 6.7

**Figure 6.7: Translocation of NF-κB to the nucleus in TNF-α treated mature HMC-1 mast cells and its suppression by Zn.**

Mature HMC-1 cells were treated as in Figure 6.3 and representative images are shown. Figure shows cytoplasmic fluorescence labelling in untreated cells (top panel), perinuclear fluorescence in compound 48/80 treated cells (LHS panels) and nuclear fluorescence in TPEN treated cells (RHS panels). Zinc suppresses nuclear translocation of NF-κB. Scale bar indicates 20 μm for all panels except for the two middle panels where scale bars indicate 10 μm.

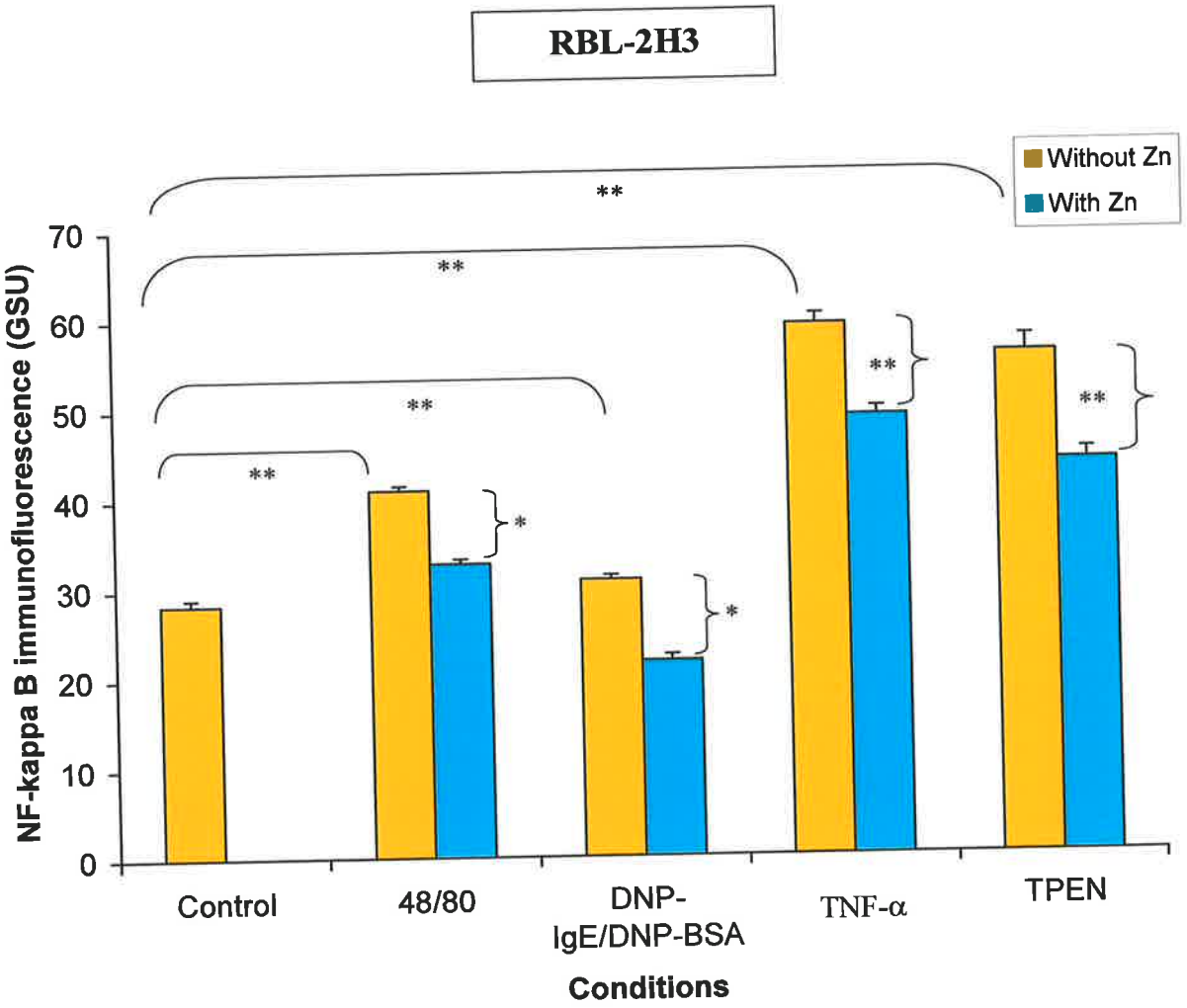
RBL-2H3
Without Zn
With Zn
NF-kappa B immunofluorescence (GSU)
70
60
50
40
30
20
10
0
**
**
**
**
*
*
**
**
Control
48/80
DNP-IgE/DNP-BSA
TNF-α
TPEN
Conditions

**Figure 6.8**

**Figure 6.8: Effect of TNF-α, TPEN or degranulators on NF-κB immunofluorescence in RBL-2H3 mast cells with and without Zn supplementation.**

RBL-2H3 mast cells were treated with 25 μM $ZnSO_4$ and 0.1μM pyrithione for 30 min to increase intracellular Zn (blue columns). Cells were then treated with 20 ng/ml of TNF-α for 2 h, or 25 μM TPEN for 4 h or degranulators for 18 h. Some cells were treated with these agents without Zn supplementation (yellow columns). Figure shows an increase in total cellular NF-κB immunofluorescence in cells treated with all agents and significant decreases in fluorescence of NF-κB following Zn supplementation.

Data are means of triplicates ± SEM for a typical experiment. Statistical significances are indicated as *$P<0.05$ and **$P<0.005$.

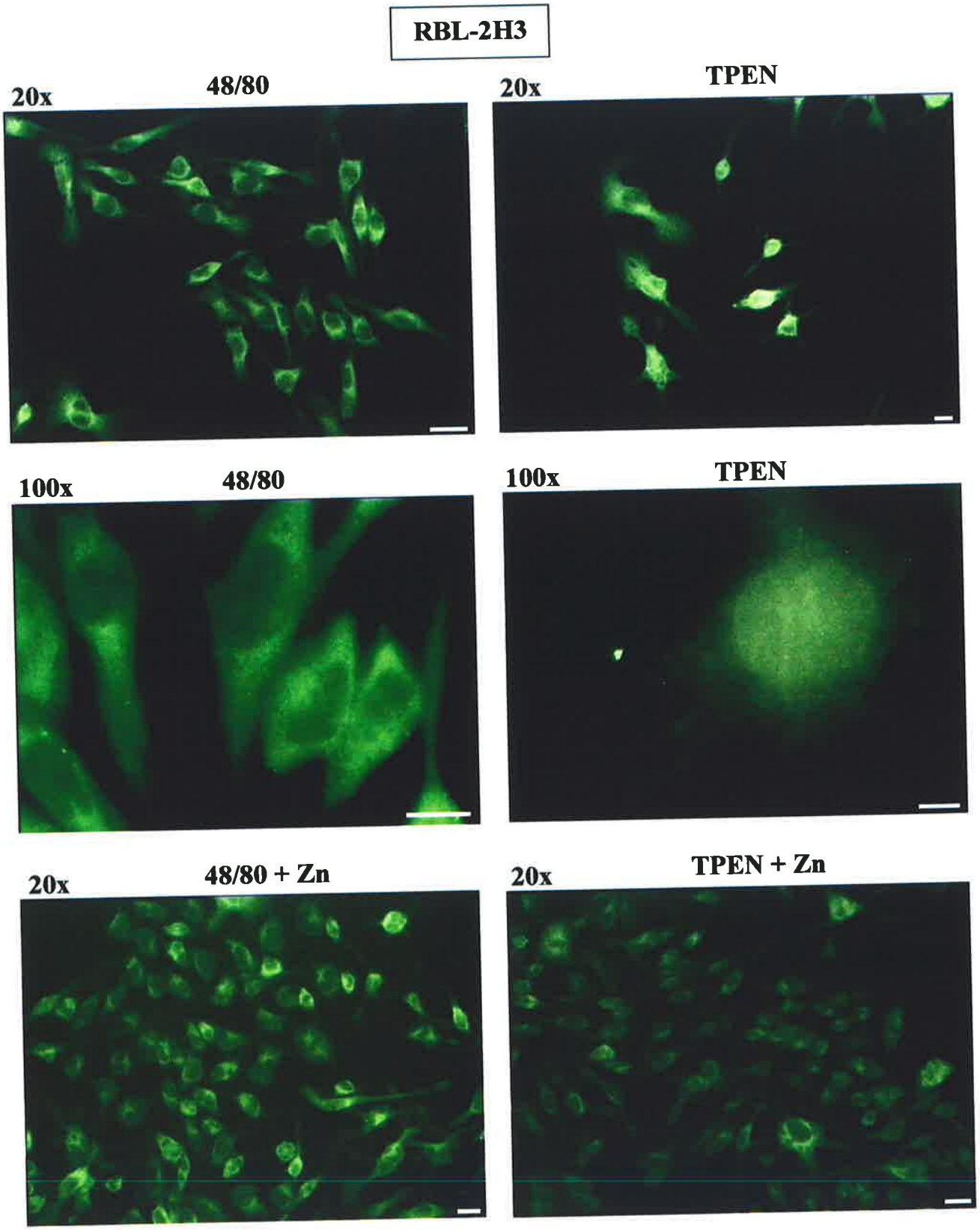
RBL-2H3
20x
48/80
20x
TPEN
100x
48/80
100x
TPEN
20x
48/80 + Zn
20x
TPEN + Zn

**Figure 6.10**

**Figure 6.10: Translocation of NF-κB to the nucleus in RBL-2H3 mast cells treated with TPEN or compound 48/80 and effects of Zn.**

RBL-2H3 mast cells were treated as in Figure 6.3 and representative images are shown. For the control untreated cells, see Figure 6.9. Figure shows cytoplasmic fluorescence labelling in compound 48/80 treated cells (LHS panels) and nuclear fluorescence labelling following treatment with TPEN (RHS panels). Zinc suppressed nuclear translocation in TPEN treated cells (bottom RHS panel). Scale bar indicates 20 μm for all panels except for the two middle panels where scale bars indicate 10 μm.

**Table 6.2 Localisation of NF-κB in mature HMC-1 cells**

| Conditions | n | %Cytoplasmic (out of total) | %Perinuclear (out of total) | %Nuclear (out of total) | %Nuclear+ %Perinuclear (out of total) |
|---|---|---|---|---|---|
| **Untreated** | 336 | 100 ± 0.0 | 0.0 ± 0.0 | 0.0 ± 0.0 | 0.0 ± 0.0 |
| **48/80** | 351 | 28.6 ± 0.6** | 57.9 ± 1.6** | 13.6 ± 2.1 | 71.4 ± 0.6** |
| **48/80+Zn** | 301 | 66.9 ± 11.4 ** | 30.6 ± 11.6 * | 2.6 ± 1.7 | 33.1 ± 11.4 ** |
| **IgE/anti-IgE** | 408 | 11.2 ± 0.8** | 67.4 ± 0.1** | 21.4 ± 0.9* | 88.8 ± 0.8** |
| **IgE/anti-IgE +Zn** | 347 | 86.5 ± 1.2 ** | 13.5 ± 1.2 ** | 0.0 ± 0.0 * | 13.5 ± 1.2 ** |
| **TNF-α** | 401 | 1.8 ± 0.2** | 24.4 ± 0.4* | 73.8 ± 0.9** | 98.3 ± 0.2** |
| **TNF-α+Zn** | 357 | 100 ± 0.0 ** | 0.0 ± 0.0 * | 0.0 ± 0.0 ** | 0.0 ± 0.0 ** |
| **TPEN** | 320 | 15.7 ± 0.9** | 21.5 ± 1.6* | 62.8 ± 1.1** | 84.3 ± 0.9** |
| **TPEN+Zn** | 345 | 87.5 ± 0.1 ** | 6.4 ± 0.7 * | 6.4 ± 0.6 ** | 12.5 ± 0.1 ** |

Data are expressed as Mean ± SEM

Cells were classified according to:

**a:** Cytoplasmic; diffused cytoplasmic labelling

**b:** Perinuclear; labelling around rim of the nucleus

**c:** Nuclear; labelling within nucleus

* P<0.05 and ** P<0.005: comparison between untreated and corresponding treated cells for each pattern of labelling.

* P<0.05 and ** P<0.005: comparison between with and without Zn treatment.

**Table 6.3 Localisation of NF-κB in RBL-2H3 cells**

| Conditions | n | %Cytoplasmic (out of total) | %Perinuclear (out of total) | %Nuclear (out of total) | %Nuclear+ %Perinuclear (out of total) |
|---|---|---|---|---|---|
| **Untreated** | 302 | 100 ± 0.0 | 0.0 ± 0.0 | 0.0 ± 0.0 | 0.0 ± 0.0 |
| **48/80** | 325 | 93.7 ± 0.8 | 6.3 ± 0.8 | 0.0 ± 0.0 | 6.3 ± 0.8 |
| **48/80+Zn** | 343 | 89.5 ± 0.7 | 10.5 ± 0.7 | 0.0 ± 0.0 | 10.5 ± 0.7 |
| **DNP-IgE/DNP-BSA** | 311 | 89.4 ± 3.8 | 7.0 ± 1.1 | 0.6 ± 0.6 | 7.6 ± 1.1 |
| **DNP-IgE/DNP-BSA +Zn** | 204 | 100 ± 0.0 | 0.0 ± 0.0 | 0.0 ± 0.0 | 0.0 ± 0.0 |
| **TNF-α** | 500 | 9.2 ± 4.1** | 71.9 ± 3.9** | 18.9 ± 1.4** | 90.8 ± 4.1** |
| **TNF-α+Zn** | 426 | 79.4 ± 3.3 ** | 16.9 ± 2.9 ** | 3.7 ± 0.6 ** | 20.6 ± 3.2 ** |
| **TPEN** | 298 | 14.3 ± 2.9** | 16.4 ± 0.3* | 69.3 ± 3.1** | 85.7 ± 2.9** |
| **TPEN+Zn** | 187 | 92.0 ± 0.8 ** | 4.3 ± 0.6 * | 4.3 ± 1.1 ** | 8.6 ± 0.7 ** |

Data are expressed as Mean ± SEM

Cells were classified according to:

**a:** Cytoplasmic; diffused cytoplasmic labelling

**b:** Perinuclear; labelling around rim of the nucleus

**c:** Nuclear; labelling within nucleus

* P<0.05 and ** P<0.005: comparison between untreated and corresponding treated cells for each pattern of labelling.

* P<0.05 and ** P<0.005: comparison between with and without Zn treatment.

other mast cells (Table 6.2). Zn supplementation decreased total cellular NF-κB fluorescence for each mast cell type (Figure 6.3, 6.6 and 6.8, $P<0.005$).

### 6.3.5 Effect Of Zn On Changes In Cell Size During Mast Cell Stimulation

Since Zn inhibits NF-κB translocation, it was next determined whether Zn also has an effect on another aspect of cell activation, namely the increase in cell size. There was a significant increase in cell size induced by degranulators in all of the mast cell types. Zn supplementation in degranulator treated immature HMC-1 cells partially decreased the increase in cell size ($P<0.005$, Table 6.4). However, this was not seen in either mature HMC-1 or RBL-2H3 mast cells (Table 6.4).

There were smaller increases of cell size in TNF-α treated cells; this was partially reversed by Zn in immature HMC-1 cells but not in the other mast cells. Similar results were found for TPEN treatment for the three types of mast cells (Table 6.4).

**Table 6.4 Effects of Zn on increase in mast cell area during stimulation.**

| Conditions | Immature HMC-1 | Mature HMC-1 | RBL-2H3 |
|---|---|---|---|
| **Untreated** | 618.4 ± 10.0 (n=361) | 681.7 ± 11.5 (n=336) | 764.2 ±15.9 (n=302) |
| **48/80** | 1477.9 ± 30.5 (n=350) | 1271.7 ± 45.8 (n=336) | 1089.6 ± 31.2 (n=325) |
| **48/80+Zn** | 1210.8 ± 31.1** (n=342) ** | 1226.8 ± 29.1 (n=301) | 1075.0 ± 37.1 (n=343) |
| **IgE/anti-IgE or DNP-IgE** | 1030.8 ± 36.2 (n=217) | 1632.3 ± 43.8 (n=408) | 1019.8 ± 31.2 (n=311) |
| **IgE/anti-IgE or DNP-IgE+Zn** | 1333.5 ± 25.8** (n=329) ** | 1616.7 ± 50.6 (n=347) | 1106.0 ± 43.1 (n=204) |
| **TNF-α** | 707.6 ± 14.3 (n=391) | 950.5 ± 22.4 (n=401) | 855.0 ±18.6 (n=500) |
| **TNF-α+Zn** | 639.9 ± 14.6** (n=318) ** | 944.7 ± 25.7 (n=358) | 836.7 ± 17.5 (n=426) |
| **TPEN** | 803.9 ± 15.3 (n=372) | 815.3 ± 23.7 (n=320) | 897.0 ±21.2 (n=298) |
| **TPEN+Zn** | 726.3 ±13.1** (n=345) ** | 781.0 ± 9.9 (n=345) | 851.5 ± 18.1 (n=187) |

Cell area was calculated from image analysis software and expressed as Mean ± SEM in square pixels.

Rat RBL-2H3 mast cells were treated with DNP-IgE/DNP-BSA as an equivalent to the IgE/anti-IgE for human mast cells.

** $P<0.005$: comparison between untreated and corresponding treated cells.

** $P<0.005$: comparison between with and without Zn treatment.

## 6.4 Discussion

The major aim of this chapter was to determine whether NF-κB mediates the effect of Zn on apoptosis in mast cells. However, the findings reported in this chapter argue against a direct role for NF-κB in actions of Zn on apoptosis. One of the major finding from these studies was that Zn depletion by TPEN was a strong inducer of NF-κB translocation to the nucleus.

Just prior to the commencement of this thesis, a number of papers appeared in the literature on up-regulation of NF-κB in mast cells (Pelletier, 1998; Richard, 1999). There were no studies at the time of NF-κB in HMC-1 cells. Therefore it was important firstly to determine whether TNF-α and other activators would up-regulate NF-κB in immature and mature HMC-1 cells and in RBL-2H3 cells. This was found to be the case and it was shown that there was both increase total immunofluorescence for NF-κB and substantial translocation of NF-κB into or around the nucleus. While the relationship between total cellular fluorescence for NF-κB and its translocation is not clear, one possibility is that the antigenic epitopes on cytoplasmic NF-κB that bind to the antibody are less available when it is complexed with IκBα inhibitory protein. This protein is lost during translocation and this loss may expose previously hidden antigenic sites.

The previous chapter has shown that Zn has anti-apoptotic effects in mast cells; since NF-κB also suppresses apoptosis (as described in 6.1), it was of interest to investigate whether Zn influences NF-κB activity in cells treated with TNF-α and other stimuli such as degranulators. Firstly, the effects of Zn supplementation were studied in cells

treated with TNF-α. Zn prevented the activation and translocation of NF-κB in each mast cell type. This confirms the findings of Connell and colleagues in endothelial cells, a non-inflammatory cell type (Connell, 1997). In that study Zn-deficient endothelial cells were supplemented with extracellular Zn for 48 h. In my study a more rapid technique for Zn supplementation was adopted where pyrithione was used to facilitate the uptake of Zn into mast cells. Pyrithione at certain concentrations has been shown to either inhibit NF-κB activation or have a toxic effect on cells (Kim, 1999). However, at the concentration used in the mast cell studies there was no effect of pyrithione alone. These results also suggest that there is no direct involvement of NF-κB in the anti-apoptotic effect of Zn, since if this were true it would be expected that Zn would promote rather than prevent the activation of NF-κB.

Next the effects of Zn depletion on NF-κB were determined. The first method of Zn depletion by TPEN treatment resulted in the activation and nuclear translocation of NF-κB. This has not previously been shown but agrees with the previous finding that an increase in intracellular Zn suppresses activation of NF-κB. It also raises important questions concerning whether NF-κB activation occurs in Zn deficient individuals.

The action of Zn in the inhibition of NF-κB activation has not been defined. One possibility is that Zn blocks the phosphorylation of IκB-α thereby preventing the translocation of NF-κB into the nucleus. Zinc is a known inhibitor of protein kinases and alters the phosphorylation pattern of cells (Beyersmann and Haase, 2001; Pang and Shafer, 1985). This could be tested by determining whether IκB-α is still present and complexed to NF-κB in TNF-α stimulated, Zn-supplemented cells. One way of

establishing this would be by immuno-precipitating the p65 subunit of NF-κB and detecting of IκB-α in the precipitate.

Other possibilities are that Zn acts either upstream or downstream of the phosphorylation of IκB-α. If Zn acts by blocking phosphorylation of IκB-α then it will be interesting to determine whether Zn depletion stimulates phosphorylation of IκB-α thereby allowing NF-κB to translocate into the nucleus. Support for this hypothesis has come from a recent study by Jeon and colleagues where it was reported that Zn inhibited NF-κB activation via the blocking of IκB kinase (IKK) (Jeon, 2000). They proposed that Zn modifies cysteine sulfhydryl groups critical for enzyme activity in the two catalytic subunits of IKK complex, IKK alpha and IKK beta. If Zn depletion does not increase phosphorylation of IκB-α and yet NF-κB does translocate into the nucleus as shown here then it would be interesting to investigate whether IκB-α is still complexed to NF-κB within the nucleus. With respect to this Shumilla and colleagues have demonstrated that Zn inhibits NF-κB binding to DNA via interactions with sulfhydryl groups (Shumilla, 1998). This is unlikely to explain the effects of Zn in mast cells because Zn supplementation prevents the translocation of NF-κB to the nucleus and therefore events such as DNA binding downstream of the translocation are irrelevant.

Another way in which Zn can inhibit NF-κB translocation is through its suppression of caspase-3. Caspase-3 has been shown to cleave IκB-α *in vitro* (Barkett, 1997), which could probably lead to release of NF-κB and its translocation to the nucleus. Therefore, by blocking caspase-3 Zn would block translocation of NF-κB into the

nucleus and thereby prevent apoptosis. It is not clear whether in mast cells NF-κB is pro-apoptotic or anti-apoptotic. The results with TPEN and Zn supplementation would agree more with the pro-apoptotic effects of NF-κB.

In Zn-depleted mast cells, NF-κB moves to the nucleus but these findings do not necessarily imply that Zn depletion promotes NF-κB mediated gene transcription. For example Prasad and colleagues have shown that HUT-78 cells grown in Zn-deficient medium had reduced binding of NF-κB to DNA and decreased gene expression of IL-2 (Prasad, 2002). A similar finding was reported by Oteiza and colleagues where there was reduced NF-κB binding to DNA in testes of Zn-deficient weanling rats (Oteiza, 2001). Future studies should test whether in TPEN-treated mast cells there is an increase in expression of genes known to be regulated by NF-κB, such as GM-CSF and IL-8.

The other mechanism of depletion of Zn by degranulation also resulted an increase in total fluorescence for NF-κB although there were some differences according to the mast cell types studied. For example, there was only partial translocation of NF-κB into the rim of the nucleus in mature HMC-1 cells while there was little translocation in immature HMC-1 and RBL-2H3 cells. The effect of degranulators in the immature cells is likely to be due to the loss of Zn rather than some other change caused by degranulation since supplementation with Zn prevented the changes in NF-κB. This implies that the granular pool of Zn in mast cells may play a role in preventing premature activation of NF-κB. The previous chapter showed that this pool of Zn was not involved in the regulation of apoptosis. This is further evidence that the effects of

Zn on apoptosis are unrelated to its effects on NF-κB and therefore probably inflammation.

Finally, the effects of Zn on increasing cell size during mast cell activation were investigated. It was found that degranulators greatly increased the size of mast cells, as determined by measuring the area of the cells, whereas TNF-α and TPEN only moderately increased cell size. Zn supplementation did not suppress the increase of cell size in mature HMC-1 and RBL-2H3 cells but it did in immature HMC-1 cells treated with some stimuli such as compound 48/80 but not with others such as anti-IgE. The reason for this is unclear and was not further investigated. Regardless of these differences, the findings do suggest that NF-κB translocation is not required for the increase in cell size because in mature HMC-1 cells treated with Zn, NF-κB translocation was completely suppressed but the cell size still increased. Zn may be an effective tool for further dissecting the mechanisms involved in the various pathways of mast cell activation.

The main aim of these experiments was to determine the possible role of NF-κB in mediating the effects of intracellular Zn on apoptosis in mast cells. It is known that both Zn and NF-κB are anti-apoptotic; therefore one would expect Zn to promote the activation of NF-κB. However, the opposite was found and further studies should explore the positive and negative interactions between these two factors.

# CHAPTER SEVEN

# SUPPRESSION OF CASPASE-3 ACTIVATION IN NEUROBLASTOMA CELLS BY INTRACELLULAR LABILE ZINC

## 7.1 Introduction

The preceding chapters have shown that labile Zn regulate apoptosis in mast cells. The aim of the experiments in this chapter was to confirm whether Zn regulate caspase activation in another cell type. For these experiments the BE(2)-C neuroblastoma cells were chosen. Firstly they were available in the laboratory. Secondly, studies with gene-knockout mice have shown caspase-3 to be important in regulating the number of neurons in the brain (Kuida, 1996). Thirdly, there are links between labile Zn, neuronal function, apoptosis and brain pathology. High concentrations of labile Zn have been found to be important for memory, cognition and behavior, and these functions are affected in moderate Zn deficiency (Golub, 1995). It is likely that the important pools of Zn in protection against premature apoptosis are the more labile (free or loosely bound) Zn. It has been suggested that deficiency in labile pools of Zn in the brain can increase apoptosis of neuronal cells (Anh, 1998). A study by the same group has demonstrated that Zn-depletion using the Zn chelator TPEN resulted in apoptosis in mouse cortical neurons (Anh, 1998). In Alzheimer's disease (AD), it has been reported that there is less Zn in the hippocampi of AD patients than those of normal individuals (Constatinidis, 1991; Cuajungco and Lees, 1997) and this may be one of the factors causing increased cell death in this region (Anderson, 1996; Smale, 1995).

In contrast, other studies have found that rapid and excessive influx of Zn into neurons can result in apoptosis *in vivo* and *in vitro* (Choi, 1988; Sheline, 2000; Weiss, 1993). Prolonged exposure of high concentrations of Zn at 20-80 μM or shorter exposure at 150-600 μM resulted in apoptosis of cortical neurons and cerebellar granule neurons

(Fraker and Telford, 1997; Manev, 1997; Yokoyama, 1986). Hence Zn seems to either have a beneficial or deleterious effect on neurons depending on its concentration and rate of influx.

Nuydens and colleagues described a cellular model of AD in which human neuroblastoma cells were induced by butyrate, to undergo essential protein synthesis leading to cytoskeletal alterations and apoptotic death (Nuydens, 1995).

Human neuroblastoma BE(2)-C cells were primed with butyrate for 18h to allow new gene expression to occur, and then further treated for up to 4 h with staurosporine or TPEN. This model was used to investigate the effect of varying intracellular Zn by treatment of cells with either a Zn chelator, TPEN to deplete labile Zn or a Zn ionophore, pyrithione to increase or supplement intracellular Zn. These pools were visualized using Zinquin. The main hypothesis being investigated in experiments described in this chapter is that changes in intracellular labile Zn influence the susceptibility of caspase-3 to be activated either spontaneously or in response to an apoptotic inducer.

## 7.2 Methods

Experiments were performed to determine the subcellular distribution of Zn and whether a correlation exists between varying levels of intracellular Zn and the activation of DEVD-caspase in human neuroblastoma BE(2)-C cells. These adherent cells are a continuously growing cell line developed from cells isolated isolated from bone marrow of a 22-month-old male with disseminated neuroblastoma (Biedler, 1978). Distribution of intracellular Zn was also determined in a more differentiated neuronal cell line, NIE-115. These cells form axon-like neurites when cultured in the presence of 2% DMSO for 10 days.

### 7.2.1 Zn Supplementation And Depletion Assays

Zn was increased in BE(2)-C cells by using varying concentrations of sodium pyrithione in the presence of 25 μM of exogenous $ZnSO_4$ for 3 h. Some cells were loaded with calcium using calcium ionophore A23187 (1 μM) for 3 h. Zn was decreased by treatment with TPEN for up to 4 h. Zn was visualized using Zinquin by both epi- fluorescence and confocal microscopy as discussed in 2.3.1.

### 7.2.2 Induction Of Apoptosis

In most experiments, BE(2)-C cells were primed with 1 mM butyrate and further treated for up to 4 h with either 1 μM staurosporine or 25 μM TPEN. In some experiments, cells were supplemented with Zn in the final 3 h. Measurement of DEVD-caspase activity was as described in section 2.3.2. DEVD-caspase activity is

expressed in the results as Units, where one Unit of DEVD-caspase activity is taken as one picomole of DEVD-AFC cleaved per h, per 50 μl of cell lysates. The amount of cleavage was determined using a standard curve with purified AFC. Apoptosis was also confirmed in randomly selected samples by morphological criteria and DNA fragmentation. All experiments were repeated at least three times.

### 7.2.4 Statistical Analysis

The results of typical experiments are described or data were pooled, as indicated in text. Statistical significance was determined by the student *t*-test and the Tukey-Kramer multiple comparisons test where appropriate.

## 7.3 Results

### 7.3.1 Distribution Of Labile Zn In Neuroblastoma Cells

Levels of labile Zn in these cells were increased or decreased following additions of Zn ionophore, pyrithione or chelator, TPEN respectively. Labile intracellular Zn was visualized in viable BE(2)-C cells using Zinquin (Figure 7.1). Figure 7.1A-C shows typical pseudo-coloured images of the levels of Zn in BE(2)-C cells obtained by epifluorescence microscopy. TPEN-treated BE(2)-C cells (panel A) had minimal fluorescence compared with the basal fluorescence in untreated cells (panel B). A marked increase in fluorescence was seen when cells were treated with $ZnSO_4$+ pyrithione (panel C). Panels C and D-E (confocal images) show the strong cytoplasmic and perinuclear Zinquin fluorescence in the Zn-loaded cells. Some fluorescence was observed in pseudopodia (Figure 7.1E).

Since neuroblastoma cells are undifferentiated and do not resemble neurons, the distribution of labile Zn in more differentiated neuronal cells was studied. It was not possible to induce differentiation in BE(2)-C cells and therefore the NIE-115 cell line was used. Differentiation of this cell line was induced by DMSO (Kimhi, 1976). Zinquin fluorescence was investigated without further addition of exogenous Zn. Typical cells are shown in panel F. There was little fluorescence in the cell body except for the golgi region (upper panel F), while there was strong fluorescence (green-red) in the neurite with an apparent cytoskeletal distribution (lower panel F). At the foot of the neurite, there was also intense fluorescence, which may correspond to Zn-rich presynaptic vesicles.

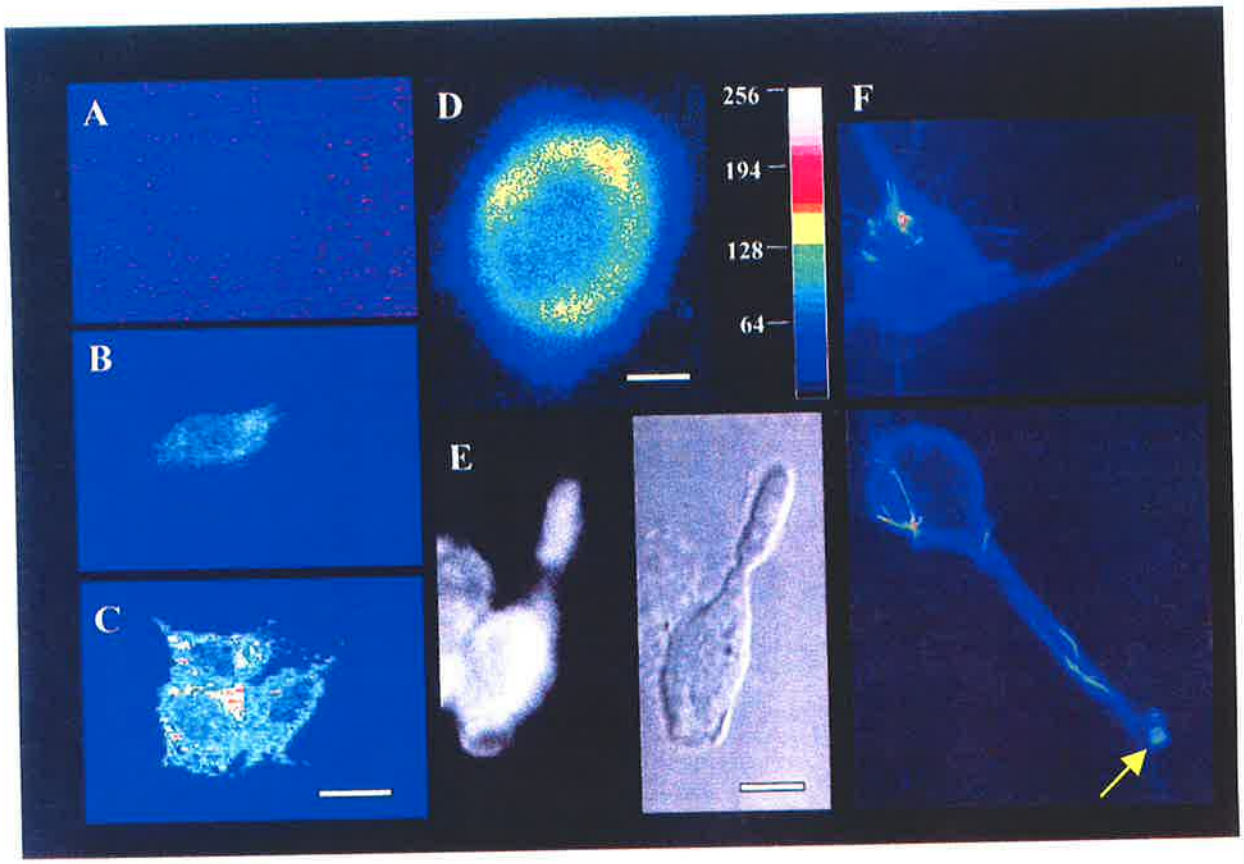


**Figure 7.1**

**Figure 7.1: Visualisation of intracellular Zn in neuroblastoma cells.**

(A-C): Pseudo-coloured images of Zn-dependent Zinquin fluorescence in BE(2)-C cells determined by epi-fluorescence microscopy. Cells were pretreated (as indicated below) for 60 min before addition of Zinquin. Typical cells are shown. Scale bar in C indicates 12 μm and applies for A-C.

(A) 25 μM TPEN (Zn-deficient).

(B) No pre-treatment (basal Zn level). One cell is shown.

(C) 25 μM $ZnSO_4$ + 4 μM pyrithione (Zn-loaded). A clump of three cells is shown.

(D-F): UV-laser confocal microscopy. (D, E) Confocal image of Zn-loaded BE(2)-C cells showing cytoplasmic fluorescence. D is a pseudo-coloured image, with vertical wedge showing the linear relationship between pseudo-colour and fluorescence intensity. E shows real fluorescence on the left panel and bright field image of the same cell on the right panel. Scale bars indicate 5 μm in D and 10 μm in E.

(F): Pseudo-coloured images of DMSO-differentiated NIE-115 cells, showing the basal fluorescence pattern. Upper panel show strong fluorescence in the Golgi region, lower panel shows an apparent cytoskeletal pattern of fluorescence and fluorescence labelling at the foot of the neurite (yellow arrow) that may represent presynaptic vesicles. Scale bar for F is shown in E and indicates 8 μm.

### 7.3.2 Effect Of Depleting Intracellular Zn In BE(2)-C Cells On DEVD-Caspase Activation

Firstly, the effects of Zn depletion using TPEN on DEVD-caspase activation were determined. Results are expressed as mean of triplicates ± SEM. When BE(2)-C cells were treated for 4 h with 25 μM TPEN, DEVD-caspase activity increased from 8.0 ± 0.2 Units to 32.2 ± 1.5 Units ($P<0.005$); Therefore, depletion of Zn by itself induces a modest increase in caspase activity.

Activation of DEVD-caspase by 25 μM TPEN was associated with morphological changes of apoptosis. Typical morphological features included presence of one or more intracellular apoptotic bodies, granularity that was often localized to one pole of the cell, exclusion of the vital dye trypan blue, membrane blebbing and, in some cells, reduction in volume.

### 7.3.3 DEVD-Caspase Activity In BE(2)-C Cells Treated With Butyrate Plus Staurosporine

Figure 7.2 shows a significant but modest increase in DEVD-caspase activity when BE(2)-C cells were treated overnight with butyrate alone (blue diamonds). Compared to untreated BE(2)-C cells which had a cytosolic DEVD-caspase activity of 11.2 ± 0.6 Units, cells treated with 1 mM butyrate had 38.1 ± 2.6 (Units, $P<0.005$), those with 2mM butyrate had 91.6 ± 4.5 Units and those with 4mM butyrate had 113.2 ± 10.3 Units ($P<0.005$). DEVD-caspase activity plateau at 2 mM butyrate with significance at 4 mM.

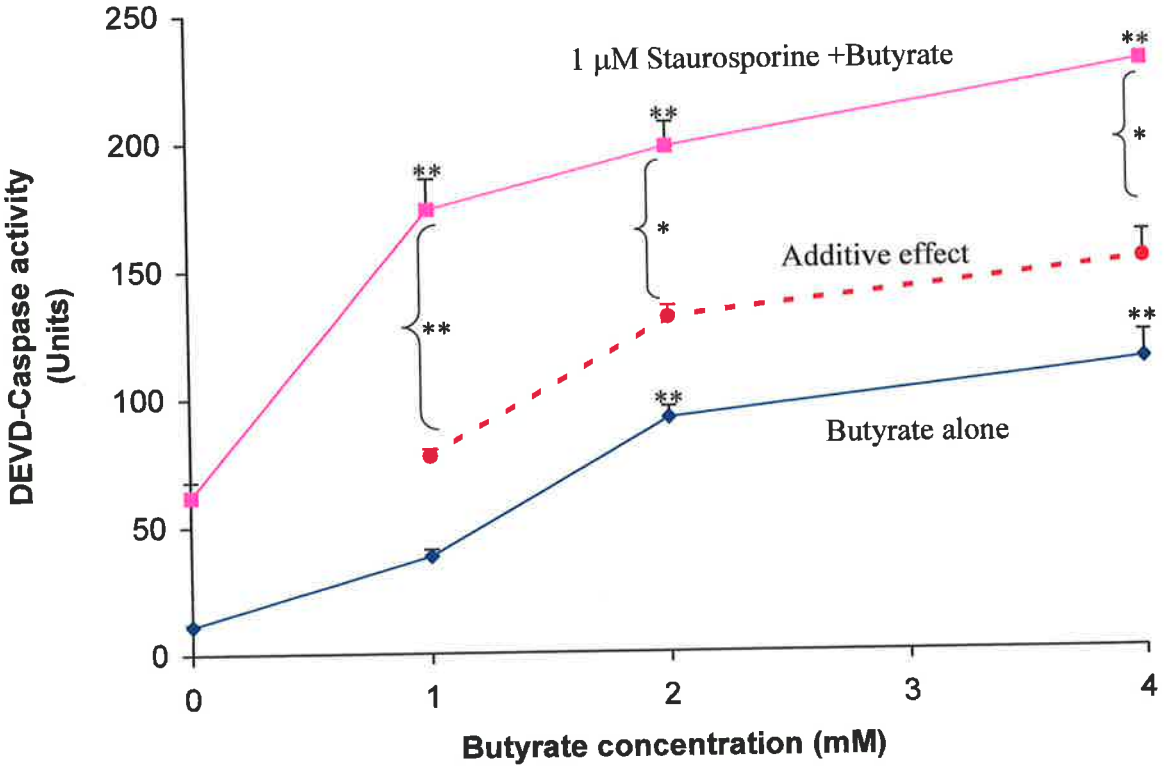
250
200
150
100
50
0
DEVD-Caspase activity (Units)
1 μM Staurosporine +Butyrate
Additive effect
Butyrate alone
**
*
0
1
2
3
4
Butyrate concentration (mM)

**Figure 7.2**

**Figure 7.2: Interaction between butyrate and staurosporine in activation of DEVD-caspase.**

Subconfluent monolayers of BE(2)-C cells in wells were treated for 18 h with the indicated concentration of butyrate before further culture for 3 h in the absence (♦) or presence (■) of 1 μM staurosporine. Floating cells were then collected and lysed together with adherent cells to yield total cell lysates, which were assayed for DEVD-caspase activity. Data are expressed as Units of activity per 50 μl of lysates ($4 \times 10^5$ cells). Bars indicate SEM for means of triplicates. Statistical significances are indicated as * $P<0.05$ and ** $P<0.005$ for comparisons with 0 butyrate conditions.

If butyrate and staurosporine act additively, the expected values for a combination of the two are indicated (-●-). Statistical significances between the expected values and the observed values are shown by the brackets and * $P<0.05$ and ** $P<0.005$. The figure shows synergy between the two toxins, especially at 1mM butyrate.

There were also increases in DNA fragmentation. Results are expressed as mean of triplicates ± SEM. Untreated cells (control) had 2.1 ± 0.7 μg/ml of cleaved DNA per mg of protein, cells treated with 1 mM butyrate had 7.5 ± 3.5 ($P < 0.05$), cells treated with 2 mM butyrate had 7.5 ± 2.6 ($P=0.06$) and cells treated with 4 mM butyrate had 8.2 ± 3.0 ($P=0.06$).

Before studying the effects of butyrate priming on TPEN-induced DEVD-caspase activation in BE(2)-C cells, staurosporine was used in combination with butyrate. When BE(2)-C cells were treated with 1 μM staurosporine alone, there was also a moderate increase in DEVD-caspase activity to 61.8 ± 5.9 Units ($P<0.005$). A much greater activation of DEVD-caspase occurred when BE(2)-C cells were treated with a combination of 1 mM butyrate and 1 μM staurosporine yielding 173.7 ± 12.1 Units ($P<0.005$) (Figure 7.2, pink squares). In the presence of 1 μM staurosporine, 2mM butyrate gave 197.7 ± 9.5 Units ($P<0.005$) and 4mM butyrate gave 229.7 ± 1.7 Units ($P<0.005$). These were all significantly greater than the additive effects of butyrate and staurosporine alone (Figure 7.2, red dashed line).

### 7.3.4 Adherent Versus Non-Adherent Cells

BE(2)-C are typically adherent cells and detach from the culture plate as a result of apoptosis. Therefore there are two populations of cells to consider, the floating (non-adherent) cells and the remaining adherent cells. To determine whether the increase in caspase activity was in both the adherent and non-adherent cells, DEVD-caspase activity was measured in the two populations of cells. Figure 7.3 shows that there was

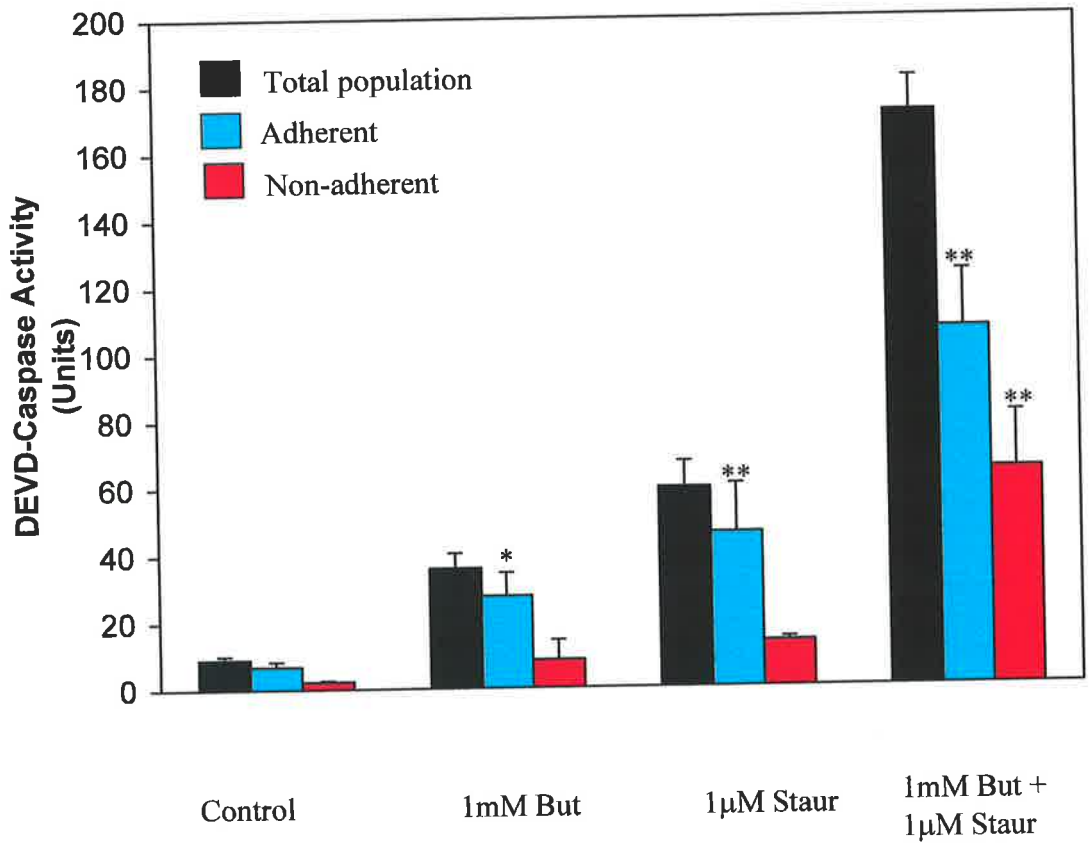
DEVD-Caspase Activity (Units)
200
180
160
140
120
100
80
60
40
20
0
Total population
Adherent
Non-adherent
*
**
**
Control
1mM But
1μM Staur
1mM But + 1μM Staur

**Figure 7.3**

**Figure 7.3: DEVD-caspase activity in adherent and non-adherent populations.**

Treatments for BE(2)-C cells were as in 3.2 except that in addition to assay of total cell population for DEVD-caspase activity (black columns), the adherent populations (blue columns) and non-adherent populations (red columns) were assayed individually. Black columns were determined by summing the mean values for the adherent and non-adherent populations. Bars indicate SEM for means of triplicates and significance is expressed as * $P<0.05$ and ** $P<0.005$. Comparisons are with the control values of corresponding adherent and non-adherent populations. The figure shows activation of DEVD-caspase in both populations, but more in the adherent cells. Abbreviations include But: butyrate and Staur: staurosporine.

an increase in DEVD-caspase activity in the total cell populations (black columns), as well as in both adherent (blue columns) and non-adherent populations (red columns). This is consistent with the onset of DEVD-caspase activity occurring before detachment of the cells from the plates. DEVD-caspase activity was significantly higher in both adherent and non-adherent populations treated with 1 mM butyrate and 1 μM staurosporine with 85.8 ± 10.2 Units compared to control of 4.5 ± 1.0 Units ($P<0.005$).

### 7.3.5 The Effect Of Priming With Butyrate On Induction Of DEVD-Caspase Activity By TPEN

Having established that BE(2)-C cells respond better to an apoptotic inducer staurosporine following overnight priming with butyrate, it was determined next whether they would also respond better to TPEN following overnight priming with butyrate. Figure 7.4 shows that this was the case. 1 mM butyrate alone gave 17.2 ± 0.5 Units of DEVD-AFC caspase activity, TPEN alone gave 32.2 ± 1.5 Units while a combination of 25 μM TPEN and 1 mM butyrate (yellow columns) resulted in 100.4 ± 8.1 Units ($P<0.005$). This was more than the additive effect shown by the dashed line in Figure 7.4. Similar synergy was seen between 4 mM butyrate and TPEN (red columns, $P<0.005$) thus indicating a higher concentration of butyrate also increases the effects of TPEN. This is similar to the effects observed with a combination of 1 μM Staurosporine and 1 or 4 mM butyrate (Figure 7.4). Thus, a combination of 1 μM staurosporine and 1 mM butyrate resulted in a significant increase in DEVD-AFC caspase activity from 21.2 ± 1.6 Units to 82.5 ± 4.9 Units ($P<0.005$) and to 122.2 ± 6.4

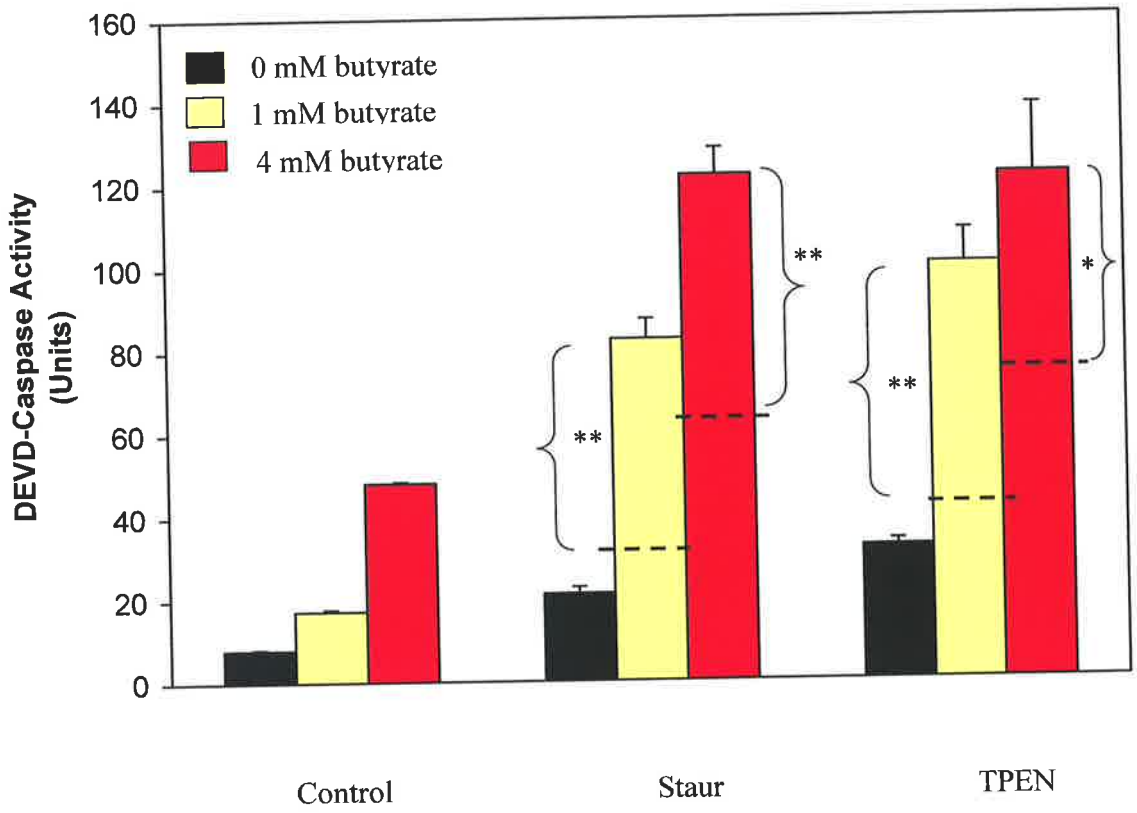
160
140
120
100
80
60
40
20
0
DEVD-Caspase Activity (Units)
0 mM butyrate
1 mM butyrate
4 mM butyrate
**
**
**
*
Control
Staur
TPEN

**Figure 7.4**

**Figure 7.4: Interactions between butyrate and staurosporine or TPEN on DEVD-caspase activation.**

BE(2)-C cells were cultured for 18 h with 0 (black columns), 1 (yellow columns), or 4 (red columns) mM butyrate and then for a further 4 h in the absence or presence of 1 μM staurosporine or 25 μM TPEN. Bars indicate SEM for means of triplicates.

If butyrate and staurosporine or TPEN act additively, the expected values for a combination of the two are indicated by dashed lines. Statistical significances between the expected values and the observed values are shown by the brackets and * $P<0.05$ and ** $P<0.005$. The figure shows synergy between butyrate and staurosporine (at both concentrations of butyrate) and between butyrate and TPEN (also at both concentrations of butyrate).

Units in cells treated with 4 mM butyrate ($P<0.005$). Therefore TPEN acts in a similar way to staurosporine in its synergy with butyrate.

The effect of TPEN was very similar to that caused by staurosporine. In agreement with this, a combination of TPEN and staurosporine had a less than additive rather than synergistic effect on DEVD-caspase activity. For example in cells treated with 25 μM TPEN alone, DEVD-caspase activity was 24.6 ± 2.2 Units, in cells treated with staurosporine alone had 73.1 ± 6.0 Units and cells treated with a combination of staurosporine and TPEN had 70.0 ± 6.6 Units.

### 7.3.6 Time Course Of TPEN Effects On DEVD-Caspase Activity In Butyrate-Primed BE(2)-C Cells

The time course of TPEN effect was then determined to establish how quickly Zn depletion acts. BE(2)-C cells were primed for 18h with 1 mM butyrate and then 25 μM or 50 μM TPEN were added and DEVD-caspase activity was measured at intervals up to 250 min (Figure 7.5). In butyrate-primed cells treated with either 25 or 50 μM TPEN, activity increased rapidly beginning about 50-100 min after the addition of TPEN and increasing up to 250 min. It is interesting that the effect of 25 μM TPEN (black squares) was similar to that of 50 μM TPEN (red triangles) and suggests that this concentration achieves a maximal effect. By contrast, 50 μM TPEN alone (no butyrate priming, blue circle) had a much greater effect than 25 μM TPEN alone (red circle). Therefore priming cells with butyrate makes TPEN much more effective.

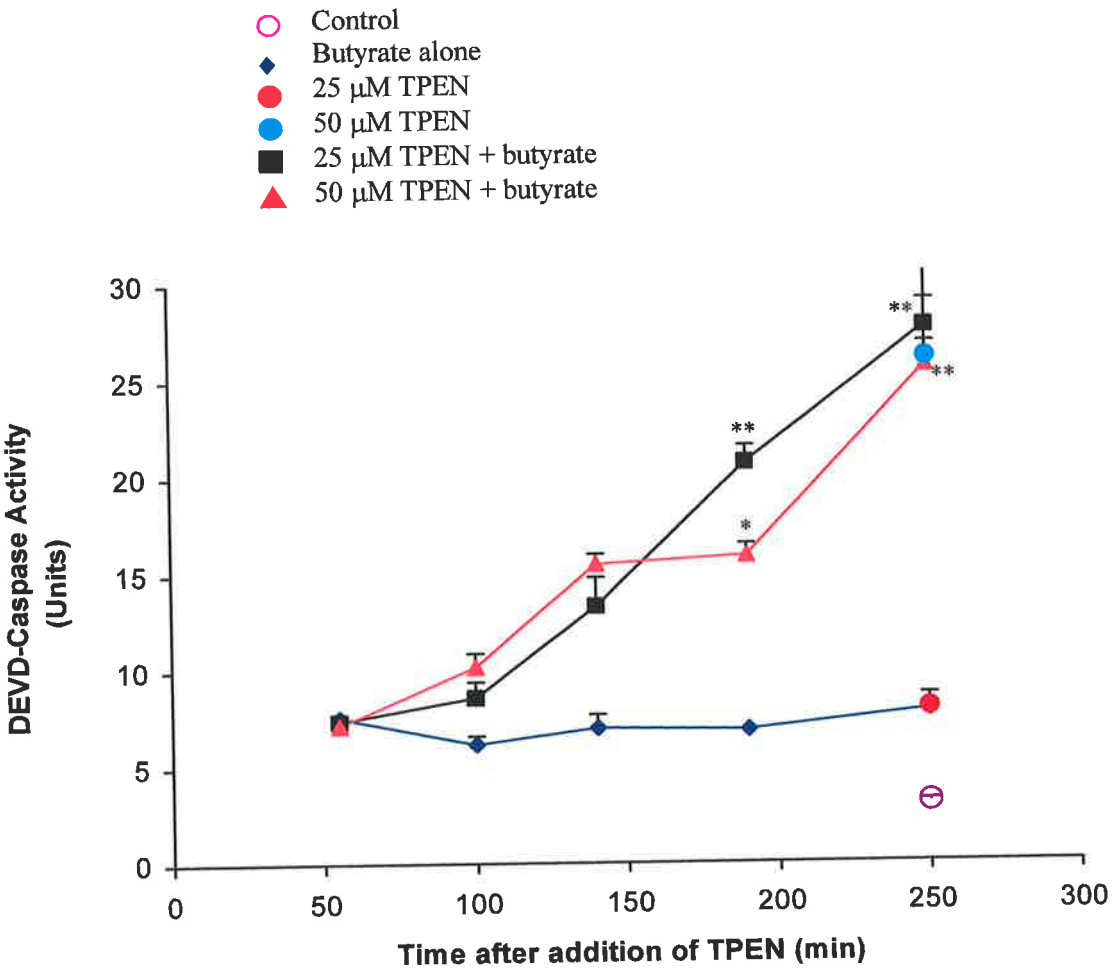
Control
Butyrate alone
25 μM TPEN
50 μM TPEN
25 μM TPEN + butyrate
50 μM TPEN + butyrate
DEVD-Caspase Activity (Units)
Time after addition of TPEN (min)
0
5
10
15
20
25
30
0
50
100
150
200
250
300
**
**
*
**

**Figure 7.5**

**Figure 7.5: Time course for action of TPEN.**

BE-(2)-C cells were cultured for 18 h with or without 1 mM butyrate (time 0) and then for up to a further 250 min in the absence or presence of 25 μM or 50 μM TPEN: Control (○), butyrate alone (♦), 25 μM TPEN alone (●), 50 μM TPEN alone (●), butyrate + 25 μM TPEN (■) and butyrate + 50 μM TPEN (▲). DEVD-caspase activity represents means of triplicates; bars indicate SEM. Statistical significances are indicated as * $P<0.05$ and ** $P<0.005$ for comparisons with 1 mM butyrate at 55 min (baseline for this experiment). The figure shows strong synergy between butyrate and TPEN, with onset of DEVD-caspase activity after a lag-phase of 100 min.

### 7.3.7 Effects Of Zn Supplementation With Pyrithione On DEVD-Caspase Activity In BE(2)-C Cells

Since decreasing intracellular labile Zn promotes DEVD-caspase activation, the effect of increasing intracellular labile Zn was also determined. To induce apoptosis, BE(2)-C cells were treated with a combination of butyrate and staurosporine as in the previous experiment. To increase intracellular labile Zn, cells were treated with 25 μM $ZnSO_4$ plus 4 μM pyrithione added during the final 3 h (Figure 7.6).

An increase in intracellular Zn strongly suppressed induction of DEVD-caspase activity by a combination of 1mM butyrate and 1μM staurosporine resulting in only 13.3 ± 0.6 Units (Figure 7.6 Zn-loaded cells - red column) compared to 187.7 ± 0.7 Units in cells treated with a combination of butyrate and staurosporine without added Zn ($P<0.005$) (unloaded cells - red column). This was also seen in cells treated with staurosporine where DEVD-caspase activity decreased from 73.1 ± 5.9 Units to 9.0 ± 0.6 Units ($P<0.005$), and in cells treated with 1 mM butyrate where it decreased from 24.9 ± 2.1 Units to 16.5 ± 1.6 Units ($P<0.05$).

By contrast, in cells loaded with calcium using the calcium ionophore A23187, there was no effect on induction of DEVD-caspase activity (Figure 7.6 calcium loaded cells). There was no change from the pattern given by the unloaded cells. Therefore the effect of Zn was not due to a general divalent cation effect.

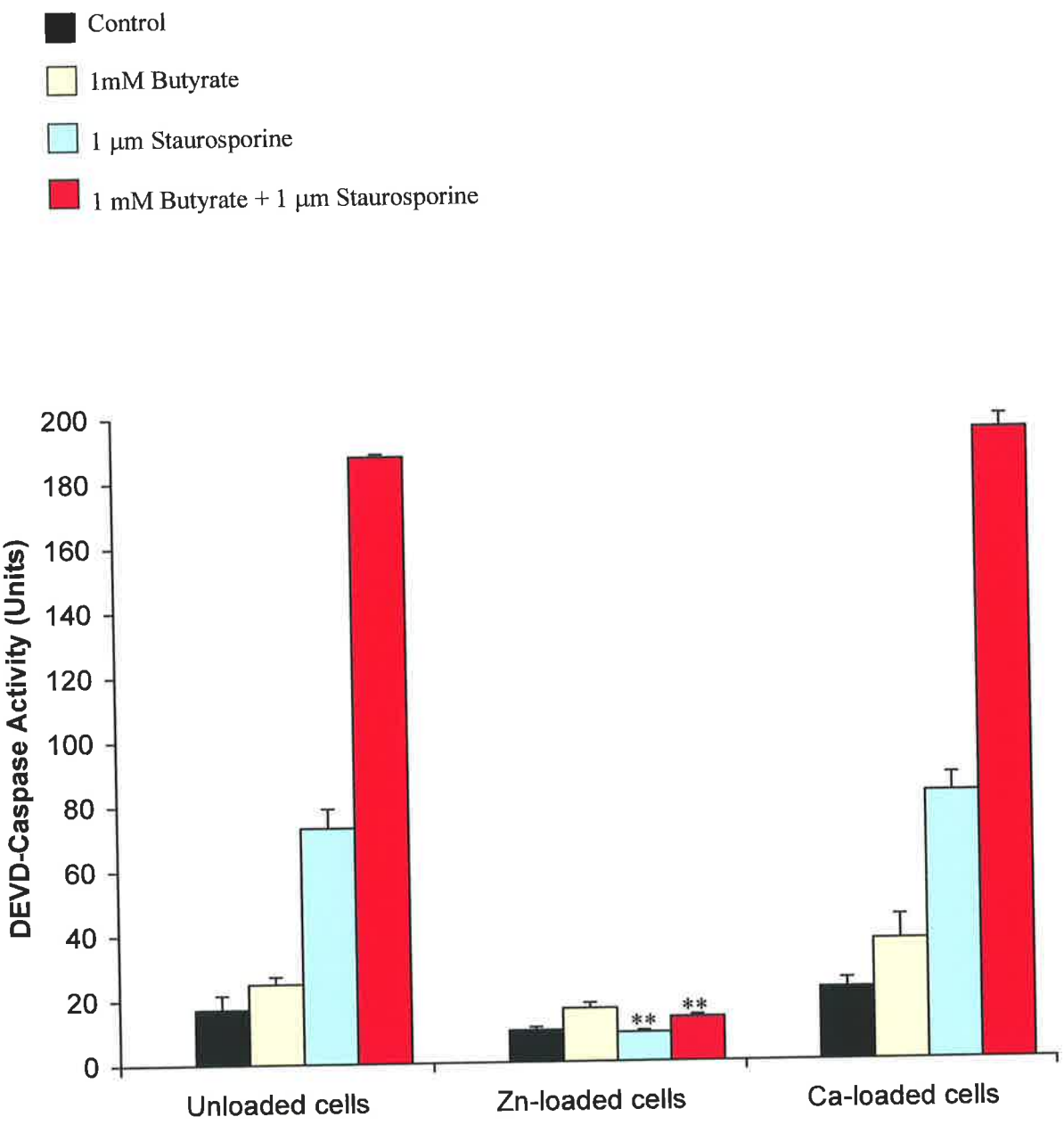
Control
1mM Butyrate
1 μm Staurosporine
1 mM Butyrate + 1 μm Staurosporine
DEVD-Caspase Activity (Units)
200
180
160
140
120
100
80
60
40
20
0
**
**
Unloaded cells
Zn-loaded cells
Ca-loaded cells

**Figure 7.6**

**Figure 7.6: Effect of increasing intracellular Zn on activation of DEVD-caspase by butyrate and staurosporine.**

Effect of increasing $[Zn^{2+}]_i$ on activation of DEVD-caspase. BE(2)-C cells were treated for 18 h without butyrate or staurosporine (black columns), with 1mM butyrate (yellow columns), with 1μM staurosporine for the final 3 h (blue columns) or with butyrate plus staurosporine (red columns). In the final 3 h cells were also treated with 25 μM TPEN (TPEN-loaded cells), 25 μM $ZnSO_4$ + 4 μM pyrithione (Zn-loaded cells), with 1 μM A23197 (Ca loaded cells) or no further addition (unloaded cells). Calcium was not added with A23187 because the medium already contains 0.6 mM Ca salts. DEVD-caspase activity represents means of triplicates and bars indicate SEM.

Significance is expressed as * $P<0.05$ and ** $P<0.005$ for comparisons between corresponding columns of Zn-loaded or Ca-loaded cells to those of unloaded cells. For example the red columns in the Zn-loaded and Ca-loaded cells are compared with the red column in the unloaded cells. The figure shows suppression of DEVD-caspase activation when cells were loaded with but not calcium, irrespective of whether caspase was activated by butyrate alone, staurosporine alone or a combination of butyrate and staurosporine.

### 7.3.8 Concentration Dependence Of Pyrithione

To determine whether pyrithione acts in a concentration dependent manner, BE(2)-C cells were treated with a combination of butyrate and staurosporine in the presence of varying concentrations of pyrithione (0.2 μM to 5 μM) and a fixed concentration of exogenous $ZnSO_4$ (25 μM, Figure 7.7). The increase in DEVD-caspase activity was completely suppressed with higher concentrations of pyrithione (1.25 μM to 5 μM) decreasing it from 56.7 ± 1.2 Units to 5.1 ± 0.3 Units. Lower concentrations of pyrithione had partial inhibitory effects with 50% inhibition of DEVD-caspase activation occurring with about 1 μM pyrithione (Figure 7.7).

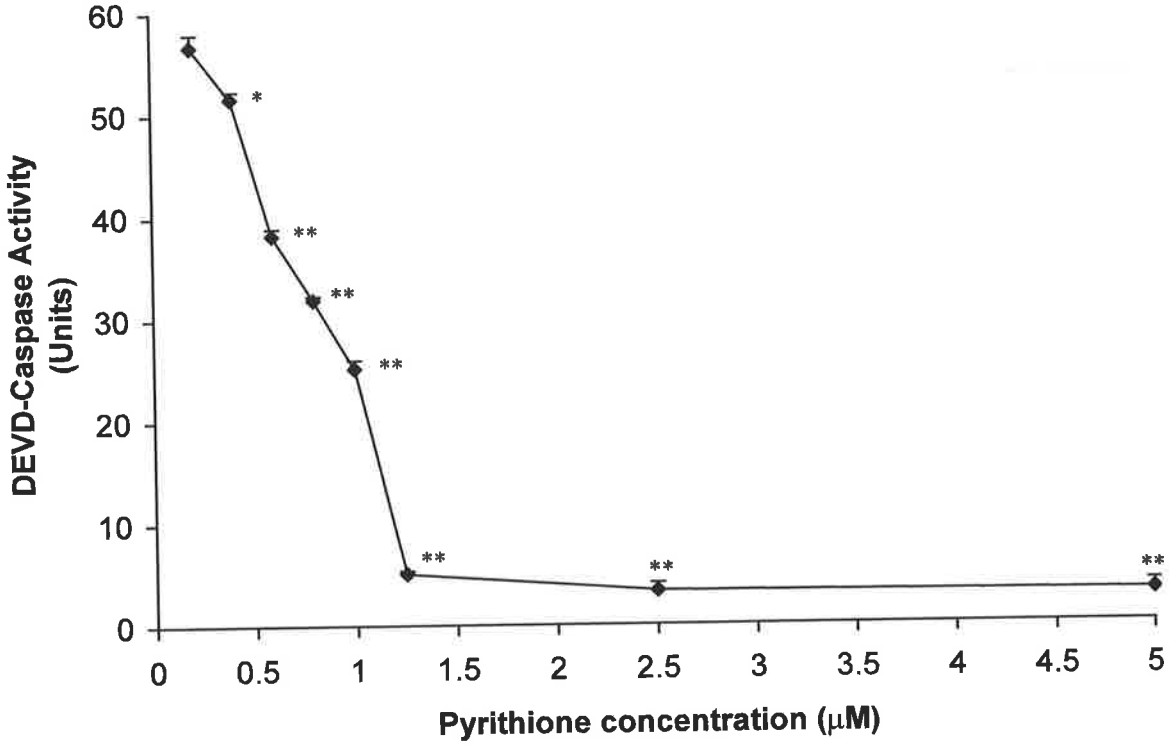
DEVD-Caspase Activity (Units)
60
50
40
30
20
10
0
*
**
**
**
**
**
**
0
0.5
1
1.5
2
2.5
3
3.5
4
4.5
5
Pyrithione concentration (μM)

**Figure 7.7**

**Figure 7.7: Concentration dependence of pyrithione effect.**

Cells were treated with a combination of butyrate and staurosporine (as in Figure 7.6) and 25 μM $ZnSO_4$ plus varying concentrations of pyrithione during the final 3 h. Bars indicate SEM for means of triplicates. Statistical significances are indicated as * $P<0.05$ and ** $P<0.005$ for comparisons with cells receiving butyrate and staurosporine but no pyrithione. The figure shows concentration-dependent suppression of DEVD-caspase activation.

## 7.4 Discussion

The main findings of the experiments reported in this chapter are: 1) BE(2)-C cells have cytoplasmic/cytoskeletal pools of intracellular labile Zn which can be further increased by Zn ionophore or decreased by Zn chelator TPEN, 2) depletion of this Zn by itself had only a moderate effect on DEVD-caspase activity, 3) priming the cells with butyrate greatly increased their susceptibility to caspase activation by TPEN or staurosporine, 4) in butyrate primed cells, TPEN depletion of Zn had a rapid effect on caspase-3 activation, and 5) increasing intracellular Zn, but not calcium suppressed activation of DEVD-caspase.

A strong synergy for the activation of DEVD-caspase and induction of apoptosis in BE(2)-C cells occurred at various concentrations of butyrate (1 – 4 mM) and 1 μM staurosporine. Staurosporine is known to trigger apoptosis and caspase-3 by direct effects on the cell cytoplasm that involved changes in mitochondrial membrane potential and Bcl-2 regulation and which are independent of new gene expression (Kluck, 1997). Although the action of butyrate is not well understood, it is known to inhibit histone deacetylase causing histone hyperacetylation and a more relaxed chromatin state which leads to new gene expression (Boffa, 1978). One or more of these new genes may prime cells to undergo apoptosis. If butyrate and staurosporine act via different pathways they are likely to act synergistically. This was found to be the case. The synergy between TPEN and butyrate may suggest TPEN also acts via a distinct pathway. The additive effects of TPEN and staurosporine together may indicate a common pathway, although in one case mediated by Zn depletion and the other by protein kinase inhibition.

Interestingly, calcium ionophore alone did not induce apoptosis of these cells nor was there synergy between calcium ionophore A23187 and butyrate. These results are in contrast to other studies that have reported A23187 to be an effective inducer of neuronal cell death. For example, A23187 has been shown to induce apoptosis in a time and concentration-dependent manner in PC12 cells and primary cortical neurons by causing an increase in intracellular calcium leading to protein synthesis, prolonged c-Fos expression and activation of p53 (Gwag, 1999; Vyas, 2002). A possible explanation would be that BE(2)-C cells do not undergo the same response following the rise in calcium ions. In addition, calcium did not mimic the effects of Zn in suppressing DEVD-caspase activation in the BE(2)-C cells.

In order to confirm apoptosis, DNA fragmentation was measured in some of the experiments. However, recently doubts have been cast on the validity of DNA fragmentation and it has largely been superseded by more efficient and sensitive techniques, in particular the cleavage of fluorogenic substrates of effector caspases. The fact that DEVD-caspase activity did not parallel DNA fragmentation results further indicates the inherent problems in DNA fragmentation assay. For example while caspase activity increased in proportion to the concentration of butyrate (Figure 7.2), the DNA fragmentation reached a plateau at 1 mM butyrate but did not increase further. The experiments on apoptosis of BE(2)-C cells were performed at an early stage of this thesis when the Hoechst dye technique for staining fragmented chromatin was not available.

The importance of Zn homeostasis in the regulation of apoptosis was confirmed from results of Zn supplementation experiments via the addition of $ZnSO_4$ and pyrithione. This further confirms other results from studies that were performed after this project commenced. These have shown that Zn prevents apoptosis by being a potent inhibitor of caspase-3 activation (Chai, 2000; Perry, 1997). However, excessive amounts of Zn are known to cause apoptosis in neuronal cells (Choi, 1988). It would only be beneficial to maintain intracellular Zn within a certain concentration range required for proper regulation of apoptosis in cells.

Others have estimated that, in general, the intracellular free Zn concentrations are in the picomolar to nanomolar range (Frederickson, 1989). The levels of Zn in neuroblastoma cells need to be determined in order to fully understand the significance of the TPEN and pyrithione experiments. In the experiments reported in this chapter, no attempt was made to quantify intensities of Zinquin fluorescence since at the time these experiments were performed, an appropriate image analysis system was not available in the laboratory. It is not possible at this stage to determine actual free Zn concentrations from the Zinquin fluorescence intensities, since it is difficult to construct a set of appropriate standards containing different intracellular Zn concentrations that would enable accurate measurements to be made.

Fluorescence images of Zinquin-loaded neuroblastoma cells revealed a paucity of nuclear labile Zn. Although Zn is expected to be abundant in the transcription factors and nucleic acid synthesizing enzymes, this Zn is tightly bound and unlikely to be available for Zinquin binding. It is unlikely that Zinquin is excluded from the nuclear compartment, since Zinquin labels Zn in other membrane bound organelles (Zalewski,

1994). Zinquin fluorescence at the neurite terminal may represent a vesicular pool of Zn analogous to the Zn-rich secretory vesicles in the presynaptic terminals of certain neurons (Frederickson, 1989).

Localization of Zinquin-stainable Zn in the cytoskeleton of neuroblastoma cells agrees with the destabilization of the microtubular cytoskeleton by Zn deprivation. In marginally Zn-deficient rats, brain Zn concentration was decreased accompanied by microtubular destabilization and tubulin polymerization; this was normalized following addition of Zn to the brain extracts (Nickolson and Veldstra, 1972; Oteiza, 1990). The microtubules are disrupted not only in Zn deficiency, but also in apoptosis where rearrangement of the microtubule is an early process (Wang, 1999). The microtubular cytoskeleton is also disrupted in AD and infusion of colchicine (microtubule toxin) into the hippocampi of rats resulted in similar alterations to those in AD (Nakagawa, 1987). These findings may have implications for AD, a disease in which there is excessive apoptosis in neurons and abnormalities in Zn homeostasis (Anderson, 1996; Constatinidis, 1991; Smale, 1995).

Zinquin also stained Zn in a pattern that resembles the golgi apparatus. This is interesting because the golgi is involved in post-translational modification of proteins and in packaging of secretory granules. Golgi Zn may be incorporated into metallopoteins and also into secretory granules.

It is still not clear whether Zn has a beneficial role (Basun, 1991; Constatinidis, 1991; Licastro, 1996; Prasad, 1993; Sandstead, 1991) or deleterious role (Bush, 1994; Danscher, 1997; Loo, 1993) on neurons. An age-associated tissue deficiency of Zn is

likely to be compounded in the brains of AD patients by sequestration of Zn within amyloid plaques (Bush, 1994) and displacement of Zn by other metals such as aluminium and lead (Shea, 1997). Intracellular neurofibrillary tangles, a hallmark of AD, may represent a cytoskeletal disturbance in a subset of neurons undergoing apoptosis. Since both Zn ions and tau (membrane associated protein) bind to tubulin and stabilize microtubules (Nickolson and Veldstra, 1972; Serrano, 1988; Yankner, 1996), tau phosphorylation and Zn deficiency may have similar effects on the cytoskeleton at the neuropathological level. Zn promotes noncovalent interaction between S100b and tau, resulting in total inhibition of tau phosphorylation by $Ca^{2+/}$calmodulin-dependent protein kinase II (Baudier and Cole, 1988). Zn supplementation may be beneficial in AD especially if commenced early to maintain adequate intracellular Zn levels. There is however a greater need to understand the mechanism of apoptosis in neuronal cells and the role of Zn deficiency in AD. The mechanism of apoptosis in neuronal cells and effects of Zn deficiency needs further study in relation to brain pathologies such as AD.

A two-stage model is proposed for the activation of DEVD-caspase by butyrate and Zn depletion (Figure 7.8). In stage I: some toxins (e.g. butyrate) induce expression of a pro-apoptotic protein, which triggers changes in neuronal vulnerability. In stage II: a Zn-deficient environment (achieved by depleting tubulin-bound Zn) destabilizes the cytoskeleton and thereby renders the neuron more susceptible to cytoskeletal damage. Since Zn appeared to be in the cytoskeleton of the differentiated neuroblastoma cells and Zn is known to stabilize the cytoskeleton (Nakagawa, 1987; Nickolson and Veldstra, 1972), TPEN may trigger apoptosis via destabilization of the cytoskeleton. Staurosporine had an effect similar to TPEN although this is a protein kinase C (PKC)

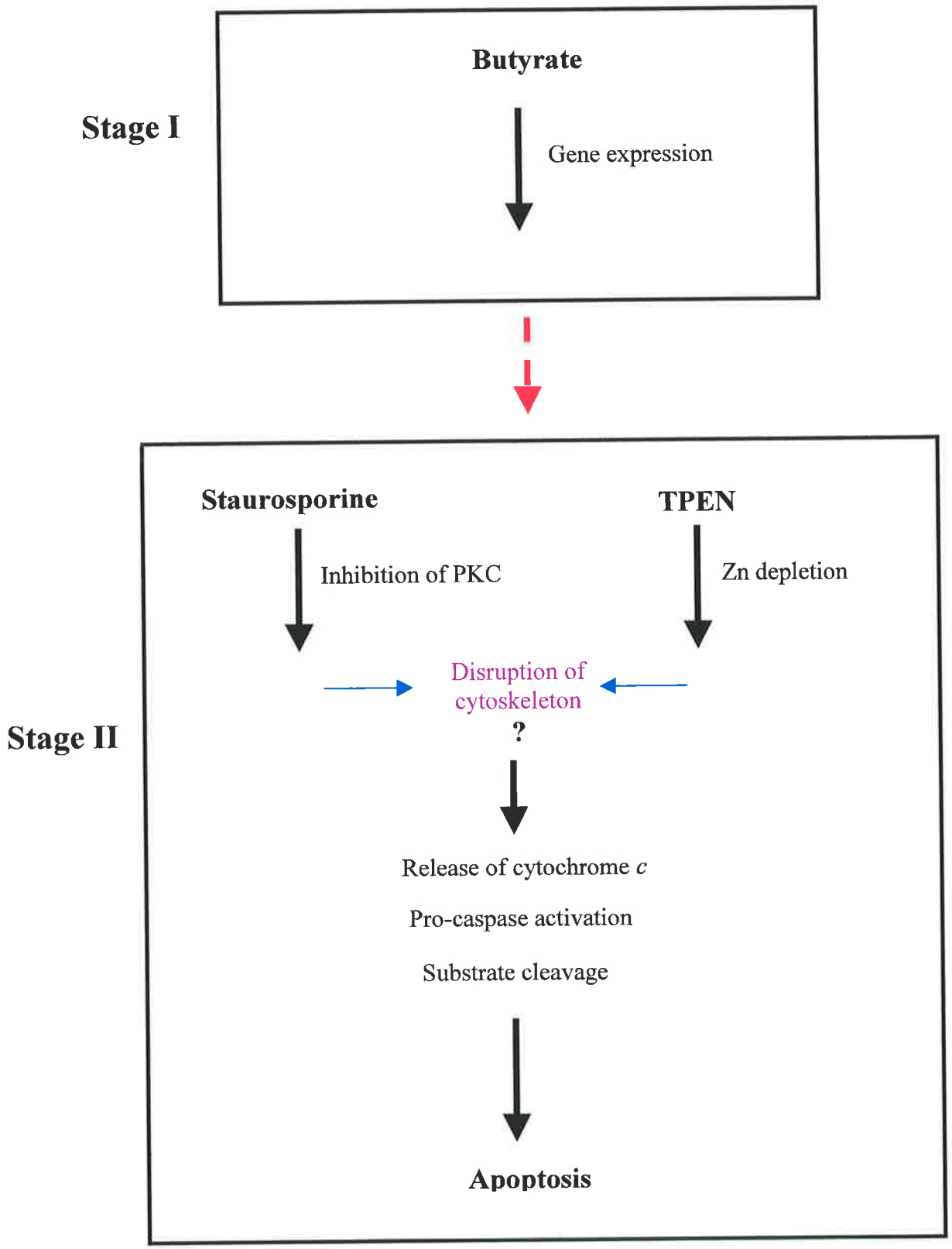
Stage I
Butyrate
Gene expression
Stage II
Staurosporine
Inhibition of PKC
TPEN
Zn depletion
Disruption of cytoskeleton
?
Release of cytochrome c
Pro-caspase activation
Substrate cleavage
Apoptosis

**Figure 7.8**

**Figure 7.8: Two-stage model of interaction between butyrate and Zn depletion.**

Figure shows a two-stage model for the activation of DEVD-caspase and apoptosis by butyrate and either Zn depletion or protein kinase inhibition. In stage I: butyrate induces expression of a pro-apoptotic protein, which predisposes the cells to a further apoptotic inducer. In stage II: disruption of the cytoskeleton is proposed to trigger downstream events of apoptosis. One mechanism is via TPEN induced Zn-depletion, since Zn is known to stabilize the cytoskeleton. Another mechanism is via the inhibition of protein kinase C caused by agents like staurosporine. Staurosporine is also known to cause disruption of the cytoskeleton. Disruption of the cytoskeleton then initiates a cascade of events involving sequentially the release of cytochrome *c* from the mitochondria into the cytosol, the proteolytic conversion of pro-caspases to their active forms, cleavage of critical proteins and cellular fragmentation into apoptotic bodies.

inhibitor. Staurosporine is also known to cause disruption of the cytoskeleton (Nishi, 2002). Disruption of the cytoskeleton can initiate a cascade of events involving sequentially the release of cytochrome *c* from the mitochondria into the cytosol (Kolenko, 2001), the proteolytic conversion of pro-caspases to their active forms, cleavage of critical proteins and cellular fragmentation into apoptotic bodies.

The experiments reported in this chapter suggest intracellular labile Zn as a critical factor in determining susceptibility of neuronal-like cells to toxin-induced activation of a major cell-death inducing protease. One limitation of these experiments is that malignant neuroblastoma cells were used and these experiments need to be confirmed in primary neurons. These results also confirm some of the findings made with mast cells. In particular Zn depletion was potently synergistic with butyrate in inducing caspase-3 activation.

Some findings in this chapter have been published in Ho et al titled: Involvement of Intracellular Labile Zinc in Suppression of DEVD-Caspase Activity in Human Neuroblastoma Cells. Biochemical and Biophysical Research Communications, Volume 268, pages 148-154. 2000.

# CHAPTER EIGHT

# GENERAL DISCUSSION AND FUTURE STUDIES

## 8.1 Introduction

Previous studies from our laboratory and others have shown that Zn regulates apoptotic DNA fragmentation and morphological changes of apoptosis in lymphocytes and various cancer cell lines. The major aim of this thesis was to determine whether there was a relationship between Zinquin-detectable intracellular pools of labile Zn and caspase activation since caspases have now been shown to be important effector enzymes in apoptosis. This was largely studied in mast cells and some findings confirmed in neuronal cells, a cell type with quite different function and cell physiology.

## 8.2 Labile Zn And $ZnT_4$ In Mast Cells

Mast cells were chosen because these cells have been shown to contain Zn rich granules. However, there have been no previous studies of labile Zn in these cells, the mechanisms by which it is accumulated and its function in relationship to apoptosis. Therefore Zinquin was used to show the levels and localization of labile Zn various types of mast cells and to compare with the distribution of a major Zn transporter $ZnT_4$.

As confirmation of earlier studies using electron microscopy (Danscher, 1980; Gustafson, 1967), mast cells were found to be rich in Zn by Zinquin fluorescence and this was mainly localized in the granules, although there was also extragranular fluorescence. Zinquin provides a rapid and sensitive technique for imaging Zn in mast cells and studying its movements during degranulation and subsequent recovery. Using Zinquin, it was demonstrated that mast cells cultured in low Zn medium have

the ability to maintain their high Zn levels. This raises the question of how mast cells regulate their uptake of Zn from their environments. Clearly these cells must have special mechanisms to accumulate large amounts of Zn and incorporate it into their granules. The mechanisms involved have yet to be identified. Evidence leading to these mechanisms may come from emerging studies of Zn transporters. The experiments reported here are the first to describe the presence of and localization of a Zn transporter in mast cells. Interestingly, there was high expression of both the messenger RNA and the protein for $ZnT_4$ in mast cells, suggesting that it is likely to be involved in the transportation of Zn either across the mast cell plasma membrane or into the granules.

Vesicular distribution of $ZnT_4$ shown by immunostaining is consistent with a role in granular localization of Zn. The absence of overlap between Zn and $ZnT_4$ may imply that only a subset of granules require $ZnT_4$ as their major Zn transporter. One possibility is that $ZnT_4$ mediates the uptake of Zn into granules and is lost from granule membranes when they have accumulated sufficient Zn. Following release of Zn during degranulation, the granules may reacquire $ZnT_4$ in the mast cell periphery and then take up more Zn. To further understand the mechanisms of Zn trafficking in mast cells, the role of other Zn transporters needs to be elucidated, such as the hZIP members, which have been shown to mediate Zn uptake in other types of cells (chapter 1). In particular, more information is needed on the mechanisms by which Zn enters mast cells, is incorporated into their granules, is secreted and is re-acquired during recovery.

As discussed in chapter one, the functions of Zn in mast cell granules are still unclear. Zn has been suggested to play a role in binding histamine and heparin within the granules analogous to the packaging of insulin by Zn in pancreatic islet beta cells. Another role of granule Zn may be in regulation of secretion since numerous studies have shown that exogenous Zn blocks histamine release from mast cells. Secreted Zn could exert a negative feedback mechanism limiting further degranulation. In order to test this, the effects of washing mast cells free of released Zn on further degranulation could be investigated. More studies are required to determine the fate of Zn secreted from mast cells, for example; is it immediately re-acquired by the same mast cell, taken up by other types of cells in the surrounding environment or remain complexed to granule components such as histamine or pro-caspases? One of the major questions addressed in this thesis was whether granular Zn plays a role in the regulation of mast cell apoptosis (discussed below).

### 8.3 Localisation Of Pro-Caspases-3 And -4 In Resting And Activated Mast Cells

When work for this thesis began (1998) there had been no previous studies of caspases in mast cells. In experiments reported in this thesis, pro-caspase-3 mRNA was found. Confirming that this mRNA was translated, pro-caspase-3 protein was also found in these cells as well as in RPMC. The same cells contained pro-caspase-4 protein. One unexpected finding was that both pro-caspases-3 and -4 were localized within granules of mast cells as shown by immunoelectron microscopy and confirmed by their release during degranulation.

There may be several explanations for why pro-caspases are localized in mast cell granules. Firstly, pro-caspases may be released and activated during degranulation and cleave extracellular substrates, such as matrix proteins. To my knowledge, there is no evidence that extracellular proteins can serve as substrates for caspases, but this hypothesis needs to be considered. Another explanation is that caspases are released and induce apoptosis in other cells. This would be similar to the situation in which smooth muscle cells undergo apoptosis in response to chymase released from mast cell granules (Leskinen, 2001). Cytotoxic T-cells induce apoptosis of target cells by releasing a caspase like enzyme, granzyme B (Barry and Bleackley, 2002). Alternatively, granular caspases may have a special function in cleaving proteins within the granules. It is not clear whether cytosolic caspases are able to enter granules to cleave intra-granular substrates. Therefore it would make sense to have some pro-caspases located within the granules awaiting the signal for apoptosis. Finally, in order to prolong their survival during activation, mast cells may release their caspases by degranulation and thereby become more resistant to noxious stimuli.

### 8.4 Interactions Between Zn Depletion And Mast Cell Apoptosis

A major conclusion from the experiments outlined in this section is that there are two distinct pools of labile Zn in mast cells. Firstly there is the pool that is contained within the granules and is released during mast cell activation. This pool is unlikely to play an important role in the regulation of mast cell apoptosis, because in cells where Zn was depleted by degranulation, these cells were no more susceptible to an apoptotic inducer than those that still contained granular Zn. In fact the extent of caspase activation in cells treated with degranulators and either staurosporine or

butyrate (as apoptotic inducers) was often less than the predicted additive effects of these agents. This may be relevant to the discussion above. If pro-caspases are released during degranulation, the cells may be less susceptible to undergo apoptosis in response to toxic stimuli. Rather than regulating pro-caspases, the functions of the intra-granular Zn are likely to be involved primarily in the regulation of secretion or packaging of histamine and heparin in the granules.

The second pool of labile Zn, which is depleted by TPEN is involved in the regulation of caspases since in cells where Zn was depleted by TPEN they were much more susceptible to an apoptotic inducer (e.g. butyrate) than those cells not treated with TPEN. This raises the question of the whereabouts of the anti-apoptotic pools of Zn in these cells. This was difficult to study using Zinquin fluorescence due to the abundance of Zn in the granules and the corresponding bright Zinquin fluorescence in these structures. It was difficult to detect and distinguish lesser pools of Zn in other organelles of the cytoplasm. The localization of extra-granular Zn may be better studied in mast cells at the electron microscopic level. This could be achieved by staining the cells for Zn using the technique of autometallography in which Zn is precipitated as microcrystals with sulphide or selenite and then visualized by deposition of silver around the precipitates (Danscher, 1980; Stoltenberg and Danscher, 2000).

One of the major current controversies concerning mast cells in the body is whether they recover following activation or whether they are removed by apoptosis and replaced by newly developed mast cells from the bone marrow. The experiments described in this thesis show that at least under *in vitro* conditions, degranulated mast

cells can recover their granular content of Zn and do not undergo apoptosis spontaneously. It may be possible that a number of mast cells do undergo apoptosis following degranulation via mechanisms that do not involve Zn and other mast cell survival factors. Other evidence from the literature supports the hypothesis that mast cells recover following degranulation. For example Dvorak and colleagues have shown that human lung mast cells regenerated their granules and histamine following IgE/anti-IgE mediated degranulation (Dvorak, 1997; Dvorak, 1988). They found that renewal of histamine granule stores occurred by multiple mechanisms including synthesis and conservation of granule materials and membranes. The mechanisms by which Zn is recovered remains to be elucidated, but is likely to involve one or more of the recently discovered Zn transporters such as $ZnT_4$ described in this thesis.

There may be a need to have both recovery and apoptosis occurring together in the mast cell population in order to maintain the balance between the generation of mast cells and their removal. If all mast cells were to recover following degranulation, the consequences of over-crowding might result in aberrations in both immune and inflammatory processes. If all mast cells were to die following degranulation, there may be excessive demand on the bone marrow for generations of replacement mast cells. The conditions in which the experiments were performed here may not resemble the exact *in vivo* conditions to which mast cells are normally exposed. This is going to be addressed in further studies that I will be undertaking using an *in vivo* model of the mast cell-deficient $Kit^{W}/Kit^{W\text{-}V}$ mice (Tsai, 2002) reconstituted with Zn depleted or Zn supplemented $ZnT_4$-ve and $ZnT_4$+ve bone marrow mast cells.

## 8.5 The Effect Of Zn On NF-κB In Mast Cells And Relationship To Apoptosis

To further understand the mechanism by which Zn may regulate apoptosis in mast cells, its effects on regulating activation of NF-κB activation were studied. NF-κB is thought to be an anti-apoptotic factor prolonging the survival of inflammatory cells (as discussed earlier); it was therefore of interest to determine whether Zn, another anti-apoptotic factor would promote the activation of NF-κB. However the opposite was found. An increase in intracellular Zn blocked activation of NF-κB in the mast cells studied, while a decrease in intracellular Zn caused by TPEN promoted the activation of NF-κB. In fact TPEN proved to be as potent a stimulator of NF-κB nuclear translocation and activation as did the classical stimulus TNF-α. This is the first demonstration that depletion of Zn can cause the translocation of NF-κB to the nucleus. However it needs to be determined whether the translocated NF-κB is still functional since it has been reported that Zn is required for DNA binding of NF-κB (Prasad, 2002). It is not clear whether TPEN will deplete the nuclear pool of Zn required for NF-κB binding to its target gene elements.

The other thing that these studies showed is that Zn does not block apoptosis via the effect on NF-κB since Zn pyrithione suppressed activation of NF-κB at the same concentration that it suppressed caspase activation. This implies that the effects of Zn on caspase activation occur by a different pathway to that of its action on NF-κB and may indicate that the anti-inflammatory effects of Zn are distinct from its anti-apoptotic properties.

In support of this concept, degranulators were effective activators of NF-κB at least moving it to the perinuclear region but had no effect on caspase-3 activation. The relationship between the granular pools of Zn and the anti-inflammatory pools of Zn has yet to be defined. This could be tested by co-culturing of mast cells with epithelial cells and determining whether Zn released from the mast cells can be taken up by the epithelial cells and suppresses pro-inflammatory events such as NF-κB activation.

### 8.6 Zn and caspase activation in neuroblastoma cells

Some experiments were repeated in neuronal cells because Zn is known to be important in the functions of these cells and apoptosis has been implicated in various brain pathologies such as Alzheimer's disease. Neuroblastoma cells were used as a model of neuronal cells because of their ready availability and because they have previously been used to study mechanisms involved in neuronal pathologies. The first aim was to investigate the distribution of labile Zn in neuroblastoma cells since this has not previously been studied. Zinquin revealed pools of intracellular labile Zn in cytoplasmic/cytoskeletal regions and these could be further increased by treatment with Zn ionophore or decreased by Zn chelator TPEN. This was interesting because previous studies have shown that Zn deprivation caused the destabilization of microtubular cytoskeleton both *in vitro* and *in vivo* and disruption of mictotubules also occurs early in the process of apoptosis in AD (discussed in chapter 1). This may have important implications for neuronal apoptosis in AD where Zn homeostasis is altered (see discussion of chapter 7). The finding that Zn may be rich in the cytoskeleton now needs to be confirmed in normal primary cortical neurons as well as the effects of neuro-degenerative diseases such as AD on Zn homeostasis.

The next set of experiments was to determine whether depletion or supplementation of Zn would affect the activation of caspase-3 in BE(2)-C neuroblastoma cells. Zn depletion by TPEN, as confirmed by the loss of Zinquin labelling, had a moderate enhancing effect on caspase-3 activity. This implies that even in severe Zn deficiency, most neuronal cells are unlikely to undergo apoptosis. However, these Zn-depleted cells were more susceptible to an apoptotic inducer namely butyrate, suggesting that in Zn-deficient patients, neurons are more likely to undergo apoptosis in response to some toxins. Zn depleted neurons were not susceptible to staurosporine, another widely used apoptotic inducer because TPEN and staurosporine did not act synergistically with each other. This was similar to the situation in mast cells. Therefore Zn depleted cells may be more susceptible to some apoptotic inducers but not others. This also suggests that the mechanism of action of butyrate and staurosporine are different, consistent with their known biochemical effects on cells.

The effects of TPEN were very rapid occurring within 2-3 h indicating that it acts relatively close to the time of activation of caspase-3. It is likely that TPEN acts upstream of caspase activation because of the lag period between addition of TPEN and induction of caspase-3 activity. This site could be the disruption of the microtubular cytoskeleton.

These experiments implicate intracellular labile Zn is a critical factor in determining susceptibility of neuronal-like cells to toxin-induced caspase activation, confirming results in mast cells. Since these experiments were performed and reported (Ho, 2000) a number of other studies have appeared in the literature confirming that Zn

depletion increases caspase-3 activation both *in vitro* and *in vivo* (Carter, 2002; Jankowski-Hennig, 2000; Kolenko, 2001; Seve, 2002). For example Jankowski-Hennig and colleagues showed that rat embryos from Zn deficient mothers had increased caspase-3 activity associated with increased apoptotic cell death.

### 8.7 General Model

The results in this thesis are summarized in the following model shown in Figure 8.1. Numbers are used to indicate the different steps in the model.

1) TPEN depletes two intracellular pools of labile Zn, granular pools as well as non-granular pools such as cytoskeletal, nuclear and mitochondrial Zn. This was best shown by the decrease in Zinquin fluorescence in TPEN treated neuroblastoma cells because in mast cells it is difficult to see non-granular fluorescence due to the intense Zinquin fluorescence of their granules.

2) Depletion of non-granular Zn leads to events, which greatly facilitate the conversion of pro-caspase-3 to its active form resulting in apoptosis. The pro-caspase-3 involved in this mast cell apoptosis is likely to be mainly that pro-caspase-3 detected outside of the granules by immuno electron microscopy. The pools of pro-caspase-3 inside of the granules may or may not be regulated by Zn as discussed below.

3) A synergy in the activation of pro-caspase-3 exists between butyrate, an apoptotic inducer and depletion of Zn. This may imply that Zn-deficient cells are more susceptible to undergo apoptosis when exposed to certain apoptotic inducers such as butyrate. It may not be all apoptotic inducers because it was shown that staurosporine,

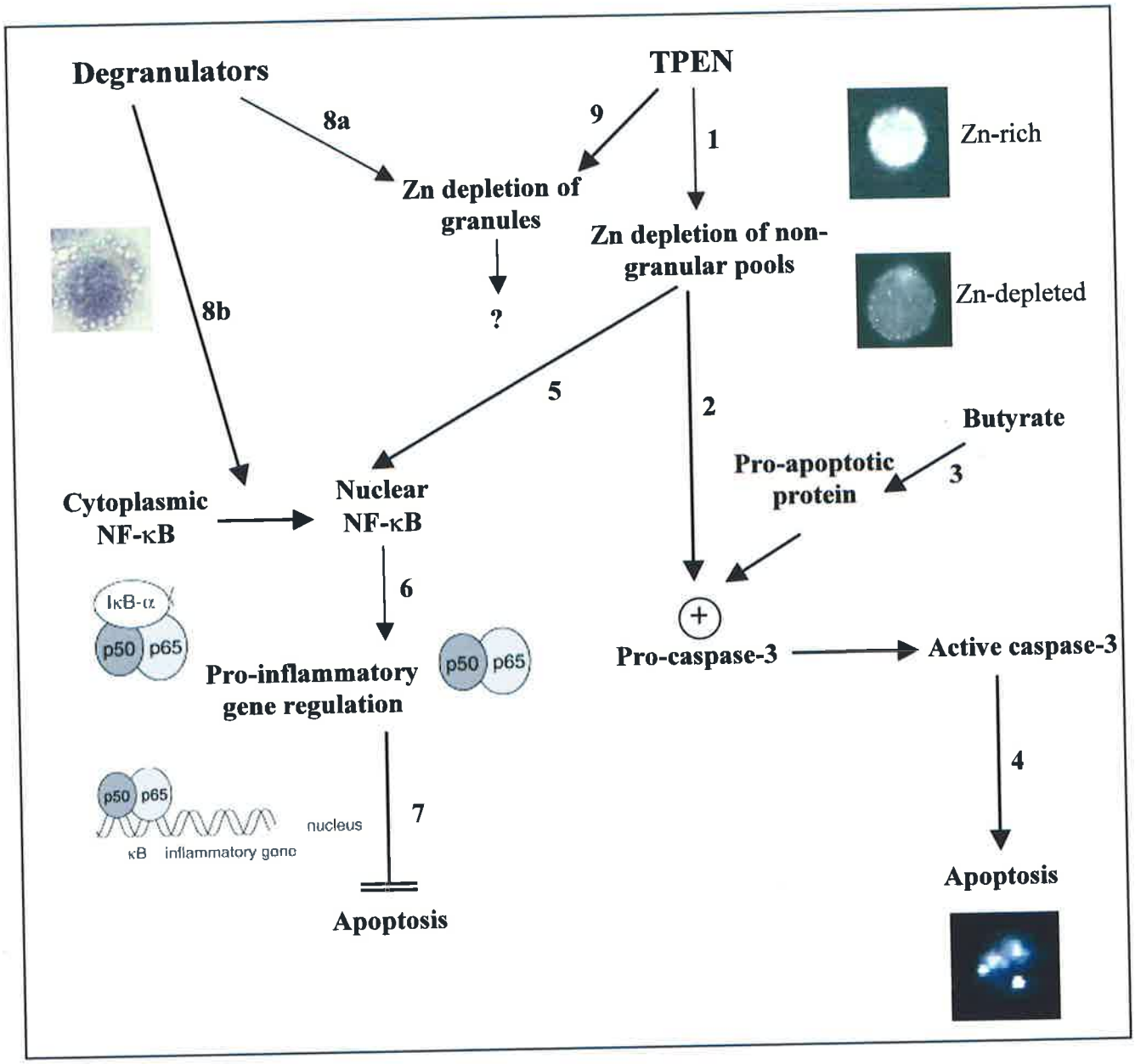


**Figure 8.1: General Model**

Figure shows a summary of the results as different steps in the model involving intracellular Zn and apoptotic pathways. See section 8.7 for discussion.

a different type of apoptotic inducer did not synergise with Zn depletion. Since the action of butyrate involves switching on of new gene expression, this may suggest that synergy requires the synthesis of a new pro-apoptotic protein. This could be further tested by determining whether other apoptotic inducers, which work via turning on new gene expression, also synergise with Zn depletion in inducing caspase activation. Another way would be to determine whether inhibitors of translation or transcription such as cycloheximide and actinomycin D block the synergy between butyrate and TPEN.

4) Activation of pro-caspase-3 leads to apoptosis in both neuroblastoma and mast cells. For mast cells, apoptosis is likely to occur to maintain cell homeostasis. However, apoptosis in neuronal cells is more characteristic of brain pathology.

5) Another effect of depletion of Zn from non-granular pools was activation and nuclear translocation of NF-κB. This was shown by the conversion of cytoplasmic immunofluorescence NF-κB labelling to a nuclear labelling in mast cells treated with TPEN. This was identical to the pattern found in cells treated with TNF-α. Consistent with the above, supplementation of Zn strongly blocked the activation of NF-κB. This is opposite to what was originally hypothesized since it was thought that Zn would activate NF-κB leading to suppression of apoptosis. As discussed in chapter one, NF-κB may have both pro-apoptotic and anti-apoptotic action depending on the cell types, nature of stimuli and other experimental factors.

There have been no studies of NF-κB in mast cell apoptosis. The finding that TPEN causes nuclear translocation of NF-κB and that Zn supplementation blocks this

translocation in mast cells would be more consistent with the pro-apoptotic effects of NF-κB. One mechanism is that caspases cleave IκBα (Barkett, 1997) resulting in the nuclear translocation of NF-κB and thereby triggering downstream events in apoptosis; by blocking caspases activation Zn would inhibit NF-κB activation. A time course experiment may help to test this mechanism. The experiment would detect caspase activation, expression level of IκBα and nuclear translocation of NF-κB in mast cells treated by TPEN to deplete Zn. If this mechanism is correct then one would expect an increase in caspase activity followed by a diminished level of IκBα and nuclear translocation of NF-κB. A second experiment would be to determine whether blocking of caspases by caspase peptide inhibitors would decrease the nuclear translocation of NF-κB in TPEN treated mast cells.

6) Activation and nuclear translocation of NF-κB leads to its binding to sites on promoter regions of inflammatory genes thereby enhancing their transcription. Products of these genes amplify the inflammatory process through the activation of lymphoid and myeloid cells (Barnes and Karin, 1997).

7) In addition to its involvement in inflammatory responses, NF-κB is also an anti-apoptotic agent. A study by Beg and Baltimore has shown that in p65 (NF-κB)-deficient mouse fibroblasts and macrophages, treatment with TNF-α resulted in a significant reduction in their viability, whereas NF-κB containing cells in wild type mice were unaffected (Beg and Baltimore, 1996). TNF-α therefore has two distinct pathways that interact with apoptosis. Firstly by activating NF-κB it causes suppression of apoptosis; secondly it acts via the death receptor ligand pathway to

activate apoptosis (Zhou, 2002). Presumably it is the balance between these two pathways, which determines whether the cells live or die. Zn depletion may also act by two similar pathways. It activates NF-κB, which would have an anti-apoptotic action while directly turning on apoptosis pathways leading to caspase-3 activation and apoptosis. There is a need to understand the particular factors that might influence the outcome of these opposing pathways.

8) Depletion of granular Zn occurs in mast cells treated with degranulators. These agents also activated NF-κB in mature HMC-1 cells. This was only partial since NF-κB fluorescence was localized to the perinuclear region rather than within the nucleus. It remains to be determined whether this action on NF-κB is a consequence of loss of granular Zn (8a in Fig 8.1) or mediated by a Zn-independent pathway (8b). Supporting the first hypothesis, Zn moderately suppressed this translocation. One possible scenario for the perinuclear translocation is that the NF-κB dimer is still complexed to IκBα inhibitory protein and thereby cannot enter the nucleus. This needs to be investigated by experiments, which look at the expression of IκBα in the complex in cells treated with degranulators. A second signal may be required to induce the nuclear localization of NF-κB in these cells. However, degranulators did not affect NF-κB in other types of mast cells and the general significance of these results are not clear.

9) Zinquin labelling experiments in this thesis have shown that Zn is rich inside the granules of various mast cell types. TPEN also depletes pools of Zn inside mast cell granules. This was shown by the decrease of Zinquin fluorescence labelling in mast

cell granules treated with this agent. These granular pools of Zn may have a role in regulating the secretion of granular contents in these cells. While they may act to regulate the pro-caspase-3 found within the granules, it is not at all clear whether the granule pro-caspase-3 is involved in apoptosis of the mast cell or whether it functions only after it is released. The role of the released pro-caspase-3 is not known and further investigation is needed to determine its action on surrounding tissues. An ideal model would be where mast cells are co-cultured with cells that are common targets of inflammatory reactions such as epithelial cells, looking at the effects of released pro-caspase-3 on these targets. Pro-caspase-4 was also released from mast cell granules and may have pro-inflammatory action. This needs to be better defined.

In conclusion the experiments in this thesis have further identified discrete pools of Zn and pro-caspases in cells and their relationship to apoptosis pathways. Some of the findings in this thesis are going to be extended using novel mouse models and gene knockout cell lines with the group of Professor Stephen Galli.

## REFERENCES


Ackland, M. and J. Mercer (1992). "The murine mutation, lethal milk, results in production of zinc-deficient milk." Journal of Nutrition 122: 1214-1218.

Aggarwal, B. (2000). "Apoptosis and Nuclear Factor-κB: A Tale of Association and Dissociation." Biochemical Pharmacology 60: 1033-1039.

Agren, M. (1991). "Enhancement of re-epithlialization with topical zinc oxide in porcine partial thickness wounds." Journal of Surgical Research 50(2): 101-105.

Aizenman, E., A. Stout, K. Hartnett, K. Dineley, B. McLaughlin and I. Reynolds (2000). "Induction of neuronal apoptosis by thiol oxidation: putative role of intracellular zinc release." Journal of Neurochemistry 75: 1878-1888.

Alnemri, E., D. Livingston, D. Nicholson, G. Salvesen, N. Thornberry, W. Wong and J. Yuan (1996a). "Human ICE/CED-3 Protease Nomenclature." Cell 87: 171.

Anderson, A., J. Su and C. Cotman (1996). "DNA damage and apoptosis in Alzheimer's disease: colocalization with c-Jun immunoreactivity, relationship to brain area, and effect of postmortem delay." Neuroscience 16: 1710-1719.

Angyal, A. and G. Archer (1968). "The zinc content of rat mast cells." The Australian Journal Experimental Biology and Medical Science 46(1): 119-121.

Anh, Y., Y. Kim, S. Hong and K. JY (1998). "Depletion of Intracellular Zinc Induces Protein Synthesis-Dependent Neuronal Apoptosis in Mouse Cortical Culture." Experimental Neurology 154: 47-56.

Antonucci, A., A. Di Baldassarre, F. Di Giacomo, L. Stuppia and G. Palka (1997). "Detection of apoptosis in peripheral blood cells of 31 subjects affected by

Down syndrome before and after zinc therapy." Ultrastructural Pathology 21(5): 449-452.

Archer, G. and A. Blackwood (1965). "Formation of Charcot-Leyden crystals in human eosinophils and basophils and study of the composition of the isolated crystals." Journal of Experimental Medicine 122: 173-180.

Arends, M., R. Morris and A. Wyllie (1990). "Apoptosis. The role of the endonuclease." American Journal of Pathology 136: 593-608.

Arquilla, E., P. Thiene, T. Burugman, T. Ruess and R. Sugiyama (1978). "Effects of zinc ion on the conformation of antigenic determinants on insulin." Biochemical Journal 175: 289-297.

Arslan, P., F. Di Virgilio, M. Beltrame, R. Tsien and T. Pozzan (1985). "Cytosolic Ca2+ homeostasis in Ehrlich and Yoshida carcinomas. A new, membrane-permeant chelator of heavy metals reveals that these ascites tumor cell lines have normal cytosolic free Ca2+." Journal of Biological Chemistry 260(5): 2719-2727.

Asai, K., J. Kitaura, Y. Kawakami, N. Yamagata, M. Tsai, D. Carbone, F. Liu, S. Galli and T. Kawakami (2001). "Regulation of mast cell survival by IgE." Immunity 14: 791-800.

Assaf, S. and S. Chung (1984). "Release of endogenous Zn2+ from brain tissue during activity." Nature 308: 734-736.

Baichwal, V. and P. Baeuerle (1997). "Activate NF-κB or die?" Current Biology: R94-R96.

Baker, S. and E. Premkumar Reddy (1998). "Modulation of life and death by the TNF receptor superfamily." Oncogene 17: 3261-3270.

Baldwin, A. (1996a). "The NF-κB and IκB proteins: new discoveries and insights." Annual Review of Immunology 14: 649-683.

Bales, K., Y. Du, R. Dodel, G. Yan, E. Hamilton-Byrd and S. Paul (1998). "The NF-κB/Rel family of proteins mediates Ab-induced neurotoxicity and glial activation." Brain research. Molecular brain research. 57: 63-72.

Barceloux, D. (1999). "Zinc." Journal of Toxicology. Clinical Toxicology 37(2): 279-292.

Barila, D., C. Murgia, F. Nobili, S. Gaetani and G. Perozzi (1994). "Substractive hybridization cloning of novel genes differentially expressed during intestinal tissue and cells." European Journal of Biochemistry 233: 701-709.

Barkett, M., D. Xue, H. Horvitz and T. Gilmore (1997). "Phosphorylation of IκBα inhibits its cleavage by caspase CPP32 in vitro." Journal of Biological Chemistry 272: 29419-29422.

Barnes, P. and I. Adcock (1997a). "NF-κB: a pivotal role in asthma and a new target for therapy." TiPS 18: 46-50.

Barnes, P. and M. Karin (1997b). "Nuclear factor-κB: a pivotal transcription factor in chronic inflammatory diseases." New England Journal of Medicine 336: 1066-1071.

Barry, M. and R. Bleackley (2002). "Cytotoxic T lymphocytes: all roads lead to death." Nature Reviews Immunmolgy 2(6): 401-409.

Basun, H., L. Forssell, L. Wetterberg and B. Winbald (1991). "Metals and trace elements in plasma and cerebrospinal fluid in normal aging and Alzheimer's disease." Journal of Neural Transmission. Parkinson's Disease and Dementia Section. 3(4): 231-258.

Baudier, J. and R. Cole (1988). "Interactions between the microtubule-associated tau proteins and S100b regulate tau phosphorylation by the Ca2+/calmodulin-dependent protein kinase II." Journal of Biological Chemistry 263(12): 5876-5883.

Beaven, M., K. Maeyama, E. Wolde-Mussie, T. Lo, H. Ali and J. Cunha-Melo (1984a). "Mechanism of signal transduction in mast cells and basophils: studies with RBL-2H3 cells." Journal of Biological Chemistry 259: 7129-7136.

Beg, A. and D. Baltimore (1996). "An essential role for NF-kappaB in preventing TNF-alpha-induced cell death." Science 274: 782-789.

Beg, A., W. Sha, R. Bronson, S. Ghosh and D. Baltimore (1995). "Embryonic lethality and liver degeneration in mice lacking the RelA component of NF-kappa B." Nature 376: 167-170.

Bergeron, L., G. Perez, G. Macdonald, L. Shi, Y. Sun, A. Jurisicova, S. Varmuza, K. Latham, J. Flaws, J. Salter, H. Hara, M. Moskowitz, E. Li, A. Greenberg, J. Tilly and J. Yuan (1998). "Defects in regulation of apoptosis in caspase-2-deficient mice." Genes and Development 12(9): 1304-1314.

Bergqvist, U., G. Samuelsson and B. Uvnas (1971). "Chemical Composition of Basophil Granules from Isolated Rat Mast Cells." Acta Physiologica Scandinavica 83: 362-372.

Bessho, R., K. Matsubara, M. Kubota, K. Kuwakado, H. Hirota, Y. Wakazono, Y. Lin, A. Okuda, M. Kawai and R. e. a. Nishikomori (1994). "Pyrrolidine dithiocarbamate, a potent inhibitor of nuclear factor kappa B (NF-kappa B)

activation, prevents apoptosis in human promyelocytic leukemia HL-60 cells and thymocytes." Biochemical Pharmacology 48: 1883-1889.

Bettger, W. and B. O'Dell (1981). "A critical physiological role of zinc in the structure and function of biomembranes." Life Sciences 28: 1425-1438.

Beyaert, R., K. Heyninck and S. Huffel (2000). "A20 and A20 binding proteins as cellular inhibitors of nuclear factor-κB-dependent gene expression and apoptosis." Biochemical Pharmacology 60: 1143-1151.

Beyersmann, D. and H. Haase (2001). "Functions of zinc in signaling, proliferation and differentiation of mammalian cells." BioMetals 14(3-4): 331-341.

Biedler, J., S. Roffler-Tarlov, M. Schachner and L. Freedman (1978). "Multiple neurotransmitter synthesis by human neuroblastoma cell lines and clones." Cancer Research 38: 3751-3757.

Bischoff, S., A. Sellge, A. Lorentz, W. Sebald, R. Raab and M. Manns (1999). "IL-4 enhances proliferation and mediator release in mature human mast cells." Proceedings of National Academy of Sciences USA 96: 8080-8085.

Blank, U., C. Ra, L. Miller, K. White, H. Metzger and J. Kinet (1989a). "Complete structure and expresion in transfected cells of the high affinity IgE receptor." Nature 337: 187-189.

Boffa, L., M. Mariani and M. Parker (1994). "Selective hypermethylation of transcribed nucleosomal DNA by sodium butyrate." Experimental Cell Research 211(2): 420-423.

Boffa, L., G. Vidali, R. Mann and V. Alfrey (1978). "Suppression of histone deacetylase *in vivo* and *in vitro* by sodium butyrate." Journal of Biological Chemistry 253: 3364-3366.

Boldin, M., T. Goncharov, Y. Goltsev and D. Wallach (1996). "Involvement of MACH, a novel MORT1/FADD-interacting protease, in Fas/APO-1- and TNF receptor-induced cell death." Cell 85(6): 803-815.

Bor, N., G. Oner, A. Noyan, A. Arcasoy, A. Cavdar and S. Sozer (1976). "Relation between mast cells and serum zinc levels." New Istanbul Contribution to Clinical Science 11(3): 136-141.

Bortner, C. and J. Cidlowski (2002). "Cellular Mechanisms For The Repression Of Apoptosis." Annual Review of Pharmacology and Toxicology 42: 259-281.

Bossy, W., D. Newmeyer and D. Green (1998). "Mitochondrial cytochrome c release in apoptosis occurs upstream of DEVD-specific caspase activation and independently of mitochondrial transmembrane depolarization." EMBO Journal 17: 37-49.

Briggs, W., M. Pederson, S. Mahajan, D. Sillix, A. Prasad and F. McDonald (1982). "Lynphocyte and granulocyte function in zinc-treated and zinc deficient hemodialysis patients." Kidney International 21: 827-839.

Browne, K., D. Johnstone, J. Jans and J. Trapani (2000). "Filamin (280-kDa actin-binding protein) is a caspase substrate and is also cleaved directly by the cytotoxic T lymphocyte protease granzyme B during apoptosis." Journal of Biological Chemistry 275: 39262-39266.

Bubien, J., L. Zhou, P. Bell, R. Frizzell and T. Tedder (1992). "Transfection of the CD20 surface molecule into ectopic cell types generates a $Ca^{2+}$ conductance found constitutively in B-lymphocytes." Journal of Cell Biology 121: 1121-1132.

Buddecke, E., A. Essellier and H. Marti (1956). "Uber die chemische Natur der Charcot Leydenschen Kristalle." Z Phys Chemie 305: 203-206.

Bullock, E. and J. E. Johnson (1996). "Nerve growth factor induces the expression of certain cytokine genes and bcl-2 in mast cells." Journal of Biological Chemistry 271: 27500-27508.

Burgoyne, R. and A. Morgan (2003). "Secretory granule exocytosis." Physiological Reviews 83(2): 581-632.

Bush, A., Pettingwell, WH, G. Multhaup, M. Paradis, J. Vonsattel, J. Gusella, K. Beyreuther, C. Masters and R. Tanzi (1994). "Rapid induction of Alzheimer A beta amyloid formation by zinc." Science 265: 1464-1467.

Butler, A. (1998). "Acquisition and utilization of transition metal ions by marine organisms." Science 281(5374): 207-210.

Butterfield, J., D. Weiler, G. Dewald and G. Gleich (1988). "Establishment of an immature mast cell line from a patient with mast cell leukemia." Leukemia Research 12(4): 345-355.

Calabresse, C., L. Venturini, G. Ronco, P. Villa, C. Chomienne and D. Belpomme (1993). "Butyric acid and its monosaccharide ester induce apoptosis in the HL-60 cell line." Biochemical and Biophysical Research Communications 195(1): 31-38.

Calesnick, B. and A. Dinan (1988). "Zinc deficiency and zinc toxicity." American Family Practice 37: 267-270.

Campo, A. J. and C. McDonald (1976). "Treatment of acrodermatitis enteropathica with zinc sulfate." Archives of Dermatology 112(5): 687-689.

Candido, E., R. Reeves and J. Davie (1978). "Sodium butyrate inhibits histone deacetylation in cultured cells." Cell 14(1): 105-113.

Carter, J., A. Truong-Tran, D. Grosser, L. Ho, R. Ruffin and P. Zalewski (2002). "Involvement of redox events in caspase activation in zinc-depleted airway epithelial cells." Biochemical and Biophysical Research Communications 297(4): 1062-1070.

Cassel, G. (1978). "Zinc: a review of current trends in therapy and our knowledge of its toxicity." Delaware Medical Journal 50: 323-328.

Castro-Alcaraz, S., V. Miskolci, B. Kalasapudi, D. Davidson and I. Vancurova (2002). "NF-kappa B regulation in human neutrophils by nuclear I kappa B alpha: correlation to apoptosis." The Journal of Immunology 169: 3947-3953.

Chai, J., C. Du, J. Wu, S. Kyin, X. Wang and Y. Shi (2000a). "Structural and biochemical basis of apoptotic activation by Smac/DIABLO." Nature 406: 885-962.

Chao, D. and S. Korsmeyer (1998). "Blc-2 family: Regulation of cell death." Annual Review of Immunology 16: 395-419.

Chausmer, A. (1998). "Zinc, Insulin and Diabetes." Journal of the American College of Nutrition 17(2): 109-115.

Chesters, J. (1989). Biochemistry of zinc in cell division and tissue growth. Zinc in Human Biology. C. Mills. London, Springer-Verlag: 109-118.

Cho, C., L. Fong, P. Ma and C. Ogle (1987). "Zinc deficiency: its role in gastric secretion and stress-induced gastric ulceration in rats." Pharmacology, biochemistry and behaviour 26(2): 293-297.

Choi, D., M. Yokoyama and J. Koh (1988). "Zinc neurotoxicity in cortical cell culture." Neuroscience 24(1): 67-79.

Chu, Z., T. McKinsey, L. Liu, J. Gentry, M. Malim and D. Ballard (1997). "Suppression of tumor necrosis factor-induced cell death by inhibitor of apoptosis c-IAP2 is under NF-kappaB control." Proceedings of National Academy of Sciences USA 94(19): 10057-10062.

Chuang, P., E. Yee, A. Karsan, R. Winn and J. Harlan (1998). "A1 is constitutively and inducible Bcl-2 homologue in mature human neutrophils." Biochemical and Biophysical Research Communications 249: 361-365.

Chung, Y., I. Song, R. Erickson, M. Sleisenger and Y. Kim (1985). "Effect of growth and sodium butyrate on brush border membrane-associated hydrolases in human colorectal cancer cell lines." Cancer Research 45(7): 2976-2982.

Chvapil, M. (1976). "Effect of Zinc on Cells and Biomembranes." Symposium on Trace Elements 60(4): 799-812.

Cohen, G. (1997a). "Caspases: the executioners of apoptosis." Biochemical Journal 326: 1-16.

Cohen, J. and R. Duke (1984). "Glucocorticoid activation of a calcium-dependent endonuclease in thymocyte nuclei leads to cell death." The Journal of Immunology 132(1): 38-42.

Cole, T., H. Wenzel, K. Kafer, P. Schwartzkroin and R. Palmiter (1999). "Elimination of zinc from synaptic vesicles in the intact mouse brain by disruption of the ZnT3 gene." Proceedings of National Academy of Sciences USA 96(4): 1716-1721.

Coleman, J. (1992). "Zinc proteins: enzymes, storage proteins, transcription factors, and replication proteins." Annual Review of Biochemistry 61: 897-946.

Connell, P., V. Young, M. Toborek, D. Cohen, S. Barve, C. McClain and B. Hennig (1997). "Zinc attenuates tumour necrosis factor-mediated activation of transcription factors in endothelial cells." Journal of the American College of Nutrition 16(5): 411-417.

Conrad, M., J. Umbreit and E. Moore (1999). "Iron absorption and transport." The American journal of the medical sciences. 318(4): 213-229.

Constatinidis, J. (1991). "The hypothesis of zinc deficiency in the pathogenesis of neurofibrillary tangles." Medical Hypotheses 35: 319-323.

Cotton, F. and G. Wilkinson (1988). Advanced Inorganic Chemistry. A Comprehensive Text. New York, Wiley-Interscience: 599.

Cousins, R. (1998ab). "A role of zinc in the regulation of gene expression." Proceedings of the Nutrition Society 57: 307-311.

Cousins, R. and R. McMahon (2000a). "Integrative aspects of zinc transporters." Journal of Nutrition 130(5S Suppl): 1384S-1387S.

Cragg, R., G. Christie, S. Phillips, R. Russi, S. Kury, J. Mathers, P. Taylor and D. Ford (2002). "A novel zinc-regulated human zinc transporter, hZTL1, is localised to the enterocyte apical membrane." Journal of Biological Chemistry 277(25): 22789-22797.

Craig, S., N. Schechter and L. Schwartz (1988). "Ultrastructural analysis of human T and TC mast cells identified by immunoelectron microscopy." Laboratory Investigation 58: 682-691.

Creagh, E. and S. Martin (2001). "Caspases: cellular and demolition experts." Biochemical Society Transactions 29(6): 696-702.

Cuajungco, M. and G. Lees (1997a). "Zinc metabolism in the brain: Relevance to human neurodegenerative disorders." Neurobiology of Diseases 4: 137-169.

Cuajungco, M. and G. Lees (1997b). "Zinc and Alzheimer's disease: Is there a direct link?" Brain Research Review 23: 219-236.

Cui, L., N. Schoene, L. Zhu, J. Fanzo, A. Alshatwi and K. Lei (2002). "Zinc depletion reduced Egr-1 and HNF-3beta expression and apolipoprotein A-I promoter activity in Hep G2 cells." American Journal of Physiology and Cellular Physiology 283(2): C623-C630.

Cunha-Melo, J., N. Dean, J. Moyer, K. Maeyama and M. Beaven (1987). "The kinetics of phosphoinositide hydrolysis in rat basophilic leukemia (RBL-2H3) cells varies with the type of IgE receptor cross-linking agent used." Journal of Biological Chemistry 262: 11455-11463.

Danscher, G. (1996). "The autometallographic zinc-sulphide method. A new approach involving in vivo creation of nanometer-sized zinc sulphide crystal lattices in zinc-enriched synaptic and secretory vesicles." Histochemical Journal 28(5): 361-373.

Danscher, G., J. Obel and O. Thorlacius-Ussing (1980). "Electron microscopic demonstration of metals in rat mast cells. A cytochemical study based on an improved sulphide silver method." Histochemistry 66(3): 293-300.

Danscher, G., G. Howell, J. Perez-Clausell and H. N (1985c). "The dithizone, Timm's sulphide silver and the selenium methods demonstrate a chelatable pool of zinc in CNS. A proton activation (PIXE) analysis of carbon tetrachloride extracts

from rat brains and spinal cords intravitally treated with dithizone." Histochemistry 83(5): 419-422.

Danscher, G., K. Jensen, C. Frederickson, K. Kemp, A. Andreasen, S. Juhl, M. Stoltenberg and R. Ravid (1997). "Increased amount of zinc in the hippocampus and amygdala of Alzheimer's diseased brains: a proton-induced X-ray emission spectroscopic analysis of cryostat sections from autopsy material." Journal of Neuroscience Methods 76: 53-59.

Dardenne, M., J. Pleau, P. Lefrancier, M. Derrien, J. Choay and J. Bach (1982). "Contribution of zinc and other metals to the biological activity of the serum thymic factor (FTS)." Proceedings of the National Academy of Sciences USA 79: 5370-5373.

Datta, R., E. Oki, K. Endo, V. Biedermann, J. Ren and D. Kufe (2000a). "XIAP regulates DNA damage-induced apoptosis downstream of caspase-9 cleavage." Journal of Biological Chemistry 275: 31733-31738.

Davies, N. (1980). "Studies on the absorption of zinc by rat intestine." British Journal of Nutrition 43(1): 189-203.

Davis, S., R. McMahon and R. Cousins (1998). "Metallothionein knockout and transgenic mice exhibit altered intestinal processing of zinc with uniform zinc-dependent zinc transporter-1 expression." Journal of Nutrition 128(5): 825-831.

de Moissac, D., S. Mustapha, A. Greenberg and L. Kirshenbaum (1998). "Bcl-2 activates the transcription factor NFkappaB through the degradation of the cytoplasmic inhibitor IkappaBalpha." Journal of Biological Chemistry 273(37): 23946-23951.

Delic, J., P. Masdehors, S. Omura, J. Cosset, J. Dumont, J. Binet and H. Magdelenat (1998). "The proteasome inhibitor lactacystin induces apoptosis and sensitizes chemo- and radioresistant human chronic lymphocytic leukaemia lymphocytes to TNF-alpha-initiated apoptosis." British Journal of Cancer 77(7): 1103-1107.

Denault, J. and G. Salvesen (2002). "Caspases: Keys in the Ignition of Cell Death." Chemical Reviews 102(2): 4489-4499.

Denburg, J. (1992). "Basophil and mast cell lineages in vitro and in vivo." Blood 79: 846-860.

Deveraux, Q. and J. Reed (1999). "IAP family proteins- suppressors of apoptosis." Genes and Development 13: 239-252.

Di Donato, J., Haykawa, M and D. Rothward (1997). "A cytokine-responsive IkappaB kinase that activates the transcription factor NF-kappaB." Nature 388(6642): 548-554.

Dineley, K., L. Malaiyandi and I. Reynolds (2002). "A reevaluation of neuronal zinc measurements: artifacts associated with high intracellular dye concentration." Molecular Pharmacology 62(3): 618-627.

Donaldson, J., T. St-Pierre, J. Minnich and A. Marbea (1971). "Seizures in Rats Associated with Divalent Cation Inhibition of $Na^+$-$K^+$-ATPase." Canadian Journal of Biochemistry 49: 1217-1224.

Dreosti, I. (2001). "Zinc and the gene." Mutation Research 475: 161-167.

Du, C., M. Fang, Y. Li, L. Li and X. Wang (2000c). "Smac, a mitochondrial protein that promotes cytochrome c-dependent caspase activation by eliminating IAP inhibition." Cell 102(1): 33-42.

DuBuske, L., K. Austen, J. Czop and R. Stevens (1984). "Granule-associated serine neutral proteases of the mouse bone marrow-derived mast cell that degrade fibronectin: their increase after sodium butyrate treatment of the cells." Journal of Immunology 133(3): 1535-1541.

Dumont, A., S. Hehner, T. Hofmann, M. Ueffing, W. Droge and M. Schmitz (1999ab). "Hydrogen peroxide-induced apoptosis is CD95-independent, requires the release of mitochondria-derived reactive oxygen species and the activation of NF-kappaB." Oncogene 18(3): 747-757.

Dvorak, A. (1991). Basophil and mast cell degranulation and recovery. Blood Cell Biochemistry. New York, Plenum Press. **4.**

Dvorak, A. (1997). "Ultrastructural localization of histamine in human basophils and mast cells; changes associated with anaphylatic degranulation and recovery demonstrated with a diamine oxidase-gold probe." Allergy 52(suppl 34): 14-24.

Dvorak, A., R. Schleimer and L. Lichtenstein (1988a). "Human mast cells synthesize new granules during recovery from degranulation. In vitro studies with mast cells purified from human lungs." Blood 71(1): 76-85.

Earnshaw, W., L. Martins and S. Kaufmann (1999). "Mammalian Capases: structure, activation, substrates, and functions during apoptosis." Annual Review of Biochemistry 68: 383-424.

Eckhart, L., J. Ban, H. Fischer and E. Tschachler (2000). "Caspase-14: analysis of gene structure and mRNA expression during keratinocyte differentiation." Biochemical and Biophysical Research Communications 277(3): 655-659.

Elmes, M. (1977). "Apoptosis in the small intestine of zinc-deficient and fasted rats." Journal of Pathology 123: 219-224.

Elmes, M. and J. Jones (1980). "Ultrastructural changes in the small intestine of zinc deficient rats." Journal of Pathology 130(1): 37-43.

Emdin, S., G. Dodson, J. Cutfield and S. Cutfield (1980). "Role of zinc in insulin biosynthesis. Some possible zinc-insulin interactions in the pancreatic B-cell." Diabetologia 19(3): 174-182.

Enari, M., H. Sakahiri, H. Yokoyama, K. Okawa, A. Iwamatsu and S. Nagata (1998). "A caspase-activated DNase that degrades DNA during apoptosis, and its inhibitor ICAD." Nature 391: 43-50.

Endre, L., W. Beck and A. Prasad (1990). "The role of zinc in human health." Journal of Trace Elements and Experimental Medicine 3: 337-375.

Evan, G. and T. Littlewood (1998). "A matter of life and cell death." Science 281: 1317-1322.

Fantuzzi, G., A. Puren, M. Harding, D. Livingston and C. Dinarello (1998). "Interleukin-18 regulation of interferon gamma production and cell proliferation as shown in interleukin-1beta-converting enzyme (caspase-1)-deficient mice." Blood 91(6): 2118-2125.

Fasset, D. and A. Hjort (1938). "Some tetrahydroisoquinolones. II. Their action on blood pressure, respiration and smooth muscle." Journal of Pharmacology Experimental Therapeutics 63: 253-271.

Fattman, C., S. Delach, Q. Dou and D. Johnson (2001). "Sequential two-step cleavage of the retinoblastoma protein by caspase-3/-7 during etoposide-induced apoptosis." Oncogene 20(23): 2918-2926.

Fernandes, G., N. Nair, K. Onoe, T. Tanaka, R. Floyd and R. Good (1979). "Impairment of cell mediated immunity function in dietary zinc deficiency in mice." Proceedings of National Academy of Sciences USA 76: 457-461.

Fernandes, P., D. Samuelson, W. Clark and R. Cousins (1997). "Immunohistochemical localization of cysteine-rich intestinal protein in rat small intestine." American Journal of Physiology 272: G751-G759.

Fernandes-Alnemri, T., G. Litwack and E. Alnemri (1994). "CPP32, a novel human apoptotic protein with homology to Caenorhabditis elegans cell death protein Ced-3 and mammalian interleukin-1 beta-converting enzyme." Journal of Biological Chemistry 269(49): 30761-30764.

Fernandes-Alnemri, T., A. Takahashi, R. Armstrong, J. Krebs, L. Fritz, K. Tomaselli, L. Wang, Z. Yu, C. Croce and G. e. a. Salvesen (1995). "Mch3, a novel human apoptotic cysteine protease highly related to CPP32." Cancer Research 55: 6405-6502.

Fesik, S. (2000). "Insights into programmed cell death through structural biology." Cell 103: 273-282.

Filippovich, I., N. Sorokina, K. Khanna and M. Lavin (1994). "Butyrate induced apoptosis in lymphoid cells preceded by transient over-expression of HSP70 mRNA." Biochemical and Biophysical Research Communications 198(1): 257-265.

Follis, R., H. Day and E. McCollum (1941). "Histologic studies of the tissues of rats fed a diet extremely low in zinc." Journal of Nutrition 22: 223-237.

Foster, M., R. Leapman, M. Li and I. Atwater (1993). "Elemental composition of secretory granules in pancreatic islets of Langerhans." Biophysical Journal 64: 525-532.

Fox, C., A. Dvorak, S. Peters, A. Kagey-Sobotka and L. Lichtenstein (1985). "Isolation and characterization of human intestinal mucosal mast cells." Journal of Immunology 135: 483-491.

Fraker, P. (1983). "Zinc deficiency: a common immunodeficiency state." Survey of Immunologic Research 2(2): 155-163.

Fraker, P. and W. Telford (1997). "A reappraisal of the role of zinc in life and death decision of cells." Proceedings of the Society for Experimental Biology and Medicine 215: 229-236.

Fraker, P., R. Caruso and F. Kierszenbaum (1982). "Alteration of the immune and nutritional status of mice by synergy between zinc and deficiency and infection with *Trypanosoma cruzi*." Journal of Nutrition 112: 1224-1229.

Frederickson, C. (1989a). "Neurobiology of zinc and zinc-containing neurons." International Review of Neurobiology 31: 145-238.

Frederickson, C., E. Kasarskis, D. Ringo and R. Frederickson (1987). "A quinolone fluorescence method for visualizing and assaying the histochemically reactive zinc (bouton zinc) in the brain." Journal of Neuroscience Methods 20: 91-103.

Frederickson, C., M. Hernandez, S. Goik, J. Morton and J. McGinty (1988). "Loss of zinc staining from hippocampal mossy fibers during kainic acid induced seizures: a histofluorescence study." Brain Research 446: 383-386.

Frigo, A., L. Bambara, E. Concari, M. Marrella, U. Moretti, C. Tambolo, G. Velo and R. Milanino (1989). Concerning the potential therapeutic value of zinc in

rheumatoid and psoriatic arthritis. Copper and zinc in inflammation. R. Milanino, G. Velo and K. Rainsford. Dordrecht, Kluwer Academic Publishers: 133-142.

Fukamachi, Y., Y. Karasaki, T. Sugiura, H. Itoh, T. Abe, K. Yamamura and K. Higashi (1998). "Zinc suppresses apoptosis of U937 cells induced by hydrogen peroxide through an increase of the Bcl-2/Bax ratio." Biochemical and Biophysical Research Communications 246(2): 364-369.

Fukushima, T., Y. Lijima and F. Kosaka (1988). "Endotoxin-induced zinc accumulation by liver cells in mediated by metallothionein synthesis." Biochemical and Biophysical Research Communications 152: 874-878.

Gaither, L. and D. Eide (2000). "Functional expression of the human hZIP2 zinc transporter." Journal of Biological Chemistry 275(8): 5560-5564.

Gaither, L. and D. Eide (2001a). "The human ZIP1 transporter mediates zinc uptake in human K562 erythroleukemia cells." Journal of Biological Chemistry 276(25): 22258-22264.

Galli, S., A. Dvorak, J. Marcum, T. Ishizaka, G. Nabel, H. Der Simonian, K. Pyne, J. Goldin, R. Rosenberg, H. Cantor and H. Dvorak (1982). "Mast cell clones: a model for the analysis of cellular maturation." Journal of Cellular Biology 95(2 Pt 1): 435-444.

Gerber, H., V. Dixit and N. Ferrara (1998). "Vascular endothelial growth factor induces expression of the antiapoptotic proteins Bcl-2 and A1 in vascular endothelial cells." Journal of Biological Chemistry 273: 13313-13316.

Ghildyal, N., H. McNeil, K. Austen and R. Stevens (1992). "Transcriptional regulation of the mucosal mast cell-specific protease gene, MMCP-2, by interleukin 10 and interleukin 3." Journal of Biological Chemistry 267: 8473-8477.

Ghosh, S. and D. Baltimore (1990). "Activation *in vitro* of NF-κB by phosphorylation of its inhibitor I-κB." Nature 344: 678.

Glass, C., D. Rose and M. Rosenfeld (1997). "Nuclear receptor co-activators." Current opinion in Cell Biology 9: 222-232.

Glucksmann, A. (1951). "Cell deaths in normal vertebrate development." Biological Reviews 26: 59-86.

Glusker, J. (1991). Structural aspects of metal liganding to functional groups in proteins. Advances in Protein Chemistry. C. F. Anfinsen, J. Edsall, D. Eisenberg and F. Richards. San Diego, Academic Press. **42:** 1.

Golub, M., C. Keen, M. Gershwin and A. Hendricks (1995). "Developmental zinc deficiency and behavior." Journal of Nutrition 125 (Suppl): 2263S-2271S.

Greenberg, A. (1996ab). "Activation of apoptosis pathways by granzyme B." Cell Death and Differentiation 3: 269-274.

Grennan, D., J. Knudson, J. Dunckley, M. MacKinnon, D. Myers and D. Palmer (1980). "Serum copper and zinc in rheumatoid arthritis and osteoarthritis." New Zealand Medical Journal 91(652): 47-50.

Grey, S., M. Arvelo, W. Hasenkamp, F. Bach and C. Ferran (1999). "A20 inhibits cytokine-induced apoptosis and nuclear factor kappaB-dependent gene activation in islets." Journal of Experimental Medicine 190(8): 1135-1146.

Gross, A., X. Yin, K. Wang, M. Wei, J. Jockel, C. Milliman, H. Erdjunment-Bromage, P. Tempst and S. Korsmeyer (1999). "Caspase cleaved BID targets

mitochondria and is required for cytochrome c release, while BCL-XL prevents this release but not tumor necrosis factor-R1/Fas death." Journal of Biological Chemistry 274(2): 1156-1163.

Grossmann, M., Y. Nakamura, R. Grumont and S. Gerondakis (1999). "New insights into the roles of Rel/NF-κB transcription factors in immune function, hemopoiesis and human disease." The international journal of biochemistry and cell biology 31: 1209-1219.

Guo, Q., N. Robinson and M. Mattson (1998). "Secreted b-amyloid precursor protein counteracts the proapoptotic action of mutant presenilin-1 by activation of NF-κB and stabilization of calcium homeostasis." Journal of Biological Chemistry 273: 123411-12351.

Gustafson, G. (1967a). "Heavy metals in rat mast cell granules." Laboratory Investigation 17(6): 588-598.

Guttridge, D., C. Albanese, J. Ruether, R. Pestell and J. A. Baldwin (1999). "NF-κB controls cell growth and differentiation through transcriptional regulation of cyclin D1." Molecular and Cellular Biology 19: 5785-5799.

Gwag, B., L. Canzoniero, S. Sensi, J. Demaro, J. Koh, M. Goldberg, M. Jacquin and D. Choi (1999). "Calcium ionophores can induce either apoptosis or necrosis in cultured cortical neurons." Neuroscience 90(4): 1339-1348.

Hague, A., A. Manning, J. van der Stappen and C. Paraskeva (1993). "Sodium butyrate induces apoptosis in human colonic tumour cell lines in a p53-independent pathway: implications for the possible role of dietary fibre in the prevention of large-bowel cancer." International Journal of Cancer 55(3): 498-505.

Hakem, R., A. Hakem, G. Duncan, J. Henderson, M. Woo, M. Soengas, A. Elia, J. de la Pompa, D. Kagim, W. Khoo, J. Potter, R. Yoshida, S. Kaufman, S. Lowe, J. Penninger and T. Mak (1998). "Differential requirement for caspase 9 in apoptotic pathways in vivo." Cell 94(3): 339-352.

Hambidge, K., P. Walvarens and K. Neldner (1977a). The role of zinc in the pathogenesis and treatment of acrodermatitis enteropathica. Zinc metabolism: current aspects in health and disease. G. Brewer and A. Prasad. New York, Alan R Liss: 329-340.

Hanada, K., R. Gange, E. Siebert and T. Hasan (1991). "Protective effects of cadmium chloride against UVB injury in mouse skin and in cultured human cells: a possible role of cadmium-induced metallothionein." Photodermatology, photoimmunology and photomedicine 8: 111-115.

Hanada, K., T. Baba, I. Hashimoto, R. Fukui and S. Watanabe (1992). "Possible role of cutaneous metallothionein in protection against photo-oxidative stress--epidermal localization and scavenging activity for superoxide and hydroxyl radicals." Photodermatology, photoimmunology and photomedicine 9(5): 209-213.

Hardy, W. and F. Westbrook (1895). "The wondering cells of the alimentary canal." Journal of Physiology 18: 490.

Harrison, N. and S. Gibbons (1994). "Zn2+: an endogenous modulator of ligand- and voltage-gated ion channels." Neuropharmacology 33(8): 935-952.

Hartmann, K., A. Wagelie-Steffen, E. Stebut and D. Metcalfe (1997). "Fas(CD95, Apo-1) antigen expression and function in murine mast cells." Journal of Immunology 159: 4006.

Hassig, C., J. Tong and S. Schreiber (1997). "Fiber-derived butyrate and the prevention of colon cancer." Chemistry and Biology 4: 783-789.

Haug, F. (1973). "Heavy metals in the brain. A light microscope study of the rat with Timm's sulphide silver method. Methodological considerations and cytological and regional staining patterns." Advances in anatomy, embryology, and cell biology. 47: 1-71.

Hengartner, M. (2000). "The biochemistry of apoptosis." Nature 407: 770-776.

Hengartner, M. and H. Horvitz (1994c). "*C, elegans* cell survival gene ced-9 encodes a functional homolog of the mammalian proto-oncogene bcl-2." Cell 76: 665-676.

Heyninck, K. and R. Beyaert (1999a). "The cytokine-inducible zinc finger protein A20 inhibits IL-1-induced NF-κB activation at the level of TRAF6." FEBS letter 442: 147-150.

Heyninck, K., D. Valck, W. Berghe, W. Criekinge, R. Contreras, W. Fiers, G. Haegeman and R. Beyaert (1999b). "The zinc finger protein A20 inhibits TNF-induced NF-κB-dependent gene expression by interfering with an RIP- or TRAF2-mediated transactivation signal and directly binds to a novel NF-κB-inhibiting protein ABIN." The Journal of Cell Biology 145(7): 1471-1482.

Hide, I., J. Bennett, A. Pizzey, G. Boonen, D. Bar-Sagi, B. Gomperts and T. PE. (1993). "Degranulation of individual mast cells in response to Ca2+ and guanine nucleotides: an all-or-none event." Journal of Cell Biology 123(3): 585-593.

Hierholzer, J., E. Castells, G. Banks, J. Bryan and C. McEwen (1993). "Sensitivity of NCI-H292 human lung mucoepidermoid cells for respiratory and other human viruses." Journal of Clinical Microbiology 31(6): 1504-1510.

Hinz, M., D. Krappmann, A. Eichten, A. Heder, C. Scheidereit and M. Strauss (1999). "NF-κB function in growth control: regulation of cyclin D1 expression and G0/G1-to-S-phase transition." Molecular and Cellular Biology 19: 2690-2698.

Hirabayashi, M., T. Matsui and H. Yano (1998). "Fermentation of soybean meal with Aspergillus usamii improves zinc availability in rats." Biological Trace Element Research 61: 227-234.

Ho, E., N. Quan, Y. Tsai, W. Lai and T. Bray (2001). "Dietary zinc supplementation inhibits NFkappaB activation and protects against chemically induced diabetes in CD1 mice." Experimental Biology and Medicine 226(2): 103-111.

Ho, L., R. Ratnaike and P. Zalewski (2000a). "Involvement of Intracellular Labile Zinc in Suppression of DEVD-Caspase Activity in Human Neuroblastoma Cells." Biochemical and Biophysical Research Communications 268: 148-154.

Hoadley, J., A. Leinart and A. Cousins (1987). "Kinetic analysis of zinc uptake and serosal transfer by vascularly perfused rat intestine." American Journal of Physiology 252(6 Pt 1): G825-G831.

Hogberg, B. and B. Uvnas (1960). "Further observations on the disruption of rat mesentery mast cells caused by compound 48/80, antigen-antibody reaction, lecithinase A and decylamine." Acta Physiologica Scandinavica 48: 133-145.

Holgate, S. and M. Church (1992a). "The Mast Cell." British Medical Bulletin 48(1): 40-50.

Horvitz, H., S. Shaham and M. Hengartner (1994ab). "The genetics of programmed cell death in the nematode *Caenorhabditis elegans.*" Cold Spring Harbor symposia on quantitative biology 59: 377-385.

Horwitz, R. and W. Busse (1995). "Inflammation and asthma." Clinics in Chest Medicine 16(4): 583-602.

Howell, G. and C. Frederickson (1989). "A retrogade transport method for mapping zinc-containing fiber systems in the brain." Brain Research 515: 277-286.

Hsu, S., M. Gavrilin, H. Lee, C. Wu, S. Han and M. Lai (1999ab). "NF-kappa B-dependent Fas ligand expression." European Journal of Immunology 29(9): 2948-2956.

Hu, X., M. Tang, A. Fisher, N. Olashaw and Z. KS. (1999). "TNF-alpha-induced growth suppression of CD34+ myeloid leukemic cell lines signals through TNF receptor type I and is associated with NF-kappa B activation." Journal of Immunology 163(6): 3106-3115.

Huang, E. (1997b). "Metal ions and synaptic transmission: think zinc." Proceedings of National Academy of Sciences USA 94: 13386-13387.

Huang, E., K. Nocka, D. Beier, T. Chu, J. Buck, H. Lahm, D. Wellner, P. Leder and P. Besmer (1990). "The hematopoietic growth factor KL is encoded by the Sl locus and is the ligand of the c-kit receptor, the gene product of the W locus." Cell 63(1): 225-233.

Huang, L. and J. Gitschier (1997a). "A novel gene involved in zinc transport is deficient in lethal milk mouse." Nature Genetics 17(3): 292-297.

Huang, L., C. Kirschke and J. Gitschier (2002). "Functional characterization of a novel mammalian zinc transporter, ZnT6." Journal of Biological Chemistry 277(29): 26389-26395.

Huo, Y., J. Ekholm and D. Hanaban (1988). "A preferential inhibition by Zn (II) on PAF and thrombin-induced serotonin secretion from washed rabbit platelets." Archives of Biochemistry and Biophysics 260: 841-846.

Ihle, J., J. Keller, S. Oersozlan, L. Henderson, T. Copeland, F. Fitch, M. Prytowsky, E. Goldwasser, J. Scradler, E. Palaszynski, M. Dy and B. Lebel (1983). "Biologic properties of homogeneous interleukin 3. I. Demonstration of WEHI-3 growth factor activity, mast cell growth factor activity, p cell-stimulating factor activity, colony-stimulating factor activity, and histamine-producing cell-stimulating factor

activity." Journal of Immunology 131(1): 282-287.

Inemura, A., M. Tsai, A. Ando, B. Wershil and S. Galli (1994). "The c-kit ligand promotes mast cell survival by suppressing apoptosis." American Journal of Pathology 144: 321-328.

Irani, A., N. Schechter, S. Craig, G. DeBlois and L. Schwartz (1986). "Two human subsets with different neutral protease composition." Proceedings of the National Academy of Sciences USA 83: 4464-4468.

Ishizuka, T., K. Chayana, K. Takeda, E. Hamelmann, N. Terada, G. Keller, G. Johnson and E. Gelfand (1999). "Mitogen-activated protein kinase activation through Fcε receptor is differentially regulated by phosphatidylinositol 3-kinase and calcineurin in mouse bone marrow-derived mast cells." Journal of Immunology 162: 2087-2094.

Jankowski-Hennig, M., M. Clegg, G. Daston, J. Rogers and C. Keen (2000). "Zinc-deficient rat embryos have increased caspase 3-like activity and apoptosis." Biochemical and Biophysical Research Communications 271(1): 250-256.

Jasim, S. and H. Tjalve (1986). "Effect of zinc pyridinethione on the tissue disposition of nickel and cadmium in mice." Acta Pharmacologica et toxicologica 59(3): 204-208.

Jeon, K., J. Jeong and D. Jue (2000). "Thiol-reactive metal compounds inhibit NF-κB activation by blocking IκB kinase." The Journal of Immunology 164: 5981-5989.

Jeremias, I., C. Kupatt, B. Baumann, I. Herr, T. Wirth and D. KM. (1998). "Inhibition of nuclear factor kappaB activation attenuates apoptosis resistance in lymphoid cells." Blood 91(12): 4624-4631.

Jiang, D., P. Sullivan, S. Sensi and O. Steward (2001). "Zn(2+) induces permeability transition pore opening and release of pro-apoptotic peptides from neuronal mitochondria." The Journal of Biological Chemistry 276(50): 47524-47529.

Jouvin, M., M. Adamczewski, R. Numerof, O. Letourneur, A. Valle and J. Kinet (1994). "Differential control of the tyrosine kinases Lyn and Syk by the two signaling chains of the high affinity immunoglobulin E receptor." Journal of Biological Chemistry 269: 5918-5925.

Jung, M., Y. Zhang, A. Dimtchev and A. Dritschilo (1998a). "Impaired regulation of nuclear factor-κB results in apoptosis induced by γ radiation." Radiation research 149: 596-601.

Kagi, J. and A. Schaffer (1988). "Biochemistry of metallothionein." Biochemistry 27: 8509-8515.

Kamada, S., M. Washida, J.-i. Hasegawa, H. Kusano, Y. Funahashi and Y. Tsujimoto (1997a). "Involvement of caspase-4(-like) protease in Fas-mediated apoptotic pathway." Oncogene 15: 285-290.

Kambe, T., H. Narita, Y. Yamaguchi-Iwai, J. Hirose, T. Amano, N. Sugiura, R. Sasaki, K. Mori, T. Iwanaga and M. Nagao (2002). "Cloning and characterization of a novel mammalian zinc transporter, zinc transporter 5, abundantly expressed in pancreatic beta cells." Journal of Biological Chemistry 277(21): 19049-19055.

Kanduc, D., A. Mittlman, R. Serpico, E. Sinigaglia, A. Sinha, C. Natale, R. Santacroce, M. Di Corcia, A. Lucchese, L. Dini, P. Pani, S. Santacroce, S. Simone, R. Bucci and F. E. (2002). "Cell death: apoptosis versus necrosis." International Journal of Oncology 21: 165-170.

Karin, M. (1998). "The NF-kappa B activation pathway: its regulation and role in inflammation and cell survival." The Cancer Journal from Scientific American 4(Suppl 1): S92-S99.

Karl, L., M. Chvapil and C. Zukoski (1973). "Effect of Zinc Viability and Phagocytic Capacity of Peritoneal Macrophages." Proceedings of the Society for Experimental Biology and Medicine 142: 1123-1127.

Kawamoto, K., T. Okada, Y. Kannan, H. Ushio, M. Matsumoto and H. Matsuda (1995). "Nerve growth factor prevents apoptosis of rat peritoneal mast cells through the trk proto-oncogene receptor." Blood 86: 4683-4644.

Kazimierczak, W. and C. Maslinski (1974). "The mechanism of the inhibitory action of zinc on histamine release from mast cells by compound 48/80." Agents and Actions 4: 203-204.

Keegan, A. and W. Paul (1992). "Multichain immune recognition receptors: similarities in structure and signaling pathways." Immunology Today 13: 63-68.

Keilin, D. and T. Mann (1940). "Carbonic anhydrase. Purification and nature of the enzyme." Biochemical Journal 34: 1163-1176.

Kerp, L. (1963). "Bedeutung vonZik fur die Histaminspeieherung in Mastzellen." International Archives of Allergy 22: 112.

Kerr, J., A. Wyllie and A. Currie (1972). "Apoptosis: a basic biological phenomenon with wide-ranging implications in tissue kinetics." British Journal of Cancer 26: 239-257.

Kerr, J., P. Searle, B. Harmon and C. Bishop (1987). Apoptosis. Perspectives of Mammalian Cell Death. C. Potten. Oxford, Oxford Uni Press: 93-128.

Khoo, C., R. Blanchard, V. Sullivan and R. Cousins (1997). "Human cysteine-rich intestinal protein: cDNA cloning and expression of recombinant protein and identification in human peripheral blood mononuclear cells." Protein Expression and Purification. 9: 379-387.

Kim, A., C. Sheline, M. Tian, T. Higashi, R. McMahon, R. Cousins and D. Choi (2000). "L-type Ca(2+) channel-mediated Zn(2+) toxicity and modulation by ZnT-1 in PC12 cells." Brain Research 886(1-2): 99-107.

Kim, C., J. Kim, C. Hsu and Y. Ahn (1999a). "Zinc is required in pyrrolidine dithiocarbamate inhibition of NF-κB activation." FEBS letter 449: 28.

Kim, C., J. Kim, S. Moon, K. Chung, C. Hsu, J. Seo and Y. Ahn (1999b). "Pyrithione, a zinc ionophore, inhibits NF-kappaB activation." Biochemical and Biophysical Research Communications 259(3): 505-509.

Kimhi, Y., C. Palfrey, I. Spector, Y. Barak and U. Littauer (1976). "Maturation of neuroblastoma cells in the presence of dimethylsulfoxide." Proceedings of National Academy of Sciences USA 73(2): 462-466.

Kimura, E. and T. Kioke (1998). "Recent development of zinc(II) fluorophore." Chemical Society Reviews 27: 179-184.

Kinet, J., U. Blank, C. Ra, K. White, H. Metzger and J. Kochan (1988b). "Isolation and characterization of cDNAs coding for the β-subunit of the high affinity receptor for immunoglobulin E." Proceedings of the National Academy of Sciences USA 85: 6483-6487.

Kinlaw, W., A. Levine, J. Morley, S. Silvis and C. McClain (1983). "Abnormal zinc metabolism in type II diabetes mellitus." American Journal of Medicine 75(2): 273-277.

Kitajima, I., Y. Soejima, I. Takasaki, H. Beppu, T. Tokioka and I. Maruyama (1996). "Ceramide-induced nuclear translocation of NF-kappa B is a potential mediator of the apoptotic response to TNF-alpha in murine clonal osteoblasts." Bone 19(3): 263-270.

Kitamura, Y. and S. Go (1978). "Decrease of mast cells in W1/W1$^{v}$ mice and their increase by bone marrow transplantation." Blood 52: 447-452.

Kluck, R., E. Bossy-Wetzel, D. Green and D. Newmyer (1997). "The release of cytochrome c from mitochondria: a primary site for Bcl-2 regulation of apoptosis." Science 275: 1132-1136.

Kochan, J., L. Pettine, J. Hakimi, K. Kishi and J. Kinet (1988a). "Isolation of the gene for the alpha-subunit of the human high affinity IgR receptor." Nucleic Acids Research 16: 35-84.

Koh, J., S. Suh, B. Gwag, Y. He, C. Hsu and D. Choi (1996). "The role of zinc in selective neuronal death after transient global cerebral ischemia." Science 272: 1013-1016.

Kohler, C., A. Gahm, T. Noma, A. Nakazawa, S. Orrenius and B. Zhivotovsky (1999). "Release of adenylate kinase 2 from the mitochondrial intermembrane space during apoptosis." FEBS letter 447: 10-12.

Kolenko, V., R. Uzzo, N. Dulin, E. Hauzman, R. Bukowski and J. Finke (2001). "Mechanism of apoptosis induced by zinc deficiency in peripheral blood T lymphocytes." Apoptosis 6(6): 419-429.

Kopper, K. and J. Adorante (2002). "Regulation of intracellular calcium in N1E-115 neuroblastoma cells: the role of Na(+)/Ca(2+) exchange." American Journal of Physiology and Cellular Physiology 282(5): C1000-C1008.

Korsmeyer, S., J. Shutter, D. Veis, D. Merry and Z. Oltvai (1993). "Bcl-2/Bax: a rheostat that regulates an anti-oxidant pathway and cell death." Seminars in Cancer Biology 4(6): 327-332.

Kreavich, M., J. Meyer and J. Waterhouse (1981). "Increased numbers of mast cells in the hyperplastic buccal mucosa of the zinc-deficient rat." Journal of Oral Pathology 10(1): 22-31.

Krebs, N. and K. Hambidge (2001). "Zinc metabolism and homeostasis: The application of tracer techniques to human physiology." BioMetals 14: 397-412.

Krebs, N., J. Wescott, L. Miller and J. Huffer (1998). "Absorption of exogenous zinc and secretion of endogenous zinc in the human small intestine." Federation of American Society for Experimental Biology Journal 12: A345.

Krikos, A., C. Laherty and V. Dixit (1992). "Transcriptional activation of the tumor necrosis factor alpha-inducible zinc finger protein, A20, is mediated by κB elements." Journal of Biological Chemistry 267: 17971-17976.

Kudrin, A. (2000). "Trace elements in regulation of NF-kappaB activity." Journal of Trace Elements in Medicine and Biology 14(3): 129-142.

Kuida, K., J. Lippke, G. Ku, M. Harding, D. Livingston, M. Su and R. Flavell (1995). "Altered cytokine export and apoptosis in mice deficient in interleukin-1 beta converting enzyme." Science 267(5206): 2000-2003.

Kuida, K., T. Zheng, S. Na, C. Kuan, D. Yang, H. Karasuyama, P. Rakic and R. Flavell (1996). "Decreased apoptosis in the brain and premature lethality in CPP32-deficient mice." Nature 384: 368-372.

Kuida, K., T. Haydar, C. Kuan, Y. Gu, C. Taya, H. Karasuyama, M. Su, P. Rakic and R. Flavell (1998). "Reduced apoptosis and cytochrome c-mediated caspase activation in mice lacking caspase 9." Cell 94(3): 325-337.

Kumar, S., M. Kinoshita, M. Noda, N. Copeland and J. NA (1994). "Induction of apoptosis by the mouse Nedd2 gene, which encodes a protein similar to the product of the Caenorhabditis elegans cell death gene ced-3 and the mammalian IL-1 beta-converting enzyme." Genes and Development 8: 1613-1626.

Kuo, I., B. Seitz, L. LaBree and P. McDonnell (1997). "Can zinc prevent apoptosis of anterior keratocytes after superficial keratectomy?" Cornea 16(5): 550-555.

Lagunoff, D., T. Martin and G. Read (1983). "Agents that release histamine from mast cells." Annual Review of Pharmacology 23: 331-351.

Lassus, P., X. Opitz-Araya and Y. Lazebnik (2002). "Requirement for caspase-2 in stress-induced apoptosis before mitochondrial permeabilization." Science 29: 1352-1354.

Lazebnik, Y., S. Cole, C. Cooke, W. Nelson and W. Earnshaw (1993). "Nuclear events of apoptosis *in vitro* in cell-free mitotic extracts: a model system for analysis of the active phase of apoptosis." Journal of Cell Biology 123: 7-22.

Le Trong, H., H. Neurath and R. Woodbury (1987). "Substrate specificity of the chymotrypsin-like proteases in secretory granules from rat mast cells." Proceedings of the National Academy of Sciences USA 84: 364-367.

Lee, D., J. Hayes, D. Pruss and A. Wolffe (1993). "A positive role for histone acetylation in transcription factor access to nucleosomal DNA." Cell 72(1): 73-84.

Lee, H., A. Prasad, G. Brewer and C. Owyang (1989). "Zinc absorption in human small intestine." American Journal of Physiology 256(1 Pt 1): G87-G91.

Lee, J. and F. Burckart (1998). "Nuclear factor kappa B: Important transcription factor and therapeutic target." Journal of Clinical Pharmacology 38: 981-993.

Leskinen, M., Y. Wang, D. Leszczynski, K. Lindstedt and P. Kovanen (2001). "Mast cell chymase induces apoptosis of vascular smooth muscle cells." Arteriosclerosis, Thrombosis, and Vascular Biology 21(4): 516-522.

Levi-Schaffer, F., K. Austin, J. Caulfield, A. Hein, P. Gravellse and R. Stevens (1987). "Co-culture of human lung-derived mast cells with mouse 3T3 fibroblasts: morphology and IgE-mediated release of histamine, prostaglandin $D_2$ and leukotrienes." Journal of Immunology 139: 494-500.

Levkau, B., M. Scatena, C. Giachelli, R. TRoss and E. Raines (1999). "Apoptosis overrides survival signals through a caspase-mediated dominant-negative NF-κB loop." Nature Cell Biology 1: 227-233.

Lewis, R. and K. Austen (1984). "The biologically active leukotrienes: biosynthesis, metabolism, receptors, functions and pharmacology." Journal of Clinical Investigation 73: 889-897.

Li, L., J. Macpherson, S. Adelstein, C. Bunn, K. Atkinson, K. Phadke and S. Krilis (1995b). "Conditioned Media from a Cell Strain Derived from a Patient with Mastocytosis Induces Preferential Development of Cells That Possess High Affinity IgE Receptors and the Granule Protease Phenotype of Mature Cutaneous Mast Cells." Journal of Biological Chemistry 270(5): 2258-2263.

Li, P., D. Nijhawan, I. Budihardjo, S. Srinivasula, M. Ahmad, E. Alnemri and X. Wang (1997a). "Cytochrome *c* and dATP-dependent formation of Apaf-1/caspase-9 complex initiates an apoptotic protease cascade." Cell 91: 479-489.

Li, P., H. Allen, S. Banerjee, S. Franklin, L. Herzog, C. Johnston, J. McDowell, M. Paskind, L. Rodman, J. Salfeld, E. Towne, D. Tracey, S. Wardwell, F. Wei, W. Wong, R. Kamen and T. Seshadri (1995a). "Mice deficient in IL-1 beta-converting enzyme are defective in production of mature IL-1 beta and resistant to endotoxic shock." Cell 80(3): 401-411.

Li, Q., G. Estapa, S. Memet, A. Isreal and I. Verma (2000ab). "Complete lack of NF-Kβ activity in IKK1 and IKK2 double-deficient mice: additional defect in neurulation." Genes and Development 14: 1729-1733.

Li, Y., W. Zhang, L. Mantell, J. Kazzaz, A. Fein and S. Horowitz (1997b). "Nuclear factor-kappaB is activated by hyperoxia but does not protect from cell death." Journal of Biological Chemistry 272(33): 20646-20649.

Li, Z., W. Chu, M. Delhase, T. Deeri9nck, M. Ellisman, R. Johnson and M. Karin (1999a). "The IKKβ subunit of IKβ kinase (IKK) is essential for nuclear factor Kβ activation and prevention of apoptosis." Journal of Experimental Medicine 189: 1839-1845.

Licastro, F., L. Davis, E. Mocchegiani and N. Fabris (1996). "mpaired peripheral zinc metabolism in patients with senile dementia of probable Alzheimer's type as shown by low plasma concentrations of thymulin." Biological Trace Element Research 51: 55-62.

Lieber, M., B. Smith, A. Szakal, W. Nelson-Rees and G. Todaro (1976). "A continuous tumor-cell line from a human lung carcinoma with properties of type II alveolar epithelial cells." International Journal of Cancer 17(1): 62-70.

Lin, E., A. Orlofsky, M. Berger and M. Prytowsky (1993). "Characterization of A1, a novel hemopoietic-specific early-response gene with sequence similarity to bcl-2." Journal of Immunology 151: 1979-1988.

Lin, K., S. Lee, R. Narayanan, J. Baraban, J. Hardwick and R. Ratan (1995). "Thiol agents and Bcl-2 identify an alphavirus-induced apoptotic pathway that requires activation of the transcription factor NF-kappa B." The Journal of Cell Biology 131(5): 1149-1161.

Lioumi, M., C. Ferguson, P. Sharpe, T. Freeman, I. Marenholz, D. Mischke, C. Heizmann and J. Ragoussis (1999). "Isolation and characterization of human

and mouse ZIRTL, a member of the IRT1 family of transporters, mapping within the epidermal differentiation complex." Genomics 62(2): 272-280.

Liu, Q., T. Sasaki, I. Kozieradzki, A. Wakeham, A. Itie, D. Dumont and J. Penninger (1999c). "SHIP is a negative regulator of growth factor receptor-mediated PKB/Akt activation and myeloid cell survival." Genes and Development 13: 786-791.

Liu, Z., H. Hsu, D. Goeddel and M. Karin (1996a). "Dissection of TNF receptor 1 effector functions: JNK activation is not linked to apoptosis while NF-kappaB activation prevents cell death." Cell 87(3): 565-576.

Lobner, D., L. Canzoniero, P. Manzerra, F. Gottron, H. Ying, M. Knudson, M. Tian, L. Dugan, G. Kerchner, C. Sheline, S. Korsmeyer and D. Choi (2000). "Zinc-induced neuronal cell death in cortical neurons." Cellular and Molecular Biology 46: 797-806.

Lonnerdal, B. (1997). "Effects of milk and milk components on calcium, magnesium, and trace element absorption during infancy." Physiological Reviews 77(3): 643-669.

Loo, D., A. Copani, C. Pike, E. Whittemore, A. Walencewicz and C. Cotman (1993). "Apoptosis is induced by beta-amyloid in cultured central nervous system neurons." Proceedings of National Academy of Sciences USA 90: 7951-7955.

Luna, L. (1992). Histopathologic methods and color atlas of special stains and tissue artifact, Gaitheresburg, MD

American Histolabs.

MacFarlane, M., K. Cain, X. Sun, E. Alnemri and G. Cohen (1997). "Processing/activation of at least four interleukin-1beta converting enzyme-

like proteases occurs during the execution phase of apoptosis in human monocytic tumor cells." Journal of Cell Biology 137: 469-479.

Malinin, N., M. Boldin, A. Kovalenko and D. Wallach (1997). "MAP3K-related kinase involved in NF-kappaB induction by TNF, CD95 and IL-1." Nature 385(6616): 540-543.

Mancini, M., D. Nicholson, S. Roy, N. Thornberry, E. Peterson, L. Casciola-Rosen and A. Rosen (1998). "The caspsae-3 presursor has a cytosolic and mitochondrial distribution: implications for apoptotic signaling." Journal of Cell Biology 140: 1485-1495.

Mandal, M., X. Wu and R. Kumar (1997). "Bcl-2 deregulation leads to inhibition of sodium butyrate-induced apoptosis in human colorectal carcinoma cells." Carcinogenesis 18(1): 229-232.

Manev, H., E. Kharlamov, T. Uz, R. Mason and C. Cagnoli (1997). "Characterization of zinc-induced neuronal death in primary cultures of rat cerebellar granule cells." Experimental Neurology 146: 171-178.

Manjo, G. and I. Joris (1995). "Apoptosis, oncosis and necrosis: an overview of cell death." American Journal of Pathology 146: 3-15.

Manna, S., H. Zhang, T. Yan, L. Oberley and B. Aggarwal (1998). "Overexpression of manganese superoxide dismutase suppresses tumor necrosis factor-induced apoptosis and activation of nuclear transcription factor-kappaB and activated protein-1." Journal of Biological Chemistry 273(21): 13245-13254.

Maret, W., C. Jacob, B. Vallee and E. Fischer (1999). "Inhibitory sites in enzymes: Zinc removal and reactivation by thionein." Proceedings of National Academy of Sciences USA 96: 1936-1940.

Marone, G., M. Columbo, A. De Paulis, R. Cirillo, R. Giugliano and M. Condorelli (1986). "Physiological concentrations of zinc inhibit the release of histamine from human basophils and lung mast cells." Agents and Actions 18(1-2): 103-106.

Martin, L. (2001a). "Neuronal cell death in nervous system development, disease, and injury." International journal of Molecular Medicine 7: 455-478.

Martin, S., G. Mazdai, J. Strain, T. Cotter and B. Hannigan (1991). "Programmed cell death (apoptosis) in lymphoid and myeloid cell lines during zinc deficiency." Clinical Experimental Immunology 83(2): 338-343.

Martins, L., I. Laccarino, T. Tenev, S. Gschmeissner, N. Totty, N. Lemoine, J. Savopoulos, C. Gray, C. Creasy, C. Dingwall and J. Downward (2001). "The serine protease Omi/HtrA2 regulates apoptosis by binding XIAP through a reaper-like motif." Journal of Biological Chemistry 277(1): 439-444.

Masuda, A., T. Matsuguchi, K. Yamaki, T. Hayakawa and Y. Yoshikai (2001). "Interleukin-15 prevents mouse mast cell apoptosis through STAT6-mediated Bcl-$X_L$ expression." The Journal of Biological Chemistry 276(28): 25107-26113.

Matsui, K., A. Fine, B. Zhu, A. Marshak-Rothstein and S. Ju (1998a). "Identification of two NF-kappa B sites in mouse CD95 ligand (Fas ligand) promoter: functional analysis in T cell hybridoma." Journal of Immunology 161: 3469-3473.

Matsushita, K., K. Kitagawa, T. Matsuyama, T. Ohtsuki, A. Taguchi, K. Mandai, T. Mabuchi, Y. Yagita, T. Yanagihara and M. Matsumoto (1996). "Effect of

systemic zinc administration on delayed neuronal death in the gerbil hippocampus." Brain Research 743(1-2): 362-365.

Maurer, M., M. Tsai, M. Metz, S. Fish, S. Korsmeyer and S. Galli (2000). "A role for Bax in the regulation of apoptosis in mouse mast cells." The Journal of Investigative Dermatology 114(6): 1205-1206.

McCabe, M., S. Jiang and S. Orrenius (1993). "Chelation of intracellular zinc triggers apoptosis in mature thymocytes." Laboratory Investigation 69: 101-110.

McDade, T., R. Perugini, F. J. Vittimberga, R. Carrigan and M. Callery (1999). "Salicylates inhibit NF-kappaB activation and enhance TNF-alpha-induced apoptosis in human pancreatic cancer cells." Journal of Surgical Research 83(1): 56-61.

McMahon, R. and R. Cousins (1998a). "Regulation of the zinc transporter ZnT-1 by dietary zinc." Proceedings of National Academy of Sciences USA 95(9): 4841-4846.

McNeil, H. (1996). "The mast cell and inflammation." Australian New Zealand Journal of Medicine 26: 216-225.

Medina, V., B. Edmonds, G. Young, R. James, S. Appleton and P. Zalewski (1997). "Induction of caspase-3 protease activity and apoptosis by butyrate and trichostatin A (inhibitors of histone deacetylase):dependence on protein synthesis and synergy with a mitochondrial/cytochrome c-dependent pathway." Cancer Research 57(17): 3697-3707.

Mekori, Y. (1997b). "Mast cell apoptosis: From the DNA to the Bedside." Allergie et Immunologie 29b(1): 4-6.

Mekori, Y. and D. Metcalfe (1994). "Transforming growth factor-beta prevents stem cell factor-mediated rescue of mast cells from apoptosis after IL-3 deprivation." Journal of Immunology 153: 2194-2203.

Mekori, Y., A. Gilfillan, C. Akin, K. Hartmann and D. Metcalfe (2001). "Human mast cell apoptosis is regulated through Bcl-2 and Bcl-$X_L$." Journal of Clinical Immunology 21(3): 171-174.

Menon, S., S. Qin, G. Guy and Y. Tan (1993). "Differential induction of nuclear NF-kappa B by protein phosphatase inhibitors in primary and transformed human cells. Requirement for both oxidation and phosphorylation in nuclear translocation." Journal of Biological Chemistry 268(35): 26805-26812.

Metcalfe, D., D. Bram and Y. Mekori (1997a). "Mast cells." Physiological Reviews 77(4): 1033-1079.

Michalczyk, A., J. Allen, R. Blomeley and M. Ackland (2002). "Constitutive expression of hZnT4 zinc transporter in human breast epithelial cells." Biochemical Journal 364(Pt1): 105-113.

Milanino, R., U. Moretti, E. Concari, M. Marella and G. Velo (1988b). "Copper and zinc status in adjuvant-arthritic rat: studies on blood, liver, kidneys, spleen and inflamed paws." Agents and Actions 24(3/4): 365-376.

Miller, H., J. Huntley, G. Newlands, A. Mackellar, J. Irvine, D. Haig, A. Macdonald, A. Lammas, D. Wakelin and G. Woodbury (1989b). Mast cell granule proteases in mouse and rat: a guide to mast cell heterogeneity and activation in the gastrointestinal tract. Mast cell and basophil differentiation and function in health and disease. S. Galli and K. Austen. New York, Raven: 81-.

Mori, H., Y. Matsumoto, Y. Tamada and M. Ohashi (1996). "Apoptotic cell death in formation of vesicular skin lesions in patients with acquired zinc deficiency." Journal of Cutaneous Pathology 23(4): 359-363.

Mousli, M., C. Bronner, J. Bockaert, B. Rouot and Y. Landry (1990a). "Interaction of substance P, compound 48/80 and mastocytoparan with α-subunit C-terminal of G-protein." Immunology Letters 25: 355-358.

Munday, N., J. Vaillancourt, A. Ali, F. Casano, D. Miller, S. Molineaux, T. Yamin, V. Yu and D. Nicholson (1995). "Molecular cloning and pro-apoptotic activity of ICErelII and ICErelIII, members of the ICE/CED-3 family of cysteine proteases." Journal of Biological Chemistry 270(26): 15870-15876.

Murgia, C., I. Vespignani, J. Cerase, F. Nobili and G. Perozzi (1999). "Cloning, expression, and vesicular localization of zinc transporter Dri 27/ZnT4 in intestinal tissue and cells." American Journal of Physiology 277(6 Prt 1): G1231-G1239.

Muzio, M., A. Chinnaiyan, F. Kischkel, K. O'Rourke, Shevchenko A, C. Ni scaffidi, D. Bretzmr, M. Zhang, R. Gentz, M. Mann, P. Krammer, M. Peter and D. VM (1996). "FLICE, a novel FADD-homologous ICE/CED-3-like protease, is recruited to the CD95 (Fas/APO-1) death--inducing signaling complex." Cell 48(6): 817-827.

Nakagawa, Y., S. Nakamura, Y. Kase, T. Noguchi and T. Ishihara (1987). "Colchicine lesions in the rat hippocampus mimic the alterations of several markers in Alzheimer's disease." Brain Research 408: 57-64.

Nakagawara, A., Y. Nakamura, H. Ikeda, T. Hiwasa, K. Kuida, M. Su, H. Zhao, A. Cnaan and S. Sakiyama (1997). "High levels of expression and nuclear

localization of interleukin-1 beta converting enzyme (ICE) and CPP32 in favorable human neuroblastomas." Cancer Research 57(20): 4578-4584.

Nakai, M., Z. Qin, J. Chen, Y. Wang and T. Chase (2000). "Kainic acid-induced apoptosis in rat striatum is associated with nuclear factor-kappaB activation." Journal of Neurochemistry 74(2): 647-658.

Nicholson, D. and N. Thornberry (1997). "Caspases- killer proteases." Trends in Biochemical Sciences (TIBS) 22: 299-306.

Nickolson, V. and H. Veldstra (1972). "The influence of various cations on the binding of colchicine by rat brain homogenates. Stabilization of intact neurotubules by zinc and cadmium ions." FEBS letter 23: 309-313.

Nilsson, G., T. Blom, M. Kusche-Gullberg, L. Kjellen, J. Butterfield, C. Sundstrom, K. Nilsson and L. Hellman (1994). "Scandinavian Journal of Immunology." 39 5(489-498).

Nishi, K., J. Schnier and M. Bradbury (2002). "Cell shape change precedes staurosporine-induced stabilization and accumulation of p27kip1." Experimental Cell Research 280(2): 233-243.

Nishibe, S., M. Wahl, S. Hernandez-Sotomayor, N. Tonks, S. Rhee and G. Carpenter (1990). "Increase of the catalytic activity of phospholipase C-gamma 1 by tyrosine phosphorylation." Science 250: 1253-1256.

Norris, D. (1985). "Zinc and cutaneous inflammation." Archives of Dermatology 121(8): 985-989.

Nuydens, R., C. Heers, A. Chadarevian, M. De Jong, R. Nuyens, F. Cornelissen and H. Geerts (1995). "Sodium butyrate induces aberrant tau phosphorylation and

programmed cell death in human neuroblastoma cells." Brain Research 688: 86-94.

O'Connell, H., M. Bennet, K. Nally, A. Houston, G. O'Sullivan and F. Shanahan (2000). "Altered mechanisms of apoptosis in colon cancer: Fas resistance and counterattack in the tumor-immune conflict." Annals of the New York Academy of Sciences 910: 178-192.

Oh, C. and D. Metcalfe (1994). "Transcriptional regulation of the TCA-3 gene in mast cells after FcRI cross-linking." Journal of Immunology 153: 325-332.

Okayama, Y. and M. Church (1992). "IL-3 primes and evokes histamine release from human basophils but not mast cells." International Archives Allergy Applied Immunology 99: 343-345.

Opipari, A., H. Hu, R. Yabkowitz and V. Dixit (1992). "The A20 zinc finger protein protects cells from tumor necrosis factor cytotoxicity." Journal of Biological Chemistry 267: 12424-12427.

Oskeritzian, C., Z. Wang, J. Kochan, M. Grimes, Z. Du, H. Chang, S. Grant and L. Schwartz (1999). "Recombinant human (rh)IL-4-mediated apoptosis and recombinant human IL-6-mediated protection of recombinant human stem cell factor-dependent human mast cells derived from cord blood mononuclear cell progenitors." Journal of Immunology 163(9): 5105-5115.

Ossina, N., A. Cannas, V. Powers, P. Fitzpatrick, J. Knight, J. Gilbert, E. Shekhtman, L. Tomei, S. Umansky and M. Kiefer (1997). "Interferon-γ modulates a p53-independent apoptotic pathway and apoptosis related gene expression." Journal of Biological Chemistry 272: 16351-16357.

Oteiza, P., M. Clegg and C. Keen (2001). "Short-term Zn deficiency affects nuclear factor-kappab nuclear binding activity in rat testes." Journal of Nutrition 131(1): 21-26.

Oteiza, P., S. Cuellar, B. Lonnerdal, L. Hurley and C. Keen (1990). "Influence of maternal dietary zinc intake on in vitro tubulin polymerization in fetal rat brain." Teratology 41: 97-104.

Palmiter, R. and S. Findley (1995a). "Cloning and functional characterization of a mammalian zinc transporter that confers resistance to zinc." EMBO Journal 14(4): 639-649.

Palmiter, R., T. Cole and S. Findley (1996a). "ZnT-2, a mammalian protein that confers resistance to zinc by facilitating vesicular sequestration." EMBO Journal 15(8): 14934-14939.

Palmiter, R., T. Cole, C. Quaife and S. Findley (1996b). "ZnT-3, a putative transporter of zinc into synaptic vesicles." Proceedings of National Academy of Sciences USA 93: 14924-14939.

Pang, D. and J. Shafer (1985). "Inhibition of the activation and catalytic activity of insulin receptor kinase by zinc and other divalent metal ions." Journal of Biological Chemistry 260(8): 5126-5130.

Paolini, R., M. Jouvin and J. Kinet (1991). "Phosphorylation and dephosphorylation of the high affinity receptor for IgE immediately after receptor engagement and disengagement." Nature 353: 855-858.

Pelletier, C., N. Varin-Blank, J. Rivera, B. Iannascoli, F. Marchand, B. David, A. Weyer and U. Blank (1998). "Fc epsilonRI-mediated induction of TNF-alpha gene expression in the RBL-2H3 mast cell line: regulation by a novel NF-

kappaB-like nuclear binding complex." The Journal of Immunolgy 161: 4768-4776.

Perez-Clausell, J. and G. Danscher (1985ab). "Intravesicular localization of zinc in rat telencephalic boutons. A histochemical study." Brain Research 337(1): 91-98.

Perry, D., M. Smyth, H. Stennicke, G. Salvesen, P. Duriez, G. Poirier and Y. Hannun (1997). "Zinc is a potent inhibitor of the apoptotic protease, Caspase-3." The Journal of Biological Chemistry 272(30): 18530-18533.

Pihl, E., G. Gustafson, B. Josefsson and K. Paul (1967b). "Heavy metals in granules of eosinophilic granulocytes." Scandanavian Journal of Haematology 4: 371-379.

Pilch, S. and F. Senti (1984). Assessment of the Zinc Nutritional Status of the US Population Based on Data Collected in the Second National Health and Nutrition Examination Survey 1976-1980. FASEB FDA. Bethesda, MD, Life Science Rsearch Office: 223, 83, 2384.

Piletz, J. and R. Ganschow (1978). "Zinc deficiency in murine milk underlies expression of the lethal milk (lm) mutation." Science 199(4325): 181-183.

Porter, A. (1999). "Protein translocation in apoptosis." Trends in Cell Biology 9: 394-401.

Powell, S. (2000). "The antioxidant properties of zinc." Journal of Nutrition 130: 1447S-1454S.

Prasad, A. (1986a). "Effect of trace metal imbalance in human diseases." Acta Pharmacologica et toxicologica 59(Suppl 7): 94-103.

Prasad, A., B. Bao, F. Beck and F. Sarkar (2002). "Zinc enhances the expression of interleukin-2 and interleukin-2 receptors in HUT-78 cells by way of NF-kappaB activation." Journal of Laboratory Clinical Medicine 140: 272-289.

Prasad, A., A. Mial, Z. Farid, A. Schulert and H. Sandstead (1963). "Zinc metabolism in patients with the syndrome of iron deficiency anemia hypogonadism, and dwarfism." Journal of Clinical and Laboratory Medicine 61: 537-549.

Prasad, A., J. Fitzgerald, J. Hess, J. Kaplan, F. Pelen and M. Dardenne (1993). "Zinc deficiency in elderly patients." Nutrition 9(3): 218-224.

Qin, J., V. Chaturvedi, M. Denning, D. Choubey, M. Diaz and B. Nickoloff (1999). "Role of NF-kappaB in the apoptotic-resistant phenotype of keratinocytes." Journal of Biological Chemistry 274(53): 37975-37964.

Raff, M. (1992). "Social controls on cell survival and cell death." Nature 356: 397-400.

Rahman, I. and W. MacNee (1998). "Role of transcription factors in inflammatory lung diseases." Thorax 53(7): 601-612.

Raja, K., P. Leach, G. Smith, D. McCarthy and T. Peters (1982). "The concentration and subcellular localisation of zinc, magnesium, and calcium in human polymorphonuclear leukocytes." Clinica Chimica Acta 123: 19-26.

Ranaldi, G., G. Perozzi, A. Truong-Tran and P. Zalewski (2002). "Intracellular distribution of labile Zn (II) and zinc transporter expression in the kidney and in MDCK cells." American Journal of Physiology- Renal Physiology in press.

Record, I., R. Tulsi, I. Dreosti and F. Fraser (1985). "Cellular necrosis in zinc-deficient rat embryos." Teratology 32(3): 397-405.

Repke, H. and M. Beinert (1987). "Mast cell activation: a receptor independent mode of substance P action?" FEBS letter 221: 236-240.

Reuther, J. and J. A. Baldwin (1999). "Apoptosis promotes a caspase-induced amino-terminal truncation of IκBα that functions as a stable inhibitor of NF-κB." Journal of Biological Chemistry 274: 20664-20670.

Reyes, J. (1996). "Zinc transport in mammalian cells." American Journal of Physiology 270: C401-C10.

Richard, M., J. Louahed, J. Demoulin and J. Renauld (1999). "Interleukin-9 regulates NF-kappaB activity through BCL3 gene induction." Blood 93(12): 4318-4327.

Robertson, J., M. Enoksson, M. Suomela, B. Zhivotovsky and S. Orrenius (2002). "Caspase-2 acts upstream of mitochondria to promote cytochrome c release during etoposide-induced apoptosis." Journal of Biological Chemistry 277: 29803-29809.

Romashkova, J. and S. Makarov (1999). "NF-kappaB is a target of AKT in anti-apoptotic PDGF signalling." Nature 401(6748): 86-90.

Sahara, S., M. Aoto, Y. Eguchi, N. Imamoto, Y. Yoneda and Y. Tsuijimoto (1999). "Acinus is a caspase-3-activated protein required for apoptotic chromatin condensation." Nature 401: 168-173.

Samali, A., B. Zhivotovsky, D. Jones and S. Orrenius (1998). "Detection of pro-caspase-3 in cytosol and mitochondria of various tissues." FEBS letter 431(2): 167-169.

Samali, A., J. Cai, B. Zhivotovsky, D. Jones and S. Orrenius (1999ab). "Presences of pro-apoptotic complex of pro-caspase-3, Hsp60 and Hsp10 in the mitochondrial fraction pf Jurkat cells." EMBO Journal 19: 2040-2048.

Sandstead, H. (1991). "Zinc deficiency. A public health problem?" American Journal of Diseases of Children 145(8): 853-859.

Sanz, C., A. Benito, M. Silva, B. Albella, C. Richard, J. Segovia, A. Insunza, J. Beuren and J. Fernandez-Luna (1997). "The expression of Bcl-X is downregulated during differentiation of human progenitor cells." Blood 89: 3199-3204.

Saunders, J. and J. Fallon (1966). Cell death in morphogenesis. Major Problems in developmental biology. M. Lock. New York, New York Academic Press: 298-314.

Savill, J. and V. Fadok (2000). "Corpse clearance defines the meaning of cell death." Nature 407: 784-788.

Schneider, A., A. Martin-Villalba, F. Weih, J. Vogel, T. Wirth and M. Schwaninger (1999). "NF-kappaB is activated and promotes cell death in focal cerebral ischemia." Nature Medicine 5(5): 554-559.

Schwartz, L. (1993). Heterogeneity of human mast cells. The mast cell in health and disease. M. Kaliner and D. Metcalfe. New York, Dekker: 219-236.

Schwartzman, R. and J. Cidlowski (1993). "Apoptosis: the biochemistry and molecular biology of programmed cell death." Endocrine reviews 14: 133-151.

Sciences, N. A. o. (1989). Recommended Dietary Allowances. Washington D.C, National Academy Press.

Sebbagh, M., C. Renvoize, J. Hamelin, N. Riche, J. Bertoglio and J. Breard (2001). "Caspase-3 mediated cleavage of ROCK I induces MLC phosphorylation and apoptotic membrane blebbing." Nature Cell Biology 3: 346-352.

Sensi, S., H. Yin, S. Carriedo, S. Rao and J. Weiss (1999a). "Preferential Zn2+ influx through Ca2+-permeable AMPA/kainate channels triggers prolonged

mitochondrial superoxide production." Proceedings of National Academy of Sciences USA 96(5): 2414-2419.

Seo, S., S. Chong, S. Lee, J. Sung, Y. Anh, K. Chung and J. Seo (2001). "Zn2+-induced ERK activation mediated by reactive oxygen species causes cell death in differentiated PC12 cells." Journal of Neurochemistry 78(3): 600-610.

Serrano, L., J. Dominguez and J. Avila (1988). "Identification of zinc-binding sites of proteins: zinc binds to the amino-terminal region of tubulin." Analytical Biochemistry 172: 210-218.

Seve, M., F. Chimienti and A. Favier (2002). "Role of intracellular zinc in programmed cell death." Pathologie et biologie 50(3): 212-221.

Shalit, M. and F. Levi-Schaffer (1995). "Challenge of mast cells with increasing amounts of antigen induces desensitization." Clinical Experimental Allergy 25: 896-902.

Shea, T., E. Wheeler and C. Jung (1997). "Aluminum inhibits neurofilament assembly, cytoskeletal incorporation, and axonal transport. Dynamic nature of aluminum-induced perikaryal neurofilament accumulations as revealed by subunit turnover." Molecular and Chemical Neuropathology 32: 17-39.

Sheline, C., M. Behrens and D. Choi (2000a). "Zinc-induced cortical neuronal death: contribution of energy failure attributable to loss of NAD(+) and inhibition of glycolysis." Journal of Neuroscience 20: 3139-3146.

Shumilla, J., K. Wetterhahn and A. Barchowsky (1998). "Inhibition of NF-kappa B binding to DNA by chromium, cadmium, mercury, zinc, and arsenite in vitro: evidence of a thiol mechanism." Archives of Biochemistry and Biophysics 349(2): 356-362.

Siebenlist, U., G. Franzuso and R. Brown (1994). "Structure, regulation and function of NF-kappa B." Annual Review of Cell Biology 10: 405-455.

Simkin, P. (1997). "Zinc, again." Clinical Experimental Rheumatology 24: 626-628.

Simon, H. (2001). "Regulation of eosinophil and neutrophil apoptosis--similarities and differences." Immunological reviews 179: 156-162.

Slee, E., C. Adrain and S. Martin (2001). "Executioner caspase-3, -6, and -7 perform distinct, non-redundant roles during the demolition phase of apoptosis." Journal of Biological Chemistry 276(10): 7320-7326.

Sloviter, R. (1985). "A selective loss of hippocampal mossy fiber Timm stain accompanies granule cell seizure activity induced by perforant path stimulation." Brain Research 330: 150-153.

Smale, G., N. Nichols, D. Brady, C. Finch and W. J. Horton (1995). "Evidence for apoptotic cell death in Alzheimer's disease." Experimental Neurology 133(2): 225-230.

Smart, T., X. Xie and B. Krishek (1994). "Modulation of inhibitory and excitatory amino acid receptor ion channels by zinc." Progress in neurobiology 42: 393-441.

Smith, C., T. Farrah and R. Goodwin (1994). "The TNF receptor super-family of cellular and viral proteins: Activation, costimulation and death." Cell 76: 959-962.

Soler, A., C. Marano, M. Bryans, R. Miller, L. Garulacan, S. Mauldin, T. Stamato and J. Mullin (1999). "Activation of NF-kappaB is necessary for the restoration of the barrier function of an epithelium undergoing TNF-alpha-induced apoptosis." European Journal of Cell Biology 78(1): 56-66.

Solomons, N. (1988). Zinc and copper. In Modern Nutrition in Health and Disease. M. Shils and V. Young. Philadelphia, Lea and Febiger: 238-262.

Song, H., M. Rothe and D. Goeddel (1996). "The tumor necrosis factor-inducible zinc finger protein A20 interacts with TRAF1/TRAF2 and inhibits NF-κB activation." Proceedings of National Academy of Sciences USA 93: 6721-6725.

Song, Z. and H. Steller (1999). "Death by design: mechanism and control of apoptosis." Trends in Cell Biology 9: 49-52.

Sorensen, J., O. Anderson and J. Nielsen (1998). "An in vivo study of the gastrointestinal absorption site for zinc chloride in mice." Journal of Trace Elements in Medicine and Biology 12: 16-22.

Srinivasula, S., M. Ahmad, T. Fernandes-Alnemri, G. Litwack and E. Alnemri (1996b). "Molecular ordering of the Fas-apoptotic pathway: the Fas/APO-1 protease Mch5 is a CrmA-inhibitable protease that activates multiple Ced-3/ICE-like cysteine proteases." Proceedings of National Academy of Sciences USA 93: 14486-14491.

Stehlik, C., R. de Martin, I. Kumabashiri, J. Schmid, B. Binder and J. Lipp (1998). "Nuclear factor (NF)-kappaB-regulated X-chromosome-linked iap gene expression protects endothelial cells from tumor necrosis factor alpha-induced apoptosis." Journal of Experimental Medicine 188(1): 211-216.

Stoltenberg, M. and G. Danscher (2000). "Histochemical differentiation of autometallographically traceable metals (Au, Ag, Hg, Bi, Zn): protocols for chemical removal of separate autometallographic metal clusters in Epon sections." Histochemical Journal 32(11): 645-652.

Strasser, A., L. O'Connor and V. Dixit (2000). "Apoptosis Signaling." Annual Review of Biochemistry 69: 217-245.

Sturniolo, G., C. Mestriner, P. Lecis, A. D'odorico, C. Venturi, P. Irato, A. Cecchetto, A. Tropea, G. Longo and R. D'inca (1998). "Altered plasma and Mucosal Concentrations of Trace Elements and Antioxidants in Active Ulcerative Colitis." Scandanavian Journal of Gastroenterology 33: 644-649.

Sumitomo, M., M. Tachibana, J. Nakashima, M. Murai, A. Miyajima, F. Kimura, M. Hayakawa and H. Nakamura (1999). "An essential role for nuclear factor kappa B in preventing TNF-alpha-induced cell death in prostate cancer cells." Journal of Urology 161(2): 674-679.

Sun, X., M. MacFarlane, J. Zhuang, B. Wolf, D. Green and G. Cohen (1999). "Distinct caspase cascades are initiated in receptor-mediated and chemical-induced apoptosis." Journal of Biological Chemistry 274: 5053-5060.

Sunderman, F. (1995). "The influence of zinc on apoptosis." Annals of clinical laboratory science 25: 134-142.

Susin, S., H. Lorenzo, N. Zamzami, I. Marzo, C. Brenner, N. Larochette, M. Prevost, P. Alzari and G. Kroemer (1999). "Mitochrondrial release of caspase-2 and -9 during apoptotic process." Journal of Experimental Medicine 189: 381-394.

Suzuki, Y., Y. Imai, H. Nakayama, K. Takahashi, K. Takio and R. Takahashi (2001). "A serine protease, HtrA2, is released from mitochondria and interacts with XIAP, inducing cell death." Molecular Cell 8: 613-621.

Takagi, M., T. Nakahata, T. Kubo, M. Shiohara, K. Koike, A. Miyajima, K. Arai, S. Nishikawa, K. Zsebo and A. Komiyama (1992). "Stimulation of mouse connective tissue-type mast cells

by hemopoietic stem cell factor, a ligand for the c-kit receptor." Journal of Immunology 148: 3446-3453.

Takano, Y., B. Harmon and J. Kerr (1991). "Apoptosis induced by mild hyperthermia in human and murine mast tumour cell lines: a study using electron microscopy and DNA gel electrophoresis." Journal of Pathology 163: 329-336.

Takuma, K., E. Lee, M. Kidawara, K. Mori, Y. Kimura, A. Baba and T. Matsuda (1999). "Apoptosis in Ca2 + reperfusion injury of cultured astrocytes: roles of reactive oxygen species and NF-kappaB activation." European Journal of Neuroscience 11(12): 4204-4212.

Talanian, R., C. Quinlan, S. Trautz, M. Hackett, J. Mankovich, D. Banach, T. Ghayur, K. Brady and W. Wong (1997). "Decreased apoptosis in the brain and premature lethality in CPP32-deficient mice." Journal of Biological Chemistry 272: 9677-9682.

Tartaglia, L., T. Ayres, G. Wong and D. Goeddel (1993). "A novel domain within the 55 Kd TNF receptor signal cell death." Cell 74: 845-853.

Thanos, D. and T. Maniatis (1995). "NF-kappa B: a lesson in family values." Cell 80(4): 529-532.

Thomas, D., C. Du, M. Xu, X. Wang and T. Ley (2000). "DFF45/ICAD can be directly processed by granzyme B during the induction of apoptosis." Immunity 12(6): 621-632.

Thompson, J., R. Phillips, H. Erdjunment-Bromage, P. Tampst and S. Ghosh (1995b). "I kappa B-beta regulates the persistent response in a biphasic activation of NF-kappa B." Cell 80(4): 573-582.

Thompson, R., D. Peterson, W. Mahoney, M. Cramer, B. Maliwal, S. Suh, C. Frederickson, C. Fierke and P. Herman (2002). "Fluorescent zinc indicators for neurobiology." Journal of Neuroscience 118: 63-75.

Thorling, E. and M. Niazy (1973). "Inhibition of leucocyte alkaline phosphatase by cyanide in vivo." Acta Medica Scandinavica 194: 271-276.

Thornberry, N. and Y. Lazebnik (1998a). "Caspases: Enemies within." Science 281: 1312-1316.

Trapani, J. (2001). "Granzymes: a family of lymphocyte granule serine proteases." Genome Biology 2(12): REVIEWS3014.

Tsai, M., S. Tam, J. Wedemeyer and S. Galli (2002). "Mast cells derived from embryonic stem cells: a model system for studying the effects of genetic manipulations on mast cell development, phenotype, and function in vitro and in vivo." International Journal of Hematology 75(4): 345-349.

Uvnas, B., C. Aborg and A. Bergendorf (1970). "Storage of Histamine in Mast Cells. Evidence for an Ionic Binding of Histamine to Protein Carboxyls in the Granule Heparin-Protein Complex." Acta Physiologica Scandinavica Supplement 336.

Uvnas, B., C. Aborg and U. Bergqvist (1975). "No role for zinc in the storage of histamine in rat peritoneal mast cells." Acta Physiologica Scandinavica 93(3): 401-408.

Valent, P., J. Besemer, C. Sillaber, J. Butterfield, R. Eher, O. Majdic, K. Kishi, W. Klepetko, F. Eckersberger, K. Lechner and e. al (1990). "Failure to detect IL-3 binding sites on human mast cells." Journal of Immunology 145(10): 3422-3427.

Vallee, B. (1995a). "The function of metallothionein." Neurochemistry International 27: 23-33.

Vallee, B. and K. Falchuk (1993). "The Biochemical Basis of Zinc Physiology." Physiological Reviews 73(1): 79-118.

Vallee, B. and D. Auld (1995b). "Zinc metallochemistry in biochemistry." EXS 73: 259-277.

Van Antwerp, D., S. Martin, T. Kafri, D. Green and I. Verma (1996). "Suppression of TNF-alpha-induced apoptosis by NF-kappaB." Science 274(5288): 787-789.

Varfolomeev, E., M. Schuchmann, V. Luria, N. Chiannilkulchai, J. Beckmann, I. Mett, D. Rebrikov, V. Brodianski, O. Kemper, O. Kollet, T. Lapidot, D. Soffer, T. Sobe, K. Avraham, T. Goncharov, H. Holtmann, P. Lonai and D. Wallach (1998). "Targeted disruption of the mouse Caspase 8 gene ablates cell death induction by the TNF receptors, Fas/Apo1, and DR3 and is lethal prenatally." Immunity 9(2): 267-276.

Vaughan, A., C. Betti and M. Villalobos (2002). "Surviving apoptosis." Apoptosis 7: 173-177.

Verhagen, A., P. Ekert, M. Pakusch, J. Silke, L. Connolly, G. Reid, R. Moritz, R. Simpson and D. Vaux (2000). "Identification of DIABLO, a mammalian protein that promotes apoptosis by binding to and antagonizing IAP proteins." Cell 102(1): 43-53.

Vincenz, C. and V. Dixit (1997). "Fas-associated death domain protein interleukin-1-beta-converting enzyme 2 (FLICE2). an ICE/Ced-3 homologue is proximally involved in CD95- and p55-mediated death signaling." Journal of Biological Chemistry 272: 6578-6583.

Vyas, S., N. Biguet, P. Michel, L. Monaco, N. Foulkes, G. Evan, P. Sassone-Corsi and Y. Agid (2002). "Molecular mechanisms of neuronal cell death: implications for nuclear factors responding to cAMP and phorbol esters." Molecular and Cellular Neurosciences 21(1): 1.

Walkup, G., S. Burdette, S. Lippard and R. Tsien (2000). "A new cell-permeable fluorescent probe for $Zn^{2+}$." Journal of the American Chemical Society 122: 5644-5645.

Walravens, P. and K. Hambidge (1976). "Growth of infants fed a zinc supplemented formula." American Journal of Clinical Nutrition 29: 1114-1121.

Wang, C., J. J. Cusack, R. Liu and A. J. Baldwin (1999b). "Control of inducible chemoresistance: enhanced anti-tumor therapy through increased apoptosis by inhibition of NF-kappaB." Nature Medicine 5(4): 412-417.

Wang, C., M. Mayo, R. Korneluk, D. Goeddel and J. A. Baldwin (1998a). "NF-κB antiapoptosis: induction of TRAF1 and TRAF2n and c-IAP and c-IAP2 to suppress caspase-8 activation." Science 281: 1680-1683.

Wang, J. and M. Lenardo (2000ab). "Roles of caspases in apoptosis, development, and cytokine maturation revealed by homozygous gene deficiencies." Journal of Cell Science 113: 753-757.

Wang, L., X. Liu, W. Kreis and D. Budman (1999ab). "The effect of antimicrotubule agents on signal transduction pathways of apoptosis: a review." Cancer chemotherapy and pharmacology 44(5): 355-361.

Wang, L., M. Miura, L. Bergeron, H. Zhu and J. Yuan (1994). "Ich-1, an Ice/ced-3-related gene, encodes both positive and negative regulators of programmed cell death." Cell 78: 739-750.

Wang, S., Y. Miura, H. Jung, V. Gagliardini, L. Shi, A. Greenberg and J. Yuan (1996a). "Identification and charaterization of Ich-3, a member of the interleukin-1 beta converting enzyme (ICE)/Ced-3 family and an upstream regulator of ICE." Journal of Biological Chemistry 271: 20580-20587.

Ward, A., S. Lincoln, W. Betts, P. Zalewski, I. Forbes, I. Mahadevan, M. Kimber and K. Hendrickson (2000). Zinquin Ester - a Reagent for the Investigation of the Role of Available Zn(II) in Living Systems. Trace Elements in Man and Animals. A. Roussel, R. Anderson and A. Favier. New York, Kluwer Academic: 995-998.

Ward, C., E. Chilvers, M. Lawson, J. Pryde, S. Fujihara, S. Farrow, C. Haslett and A. Rossi (1999). "NF-κB activation is a critical regulator of human granulocyte apoptosis *in vitro*." The Journal of Biological Chemistry 274(7): 4309-4318.

Warner, J. and C. Kroegel (1994). "Pulmonary immune cells in health and disease: mast cells and basophils." European Respiratory Journal 7: 1326-1341.

Warren, L., M. Glick and M. Nass (1966). "Membranes of Animal Cells. I. Methods of Isolation of the Surface Membrane." Journal of Cellular Physiology 68: 269-288.

Wasserman, S. (1994). "Mast cells and airway inflammation in asthma." American Journal of Respiratory Critical Care Medicine 150: S39-S41.

Weidner, N. and K. Austen (1991). "Ultrastructural and immunohistochemical characterization of normal mast cells at multiple body sites." Journal of Investigative Dermatology 96: 26S-31S.

Weiss, J., D. Hartley, J. Koh and D. Choi (1993). "AMPA receptor activation potentiates zinc neurotoxicity." Neuron 10: 43-49.

Whitehouse, M., K. Rainsford, R. Taylor and B. Vernon-Roberts (1990). "Zinc monoglycerolate: A slow-release source of zinc with anti-arthritic activity in rats." Agents and Actions 31(1/2): 47-58.

Whyte, M. (1996). "ICE/CED-3 proteases in apoptosis." Trends in Cell Biology 6: 245-248.

Williams, R. (1987). "The Biochemistry of zinc." Polyhedron 6: 61-69.

Wilson, R. (1987). "Vitamin, selenium, zinc and copper interactions in free-radical protection against ill-placed iron." The Proceedings of the Nutrition Society 46: 27-34.

Wyllie, A. (1997). "Apoptosis: an overview." British Medical Bulletin 53: 451-465.

Xiang, Z., A. Ahmed, C. Moller, K. Nakayama, S. Hatakeyama and G. Nilsson (2001). "Essential roleof the Pro-survival bcl-2 Homologue A1 in Mast Cell Survival After Allergic Activation." Journal of Experimental Medicine 194(11): 1561-1569.

Xu, Y., S. Bialik, B. Jones, Y. Iimuro, R. Kitsis, A. Srinivasan, D. Brenner and C. MJ (1998). "NF-kappaB inactivation converts a hepatocyte cell line TNF-alpha response from proliferation to apoptosis." American Journal of Physiology 275(4 Pt1): C1058C1066.

Yamaguchi, M., K. Sayama, K. Yano, C. Lantz, N. Noben-Trauth, C. Ra, J. Costa and S. Galli (1999b). "IgE enhances Fcε receptor I expression and IgE-dependent release of histamine and lipid mediators from human umbilical cord blood-derived mast cells: synergistic effect of IL-4 and IgE on human mast cell Fcε receptor I expression and mediator release." The Journal of Immunology 162(9): 5455-5465.

Yang, E. and S. Korsmeyer (1996a). "Molecular thanatopis: A discourse on the BCL2 family and cell death." Blood 88: 386-401.

Yankner, B. (1996). "Mechanisms of neuronal degeneration in Alzheimer's disease." Neuron 16(5): 921-932.

Yatsuyanagi, J., K. Iwai and T. Ogiso (1987). "Suppressive Effect of Zinc on Some Functions of Neutrophils: Studies with Carregeenan-Induced Inflammation in Rats." Chemical and Pharmaceutical Bulletin 35(2): 699-704.

Yee, N., I. Paek and P. Besmer (1994). "Role of c-kit ligand in proliferation and suppression of apoptosis in mast cells. Basis for radiosensitivity of white spotting and steel mutants." Journal of Experimental Medicine 179(6): 1777-1787.

Yokoyama, M., J. Koh and D. Choi (1986). "Brief exposure to zinc is toxic to cortical neurons." Neuroscience Letters 71: 351-355.

Yoshikawa, H., Y. Nakajima and K. Tasaka (1999). "Glucocorticoid suppresses autocrine survival of mast cells by inhibiting IL-4 production and ICAM-1 expression." Journal of Immunology 162: 6162-6170.

Yoshikawa, H., Y. Nakajima and K. Tasaka (2000b). "Enhanced expression of Fas-Associated Death Domain-Like IL-1-Converting Enzyme (FLICE)-Inhibitory protein induces resistance to Fas-mediated apoptosis in activated mast cells." Journal of Immunology 165: 6262-6269.

Yuan, J., S. Shaham, S. Ledoux, H. Ellis and R. Horvitz (1993). "The C. elegans cell death gene *ced*-3 encodes a protein similar to mammalian interleukin-1β–converting enzyme." Cell 75: 641-652.

Zalewski, P. and I. Forbes (1993a). Intracellular zinc and the regulation of apoptosis. Programmed cell death: the cellular and molecular biology of apoptosis. M. Lavin and D. Watters. Melbourne, Harwood Academic: 73-86.

Zalewski, P., I. Forbes and C. Giannakis (1991). "Physiological role for zinc in prevention of apoptosis (gene-directed death)." Biochemistry International 24(6): 1093-1101.

Zalewski, P., I. Forbes and H. Betts (1993b). "Correlation of apoptosis with change in intracellular labile Zn(II) using Zinquin [(2-methyl-8-*p*-roluenesulphonamido-6-quinolyloxy) acetic acid], a new specific fluorescent probe for Zn(II)." Biochemical Journal 296: 403-408.

Zalewski, P., S. Millard, I. Forbes, O. Kapaniris, A. Slavotinek and H. Betts (1994a). "Video image analysis of labile zinc in viable pancreatic islet cells using a specific fluorescent probe for zinc." Journal of Histochemistry and Cytochemistry 42(7): 877-884.

Zalewski, P., I. Forbes, R. Seamark, R. Borlinghaus, H. Betts, S. Lincoln and A. Ward (1994b). "Flux of intracellular labile zinc during apoptosis (gene-directed cell death) revealed by a specific chemical probe, Zinquin." Chemical and Biology 1(3): 153-161.

Zalewski, P., X. Jian, L. Soon, W. Breed, R. Seamark, S. Lincoln, A. Ward and F.-Z. Sun (1996a). "Changes in Distribution of Labile Zinc in Mouse Spermatozoa during Maturation in the Epididymis Assessed by the Fluorophore Zinquin." Reproduction, Fertility and Development 8: 1097-1105.

Zen, K., A. Karsan, A. Stempien-Otero, E. Yee, J. Tupper, X. Li, T. Eunson, M. Kay, C. Wilson, R. Winn and J. Harlan (1999). "NF-kappaB activation is required

for human endothelial survival during exposure to tumor necrosis factor-alpha but not to interleukin-1beta or lipopolysaccharide." Journal of Biological Chemistry 274(40): 28808-28815.

Zheng, T., S. Schlosser, T. Dao, R. Hingorani, I. Crispe, J. Boyer and R. Flavell (1998). "Caspase-3 controls both cytoplasmic and nuclear events associated with Fas-mediated apoptosis in vivo." Proceedings of National Academy of Sciences USA 95: 13618-13623.

Zhivotovsky, B., A. Samali and S. Orrenius (1999c). "Caspases: their intracellular localization and translocation during apoptosis." Cell Death and Differentiation 6: 644-651.

Zhou, T., J. Mountz and R. Kimberly (2002). "Immunobiology of tumor necrosis factor receptor superfamily." Immunologic Research 26(1-3): 323-336.

Zong, W., L. Edelstein, C. Chen, J. Bash and C. Gelinas (1999). "The prosurvival Bcl-2 homolog Bfl-1/A1 is a direct transcriptional target of NF-kappaB that blocks TNFalpha-induced apoptosis." Genes and Development 13(4): 382-387.

Zou, H., Y. Li, X. Liu and X. Wang (1999). "An APAF-1/Cytochrome *c* multimeric complex is a functional apoptosome tha activates procaspase-9." Journal of Biological Chemistry 274: 11549-11556.

# APPENDIX 1A

# CELL CULTURES AND BUFFERS

# APPENDIX 1A- Cell Cultures and Buffers

## 1. Cell Cultures

-American Type Culture Collection, VA, USA supplied the following cell lines:

A549 human lung carcinoma cell, Cat # CCL-185

NCI-H292 human alveolar epithelial carcinoma cells, Cat # CRL-1848

RBL-2H3 rat basophilic leukemia cells, Cat # CRL-2256 and courtesy of Dr Russell Ludowyke, Centre of Immunology, St Vincent's Hospital, NSW, AUS.

-European Collection of Cell Cultures, Wiltshire, UK supplied the following cell line:

BE (2)-C human neuroblastoma cells, Cat # 95011817

-Dr Stephen R. Bolsover, Department of Physiology, University College London, London, UK kindly provided:

NIE-115 mouse neuroblastoma cells

-Professor Joseph H. Butterfield, Division of Allergy and Outpatient Infectious Diseases, Mayo Clinic and Foundation, Rochester, Minnesota, USA, kindly provided:

HMC-1, human leukemia mast cells

-Human lung and umbilical cord blood mast cells were isolated from samples with permission of the Human Ethics Committee. Protocols are described below in General Method's section (1).

-Human bone marrow-derived mast cells: courtesy of Dr Steven Krilis, Department of Immunology, Allergy and Infectious Disease, St George Hospital, NSW, AUS.

## 2. Buffers

**-Acetate buffer**: 0.2M acetic acid and 0.2M sodium acetate, pH 5.2 and store at 4°C.

**-Caspase substrate buffer (total 200 ml)**: 20 mM Hepes, 10% sucrose and 0.1% CHAPS in Milli-Q water pH 7.4 and store at 4°C. 10 mM Dithiothrietol (DTT) is added to buffer the same time as caspase fluorogenic substrate on the day of assay.

**-Citrate buffer (0.1M)**: 29.41 g of citric acid in 1 L of Milli-Q water, pH 4.5.

**-1X gel RNA gel loading buffer**: 500 µl deionised formamide, 100 µl 10X MOPS buffer, 167 µl 37% formaldehyde, 133 µl DEPC-treated water, 100 µl glycerol and a few grains of bromophenol blue enough to colour the solution. Store at –20°C.

-6X DNA loading gel buffer: 0.25% bromophenol blue and 40% w/v sucrose in water. Store at 4°C.

**-HBSS buffer**: N-2-hydroxyethyl-piperanzine-N'-2-ethanesulphonic acid (Hepes): 137mM NaCl, 5mM D-Glucose, 0.4mM $NaH_2PO_4$, 2.7mM KCl and 10mM Hepes. pH 7.2, autoclave and store at 4°C.

**-HBSS-protein buffer**: HBSS + 2% FBS with 10% horse serum, 1% BSA and 50µg/ml human IgG.

**-MOPS (10X)**: 0.2 M MOPS free acid, 0.5 M EDTA pH 8.0 and 0.05 M sodium acetate. Dissolve chemicals in DEPC-treated water and adjust pH to7.0 and store at 4°C.

**-Phosphate Buffered Saline (PBS)**: 0.27M NaCl, 0.005M KCl, 0.02M $Na_2HPO_4$ and 0.004M $KH_2PO_4$. pH 7.4 autoclave and store at 4°C.

**-Saline Sodium Citrate buffer (SSC) 20X**: 3 M sodium chloride, 0.3 M sodium citrate in Milli-Q water. Ph 7.0, autoclave and store at room temperature.

**-Tris-buffered saline with 0.05% Tween 20 (TTBS)**: 0.05M Tris-HCl pH 7.4,0.15M NaCl and 0.15% Tween 20. Store at 4°C.

**-Tyrode's buffer**: 0.14M NaCl, 0.003M KCl, 0.0004M $NaH_2PO_4$, 0.002M $CaCl_2.2H_2O$, 0.001 M $MgCl_2.6H_2O$ and 0.006 M glucose. pH 7.4, autoclave and store at 4°C.

**-TAE buffer (50x)**: 40mM Trizma base, 5.7% v/v glacial acetic acid and 1mM EDTA (pH 8.0) in distilled water. Store at room temperature.

# APPENDIX 1B

# ANTIBODIES, ENZYMES,

# SUBSTRATES AND KITS

## APPENDIX 1B- Antibodies, Enzymes, Substrates and Kits

### 1. Antibodies:

Anti-*c-Kit* Monoclonal Antibody YB5.B8- a kind gift of Dr Leonie Ashman Division of Haematology, Hanson Centre for Cancer Research, SA, Australia.

Goat anti-mouse IgG coated Dynabeads (Cat # MP-450), Dynal, Oslo, Norway.

Magnetic Particle Concentrator (MPC-1): Dynal, Oslo, Norway.

Monoclonal Anti-DNP IgE (Clone SPE-1), Cat # D-8406, Sigma

Human IgE monoclonal antibody, Cat # I-6510, Sigma

Polyclonal rabbit anti-CPP32 (human caspase-3), Cat # 556425, Pharmingen Becton Dickinson, New South Wales, AUS.

Polyclonal rabbit anti-p65 IgG, Cat # SC-109, Santa Cruz Biotechnology, California, USA.

Goat anti-rabbit IgG FITC, Cat # SC-2012, Santa Cruz Biotechnology, California, USA.

Bovine anti-goat IgG FITC, Cat # SC-2348, Santa Cruz Biotechnology, California, USA.

Polyclonal goat anti-caspase-4, Cat # SC-1229, Santa Cruz Biotechnology

Rabbit anti-rat $ZnT_4$ serum portion, a kind gift of Dr Chiara Murgia, Istituto Nazionale Ricerca per gli Alimenti e la Nutrizione, Rome, Italy.

Aurion goat anti-rabbit IgG EM grade immunogold antibody (10nm), Cat # 810.011, Jomar Diagnostics, South Australia, AUS.

Aurion rabbit anti-goat IgG EM grade immunogold antibody (10nm), Cat # 810.077, Jomar Diagnostics, South Australia, AUS.

**2. Caspase fluorogenic substrates:** supplied by Calbiochem-Novabiochem Corporation, California, USA:

7-amino-4(trifluoromethyl)coumarin (DEVD-AFC) Cat # 164580

Caspase-1, substrate I Cat # 218743 [z-Val-Ala-Asp-AFC or (z-VAD- AFC)]

Caspase-2, substrate II Cat # 218740 [z-Val-Asp-Val-Ala-Asp-AFC or (z-VDVAD-AFC)]

Caspase-3, substrate IV Cat # 264150 [z-Asp-Glu-Val-Asp-AFC or z-DEVD-AFC)]

Caspase-4, substrate II Cat # 218748 [Ac-Leu-Glu-Val-Asp-AFC or (Ac-LEVD-AFC)]

Caspase-5, substrate II Cat # 218754 [Ac-Trp-Glu-His-Asp-AFC or (Ac-WEHD-AFC)]

Caspase-6, substrate III Cat # 218763 [z-Val-Glu-Ile-Asp-AFC or (z-VEID-AFC)]

Caspse-9, substrate I Cat # 218765 [Ac-Leu-Glu-His-Asp-AFC or (Ac-LEHD-AFC)]

**3. Enzymes:**

Collagenase Type IA, Cat # C-9891, Sigma

Hyaluronidase Type 1-S, Cat # H-3506, Sigma

Reverse Transcriptase Cat: M-MLV, Life Technologies, California USA.

poly Taq polymerase, Cat # M2031, Promega, California, USA.

**4. Restriction enzymes and corresponding buffers:**

BamH I [GGATCC], Cat # RO136S, New England Biolabs, Hertfordshire, England.

EcoR I [GAATTC], Cat # RO101S, New England Biolabs, Hertfordshire, England.

Not I [GCGGCCGC], Cat # RO189S, New England Biolabs, Hertfordshire, England.

Xba I [TCTAGA], Cat # RO145S, New England Biolabs, Hertfordshire, England.

**5. Molecular Markers:**

GeneWorks, Bresatec, SA, AUS supplied:

SPP1-*Eco*RI DNA molecular weight marker, Cat # DMW-S1

1 kb DNA ladder Plus marker, Cat # DMW-1

**6. Primers:**

SP6 promoter primer, Cat # Q5011, Promega, MA, USA.

T7 promoter primer, Cat # Q5021, Promega, MA, USA.

Hexamer random primers, Promega, MA, USA.

**7. Dyes and Stains:**

Hoechst 33342, Cat # 33342, Sigma Chemical Company

Toluidine Blue, Cat # T0394, Sigma Chemical Company

Trypan Blue, Cat # T6146, Sigma Chemical Company

**8. Kits:**

Ambion Inc, Austin, Texas, USA supplied:

DECAprime II randon priming DNA labelling kit, Cat # 1455

GeneWorks, Bresatec, SA, AUS supplied:

GPK-1 giga prime DNA labelling kit, Cat # K-140

Immunotech - Beckam Coulter Company, Marseille, France supplied:

Enzyme immunoassay histamine kit, Cat # 2015

Qiagen GbmH, Hilden Germany supplied:

Qiagen plasmid midi/maxi kit, Cat #

QIAquick gel extraction kit protocol, Cat # 28704

RNeasy mini kit, Cat # 74104

**9. Others:**

Ambion Inc, Austin, Texas, USA supplied:

Bright star Plus positively charged nylon membrane, Cat # 10102

Dako Australia PTY Ltd, Botany, NSW, AUS supplied:

Fluorescent Mounting Medium, Cat # S.3023

NEN Life Products Inc, MA USA supplied:

Gene Screen Plus Hybridization transfer membrane, Cat #NEF986

Whatman International, Maidstone, England supplied:

Standard grade 1 (11μm) filter paper with diameter 4.7cm, Cat # 1001-047

# APPENDIX 1C

# CHEMICALS AND EQUIPMENT

# APPENDIX 1C- Chemicals and Equipments

## 1. Chemicals:

Ajax Chemicals, NSW, AUS supplied the following materials:

Calcium chloride ($CaCl_2.6H_2O$), Cat # 33138

$_D$-Glucose, Cat # 402103

Potassium chloride (KCl), Cat # 201751

Potassium dihydrogen orthophosphate ($KH_2PO_4$), Cat # 805286

Magnesium chloride ($MgCl_2.6H_2O$), Cat # 107536

Sodium hydrogen carbonate ($NaHCO_3$), Cat# 308072

Amersham Pharmacia Biotech, Uppsala, Sweden supplied:

Percoll (density 1.128g/ml), Cat 17-0891-02

BDH/Analar-Merck Pty Ltd, VIC, AUS supplied the following materials:

Absolute ethanol, Cat # 10107.9010

Acetone, Cat # 10003.4Q

Chloroform, Cat # 10077.6C

Formaldehyde (40%), Cat # 10113.6C

Glacial acetic acid, Cat # 100015N

Isopropanol, Cat # 10244 5K

Methanol, Cat # 10158.6B

Sodium chloride (NaCl), Cat # 1024.4J

Sodium dihydrogen orthophosphate ($NaH_2PO_4$), Cat # 307164T

BioRad Laboratories, California, USA supplied:

Analytical grade mixed bed resin (20-50 mesh), Cat # AG 501-X8

Bradford protein assay, Cat # 500-0006

$D_c$ protein assay [Reagent A, Cat # 500-0114, reagent B, Cat # 500-0113, reagent S]

Bresatec Pty Ltd, South Australia, AUS supplied the following:

Geneworks SPP1/*Eco*RI DNA molecular weight marker, Cat # DMW-S1

Flow Laboratories, NSW, AUS supplied:

Horse donor serum, Cat # 29-211-54

ICN Biomedicals Inc, Ohio, USA supplied the following materials:

Glycerol, Cat # 800688

Ham's F-12 Medium, Cat # 1042120

Ficoll Paque Plus (density 1.077g/ml), Cat # 17-1440-02

200X Penicillin (10000 IU/ml)-Streptomycin (10 mg/ml), Cat # 1670249

1X Trypsin-EDTA 1:250, Cat # 1689149

Invitrogen, Life Technologies, CA, USA supplied:

Trizol, Cat # 15596

May and Baker Ltd, Dagenham, England supplied:

Bromophenol blue, Cat # B97/18/61

Merck-Schuchardt, Hohenbrunn, Germany supplied:

Sodium Butyrate ($C_4H_7NaO_2$), Cat # 8.20236.0250

Molecular Probes Inc, Oregon, USA supplied:

Albumin from bovine serum, 2,4-dinitrophenylated (DNP-BSA),

Cat # A23018

National Diagnostics, Georgia, USA supplied the following materials:

Histoclear, Cat # HS-202

Histomount, Cat # HS-103

Pharmacia and Upjohn Pty Ltd, WA, AUS supplied:

Gentamicin sulfate (80 mg/2ml) injection ampoule, Cat # R-580A

G50 Sephadex, Cat # 17004301

Perkin Elmer Life Sciences Inc, MA, USA supplied:

Nucleotides, [$\alpha$-$^{32}$P ] dATP- specific activity 111 TBq/mmol

Progen Industries Ltd, Qld, AUS supplied:

DNA grade agarose, Cat # 200-0011

Low melting point agarose, Cat # 200-0030

Promega Corporation, Sydney, AUS supplied:

pGEMT-Easy vector, Cat # A1360 [see Appendix ]

ProSciTech, Qld, AUS supplied:

Epoxy Procure aradite embedding kit (Epoxy resin), Cat # C039

Lead Citrate stain, Cat # C073

LR White resin medium grade, Cat # C023

Nickel grid, Cat # GMNi200

Normal rabbit serum, Cat # JBSR5

Osmium tetroxide, Cat # C010, C012

Uranyl acetate stain, Cat # C079

Riedel-de-Haën Laborchemikalien, GmbH, Germany

30% w/v Hydrogen peroxide, Cat # 2014

Serotec, Oxford, UK supplied:

Human IgE Kappa Myeloma-purified protein, Cat # PHP008

Sigma Chemical Company, St Louise, MO, USA supplied the following materials:

Albumin Bovine (BSA)-fraction V, Cat # A-7030

3-amino-9-ethylcarbizole, Cat # A-5754

Calcium Ionophore A23187, Cat # C-7522

CHAPS, Cat # C-3023

Compound 48/80, Cat # C-2313

Dextran sulfate, Cat # D-8906

Diethyl pyrocarbonate (DEPC), Cat # D-5758

Dimethyl sulfoxide (DMSO), Cat # D-5879

Dithiothrietol (DTT), Cat # D-5545

EDTA, Cat # E-5134

Ethidium Bromide, Cat # E-1510

Fast Blue RR, Cat # F-0375

Formamide, Cat # F-7508

Glutaraldehyde, Cat # G-6257

Hepes, Cat # H-7523

Herring Sperm DNA, Cat # D-3159

Human IgG, Cat # I-4506

Igepal Ca-6330 (NP-40), Cat # I-3021

Human Interleukin-5, Cat # I-5273

Human Interleukin-6, Cat # I-1395

L-Glutamine, Cat # G-7145

2-Mercaptoethanol, Cat # M-7522

Metrizamide, Cat # M-3383

MOPS (3-[N-Morpholino]propanesulfonic acid), Cat # M-8899

100X Non essential amino acids (NEAA), Cat # M-7145

Ovalbumin (hen egg white), Cat # A2512

Paraformaldehyde, Cat # P6148

Phorbol 12-Myristate 13-Acetate (PMA), Cat # P-8139

p-ntirophenyl-N-acetyl-$\beta$-$_D$-glucosaminidase, Cat # N-9376

RPMI-1640 culture medium, Cat # R-6504

Sodium acetate ($CH_3COONa$), Cat # 003571

Sodium citrate, Cat # S-4641

Sodium dodecyl sulfate, Cat# L-4509

Sodium Pyrithione (Zn pyrithione), Cat # H-3261

Staurosporine, Cat# S-4400

Stem cell factor human recombinant (rhSCF), Cat # S-7901

Sucrose, Cat # S-1888

Toluidine Blue (basic blue), Cat # T-0394

Tris -HCl, Cat # T-6666

TPEN (N, N,N',N'-Tetrakis(2-pyridylmethyl)ethylenediamine),

Cat # P-4413

Triton X-100, Cat # T-9284

Trizma base, Cat # T-1503

Tween-20, Cat # P-5927

Trace Scientific Ltd, Melbourne, AUS supplied:

Foetal Bovine Serum (FBS), Cat # 15-010-0500V

**2. Equipments:**

Adelab Scientific, SA, AUS supplied:

Electronic UV transilluminator

CEMMSA, University of Adelaide, South Australia, Aus provided:

Philips CM 100 TEM electron microscope

Bio-Rad, Hemel Hempstead, UK supplied:

Confocal Microscopic System

Bio-Rad MRC-1000 UV Laser Scanning Confocal Microscope

Eastman Kodak Company, Pty Ltd supplied:

Electrophoresis Documentation and analysis system 120- Kodak 1D image analysis software.

Leading Edge Pty Ltd, South Austalia, AUS supplied:

Video Pro Image Analysis System

Eppendorf, Hamburg, Germany supplied:

Microcentrifuge (5414s)

Flow Laboratories Pty Ltd, NSW, AUS supplied:

Titertek Multiskan MC plate reader

Hybaid, Middlesex, UK supplied:

Hybaid Micro-4 hybridisation oven

International Equipment Co, USA supplied:

Centrifuge (IEC-Centra-7R)

Millipore Australia Pty Ltd, NSW, AUS supplied:

Milli-Q Plus System- ultra pure water unit

MJ Research Inc, MA, USA supplied:

PTC DNA engine 200- Peltier thermal cycler

Olympus, Tokyo, Japan supplied:

UV Fluorescence microscope (BH-2)

Phase Contrast Microscope

Perkin Elmer Connecticut, USA supplied:

Perkin Elmer Gene Amp PCR system 9700

Spectrofluorimeter LS50

Spectrophotometer

Stratagene, California, USA supplied:

UV Stratalinker 1800

Thermo Shandon Inc, Pittsburgh, PA, USA supplied the following:

Shandon -Elliot Cytospin 2 Centrifuge

Funnel cyto-single disposable sample chamber with white filter card and cap, cat # 59910040

# APPENDIX 1D

# JOURNAL PAPERS

Ho, L.H., Ratnaike, R.N. & Zalewski, P.D. (2000) Involvement of intracellular labile zinc in suppression of DEVD-caspase activity in human neuroblastoma cells.
*Biochemical and Biophysical Research Communication, v. 268(1), pp. 148-154*

Ho, L.H., Ruffin, R.E., Murgia, C., Li, L., Krilis, S.A. & Zalewski, P.D. (2000) Labile zinc and zinc transporter ZnT4 in mast cell granules: role in regulation of caspase activation and NF-KB translocation.
*Journal of Immunology, v. 172(12), pp. 7750-7760*